CENTRO DE INVESTIGACIÓN Y DE ESTUDIOS AVANZADOS DEL INSTITUTO POLITÉCNICO NACIONAL

PROGRAMA DE DOCTORADO EN NANOCIENCIAS Y NANOTECNOLOGÍA, UNIDAD ZACATENCO, CDMX

Título de Tesis:

"SÍNTESIS, CARACTERIZACIÓN Y EVALUACIÓN DE NANOPARTÍCULAS NÚCLEO-ENVOLTURA Au $_x$Fe$_2$O$_4$ (x= Fe, Co, Mn, Zn) FUNCIONALIZADAS (CD-44, DOCETAXEL Y BICALUTAMIDA) PARA EL TRATAMIENTO *IN VITRO* DE CANCER DE MAMA TRIPLE NEGATIVO"

Sustentante de la Tesis:

MAURICIO ALBERTO MEDINA PÉREZ

Para obtener el grado de: Doctorado en Ciencias

En la Especialidad de Nanociencias y Nanotecnología

Directores de la Tesis:

Dr. JOSÉ MANUEL HERNÁNDEZ HERNÁNDEZ

(Departamento de Biología Celular)

Dr. JOSE ISABEL TAPIA RAMÍREZ

(Departamento de Genética y Biología Molecular)

Ciudad de México; Diciembre, 2020

CENTER FOR RESEARCH AND ADVANCED STUDIES OF THE NATIONAL POLYTECHNIC INSTITUTE

DOCTORATE PROGRAM IN NANOSCIENCES AND NANOTECHNOLOGY, ZACATENCO, CDMX

Thesis title:

"SYNTHESIS, CHARACTERIZATION AND EVALUATION OF CORE-SHELL Au xFe_2O_4 (x = Fe, Co, Mn, Zn) NANOPARTICLES FUNCTIONALIZED (CD-44, DOCETAXEL-BICALUTAMIDE) FOR THE IN VITRO TREATMENT OF TRIPLE NEGATIVE BREAST CANCER"

Thesis Sustainer:

MAURICIO ALBERTO MEDINA PÉREZ

To obtain Ph.D. degree in the specialty of Nano-sciences and Nanotechnology

Thesis Directors:

Dr. JOSÉ MANUEL HERNÁNDEZ HERNÁNDEZ

(Cell Biology Department)

Dr. JOSE ISABEL TAPIA RAMÍREZ

(Genetics and Molecular Biology Department)

Mexico City; December 2020

DEDICATIONS

My experiences with science led me to God. They challenge science to prove the existence of God. But must we really light a candle to see the sun?

—Wernher von Braun

Dedicated to God…with love.

ACKNOWLEDGEMENTS

A good engineer gets stale very fast if he doesn't keep his hands dirty.

—Wernher von Braun

Thank you:

Dr. José Isabel Tapia Ramírez

Dr. José Manuel Hernández Hernández

If you want to find the secrets of the universe, think in terms of energy, frequency and vibration.

— Nikola Tesla

Thank you:

Dr. Goldie Oza

It is not the healthy who need a doctor, but the sick.

—Jesus Christ

Everyone is the other, and no one is himself

—Martin Heidegger

Thank you:

María Teresa Pérez González

Dr. Miguel Alberto Medina Escobar

Dr. Luis Romero Arce

Dr. Amanda Haglund

Dedicated to all those medical doctors, nurses, biomedical-engineer researchers and healthy personnel who fight against the disease and help their patients tirelessly.

" SYNTHESIS, CHARACTERIZATION AND EVALUATION OF SUPER-PARAMAGNETIC CORE-SHELL NANOPARTICLES Au xFe_2O_4 (x = Fe, Co, Mn, Zn) FUNCTIONALIZED (CD-44, DOCETAXEL-BICALUTAMIDE) FOR THE IN VITRO TREATMENT OF TRIPLE NEGATIVE BREAST CANCER".

Examination Committee

Examination committee: Supervisor Dr. José Manuel Hernández Hernández (Cell Biology Department) Co-supervisor Dr. Jose Tapia Ramirez (Department of Genetics and Molecular Biology) Committee members: Dr. Gerardo Cabañas Moreno (Nanoscience and Nanotechnology Department) Dr. Jaime Santoyo Salazar (Physics Department) Dr. Miguel García Rocha (Physics Department).

Thanks to:

Dr. Goldie Oza, (CIDETEQ), Dr. Alvaro Angeles Pascual (LANE), Dr. Sirenia González Pozos (TEM LANE), M. S Miguel Avendaño Ibarra (CINVESTAV-SEES, Raman spec), Dr. Jesús Angel Arenas Alatorre (Physics department UNAM HR-TEM SQUID), Dr. Samuel Tehuacanero Cuapa (Physics department UNAM HR-TEM), M. S Adolfo Tavira Fuentes (CINVESTAV-SEES, XRD analysis), Dr. Jorge Roque De la Puente (SEM-Auriga), M. en C. José Hugo Zepeda Peralta (Bioelectronics CINVESTAV), Dr. Arturo Vera (Bioelectronics department, Hyperthermia measurements), Victor Tapia Ramírez, Dr. Humberto Santana Román, Dr. Daniel Bahena Uribe, last and not least collaborations from various departments (Physics, Cell biology, Electrical engineering – SEES, Chemistry department, Toxicology department and National Council for Science and Technology (CONACYT).

Regarding conflicts of interests and economic compensations.

We declare that this project does not present any conflict of economic interests since it has been created with resources from CONACYT / CINVESTAV. Both, the main author and collaborators of this project, we all declare that there will be NO economic remuneration, from any source (company, university, cooperative group, NGO) for the realization of this research.

DECLARATION

I declare: This thesis entitled "SYNTHESIS, CHARACTERIZATION AND EVALUATION OF SUPER-PARAMAGNETIC CORE-SHELL NANOPARTICLES Au xFe_2O_4 (x = Fe, Co, Mn, Zn) FUNCTIONALIZED (CD-44, DOCETAXEL-BICALUTAMIDE) FOR THE IN VITRO TREATMENT OF TRIPLE NEGATIVE BREAST CANCER" is submitted for the degree of Doctor of Philosophy in Science (Specialized in Nano-sciences and Nanotechnology) and has been made by myself at Center for Research and Advanced Studies of the National Polytechnic Institute (CINVESTAV-IPN), Zacatenco, Mexico City under the supervision of Dr. José Manuel Hernández Hernández and Dr. Jose Isabel Tapia Ramirez. The Project was conceived by our group which is a multidisciplinary team and all the ideas are genuine and have not been submitted in part or full in order to get another degree or diploma in any other university or research institution. This work is original, an effort to optimize therapeutic effects of Nanoparticles for applications in the ***Nanomedicine*** field.

Dr. Mauricio A. Medina-Pérez M.D. M. Sc

ABSTRACT

Breast cancer continues to be a major public health problem. The incidence is increasing in most countries and is expected to increase further in the next 20 years despite current efforts to prevent the disease. Some risk factors for breast cancer are lower age of menarche, late age of first pregnancy, fewer pregnancies, having had dysfunctional or shorter lactation periods, late menopause, obesity, alcohol consumption, physical inactivity, and therapy of hormone replacement (HRT). In addition to the known mutations of the BRCA-1 and BRCA-2 genes, the latter has quadrupled its presence in recent decades. Above all the molecular subtypes of breast cancer, the triple negative (TNBC) has the worst prognosis and the lowest response rate to treatment. In the present day, there is no specific oncological treatment for this type of cancer and the side effects are terrible, affecting healthy cell-tissue and organs due to the lack of specificity in conventional therapy.

This work consisted of synthesizing super-para-magnetic iron oxide nanoparticles (SPIONs) doped with cobalt (Co), manganese (Mn), and zinc (Zn) with a gold-coating, functionalized for triple negative breast cancer (TNBC) therapy. The main advantage of this core-shell nanoparticle is that it is constituted by two different nanomaterials, which can be effectively used for drug delivery and hyperthermia. The gold (Au) surface will be functionalized with drugs such as Docetaxel and Bicalutamide for the effective treatment of triple negative breast cancer (MDA MB-231 cell line). The gold-coated complex with surface functionality was characterized and evaluated for *"In Vitro"* cytotoxicity studies to ensure that the nanoparticle complex shows no toxic effects in normal cells. After

performed characterizations, our research group decided to use $CoFe_2O_4$ armada to continue functionalization.

Firstly, the release of the drug will be studied using the dialysis membrane technique at different pH levels, which is why it is necessary to adapt it to several mathematical models of drugs to find the appropriate release adjustment. Finally, under an alternating magnetic field, the study focused on detecting the amount of heat produced by SPIONs to induce apoptosis over cancer cell lines by using hyperthermia, either for releasing drug at high temperature or producing apoptosis *"In Vitro"*. Interestingly, our results suggested when combining therapy (hyperthermia and drug delivery) produced irreversible damage to malignant cells because its higher specificity. Therefore, we propose to design a complex system for personalized nanomedicine in cancer therapeutics.

Keywords: *Triple Negative Breast Cancer (TNBC), Nanomedicine, Hyperthermia, Super-para-magnetic iron oxide nanoparticles (SPIONs), Personalized Medicine.*

RESUMEN

El cáncer de mama sigue siendo un problema importante de salud pública. La incidencia está aumentando en la mayoría de los países y se espera que se incremente aún más en los próximos 20 años a pesar de los esfuerzos actuales para prevenir la enfermedad. Algunos factores de riesgo de cáncer de mama son: menor edad de la menarquia, edad tardía del primer embarazo, menos embarazos, haber tenido períodos de lactancia disfuncionales o más cortos, menopausia tardía, obesidad, el consumo de alcohol, la inactividad física y la terapia de reemplazo hormonal (TRH). Además de las conocidas mutaciones de los genes BRCA-1 y BRCA-2, éste último ha cuadriplicado su presencia en las últimas décadas. De todos los subtipos moleculares de cáncer de mama, el triple negativo (TNBC) tiene el peor pronóstico y menor tasa de respuesta a tratamiento. En los días actuales no existe tratamiento oncológico específico para este tipo de cáncer y los efectos adversos de la terapia convencional actual son devastadores para las células, tejidos y órganos sanos en estos pacientes, en parte por la falta de especificidad.

En el presente trabajo, sintetizamos nanopartículas de óxido de hierro súper-paramagnético (SPION), dopadas con iones de cobalto (Co), manganeso (Mn), y zinc (Zn) para terapia de cáncer de mama triple negativo. La principal ventaja de esta nanopartícula núcleo-cubierta es que está constituida por dos nanomateriales diferentes, que se pueden usar de manera efectiva para el suministro de medicamentos y la hipertermia. La superficie de oro (Au) se funcionalizó con medicamentos como Docetaxel y Bicalutamida para el tratamiento efectivo del cáncer de mama triple negativo (línea celular MDA MB-231). El complejo recubierto de oro con funcionalidad superficial se caracterizó y evaluó para

estudios de citotoxicidad *"In vitro"* para garantizar que el complejo de nanopartículas no muestre efectos tóxicos en las células normales. El complejo ganador, para realizar la funcionalización después de las caracterizaciones y ensayos MTT fue $CoFe_2O_4$.

Primero, se estudió la liberación del fármaco utilizando la técnica de membrana de diálisis a diferentes niveles de pH, por lo que fue necesario adaptarlo a varios modelos matemáticos de fármacos para encontrar el ajuste de liberación adecuado. Finalmente, bajo un campo magnético alterno, el estudio se centró en detectar la cantidad de calor producida por los SPIONs para inducir apoptosis sobre las líneas celulares cancerosas mediante el uso de hipertermia, la cual funciona para liberar el fármaco a alta temperatura o para producir apoptosis (muerte celular) *"In vitro"*. Interesantemente, nuestros resultados sugieren que la terapia combinada (hipertermia y terapia con medicamentos) produce daño irreversible a las células malignas debido a su alta especificidad. Por lo tanto, proponemos diseñar un sistema complejo para nanomedicina personalizada en el teranóstico de cáncer.

Palabras clave: *Cáncer de mama triple negativo, Nanomedicina, Hipertermia, Nanopartículas súper-paramagnéticas de óxido de hierro, Medicina personalizada.*

INDEX CONTENTS

Chapter 1: Nanomedicine.

Chapter 6: Nanotechnology Future Trends.

List of Figures.

List of Tables

LIST OF ABBREVIATIONS

A

AI Artificial Intelligence

APCs Antigen-presenting cells

ATCC American Type Culture Collection

B

B Flux density

C

CASIS Center of the Advancement of Science in Space

CLSM Confocal laser scanning microscopy

CRT TV-type-cathode-ray tube

CSNPs Core-Shell Nanoparticles

CTAB Hexadecyltrimethylammonium bromide

CT- Scan Computed Tomography

D

3D Three dimensional

4D Fourth dimensional

DC Dendritic cells

DI Deionized water

DMEM Dulbecco's Modified Eagle Medium

DMSO Dimethyl sulfoxide

DNA Deoxyribonucleic acid

E

EDS Energy Dispersive X-Ray Spectrometer

EGFR Epidermal growth factor receptor

EPR Enhanced Permeability and Retention effect

F

FBS Fetal Bovine Serum

FDA Food and Drug Administration

FTIR Fourier Transform Infrared Spectroscopy

G

Gd Gadolinium

H

H - magnetic field

HA Hialuronan

HAADF-STEM High-Angle Annular Dark-Field Scanning Transmission Electron Microscopy

HAuCl4 Chloroauric acid

HRTEM High Resolution Transmission Electron Microscopy

Hz Hertz

I

IONPs Iron oxide nanoparticles

IV Intravenously

L

LASER Light amplification by stimulated emission of radiation

LSCM Laser Scanning Confocal Microscopy

M

M Magnetization

mAb Monoclonal Anti-body

MALDI-TOF Matrix Assisted Laser Desorption Ionization-Time Of Flight mass spectrometry

MERIT (Systematic Analysis and Characterization of Mutational Effect on RNA Interactome Topology)

MNPs@Au Gold coated magnetic nanoparticles

MRI Magnetic Resonance Image

MS Magnetic saturation

MTT 3-(4,5-dimethylthiazol-2-yl) 2,5-diphenyltetrazolium bromide

Mw Microwave

MwA Microwave Ablation

MW Molecular Weight

N

Nex: Number of excitations

ND Nanodiamonds

NHS N-Hydroxysuccinimide

NHEJ Non-homologous end junctions

Nm Nanometer

NIR Near-Infrared

NPs Nanoparticles

O

O Oxygen

P

PBS Phosphate buffer saline

PEG Polyethylene glycol

PET Positron Emission Tomography

pH Potential of Hydrogen

PK Pharmacokinetics

PL Photoluminescence

PTT Photothermal therapy

Q

QDs Quantum dots

R

RES Reticuloendothelial system

RF Radio Frequency

RNA Ribonucleic acid

ROS Reactive oxygen species

S

SAR Specific absorption rate

SAED Surface analysis of electron diffraction

SNPs Single Nucleotide Polymorphism

SEM Scanning electron microscopy

SERS Surface enhanced Raman spectroscopy

siRNA small interfering RNA

SPIONs Superparamagnetic Iron Oxide Nanoparticles

SPR Surface Plasmon Resonance

SQUID Superconducting Quantum Interference Device

T

T1 Spin-lattice relaxation

T2 Spin-spin relaxation

TB Blocking temperature

TD Thermal decomposition

TE Echo time

TGA Thermogravimetric Analysis

TNF Tumor necrosis factor

TR Repetition time

U

UV-Vis Ultra Violet-Visible

USD United States Dollar

W

WHO World Health Organization

X

XPS X-ray Photoelectron Spectroscopy

XRD X-Ray Diffraction

Y

Ys Yoctosecond

Z

Z Z Potential

LIST OF SYMBOLS

α Alpha

γ Gamma

χ Magnetic susceptibility

% Percentage

Θ Theta

Au Gold

C Celcius

cm Centimeter

Co Cobalt

CO_2 Carbon dioxide

eV Electron-Volt

Fe Iron

Fe_2O_3 Maghemite

Fe_3O_4 Magnetite

GHz GigaHertz

gm Gram

H Hydrogen

J Joule

kDa KiloDalton

kOe KiloOersted

Mn Manganese

$MnFe_2O_4$ Manganese Ferrite

M/mol Molarity

mg Milligram

min Minutes

ml Millilitre

mm Millimetre

mM Millimolar

mW MilliWatt

mV MilliVolt

N_2 Nitrogen

NaOH Sodium hydroxide

NaCl Sodium chloride

nm Nanometre

r2 Transverse relaxivity

sec Seconds

μf - permeability of ferromagnets (and ferrimagnets)

μp - permeability of paramagnets

μ0 - permeability of free space (4*π*10-7 H/m)

μd - permeability of diamagnets

μg Microgram

μl Microlitre

W Watt

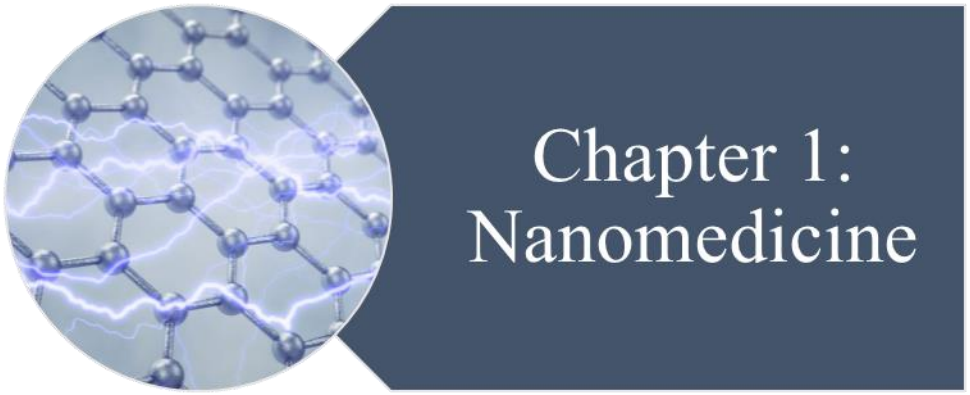

1.- Introduction.

1.1. Nanomedicine: The future of Medicine.

The contemporary *Homo Sapiens,* having around 1345 cm^3 brain-volume [1], have tried to explain the reality and nature phenomena as environment, life, death or illness. The first human civilizations based their medical practice on primitive and pragmatic empiricism (applied fundamentally to the use of herbs obtained from environment) and a magic-religious medicine, which resorted to gods and mythical beings to try to understand the unexplained phenomenon, likewise, this implied an effort to keep the groups together and guarantee the survival.

In the twentieth century, medicine was driven by scientific and technical development, through the discovery of microorganisms causing the disease, emerged the so-called ***Evidence-Based Medicine***, which is based on a fundamentally biological paradigm by using the best scientific evidences obtained by the clinical research but also admits and proposes a health-disease model determined by biological, psychological and sociocultural factors [2]. On this basis the new models in health are built acquiring unsuspected dimensions for the thinkers and researchers of the last century. However, evidence-based-medicine, a term that is falling into disuse, is being slowly displaced by ***Personalized***

Medicine, a new concept in medicine which uses molecular biomarkers to describe metabolic signaling, giving to the clinician valuable information not only about patient status but also a complete molecular profile [3].

It is necessary to make pharmacogenomics studies personalized to each patient because of the emergence of more complex diseases (Cancer, neurological diseases as Alzheimer's and Parkinson's, point mutations, prion diseases as *Creutzfeldt Jakob disease and Transmissible Spongiform Encephalopathies*). These diseases, along with increasing antimicrobial resistance, make it clear that medicine must evolve to a personalized approach in a multidisciplinary context.

New research reveals through complex mathematical models of chaos that to deal with certain types of cancer [4], requires thousands of variables, sophisticated and multidisciplinary equipment is necessary. Currently, the joint work of physicists and bio-engineers have produced nanoplatforms that generate heat (hyperthermia) to destroy tumors [5], or higher efficacy nanomaterials and the ability of engineered nanoparticles to cross through the blood-brain barrier to provide a platform for brain diseases groundbreaking innovations. Also, there are molecular biologists and geneticists researching chronic diseases using tools such as ion-proton sequencers, microarrays and gene therapy in combination with nanotechnologies. Therefore, 21st century medicine is dealing against dangerous and complex diseases, also new challenges in the field of *Aerospace Medicine* to get humans on Mars overcoming microgravity conditions [6] since physiological human body parameters changes at high altitudes and space, so it is imperative in this sense, to embrace the arrival of the *"New era in Medicine"* where powerful disciplines as *Physics, Chemistry, Robotics, Quantum Mechanics, Valleytronics, Quantum computation, Informatic Networks (Big Data), Synthetic Biology, Synthetic Epigenetics, Artificial Intelligence, Cybernetics, Omics (genomics, transcriptomics, proteomics, metabolomics, interactomics and fluxomics), Molecular Cell Biology and Nanotechnology* are involved, converging to enhance not only human health conditions but planetary conditions.

According to *The National Nanotechnology Initiative* (NNI) , *Federal Drug Administration* (FDA) and the *Patent and Trademark Office* (PTO), *Nanotechnology* can be defined as the science and engineering involved in the design, synthesis, characterization, and application

of materials and devices whose smallest functional organization, in at least one dimension, is on the nanometer (nm) scale 1 and 100 nm (0.001-0.1 μm) or one billionth of a meter (10^{-9}, of a meter) [7, 8]. At this size, the properties of matter change, so effects are important at this quantum-realm scale. Applications in Nanotechnology are not restricted to Medicine ***(Fig. 1)***.

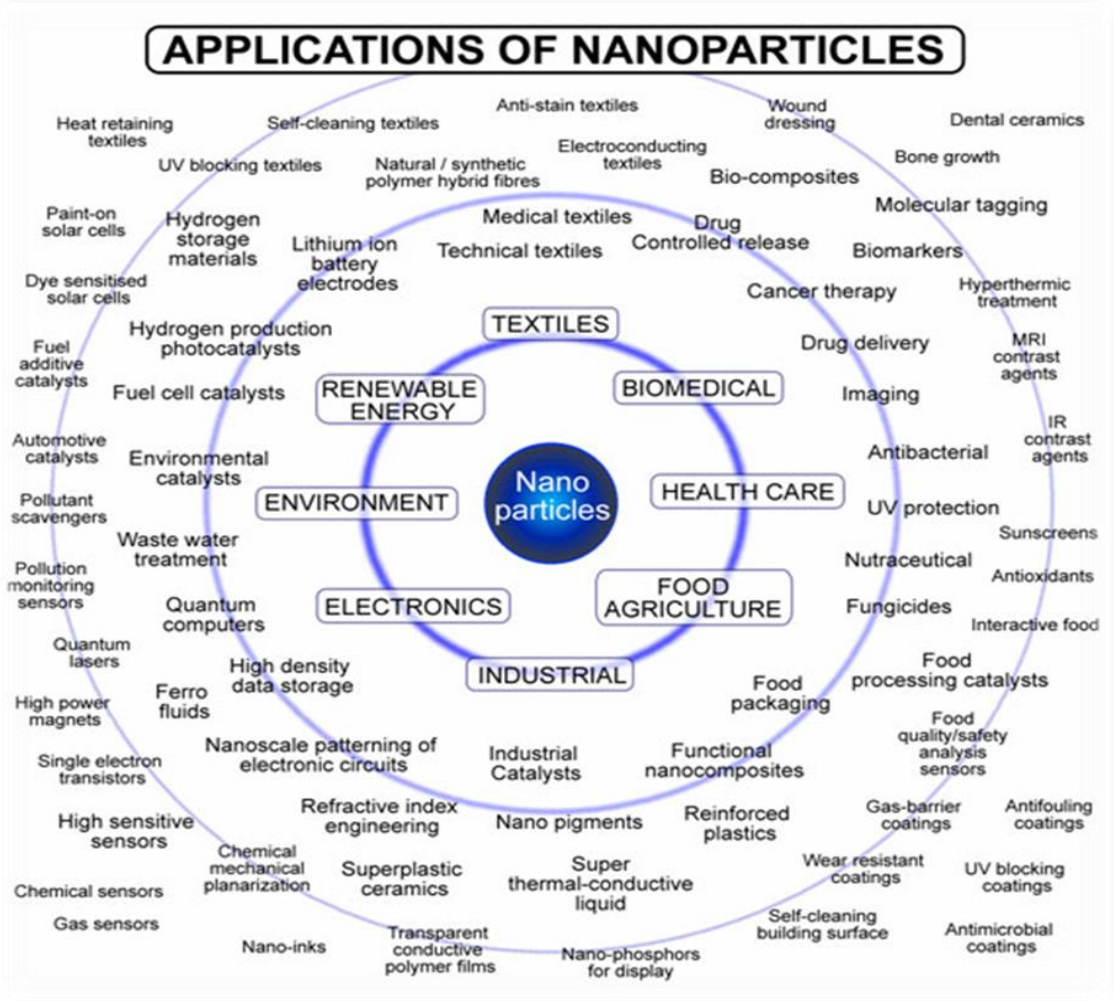

Figure 1. Applications in Nanotechnology. *Source: "Commercial scale production of inorganic nanoparticles".*

1.2 – Properties of the Nanoscale applied in Nanomedicine.

1.2.1-Size matters but isn't everything.

The properties of matter exhibit unique properties at the scale from 1 to 100 nm, nanoparticles (NPs) possess novel structural, optical, and electronic properties that many larger molecules or bulk cluster materials lack, that's the reason why nanotechnology is a convergent discipline, various research areas such as chemistry, biology, physics, mathematics, medicine and engineering are involved to bring it up smart solutions for a such complexity challenges that humankind is facing on 21st and next century [9].

Nanomedicine is the science field which uses *Nanotechnology* for applications in healthcare, including diagnosis-therapy, a dual effect called *Theranostics* [10] drug delivery and image and uses tools such as genetics, flux-omics, molecular and cell biology, material science, and bioengineering among others for this purpose. Moreover, *Nanomedicine* novel works have to do with prognosis due to its bigger capacity for finding biomarkers related to patient survival and quality-life expectations. The applications are unlimited, worldwide-market for healthcare-nanotechnology (Nanomedicine) is expected to reach USD 196.02 billion by 2020, according to a study made by the Grand View Research, Inc [11].

The "*Nano-world"* already exists in nature, daily allows our lives continue, example of this are the vital processes in the organism of living beings since the dimensions of many natural molecules like DNA (2nm), glucose (150 nm), antibodies, proteins (insulin, hemoglobin fibrinogen), enzymes, receptors, virus and amino acids are already within the nanoscale.

Class	**Material**	**Mw (Da)**	**Size of different biological substances (nm)**
Amioacids	Glicine	75	0.42
	Triptophan	246	0.67
Proteins	Insulin	6000	2.2
	Hemoglobin	68000	7.0
	Fibrinogen	40000	50
	Albumine	69000	9.0
Other molecules	Plants Clorophyll	720	1.1

Table 1: A nano-perspective. Adapted chart from Charles P. Poole Jr.

An example of size matters but isn't everything has been traced in ancient civilizations. Nanotechnology (although probably not voluntarily) were found in 4th-century Roman civilization in the manufacture of a dichroic glass cup, the famous *Lycurgus cup.* [12] The dichroic effect of the Lycurgus glass-cup is achieved by a small quantity of gold and silver nanoparticles dispersed in colloidal form in the glass, the optical properties are not only interesting but beautiful, when the light falls on the glass frontally, the glass turns into color green, but the light is red when lit from behind. It is probable that the artisans of that period did not understand nanotechnology, nor could they manipulate materials at a nanoscale, but by accidentally "Polluting" the glass with finely ground gold and silver powder, the Lycurgus cup achieved that peculiar design. If anything can show us the design of the Lycurgus cup is that size isn't everything since the shape, structure and materials composition, all of them also are essential features, critical for the final application.

1.2.1.2- Shape.

The shape of the NPs is decisive to develop a certain application as thermal-ablation, as plasmonic nano-sensors [13] or image contrast agents; For example, nanoparticles can acquire spherical shapes, tubes, rollers, stars, cells, cages or jails, cones, cylinders, matryoshkas, core-shell, wires, triangles, cubes, discs. In addition to these forms the nanoparticles can contain pores, can be rigid, solid or hollow (depending on the application whether they are hollow they can transport substances or materials) [8]. Researchers have begun to develop nanoparticles with more dynamic materials: anisotropic nanoparticles with a quasi-spherical shape, which helps in optoelectronic applications (surface plasmon response). However, the ideal nanoparticle enabled to travel into the bloodstream should have the shape of the erythrocyte (biconcave disc) to overcome the problems of vascular transport, specifically being related to the forces of *Frank Starling* [14] and the difference between vascular pressure and interstitial fluid pressure (IFP), known as the *Hydrostatic Pressure Gradient* (HPG). Understanding how the HPG interacts with a given shape of nanoparticle allows scientist to optimize drug delivery; with the ideal hydrodynamic shape, NPs can travel with decreased resistance through the bloodstream in contrast for instance, if they had a square shape [15]. The size and geometry of nanoparticles are also essential elements to escape from the cellular immune response, increasing the half-life of the *nano-*

drug or nano-vehicle and its bioavailability in blood serum. Moreover, there are in existence many more geometric shapes such as gold nano-stars or nano-urchins [16] which have interesting tunable properties that can be exploited in different nanomedicine applications, although these could have other kinds of inconveniences [17]. Other useful forms such as nano wires and quantum dots have luminescent properties [18], while nanorods [19] and nano-matryoshkas [20] can carry multiple drugs at once. Thus, nanoparticle shape is highly important for a given desired application.

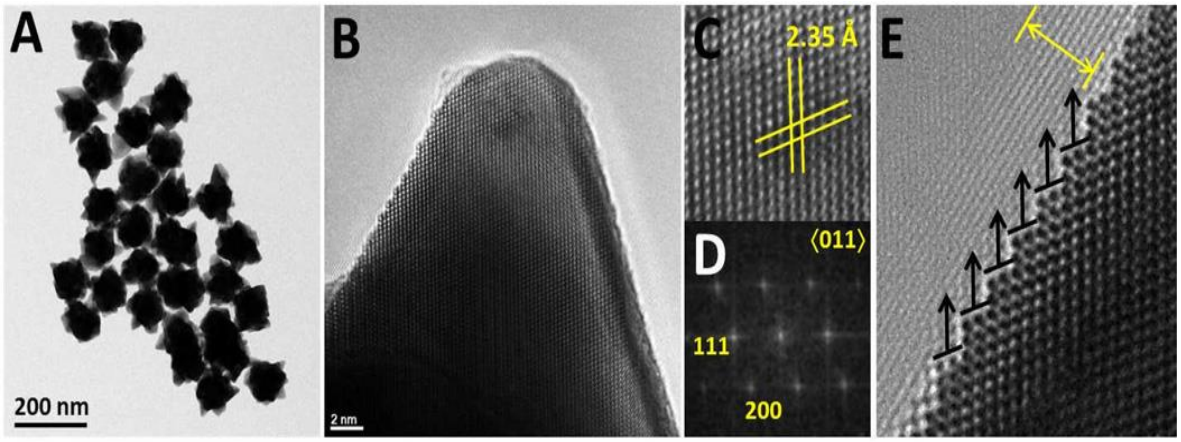

Figure 2: Representative scheme of the Gold nanostars shape. Example: Au nanoparticles are generally recognized as biocompatible materials due to their relatively low reactivity, lacking in most cases adverse and acute cytotoxic effects, making them suitable for nanomedicine applications. **(A)** BF-TEM. **(B)** Detail of atomic structure of a gold nanostar branch. **(C)** Interplanar distance. **(D)** FFT patterns of area selected at **(C)**. **(E)** Detail showing direction of growth on branches and presence of organic coating. Maysinger D, Moquin A, Choi J, Kodiha M, Stochaj U. Gold nanourchins and celastrol reorganize the nucleo- and cytoskeleton of glioblastoma cells. Nanoscale. 2018;10(4):1716-26. [17].

1.2.1.2.1 Core/shell Nanoparticles.

The core-shell nanoparticles are nanomaterials of two or more layers, which lead function as drug carriers and are of great interest for biomedical applications due to their interesting characteristics and optoelectronic properties. The core-shell NPs can incorporate distinctive characteristics depending on the material that constitutes them; they usually have a size smaller than 100 nm and their stability and practicality have made them the preferred drug

delivery NPs. The core-shell platform can also incorporate magnetism, heat generation and Cancer imaging capabilities [21], as well as photodynamic therapy (PDT) capabilities to generate reactive oxygen species in the tumor microenvironment. Its applications range from diagnostic imaging (MRI) to the delivery of siRNA (small interfering RNA) and other molecules of higher complexity [22].

1.2.1.3 Surface area.

The so-called 4th industrial revolution [23, 24] brought by the nanotechnology field (among other technologies such as artificial intelligence), has involved billions of dollars investment [25] due to the number of promises in areas such as the energy sector (green energy and more efficient transistors), the study of artificial photosynthesis [26], in the resolution of ecosystem problems [27], the cosmetics industry [28], aerospace engineering [29] and of course, in nanomedicine [8].

One of the properties of nanomaterials that has attracted most interest to investors and scientists is the ownership of the largest surface area. Because increase in surface area means that a greater proportion of atoms are located on the particle surface relative to the core, NPs are more reactive compared with conventional larger materials [30]. Moreover, the large surface area of NPs also allows them to be designed to include a broad range of surface characteristics, including conjugation with electrostatic charges or biomolecules *(Nano-functionalization)* [31].

For medical purposes, it is convenient that the shape and the increased surface area of the nanomaterials increase the effectiveness of a specific drug (drug delivery), for this reason the materials should not be toxic or at least having low toxicity, they should be biocompatible, soluble (increased surface area is also responsible for the enhanced water solubility and bioavailability) and must have pharmacokinetic and pharmacodynamic characteristics superior to those of conventional medications [32].

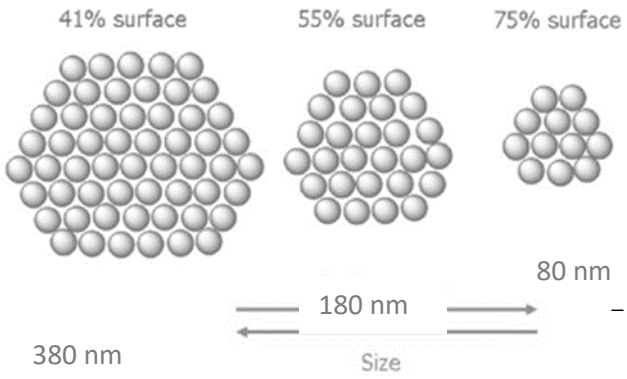

Figure 3: The smaller the scale, the more surface area available for activation. Scheme modified from Gene Lacson 2013

1.2.1.4 Optoelectronics.

One of the most celebrate features related with shape and size is the so called "Surface Plasmon Resonance" (SPR) on which peaks of gold, silver or copper nanostructures can be tuned from the visible to the near infrared region by controlling the shape and size [33]. The plasmon resonance can either radiate light (Mie scattering), a process that finds great utility in optical and imaging fields or to be rapidly converted to heat because surface plasmon oscillation decays by radiating its energy resulting in light scattering or decays non radiatively as a result of conversion of absorbed light to heat [34]. In the presence of the oscillating electromagnetic field of the light, the free electrons of the metal nanoparticle undergo a collective coherent oscillation with respect to the positive metallic lattice. The gold and silver nanoparticles do not oxidize as easily as copper nanoparticles and are therefore ideal for use in diagnostic applications, because this type of nanoparticles have enhancement optical and photothermal properties of noble metal nanoparticles arises from resonant oscillation of their free electrons in the presence of light, also known as localized surface plasmon resonance (LSPR) [35].

The optoelectronic applications are incredible, because nanoparticles can be sent to a tissue of interest, for example, tumor tissue and can detect the tumor at an early clinical stage or analyze the progression of the tumor [36]. Currently, researchers are working on surgical lenses that will allow the surgeon to remove the tumor with greater success, given that the tissues would be dyed with contrast and send a signal in real time to the user's lenses. This

technology is innovative because it would allow fewer cases of Cancer recurrence by removing the margins of the tumor with greater precision.

1.2.1.5 Magnetic properties.

Magnetism is a physical phenomenon resulting from the electric currents and the magnetic moments of the materials, this due to: 1.- The spinning motion of the electrons, 2.- temperature as well, 3.- electro-magnetic source applied and 4.- Pressure [37].

There are 4 types of magnetism based on orientations of the magnetic moments in materials: diamagnetism, para-magnetism, ferromagnetism and anti-ferromagnetism [38]. There is a fifth one type called super-para-magnetism which appears in small ferromagnetic nanoparticles [39].

1.2.1.5.1 Diamagnetism.

Diamagnetic materials oppose the applied magnetic field, so they have a negative susceptibility ($\chi < 0$) which is very weak, compared to para-magnetism or ferromagnetism [40]. Diamagnetism is observed in materials with filled electronic subshells where the magnetic moments are paired and overall cancel each other.

1.2.1.5.2 Para-magnetism.

Materials whose atomic magnetic moments are uncoupled display para-magnetism; thus, paramagnetic materials have moments with no long-range order, and there is a small positive magnetic susceptibility ($\chi \approx 0$).Some studies have added efforts to understand the paramagnetic behavior of biomolecules [41].

1.2.1.5.3 Ferromagnetism.

Ferromagnetic materials have aligned atomic magnetic moments of equal magnitude, and their crystalline structures allow for direct coupling interactions between the moments, which may strongly enhance the flux density (e.g., Fe, Ni, and Co). Furthermore, the aligned moments in ferromagnetic materials can confer a spontaneous magnetization in the absence of an applied magnetic field whereas superparamagnetic NPs will exhibit no

magnetization due to rapid reversal of the magnetic moment *(See figure 4 μf weak vector behave)* [42].

1.2.1.5.4 Anti-ferromagnetism.

It has been reported that antiferromagnetic materials (Cr, Mn, Pd, Bi) show the coexistence of antiferromagnetic and superconducting phases and they have thermal and magnetic superconductivity properties, even when they offer great magnet-resistance, above the Néel temperature, materials exhibit paramagnetic behavior. Therefore, magnetic susceptibility depends on temperature [43]. Moreover they can be useful for applications in nanomedicine, they also could be used in biosensors and the clinical diagnosis of diseases through biomarkers since they are good as spin detectors and magnetic memory storage-devices [37].

1.2.2 Super-para-magnetism: Super-Para-Magnetic Iron Oxide Nanoparticles (SPIONs).

There are several types of magnetism described above, but the effect that interests applications in nanomedicine field is about of ***super-paramagnetic*** features. In the presence of an external magnetic field, iron oxide nanoparticles between 10–20 nm size become magnetized up to their saturation magnetization, and on removal of the magnetic field, they no longer exhibit any residual magnetic interaction. Thus, on application of a magnetic field, these nanoparticles provide a stronger and more rapid magnetic response compared with bulk magnets with negligible remanence (residual magnetization) and coercivity (the field required to bring the magnetism to zero) [44].

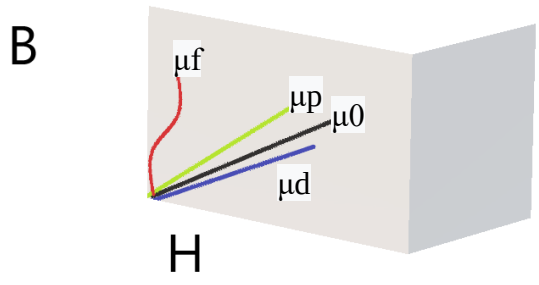

Fig 4: Magnetic permeability (not to scale): B - flux density, H - magnetic field, μf - permeability of ferromagnets (and ferrimagnets), μp - permeability of paramagnets, μ0 - permeability of free space (4*π*10-7 H/m), μd - permeability of diamagnets

In the context of superparamagnetic iron oxide (Fe_3O_4) nanoparticles (SPIONs), the precession moment could be used to generate image through the CAT (Computerized Axial Tomography), MRI (Resonance Magnetic Image) or PET (Positron Emission Tomography), to stronger the magnetic field, to stronger the precession frequency (wobble movement of protons in the presence of a magnetic field) [45].

It is very important to calculate this frequency (the number of times that the protons perform this precession movement.) To calculate this frequency the *Larmor equation* is used, which is expressed as follows [46]:

$$\omega 0O = \gamma B0$$

Where: $\omega 0O$ is the precession frequency (Hz or MHz)

$B0$ represents the external magnetic field (Tesla)

γ is the Gyromagnetic ratio.

For example, the precession frequency for H protons is 42 MHz in a magnetic field of 1 Tesla, it means that protons precession is over 42 million times per second. The vectors of protons that do not cancel each other form a longitudinal magnetic vector, such as those generated in patients when they are studied in an RMI.

The longitudinal magnetization can't be measured directly, a transverse magnetization is needed to measure the magnetic field of the patient.

The RMI works by sending an electromagnetic radio wave, called the RF pulse, the purpose is to disturb the alignment of the protons, this RF pulse must have the same frequency as the protons to exchange energy, this exchange phenomenon is called " Resonance" [47].

1.2.2.1 Permeability, electromagnetism.

It is the phenomenon presented by some materials such as iron, in which the lines of the magnetic field travel more easily through the iron material than through the maire or vacuum. Relative permeability denoted by the symbol:

$\mu r = {}^{\mu}/_{\mu 0}$ Where $\mu 0 = 4\pi\ X\ 10^{-7}$ N·A^{-2} is the (exact) magnetic permeability of free space.

Nanomedicine seeks contrast agents (Cas) to use its superparamagnetic properties SPIONs Fe, Ni, Co, Mn, Zn because of the magnetic flux lines flow more easily unlike air or vacuum, nevertheless, commercial production of FDA-approved SPION-CAs ceased due to unexpectedly severe side effects seeing onto clinical trials [48].

1.2.2.2 Spin-echo sequence.

It consists of two pulses, a 90 ° pulse and a 180 ° pulse, the 90 ° pulse establishes the transversal magnetization but this does not produce a signal or image, a time later (TE2) we send a 180 ° pulse which places protons phased out in phase. After the TE time, we obtain the Echo of spin, so the image parameters that influence the image capture of the MRI are [49]:

TE: the time between the 90 ° pulse, the echo and the TR, TE is responsible for the potentializing of the image in T2.

TR: The time between two pulse sequences (the time between a 90 ° pulse to the next 90 ° pulse), TR is responsible for the image enhancement in T1.

T1: Represents longitudinal relaxation.

T2: Represents the transversal relaxation.

The amount of signal obtained with a Spin-echo sequence to produce an image is TE dependent (the time we wait after the 90 ° pulse). Because of the signal that comes from the patient's tissues, many measurements must be captured to obtain a 1024 x 768-pixel matrix, there is an equation to describe the image acquisition time:

TA= TR X N X Nex Where: TA: Acquisition time N= number of rows in a matrix

Nex: Number of excitations

The atoms have a nucleus constituted of protons and neutrons; an exception is hydrogen (H) since it is only formed by a proton. The H nucleus is the best for capturing images (it

has the strongest signal) in MRI because the human body is full of H, today all diagnostic images are captures of images of H protons [50].

We can only use cores that have 1 spin, the electrical charge in motion is the current that causes the magnetic field of the proton, without spin there is no magnetic field.

The nucleus must have an odd field of neutrons and protons. The odd number ensures that a proton with a magnetic moment is left over and can generate the MRI signal. For example, 13 carbons, 19 fluorine, 23 Sodium, 31 phosphorus.

1.3 Nanomedicine: Imaging.

The magnetic capabilities of the materials like magnetite (Fe_3O_4) provide unprecedented promises and applications for molecular and imaging diagnostics. Because materials used at nanoscale have improved and enhanced properties for biomedical applications [51] it is necessary to bear in mind certain biosafety parameters of already mentioned nanoparticles for using in the human body. *"In Vitro"* preclinical models must be scaled to animal models or lab-on-a-chip and subsequently used in human clinical trials.

Currently, there is no precise legislation on biosafety in nanotechnology, but it has been seen that some of these materials can be metabolized by the human body such as the surfactants that can be used for envelope metals like SPIONs. Thus, a biocompatible cover has the function of improving the anisotropic, steric properties, coulomb repulsions, improving NPs-monodispersity and also preventing phagocytic monocytic system in the human body from recognizing them and phagocytizing them [52]. Moreover, NPs coated with surfactants should be stable in water at physiological pH 7.35-7.45 [53].

These surfactants are numerous, and have been used and described by many researchers, we will thoroughly address the issue of surfactants in *Chapter 3.*

The conventional imaging technology provided by X-rays, Ultrasound, MRI, CT-Scan, PET allows doctors to diagnose by using imaging methods with a properly sensitivity and specificity for each disease, some of these techniques are currently the *Gold-Standard* for the diagnosis of vascular diseases. Latest techniques are indispensable for the clinician-doctor or surgeon in oncology.

To date, diagnostic imaging technology has many disadvantages such as cost, the risk of developing contrast media allergies for example in a PET or MRI, the use of radioisotopes or exposure to radiation that, although it does not present a highly risk, it is considerable risk when chronic exposure take place, so they are latent concerns. Perhaps the biggest problem with conventional techniques can be technological, since sensitivity and specificity are low still.

Sensitivity is the ability of the test to detect the disease in sick subjects and the specificity the ability of the test to detect the absence of the disease in healthy subjects. Although in some diseases the sensitivity and specificity reach 97%, it is true that in diseases such as ovarian Cancer the sensitivity reaches only 70% and the specificity 83% [54] so that the arrival of new technologies for the improvement of conventional ones could increase the improvement in the prognosis of these patients.

Novel technologies have been subjected to experimentation, in nanomedicine for example, the arrival of SPIONs can increase the sensitivity and MRI-specificity. SPIONs can generate T2 image contrast medium, superparamagnetic properties, unlike ferromagnetic tend to be at a zero moment when the external magnetic field stops, this means that the control of nanoparticles is greater and is more stable than the conventional chemical or radio-isotopic contrast medium, having several advantage not only for their high coercivity and magneto-crystalline anisotropy [52] but they can be purified by renal route safely and this leads for a reduction of adverse effects.

Diamonds have also appeared as a solution in this trend of nanomedicine in diagnosis, nano-diamonds (ND) have fluorescence properties that can guide diagnosis of tumors [38]. The NDs are mentioned in detail in *Chapter 2.*

1.3.1 Magnetic Resonance Imaging (MRI).

Magnetic resonance is considered a mapping of H protons [55], the human body is constituted by approximately 75% water, H has a proton and an electron, its precession movement makes it act as a magnet most of the equipment of MRI are 1.5 Tesla, 1 Tesla = 10,000 Gauss, the magnetic field of the earth is 0.5 Gauss.

The magnetic field of the MRI device is obtained from an electric current that flows through cables in the form of handles, at superconducting temperatures so that they can produce a magnetic field, the signals are transmitted to a computer that processes the image. Cables that are at superconducting temperature must be cooled with Helium [56].

Protons have the precession in different orientation normally, however, when we subject the patient to a magnetic field (radiofrequency waves), the precession movements of the hydrogen protons are aligned, converted from longitudinal magnetization (relaxation time T1) to transverse magnetization T2, the magnetic field transfers energy in the same frequency and speed as the protons, a hydrogen proton has a precession movement of 64 million times per second in a magneto of 1.5 Tesla, calculated with hydrogen's gyromagnetic ratio of 42.6 MHz [56].

Transverse magnetization releases energy and it is capable of being measured to produce the image. Each tissue, depending on the amount of Hydrogen will have a different magnetization, the T1 (relaxation time) is different in each tissue.

The image in T1 depends on the repetition times, each time the RF pulses are sent (radio frequencies) first a RF pulse of 90 ° is sent, then an echo time or transverse relaxation time (TE) is needed after a RF pulse of 180 °, to obtain images in T1 a brief time is needed, the image in T1 shows liquids with hypointense image, the soft tissues are hyperintense. Therefore, the production of the image in MRI depends on the RF pulse, the tissue relaxation time, T1, T2, the number of protons in the tissues and whether contrast medium is added, for example Gadolinium GTP [57]. The images in T2 shows hyperintense liquids, hypointense soft tissues. The SPIONs are capable of being magnetized and used in MRI to direct the Nps to their therapeutic objective and to produce images T2 * [58].

1.3.2 Computed Tomography Scan (CT-Scan).

Since Wilhelm Röntgen discovered X-rays in 1895, conventional radiography has advanced significantly in the diagnosis of diseases [59]. Conventional radiography is still the gold standard for diagnosis in small bowel pathology in hospitals, due to its inexpensive cost, however, MRI and Computed Tomography scan (CT-Scan) also have good sensitivity and specificity for inflammatory pathology in acute inflammatory abdominal syndrome, having

the advantage that it does not use ionizing radiation and can be used to diagnose other pathologies such as Cancer, cerebral vascular events among others [60]. The main disadvantage continues being the higher radiation. CT-Scan is used since 1970, it uses computer-processed combinations of many X-ray measurements taken from different angles to produce cross-sectional tomographic images of the body. Other terms include computed axial tomography (CAT scan) and computer aided tomography which can generate 3-D and 4-D models [61], this is especially useful in disciplines as obstetrics, neurology, nephrology and cardiology.

CT scan has been shown to decrease hospital admissions and has reduced the need for emergency surgery by 13%, its chemical applications ranging from CT angiography to thorax and head CT [62]. At the present day, there are studies in murine models that evaluate the potential use of nanoparticles (nano-CT) to create images in lung tissue with an improved spatial resolution [63].

1.3.3 Positron Emission Tomography (PET).

PET can often distinguish between benign and malignant lesions unlike computed tomography (CT) or magnetic resonance imaging (MRI), its use in oncology is essential and to get the mapping of the body it uses markers such as sugars glucose, ^{18}F-2-fluoro-2-deoxy-D-glucose (FDG) [64], amino acids, nucleic acids, receptor-binding ligands water and molecular oxygen, with positron-emitting radionuclides, then these positron-emitting tracers undergo radioactive decay, their positions can be detected by the PET scanner [65]**.** Recently, nanotechnology began to be associated with PET studies to improve the diagnosis of Cancer, applications for PET-nanotechnology means enhancing security, sensibility, specificity and spatial visualization or Cancer in real time [66].

1.3.4 Hyperthermia.

The improved tunable magnetic capacities of iron oxides (super-para-magnetism) not only help the creation of images in real time by means of RMI, they also can generate heat through vibration and excitation generated by magnetic fields or microwaves [67]. Hyperthermia is the process of heating in the range of 41-50°C. Hence, these temperatures may be using to generate apoptosis in malignant cells, specifically solid tumors [68]. The

ability of NPs to diagnose and provide treatment at the same time is known as *Theranostics*. Concept that is widely described within the next chapter.

1.4 Characterization: Generalities.

SEM: Scanning Electron Microscope.

Within the optical characterization techniques of the nanoparticles, the *Scanning Electron Microscope* (SEM) occupies an essential place when evaluating the size and shape of the nanoparticles afterwards synthesis because unlike *Transmission Electron Microscope* (TEM), SEM can examine relatively thick species with better spatial resolution. The SEM was developed in 1951 after the second world war and is currently a tool used in the investigation of materials, energy industry, forensic laboratories among many other applications, since it provides a resolution between 1 and 10 nm, not as good as TEM but a superior conventional light-optical microscope [69].

It works by the interaction of an electron beam typically in the order of 0.2-30 kV and 10 nm diameter with atoms at various depths within the sample. The electron source can be LaB6 (lanthanum hexaboride) or a tungsten filament, the beam passes through deflector plates which forming raster-scan signals which deflect the beam in the "*X* and "*Y"* axes into a display device as TV-type-cathode-ray tube (CRT) on which SEM image appears. In a modern SEM, the scan signals are generated digitally, thereby modern SEM has the advantage that the computer can adjust the intensity of the image in each pixel and save the data in the magnetic disk of a computer [70]. The interaction of the electron beam and the sample results in the reflection of high-energy electrons by elastic dispersion, emission of secondary electrons by inelastic scattering and emission of electromagnetic radiation, each of which can be detected by specialized detectors.

The most used are the secondary electrons *SE* (atomic electrons ejected from the specimen because of inelastic scattering) and the backscattered electrons (incident electrons elastically scattered through more than 90 degrees). SEM based on secondary electrons was developed at RCA laboratories in New Jersey, the principle is based on conservation of energy, lost energy of the primary electrons will appear as gain in the energy of the atomic

electrons that are responsible for the inelastic scattering, these secondary electrons escape from the solid materials (according to the kinetic energy) towards the vacuum, which generate the signal SE in SEM [69]. Moreover, deflection angles greater than 90° lead to the dispersion of elastic and inelastic electrons, the former are created by the electrostatic interaction with the atomic nuclei and the inelastic ones by the interaction with atomic electrons, the high kinetic energy carries the backscattered electrons to abandon the sample and re-enter the vacuum where by means of a special detector they are susceptible to being measured as a signal of backscattered-electron (BSE). SEM allows to see living specimen as virus and bacteria [71].

It is possible to extend the capabilities of these microscopes using various detectors, such as "Robinson detector", Solid-state detector, or even SEM modalities such as Specimen-current image, *Electron-Beam Induced Conductivity* (EBIC) [72]. For practical purposes they are not mentioned in this work, since they were not used.

1.4.1 TEM: Transmission Electron Microscope.

Whereas SEM is scanned horizontally across the specimen in two perpendicular directions "X & Y", TEM uses a stationary incident beam which allows electrons to penetrate a thin specimen and then create an image, since electrons behave as negative particles and are deflected by magnetic fields which may be visualized through CRT. Modern TEMs use a voltage between 100 kV and 300 kV and display magnification in the range 10^3 to 10^6. The system is convenient for analyzing crystalline specimen and its resolution is in the order of 0.2 nm [73].

The device is composed of an electron gun with condensing lenses that produces a beam of electrons with high kinetic energy, the source of electrons is usually a filament made of tungsten (W) wire that is heated to 2700 K, this process is called thermo-ionic emission. TEM also has another component called specimen stage and an imaging system composed of three lenses that magnify the image or produce a diffraction pattern by means of a fluorescent screen, a photographic film or on the monitor [73].

The thermo-ionic emission of electrons could be increased using an electrostatic field, this reduces the potential sweep by keeping the electrons inside the cathode, for this purpose it

is known as *Schottky effect* [74]. Unfortunately, one of the disadvantages of TEM is that it uses electrons at high energies (ionizing radiation like X-rays and gamma rays), so it is almost impossible to study living tissue; however, for that purpose researchers can use *Scanning Helium Ion Microscope* [75].

Also, it is possible to measure other electrons which are coming from the opposite side of the specimen employing a fine-probe/scanning technique called *Scanning-Transmission Electron Microscope* (STEM) [76], now it is common to find the dual mode TEM/STEM integrated in new equipment and line scanning shows the distribution of elements within the sample.

1.4.2 HR-TEM: High Resolution Transmission Electron Microscopy.

Another useful technique for studying atomic properties of materials is *High Resolution Transmission Electron Microscope* (HR-TEM). This consists of a specialized modality of TEM that works by contrast phase image produced by electronic wave interference. The electron wave phase hides information that can be measured if defocus is provided. Basically, there are several defocuses like *Gaussian, Scherzer, Gabor and Lichte* we won't discuss in here, but they remarkably allow unique capacities for microscope techniques [77].

1.4.3 EDS: Energy-Dispersive X-ray Spectroscopy.

An electron from an outer, higher-energy shell substitute an electron from an inner, low-energy shell which was displaced because of the energy of an incident beam, so then difference in energy between the higher-energy shell and the lower energy shell may be released in the form of an X-ray. *EDS (Energy-disperse X-ray Spectroscopy)* is an analytical technique used for characterization, basic principle is that each element has a unique atomic structure allowing a unique set of peaks on its electromagnetic emission spectrum [78].

1.4.4 UV-Visible Spectroscopy.

Since Beer's law was discovered by Pierre Bouguer in 1729, Johann Heinrich Lambert in 1760 and August Beer in 1852, it is known empirically that there is an exponential relation between the transmission of light through a substance and the concentration of the substance, as well as between the transmission and the length of the body that the light goes through [79].

UV visible spectroscopy uses electromagnetic radiation from the visible, near ultraviolet (UV) and near infrared (NIR) regions of the electromagnetic spectrum. It works by emitting photons at a wavelength between 160 nm and 780 nm. The UV radiation absorbed by the molecules of the specimens in this region of the spectrum causes electronic transitions (π-π *, n-π *, σ-σ *, and n-σ *) that are susceptible to being quantified, in other words, the signal depends on the absorbance (A) because UV-Vis detects wavelengths where absorption takes place, and then it quantifies that absorption.

Most applications of UV-Visible spectroscopy are based on transitions that occur in π-π * (Far 10-200 nm and near UV-region 200-400 nm) and n-π * (Uv-visible region spectrum 400 to 800 nm). Applications for UV-visible spectroscopy are often used to identify content of substances and some functional groups of molecules in Cancer research [80]. Hence, if it is intended that the core-shell or nanocomposites design of the nanoparticles can transport drugs or ligands, it is necessary to study the functional groups of the transition metals that make up the nanoparticles. More details regarding the results of this work are provided within *chapter 3 "Nano-engineering"*.

1.4.5 XRD: X-Ray Diffraction

In 1915 William Henry Bragg and William Lawrence Bragg received the Nobel Prize in Physics for their work in the identification of diamond crystals, ZnS and NaCl.

Thanks to the so-called *Bragg's Law*, scientists can study and predict the angles at which X-rays are diffracted by a crystalline material (minerals or inorganic compounds) [81]. Bragg diffraction occurs when monochromatic radiation is specular dispersed by the atoms of a crystalline system and undergoes constructive interference. In solid crystals, the radiation is

scattered by the atoms and is separated by an interplanar distance called *d*. The path difference between two waves that experience interference is given by $2dsin\theta$, where θ is the scattering angle. Bragg's law describes the condition in θ for constructive interference to be stronger [82]:

$2dsin\theta = n\lambda$ *Where: n* is a positive integer and λ is the wavelength of the incident wave.

This law relates the wavelength of the electromagnetic radiation with the diffraction angle and the reticular spacing in a crystalline sample.

The diffracted X-rays are detected and analyzed in a modern XRD equipment composed of three elements: An X-ray tube, a sample holder, and an X-ray detector. Subsequently, the sample is scanned through a range of $2\ \theta$ *angles*, all possible diffraction directions must be reached due to the random orientation of the powder material. The conversion of the diffraction peaks to d-spacings allows the identification of the mineral because each mineral has a set of unique *D-spacings*. Then, the technician or user compares the *D-spacings* with standards for certain materials [83].

The importance of XRD quantitative analysis in iron oxide and gold nanoparticles lies in characterizing the specific peaks of super-paramagnetic magnetite Fe_3O_4; the characterization is important since contamination with other materials or maghemite Fe_2O_3 formation is never desired for specific applications.

1.4.6 Raman Spectroscopy.

Sir Chandrasekhara Venkata Raman was an Indian physicist who won the Physics Nobel Prize in 1930. He discovered that a small amount of light changed in frequency while observing the effect in organic liquids by means of sunlight, he would lay the foundations for the discovery of the Raman spectrum [84].

Because Raman scattering is too weak, the main difficulty of Raman spectroscopy is to separate the weak light dispersed inelastically from the intense scattered Rayleigh laser light so then, modern Raman spectroscopy devices have edge filters for laser rejection.

A Raman microscope is formed by a standard optical microscope, with the addition of an excitation laser, a monochromator, and a sensitive detector to observe frequencies of

plasmons, magnons, and superconducting gap excitations. A Raman microscope device is frequently used for the characterization of materials like metals, minerals, crystals, polymers, chemical bonding, and ceramics, and it also has many other applications in nanotechnology and medicine because it can study enzymes, cells, and proteins [85].

There are advanced types of Raman spectroscopy include Transmission Raman, Tip-enhanced Raman spectroscopy (TERS), surface-enhanced Raman (SERS), Resonance Raman spectroscopy, Surface-enhanced resonance Raman spectroscopy (SERRS) [86], Hyper Raman, Stimulated Raman spectroscopy (SRS) [87], Surface plasmon polariton enhanced Raman scattering (SPPERS) among others. The purpose of the Raman variants is to improve the optical resolution or to offer greater sensitivity depending on the desired application (medicine, biology, geology, forensics) and the materials that are intended to be studied.

1.4.7 FTIR: Fourier-transform infrared spectroscopy.

The Fourier transform (FT) decomposes a signal, a time function, into the frequencies that compose it, it is the frequency domain representation as to the mathematical operation that associates the frequency domain representation to a time function. Fourier-transform infrared spectroscopy (FTIR) is based on this complex mathematical algorithm where spectrum data are collected over a wide spectral range using a broadband beam containing many frequencies of light and measures how much of that beam is absorbed by the specie [88]. Then, the beam gets a different combination of frequencies, giving a second data point going through a Michelson interferometer. The process needs to be repeated many times and finally, computer takes raw data collected (interferogram) and find out what the absorption is at each wavelength.

FTIR spectrometers are mostly used for measurements in the mid 2−25 μm (5000–400 cm−1) and near IR 1−2.5 μm (10000–4000 cm−1) regions. It allows to reach 0.001 cm-1 resolution, its applications go from medicine, biology, geology, to materials research and Nanotechnology characterization because allows study small quantities (nano-FTIR) [89]. FTIR is useful to confirm successful functionalization of the nanoparticles surface [90].

1.4.8 SQUID: Superconducting Quantum Interference Device.

Superparamagnetic iron oxide nanoparticles (SPIONs) do not contain any residual para-magnetism after removal of the external magnetic field [90] so they are attractive for medical applications, given the effective control that can be had on their magnetic properties, especially for the generation of heat and for their tracking in a living system by means of magnetic resonance imaging.

The superconducting quantum interference device (SQUID) is used to measure extremely small magnetic fields (5×10^{-18} T). There are two types of SQUID: DC invented in 1964 and RF invented in 1965. The RF SQUID only have one Josephson's junction, while the DC SQUID have two or more. The so-called Josephson junctions occurs when two superconductors separated by a thin insulating layer can experience tunneling of Cooper pairs of electrons (they act as a Bosons) through the junction [91]. Josephson junctions are used in SQUID devices for the detection of minute magnetic fields, the basic principle is the quantization of magnetic flux.

The applications range from measurement of magnetic nanoparticles [92] and gravitational wave measurements to magnetic measurements as tiny as those of the heart and brain of living beings, in fact, this latter application is highly used in neurosciences. Currently, modern SQUID devices are used to create super quantum computers that work at subzero temperatures [93].

1.4.9 IR (Infra-red).

IR (Infra-red) radiation is electromagnetic radiation with wavelengths between 760 nm and 100,000 nm [94]. In this work, IR was used to determine the chemical functional groups that made up the nanoparticles in order to analyze the possibility of functionalizing them.

1.5 Synthesis of Nanoparticles (NPs).

Currently, there are several ways for synthesizing magnetite nanoparticles to obtain the desired size and shape depending on the biomedical interests that are to be executed. Some of the procedures are physical and chemical [95], involving methods like *co-precipitation, microemulsion, thermal decomposition, solvothermal, sonochemical, microwave assisted,*

chemical vapor deposition, microfluidics, nanofluidics, combustion synthesis, carbon arc, laser pyrolysis synthesis, etc. The thermal decomposition and hydrothermal methods are good candidates for obtaining appropriate super-paramagnetic nanoparticles [52]. The thermal decomposition process is described in greater detail in *Chapter 3*; thus, this synthesis method was used for the synthesis of NPs in this work.

1.6 Nano-functionalization.

The NPs can be functionalized to reach the desired destination for example molecular targets or markers in tumors in Cancer or in any other disease, this provides greater specificity to carry and deliver a cytotoxic drug and thus not affect the healthy cells of the organism.

The functionalization requires a complete mastery of the synthesis technique, the technique of nano synthesis depends on the application and design or engineering of the nanoparticle that is required. For example, whether application is to build a fuel cell, nanomaterials and designs will be different from the designs of NPs engineered for medical application [96]. In the case of materials in nanomedicine, it is appropriate not to use toxic or radioactive materials, materials friendly with biological systems should be used, and it is imperative to know about physiology and medicine, as well as multiple disciplines such as physics, chemistry, molecular biology, omics, pharmacology, etc.

1.6.1 Nanoengineering and Nanomedicine.

In the field of nanomedicine, materials must be safe for metabolic processes and must be materials that conform a dynamic design capable of traveling through fluids such as blood, overcoming the problem of viscosity, protein crown (governed by Van der Waals forces, and steric repulsive interactions), transport into the plasmatic cell membrane and cytosol and evasion of the monocyte system phagocytic or reticuloendothelial, must therefore have a certain "intelligence" [97]. Moreover, the laminar or turbulent flow expressed in the number of Reynolds that also corresponds to the geometry of the nanoparticles, the smaller the NPs, the easier to overcome the flow resistance, the blood viscosity, and the better the response to avoid to the macrophages. For now, there is no such thing as nanorobots, but someday they may be perfectly possible.

Several studies point to successful methods to functionalize nanoparticles, this is achieved by incorporating amine or carboxylic bonds as double-sided bridges or bonds that fix a carboxyl bond of the drug or the molecule to be loaded with polymer surface of the nanoparticle, this the way through nanoparticles can carry drugs or antibodies [98]. In another design, the nanoparticles can contain the drugs engineered as nanocages, nano-matryoshkas or containers which transport the substance to be delivered. To improve the electrostatic attraction of the polymers to the materials-base of the nanoparticles, it is convenient to carry out studies of *Zeta potential Analysis* described in *Chapter 3* [99].

The release method can occur within the cytoplasm by modifications in the PH that degrades the shell containing the drug; other methods of release are excitation by temperature, magnetization, microwave signals and *LASER'S* (light amplification by stimulated emission of radiation) that stimulate the nanoparticles to release the drug [100]. The nanoengineering techniques at functionalized details (High-performance liquid chromatography-HPLC, IR, TGA, UV-Spec.) are described in *Chapter 4.*

What is your preference?

… *"Primum succurrere* **or *Primum non nocere*"**

-Dr. Mauricio A. Medina-Pérez M.D.

CHAPTER 2

2. The War on Cancer: Motivation for Cancer research.

The word Cancer came from a Greek concept *"karkinos"* to describe carcinoma tumors described by Hippocrates (460–370 B.C), although Cancer had already been documented since ancient Egypt in 1600 B.C [101]. Cancer is a group of diseases in which cells behave under uncontrolled proliferation leading to the invasion towards other organs and tissues [102]. Cancer can occur in almost all the body, its multifactorial origin depends on genetic mutations, oncogenes [101], hypoxia states, environmental contamination, radiation exposures of any kind (UV, X ray, gamma rays) [103], exposure to certain products

(agrochemicals, cosmetics, industrial products), exposures to certain viruses [101], the type of food, stress, smoking [104] [105] and an idiopathic percentage (roughly 15-20%) whose origin is unknown. Moreover, intercellular communication plays an important role in Cancer initiation and progression through secretory molecules, including growth factors and cytokines [106]. In this group of diseases, the abnormal cells become immortal, they evade all the signals that indicate them apoptosis and the old cells join to young cells that never specialize, later they continue dividing until they form tumors [102].

It is estimated that by 2020, more than 15 million people in the world will suffer some type of Cancer (WHO) and is expected to rise to 26 million new Cancer cases by 2030 [107].

There have been too many efforts to face this range of extremely complex diseases called "Cancer", since 1971 when in that infamous episode president Nixon (1969-1974 U.S president) declared war on Cancer and 40 years later there is no cure still. So far there are more questions and the results are not encouraging, the new generation of scientists studies the tumor microenvironment emulating using sophisticated software and predictive mathematical models, using Nanoelectromechanical-systems (NEMS) or Micro electromechanical-systems (MEMS) for a better understanding of Cancer complexity behavior [108], because the truth is that Cancer becomes resistant to therapeutic drugs, and acts under an adaptive behavior without parallel, as any micro-organism that is in danger and needs to adapt to survive, Cancer mutates rapidly, even worst Cancer is able to use all the resources of the body kidnaping the cell signal machinery, in other words, Cancer has unlimited resources of the body, unfortunately that includes immune response and consequently lead to death.

This ability to survive has led researchers to build a theory about asexual species, that is, malignant cells are doomed to extinction unless they have a stabilization mechanism for their karyotypes to escape the *muller ratchet* (accumulation of spontaneous mutations) getting in this process a sort of speciation which leads to immortality:

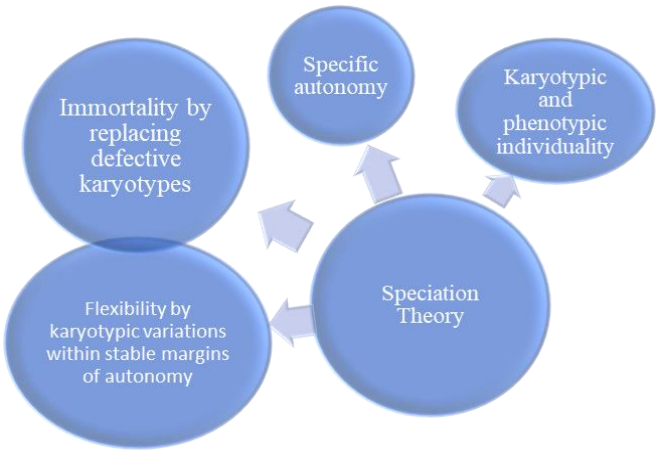

Figure 5: Speciation theory. Duesberg P, Mandrioli D, McCormack A, Nicholson JM. Is carcinogenesis a form of speciation? Cell cycle. 2011;10(13):2100-14. [109]

Cancer is a pathology of diseases where proliferation and cell immortality occur, and this clonal population of malignant cells can expand to several tissues and organs into the human body [110]. The causes that produce it are not apparent yet, but it can be multifactorial viz., diet [111], expression of oncogenes [112], exposure to certain chemical substances [113] or ionizing radiation [114], etc.

2.1 Statistics on Cancer.

As per the World Health Organization (WHO), breast Cancer (BC) causes most massive of women in the age group of 20–59 years worldwide (World Health statistics 2013). According to the global Cancer project (GLOBOCAN 2018) breast Cancer is the second most common Cancer in the world, one million cases of breast Cancer are diagnosed annually worldwide [115]. Breast Cancer is considered as the most common Cancer in less developed and industrialized countries, and is the second cause of death in Europe and United States after lung Cancer [115, 116]. **Fig 6:** Estimated age-standardized incidence rates (World) in 2018, breast, females, all ages.

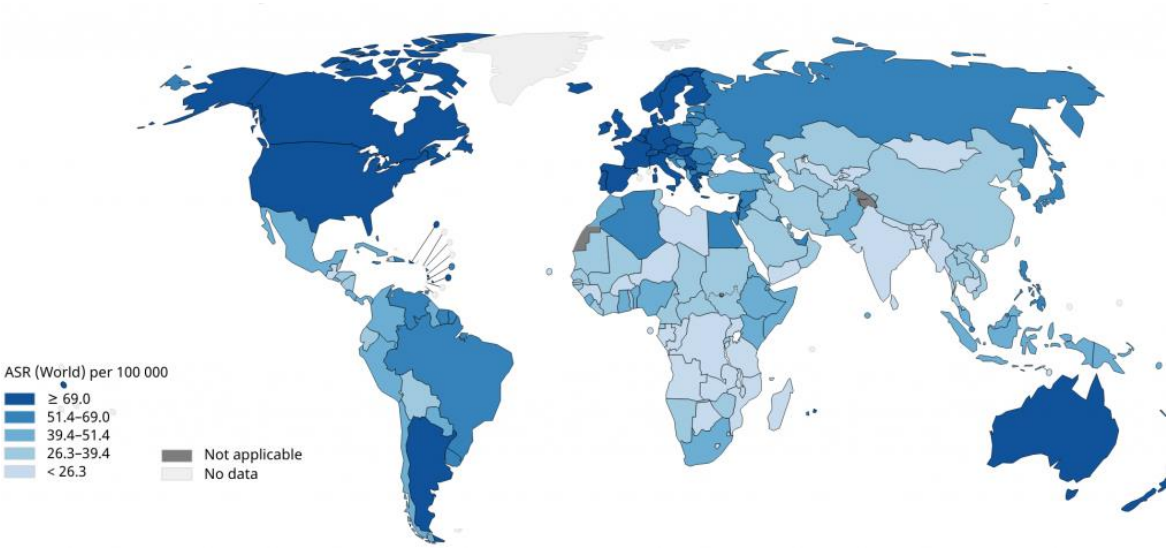

2.2 Breast Cancer: Conventional clinical approach

In everyday clinical practice breast Cancer diagnosis relies on three main types of analyses: A) clinical examination; B) radiological/image exams (mammography, ultrasonography, magnetic resonance imaging, etc.) and C) pathological tests (biopsies) [117]. Gathering all the previous information, the clinical oncologist can stage the disease using TNM classification [118] and reviewing the guidelines established in rigorous clinical trials, although, they can also use genetic profiling tests such as MammaPrint [119] and Oncotype DX [120] to understand disease prognosis better.

However, two decades ago, before the arrival of the current therapeutic, something was still missing, a stronger diagnostic tool was needed. New advances in personalized medicine emerged the technology of micro-arrangements and the discovery of molecular profiles.

There are different histological subtypes of Cancer within the same organ, but biopsies are heterogeneous because they include diverse types of cells. This heterogeneity includes breast Cancer, which also has tried to classify the various kinds of invasive carcinoma, yet the clinical importance of its classification is limited because different patients diagnosed with breast Cancer may have tumors with different molecular profiles.

Breast Cancer includes molecular biomarkers [121] which are as follows:

1.-ERα+ (Estrogen receptor a-positive)

2.-PR+ (progesterone receptor-positive)

3.- HER-2 (Human epidermal growth factor receptor-2)

4.-EGFR(epidermal growth factor receptor) 45%–70% of Triple Negative Breast Cancer (TNBC) patients show this biomarker [122],

5.- CK5/6,

6.- VEGF (vascular endothelial growth factor),

7.-KI67, etc.

Currently, thanks to microarray technology, there has been a better understanding of the molecular heterogeneity in tumors [123], because this technology allows the quantification of the expression of thousands of genes.

The classification of breast cancer cell types is considered as below:

(1) Luminal A subtype, ERα+/PR+ or −/HER-2-;
(2) Luminal B subtype, ER+/PR+/HER-2+;
(3) HER-2 enriched subtype ER- and or/PR−/HER-2+;
(4) Basal-like subtype ER^- and/or PR^-, $HER2^-$, CK5/6+, CK14+, CK17+ and EGFR+;

Normal breast-like type (ER− and/or PR^-, $HER2^-$, $CK5/6^-$, $CK14^-$, $CK17^-$, $EGFR^-$) [124] [125] [126].

2.2.1 Triple Negative Breast Cancer (TNBC).

TNBC phenotype lack ER, PR, HER2 although retain EGFR and CK5/6, but recently, researchers are mentioning there is another phenotype called “5 negative” which is deficient of all five markers [127].

Novel molecular classifications are essential to provide personalized medicine and thus helps in selecting more specific drug according to the molecular profile of the tumor. Jézequel et al. found four stable TNBC subtypes:

1.- Luminal Androgen Receptor-AR (LAR)

2.- Mesenchymal (MES)

3.- Basal-Like Immune-Suppressed (BLIS)

4.- Basal-Like Immune-Activated (BLIA).

Their results suggest that prognosis is worst for BLIS tumors and best for BLIA [128] [129]. Moreover, Lehman researchers described six subtypes of TNBC, which includes, [130] basal-like viz., BL1 and BL2, a mesenchymal (M), mesenchymal stem-like (MSL), an immunomodulatory (IM), as well as a luminal androgen receptor (LAR) subtype.

The different TNBC subtypes correlate well with the different chemotherapeutic responses as per retrospective studies. [131].

2.3 Signaling pathways involved in TNBC therapeutics.

2.3.1 Notch signaling pathway.

Thomas Hunt Morgan described in 1917 a family of transmembrane ligands and receptors called Notch [132]. This signaling pathway has a pertinent role in cell proliferation as well as differentiation and, the elevated expression of a group of signaling molecules belonging to this pathway is correlated with the poorest outcome of patients [133]. There are four Notch receptors (Notch-1,2,3 and 4); and five known ligands (Delta-like 1, Delta-like 3, Delta-like 4, Jagged-1, and Jagged-2). Researchers found out high expression of Delta 1 and Jagged 1 in breast cancer [125] [134] [135]. Notch 1 is also involved in human mammary tumorigenesis as a downstream effector of oncogenic Ras [136]. To date, it also has been figured out on the participation of the Notch channel in different types of hematological malignancies [137], pancreatic cancer [138] and many others.

Many studies suggest that Notch-3 and Notch-4 are related to survival and proliferation of tumors, in contrast overexpression of Notch-2 in the context of TNBC MDA-MB-231 cell line appears to act as a protective factor [139]. Since Notch receptor and ligand overexpression is linked with TNBC, researchers believe that the receptor can be targeted by a monoclonal antibody (mAb) [140]. The current studies about inhibition of Notch-1 signaling by mAbs have shown effectiveness in reducing the expression of HES family,

and HEY-L in the breast Cancer cell line MDA-MB-231, thus showing decrease in cell proliferation and increasement in the induction of apoptosis [141]. Additionally, the DLL4 (Delta-like ligand 4 Notch ligand) mAb therapy has shown effectiveness for the treatment of TNBC [142]. Notch signaling in many transcription factors codifies genes related to tumorigenesis, for example HES family, HEY family, Akt, p53, VEGF and PI3K-AKT-mTOR among others [143] [138] [144]. Medications that interrupt Notch signaling pathway act at the level of the second proteolytic cleavage in the cell cytoplasm by blocking the multimeric γ-secretase complex and hence these drugs are known as γ-secretase inhibitors (GSIs) [144]. Unfortunately, most of the drugs that act by blocking the Notch pathway have not met expectations required for approval by the FDA (Federal Drug Administration) presumably because of side effects.

Activation of the Notch receptor **(Figure 7)** occurs following binding of membrane-bound Delta or Jagged ligands during cell-to-cell contact. Following absorption and proteolysis of the heterodimer Notch receptor (by ADAM and γ-secretase complex), a soluble fragment—the NICD—is released into the cytoplasm. The NICD translocates to the nucleus where it serves as a transcriptional activator of Notch-associated target genes, including *HES*, *Myc* and *p21*. Potential therapeutic inhibitors of Notch signaling target events such as γ-secretase complex proteolysis and transcriptional activation. Abbreviations: ADAM, A disintegrin and metalloproteinase; CSL, CBF1/Su(H)/Lag-1; DLL, delta-like ligand; HAT, histone acetyltransferase; MAML1, Mastermind-like 1; mAbs, monoclonal antibodies; NICD, Notch intracellular domain; SKIP, ski-interacting protein; TACE, TNF-α-converting enzyme.

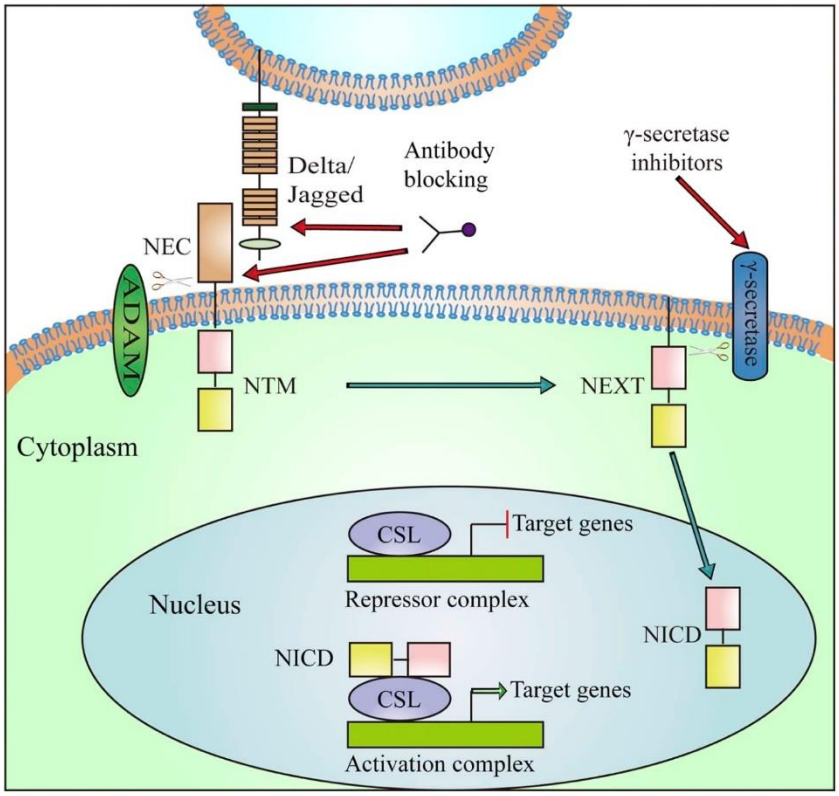

Fig. 7. Diagram of Notch receptor activation and therapeutic target in clinical development. Notch signaling is initiated by ligand binding to Notch receptor, which undergoes a two-step proteolytic cleavage by ADAM family proteases and γ-secretase, releasing the Notch intracellular domain (NICD). The NICD translocates to the nucleus where it binds to CSL and converts the complex from a repressor to an activator of Notch target genes. Notch signaling could be inhibited by two major classes of Notch inhibitors: γ-secretase inhibitors and monoclonal antibodies directing against Notch receptors or ligands. Abbreviations: NEC, Notch extracellular subunit; NTM, Notch transmembrane fragment; NEXT, Notch extracellular truncated; CSL, C protein binding factor 1/Suppressor of Hairless/Lag-1; NICD, Notch Intracellular Domain. Reproduced with permission from Yuan X, Wu H, Xu H, Xiong H, Chu Q, Yu S. Notch signaling: An emerging therapeutic target for cancer treatment. Cancer Letters. 2015, 369, 20–27 [145].

2.3.2 Hedgehog signaling pathway.

Sonic Hedgehog (Shh) [146] network morpho-genes have their impact on Cancer stem cell (CSC) maintenance, polydactyly syndromes, basal cell carcinoma (Gorlin Syndrome) and recent studies suggest that they are altered in clinical samples of several human cancers including breast cancer cell lines [147, 148]. Hedgehog signaling involves three ligands:

a) Sonic (SHH) highly expressed during embryogenesis,

b) Indian (IHH) [149] mostly expressed in hematopoietic cells, endochondral skeleton, and cartilage,

c) Desert (DHH) [150] exhibit expression in the peripheral nervous system and testes, in fact, mutations of the DHH gene could lead to pure gonadal dysgenesis (PGD) [151]

The Hedgehog signaling pathway is involved in cancer cell invasion, metastasis, drug resistance and tumor recurrence cancer therapy [152]. The Kaplan Meier survival studies indicate that overexpression of Shh is responsible for poor prediction of mortality in the case of breast Cancer patients and especially, TNBC patients. (43)

SHH has an important role in the erroneus origin of malignancy in breast Cancer because it maintains abnormal proliferation and promotes invasion to other tissues (metastasis)., Researchers have designed novel experimental drugs viz., Thiostrepton, whose pharmacological action consists of targeting the sonic Hedgehog signaling **(Figure 8)**, Thiostrepton suppresses the population of CD44 + / CD24-Cancer stem cells (CSCs) of TNBC cell lines [153]. Nevertheless, it is necessary to clarify the role of Hedgehog pathway in breast CSCs [154] since it has not been determined yet [155, 156]. As a result, there are few drugs authorized by the FDA to date to address this pathway such as Vismodegib, which is used in basal cell carcinomas [157]. However, more research is needed for SHH signaling potentially leading to the design of new prevention tools and novel molecular markers for evaluation of recurrence, survival, and prognosis.

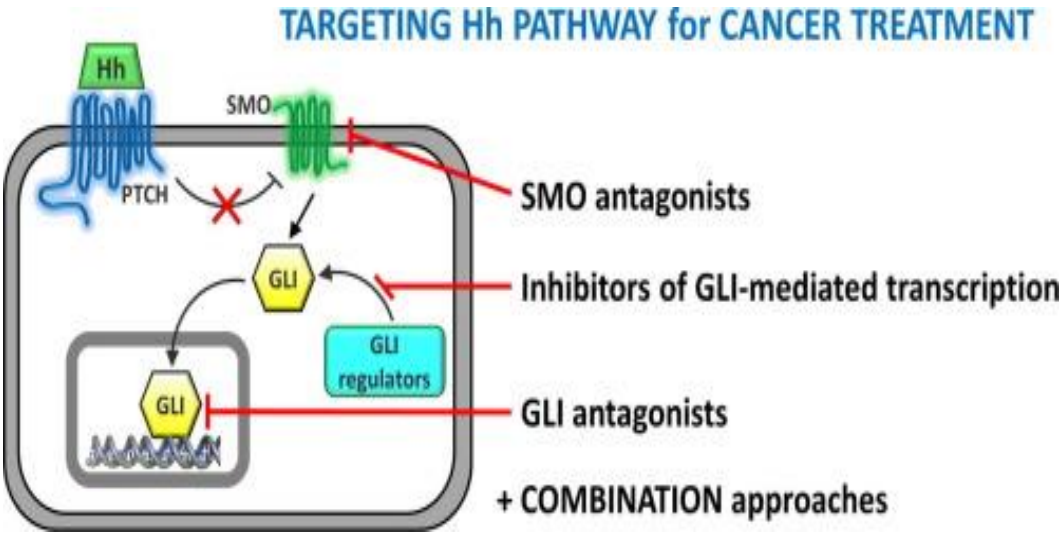

Figure 8. Current trends in Hedgehog signaling pathway inhibition by small molecules, Reproduced with permission from [158] Francesca Ghirga MM, Paola Infante. Current trends in Hedgehog signaling pathway inhibition by small molecules. Bio-organic & Medicinal Chemistry Letters. 2018; Volume 28, (Issue 19):3131-40.

2.3.3 Wnt/ β -Catenin pathway.

Wnt / β-catenin is the most commonly overexpressed pathway (49) leading to transcriptional factor activation responsible for the stimulation of epithelial cells to mesenchymal cells (EMT) transitions in CSCs (50). Wnt signaling **(Figure 9)** is also dysregulated in both canonical and non-canonical molecules on TNBC [159]. To the best of our knowledge, there are 19 human Wnts and 10 Frizzled (FZD) receptors and coreceptors [160]. Wnt ligands (WNT5A, WNT11, and WNT3A) are pertinent in promoting migration and invasion [161]. FZD6 receptor is the most important representative in TNBC due to its capacity to produce metastasis through increasing the motility characteristics of the malignant cells in TNBC [162]. Some novel drugs target Frizzled receptors, for example, OMP-18R5 an antibody targeting Frizzled receptors diminishes proliferation of tumor cells in the lung, breast, colon, and pancreatic tumors [160]. Additionally, overexpression and accumulation of β-catenin protein stimulates cell migration consequently leading to resistance in TNBC cells [159].

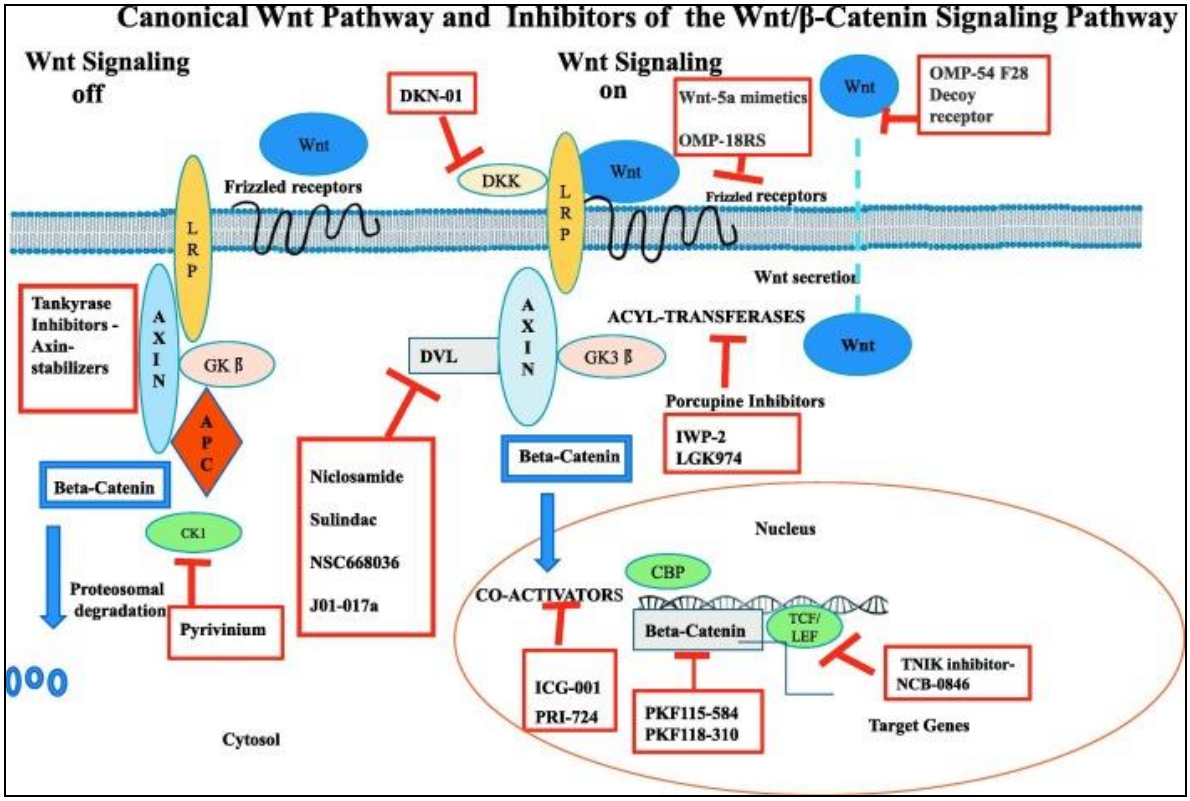

Fig. 9 WNT signaling, Canonical Wnt Pathway and Inhibitors of the Wnt/beta-Catenin Signaling Pathway schematic representation of the Canonical Wnt Pathway and pharmacologic inhibitors of the Wnt/beta-catenin signaling pathway. Reproduced with permission from Krishnamurthy N, Kurzrock R. Targeting the Wnt/beta-catenin Pathway in Cancer: Update on Effectors and Inhibitors. Cancer Treatment Reviews. 2018, 62, 50–60 [163].

Wnt inhibitors and modulators can eradicate CSC clonal cells and drug-resistant cells [164], but we further need to determine their safety in maintenance of tissue homeostasis and repair. The activation of Wnt/ β signaling pathway is correlated to diminished clinical outcome in TNBC [165] as it presents the threat of lung and brain metastasis [166]. To date, scientists believe that pluripotent CSCs play key role in the formation of the primary malignant solid tumors. These CSCs are also responsible for the formation of drug resistance protein against breast Cancer and are strongly implicated in metastasis For instance, besides immortality and ability to invade other tissues, the mitochondrial respiration of CSCs is improved, they have a greater mitochondrial mass, and they can produce reactive oxygen species (ROS) more effectively than non/CSCs. ROS production

is one of the mechanisms to overcome the damage produced in their DNA and therefore the resistance to drugs [159].Wnt signaling has an important role in the proper operation of breast stem cells as well as in the progression of mammary gland during embryogenesis [167]. Thus, erroneus Wnt signaling pathway in breast CSCs is an important parameter in tumor generation. Finally some previous reports also confirmed that this signaling pathway also has a role in TNBC tumorigenesis [168].

2.3.4 PARP inhibitors.

The polyadenosine diphosphate-ribose polymerase also called poly (ADP-ribose) polymerase (PARP) is a superfamily of 18 proteins that effect all the molecular events that leads to recovery of the cells from DNA damage (participate in DNA base excision repair), gene transcription, apoptosis and genomic stability [169]. **See Figure 10.**

PARP inhibitors are considered perhaps the most important therapeutic drugs under investigation for the BRCA-1 and BRCA-2 mutations (59) as well as against TNBC (60). PARP expression in TNBCs is a consequence of exposure to chemotherapy (61). PARP-1 and PARP-2 proteins are induced by DNA strand breaks and are associated in DNA repair processes (62). PARP synthesized ADP-ribose polymer drives both BER (excision repair pathway) and single-strand break repair (SSBR) pathways [170]

Suppression of PARP activity blocks the formation of ADP-ribose complex, so PARP-dependent DNA-damage repair complexes such as DNA polymerase ε [171] cannot be efficient for repairing DNA-damage [172]. Trapped PARP-DNA complexes are extremely cytotoxic exhibiting high anti-proliferative activity (and therefore anticancer activity) [173]. Furthermore, PARP inhibitors such as Olaparib (AZD-2281) and Veliparib (ABT-888) also differed markedly with respect to their catalytic inhibitory propensities. Thus, the clinical as well as experimental results of each PARP inhibitor also varies with respect to inhibition [174, 175]. Since PARP inhibitors are different with respect to trapping PARP-DNA complexes [173, 176] differences can be seen while comparing the two (Olaparib and Velipamib) with Velipamib the less dominant drug repressor of PARP1 and PARP2 than Olaparib [173].

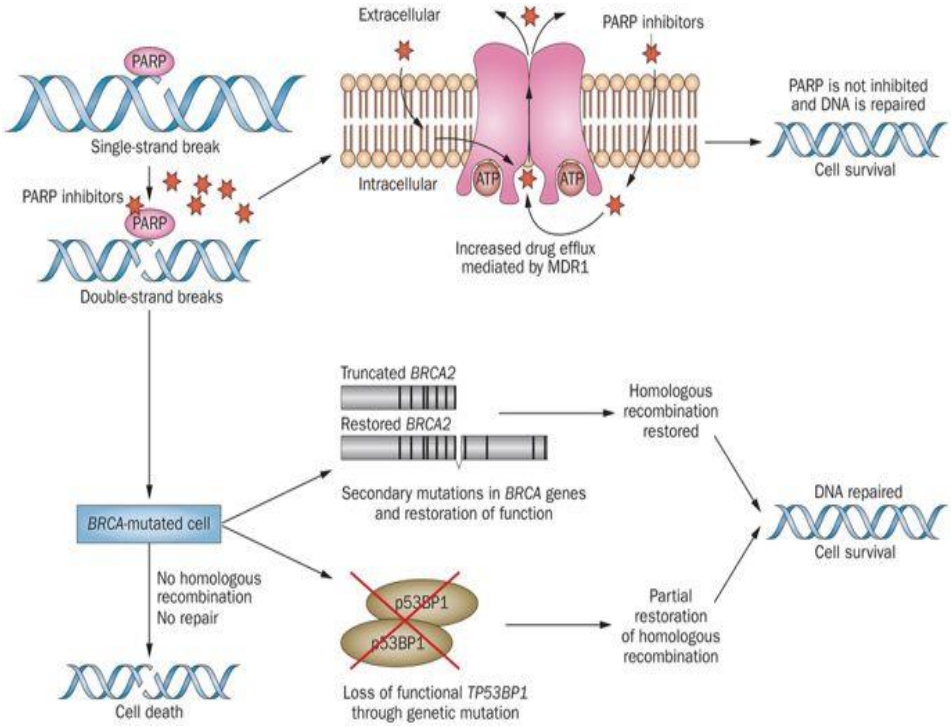

Figure 10. Major steps of the DNA strand break signaling model. Reproduced with permission from Amir Sonnenblick EdA, Hatem A. Azim Jr & Martine Piccart An update on PARP inhibitors—moving to the adjuvant setting. Nature Reviews Clinical Oncology (2015); volume12:pages27–41. [177]

2.3.5 mTOR inhibitors.

The erroneous regulation of mTOR signaling, especially PI3K/Akt/mTOR pathway has a direct relationship with malignancy (64). The mTor pathway is transformed in TNBC patients, thus is responsible for poor prognosis (aggressive and tissue invasion) (65) (66).

Phosphorylation reactions, stimulated due to the phosphoinositide- 3 kinases PI3K/Akt/mammalian target of rapamycin (mTOR), are responsible for Cancer cell growth, cell proliferation and angiogenesis (67). Phosphoinositide- 3 kinase (PI3K) dysregulation leads to mutations augmenting the carcinogenesis process (68). Moreover, overexpression of Akt, a protein kinase, is also correlated with tumor metastasis and invasion (69). The downstream signaling cascade of the PI3K/Akt pathway is mTOR that is present in two functionally different complexes (mTORC1 and mTORC2). The mTORC1 pathway

promotes mRNA translocation as well as phosphorylates a wide range of of substrates that accompany many anabolic processes (70) (71).

There are six types of inhibitors in clinical trials that target the PI3K/AKT/mTOR network: 1.- Pan-class I PI3K inhibitors, 2.- Isoform-selective PI3K inhibitors, 3.-Rapamycin analogs (Rapalogs: Everolimus, Temsirolimus, Deforolimus), 4.-Active-site mTOR inhibitors, 5.- Pan-PI3K/mTOR inhibitors, and 6.- AKT inhibitors [178]. Additionally combined targeting of mTOR and one PI3K isoform might increase efficacy compared to single PI3K inhibition [178].

Combined targeting of mTOR and one PI3K isoform might increase efficacy compared to single PI3K inhibition ***(Figure 11).***

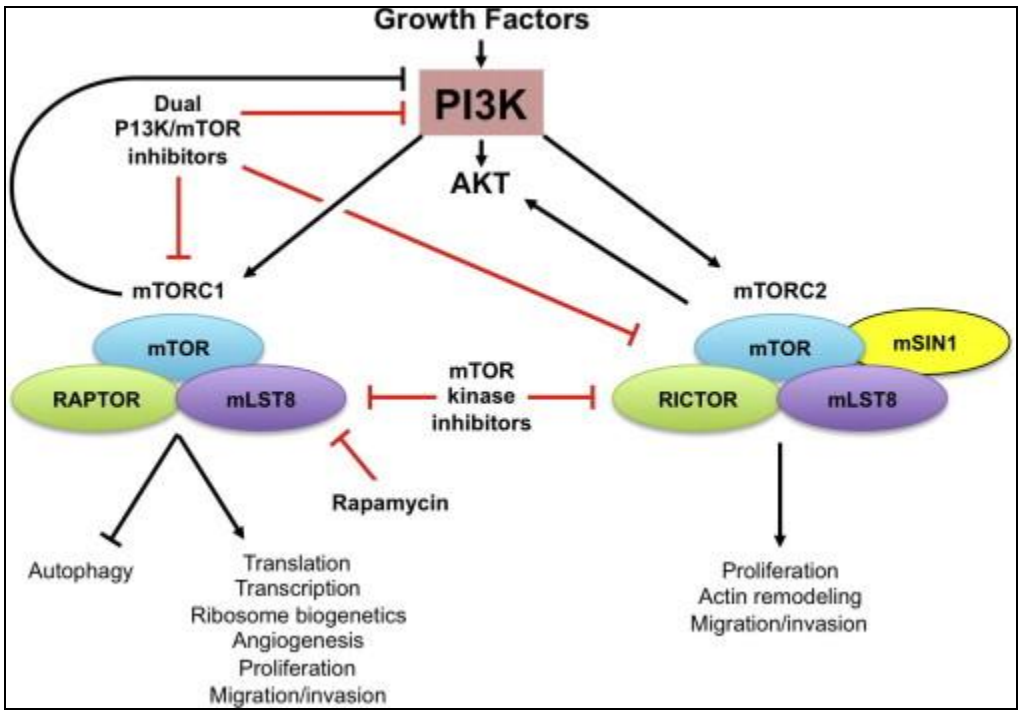

Figure 11. Mammalian target of rapamycin (mTOR) signaling pathway. mTOR is a subunit of two distinct multi-protein complexes, mTORC1 and mTORC2. Both mTORC1 and mTORC2 can be activated in response to growth-factors stimulation, whereas mTORC2 is a major kinase that phosphorylates and activates Akt. The importance of mTORC1 and mTORC2 in regulation of multiple cell functions vital for development of cancer and their strong interaction with oncogenic pathways make mTOR an attractive

target for therapeutic intervention. The mechanisms of action of currently available mTOR inhibitors are shown. Reproduced with permission from Zaytseva YY, Valentino JD, Gulhati P, Evers BM. mTOR inhibitors in cancer therapy. Cancer Letters. 2012, 319, 1–7 [179].

2.3.5.1 Rapalogs

Rapamycin as well as paclitaxel both affect the PI3K/AKT/mTOR pathway, thus playing an important role in therapeutics of TNBC. The mTOR antibodies coupled with EGFR inhibitors are more effective as compared to anti-mTOR alone, even though there is no known evidence about the synergy between anti-EGFR as well as mTOR inhibitors(73, 74). There is a need to develop other candidates for inhibition of PI3K/AKT/mTOR pathway (75) since there are many new molecular signatures that can be designed for novel treatment in TNBC (76).

2.3.6 EGFR (Epidermal Growth Factor Receptor).

Targets of receptor tyrosine kinase (RTK) such as epidermal growth factor receptor (EGFR) expression are reported in 89% of TNBC cases, and hence considered to be a therapeutic target, especially for BL2-subtype tumors that are augmented in EGFR gene expression [180]. Activation of this gene stimulates primary tumorigenesis as well as metastasis through increased proliferation, epithelial-mesenchymal transition (EMT), migration, invasion as well as angiogenesis. The EGFR inhibitor gefitinib reduces proliferation and enhances the cytotoxicities of carboplatin and docetaxel. [181] [182] There are a number of different anti-EGFR therapies trialed against TNBC that include the tyrosine kinase inhibitors (TKIs), such as erlotinib and lapatinib along with the monoclonal antibodies (mAbs) such as cetuximab and panitumumab [183] [183] [184] [185] [186]. The reports of failures of EGFR-TKIs and mAbs however, were while combination therapy that includes mAbs and chemotherapeutics proved to be a more efficacious. As an example, cetuximab, in combination with carboplatin in advanced TNBC patients, showed doubled response rates [187] [188]. Moreover, the triple combination of gefitinib, carboplatin, and docetaxel synergistically increased the cytotoxicity of TNBC cells [189].

Another drug, cannabidiol caused inhibition of breast Cancer growth and metastasis through novel mechanisms by the inhibition of EGF/EGFR signaling pathways **(Figure 12)** and alteration of the tumor milieu [190]. Hence, cannabidiol could also be used for the treatment of highly aggressive breast Cancer subtypes, i.e., TNBC [191].

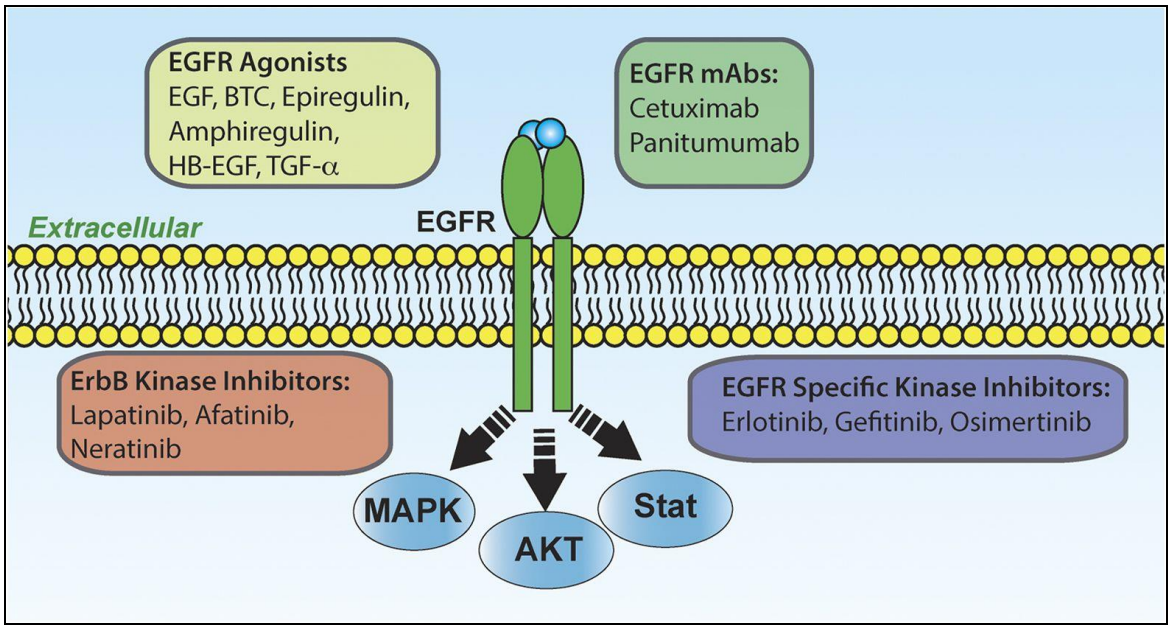

Figure 12. A schematic representation of the activators, inhibitors and outcomes of epidermal growth factor receptor (EGFR) signaling. EGFR is part of the four-member ErbB superfamily (ErbB1–4). These receptors form several different homo- and heterodimers (here we only depict the EGFR homodimer). EGFR is capable of binding several different extracellular ligands that agonize the receptor leading to activation of several downstream signaling events including, but no limited to those listed. Several therapeutics have been developed to antagonize EGFR including monoclonal antibodies (mAbs) that block ligand binding as well as several different kinase inhibitors. In addition to EGFR, some of these kinase inhibitors also target other ErbB receptors, supporting their use in human epidermal growth factor receptor-2 (Her2)-amplified breast cancer (BC). All of the listed therapies are Food and Drug Administration (FDA) approved for various cancers with the exception of Neratinib. Reproduced with permission from Ali R and Wendt MK. The paradoxical functions of EGFR during breast cancer progression. Signal Transduction and Targeted Therapy 2017, 2(16042), 1–7 [192].

2.3.7 TGF-β signalling pathway.

The TGF-β signaling pathway is linked to embryonic cell growth, cell differentiation, cellular homeostasis, apoptosis in adult organs. TGF-β1 belongs to the TGF-β superfamily of cytokines that is encoded by the *TGF-β1 gene.* [193] . Human platelets, which is a 25kDa protein have an important role in wound healing as well as having an important role in immune regulation. Thus, inhibits the secretion and activities of different cytokines such as IFN-gamma, TNF-alpha, and IL-2. TGF-beta 1 has an important role in breast Cancer stem cells, as they overexpress TGF-β1 *and the* TGF-β1 receptor [194] [195]. TGF-β inhibitors possess the ability to block the expansion of chemotherapy-resistant tumor-initiating cells (TIC) *in vivo* [195] forming the basis for combinational chemotherapy for patients suffering from TNBC. TGF-β stimulates an epithelial-to-mesenchymal transition (EMT) within mammary cells, leading to an exhibition of tumor-like properties. It is possible to reverse EMT via TGFBR1/2 inhibitors while stimulating mesenchymal-to-epithelial differentiation inside mammary epithelial cells [196]. TGF-β is frequently found overexpressed in the TNBC tumor microenvironment, especially in tumor cells, or by tumor-associated immune and stromal cells. These cells also generate SMAD2/3 and SMAD4 **(Figure 13)**, thus leading to similar effects such as protein synthesis, proliferation, metastasis, and angiogenesis. This explains to us that the TGF-β pathway is leading to the development of breast carcinomas, while TGF-β inhibitors are playing an important role as anti-metastatic therapies in patients with Cancer [196].

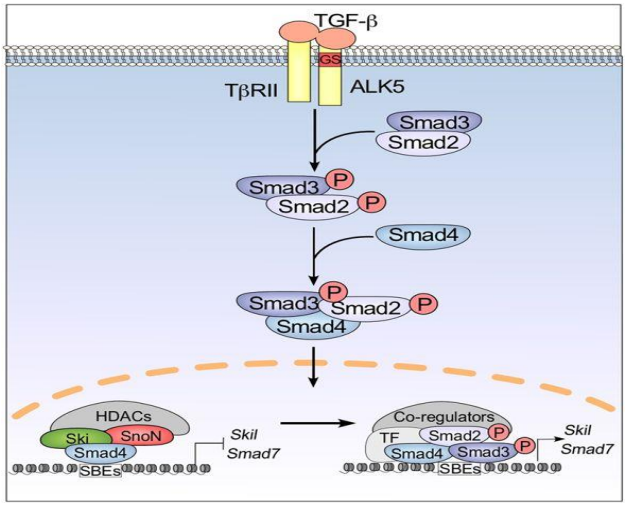

Figure 13. TGF-β stimulates Smad family. Tecalco-Cruz, A.C., Ríos-López, D.G., Vázquez-Victorio, G. *et al*. Transcriptional cofactors Ski and SnoN are major regulators of the TGF-β/Smad signaling pathway in health and disease. *Sig Transduct Target Ther* **3,** 15 (2018). https://doi.org/10.1038/s41392-018-0015-8

2.3.8 CSPG4 protein signalling pathway.

The CSPG4 or (non-glial antigen or melanoma chondroitin sulfate proteoglycan) a cell-surface proteoglycan expressed by basal breast carcinoma cells. Inhibition of CSPG4 is found to be therapeutically effective for breast Cancer therapy. This protein leads to the dissemination of the endothelial basement membrane protein, thus stabilizing the cell-substratum interaction similar to the effects that occur in TNBC. CSPG4 monoclonal antibodies can cause a blockade of essential migratory, mitogenic and survival signaling pathways in tumor cells, making CSPG4 a new target for antibody-based immunotherapy of TNBC [197]. Moreover, there is overexpression of CSPG4 in TNBC cell types, resulting in inhibition with no migration of TNBC cells when CSPG4 specific monoclonal antibody targeted such cells. CSPG4 specific monoclonal antibodies are not only effective therapeutic agents but also a diagnostic biomarker for TNBC detection [197] [198].

2.4 Cancer stem cells (CSCs) and autophagy.

As mentioned, numerous biochemical pathways in TNBC are related to Cancer stem cells (CSCs), thus, efforts are ruining into mAbs, dendritic cells (DC) and pluripotent cells Cancer vaccines as well as adoptive immunotherapy [199].

TNBC Cancer stem cells (CSC) are related to enhanced proliferative capacity, refractory treatment which leads recurrence and metastasis (CD-24, CD-44) [200]. Several biomarkers have been designed to detect CSCs. However, most biomarkers are also shared by normal stem cells, therefore these biomarkers become to unspecific molecules leading side effects. Chemo-resistance is present in TNBC stem cells, and they are the generals who lead the battle in a tumor micro-environment riddled with hypoxia [201]. Hypoxia is responsible for increasing chemo-resistance of autophagic TNBC stem cells. Blocking autophagic cascade network can increase chemo-response [202].

Autophagy is required for Cancer stem cells, autophagy processes are involved in the maintenance of cellular homeostasis and, therefore, represents a survival pathway in cells. Unfortunately, Cancer cells can regulate the autophagy pathway to develop resistance to chemotherapy. Therefore, molecular inhibition of the malignant autophagic pathway could reverse resistance to chemotherapy [202]. More research needs to be done regarding abnormal stem cells autophagy mechanism, since it may harbor the key to get a definitive cure not only against TNBC but against many types of Cancer.

Currently, efforts are focused on micro and nanofluidics to study the tumor microenvironment and understand more about the dynamic processes of Cancer. Nanomedicine could involve the design of new materials and surfaces for engineering sensors by means of *Nanoelectromechanical systems-NEMS and Microelectromechanical systems-MEMS* [203] tracing exosomes (cell vesicles with specific surface markers) [204] that are not present in healthy pluripotential cells, but only in the tumor microenvironment.

2.5 Different strategies for TNBC therapeutics.

Despite the discovery of new metabolic and biochemical pathways within tumor microenvironment, scientists and physicians continue to develop strategies to block

network routes and signals of neovascularization, metastasis, activating apoptosis, and "awakening" the immune response [205]. This effort is made challenging by the dynamic and chaotic molecular configuration of tumors, allowing tumors to recruit stromal cells, use valuable resources such as organic metals, vitamins, and create their own blood supply through the use of aberrant signaling. The standard approach has been to use cytotoxic therapeutics, the chemotherapies that since the 70's have been assisting oncology patients, however, these approaches lack the desired selectivity

Promising unconventional therapeutics are based on nanopolymers, liposomal drug delivery and nanostructured materials [206] In 1995, the FDA approved Doxil®, the first liposomal nanodrug part of a novel chemotherapy superior to the conventional [207] and a year later the FDA also approved Feridex®, nanoparticles for magnetic resonance imaging [208]. In this context, conventional chemotherapy is embracing the field of nanotechnology, promising to provide valuable specificity to the treatment of Cancer.

2.5.1 Conventional therapeutics.

Conventional therapeutics has demonstrated to be effective. However, The more advanced the stage, the prognosis will be adverse and ominous, not only due to tumor activity, but also due to chemotherapy sideeffects.

2.5.1.1 Neoadjuvant Therapy.

TNBC patients initially respond to neoadjuvant treatments, unfortunately the survival curve of these patients is not greater than 5 years [209]. Nevertheless, neoadjuvant chemotherapy is considered to be the "***Gold standard"*** of treatment for TNBC [210]. It is essential to select the agents most likely to improve prognosis [211]. Moreover, neoadjuvant anthracycline–cyclophosphamide (AC-scheme) chemotherapy is using in TNBC patients for getting good results although recently there are reports on drug-resistance for these drugs [212]. Scheme AC in presence of BRCA mutations has pathological complete response (pCR) rate of 27-30% in women [213] and consist on: Doxorubicin 20mg/m^2 plus Cyclophospamide 600mg/m^2 4 weeks followed by Paclitaxel 80mg/m^2 12 weeks, although the prognosis may be improved 61% if they associate drugs such as Cisplatin 75mg/m^2 q/3

weeks IV x 12 weeks [214].Other drugs can be used as Carboplatin (CALGB40603 study) AUC dose calculation or Abraxane 125 mg/m^2 (Nab-Paclitaxel nanoparticles) or immunotherapy using Bevacizumab 10mg/kg 2 weeks x 9 cycles (GeparSixto trial) [215] [216]. On the other hand, after treatment, the monitoring of the disease must be evaluated by imaging techniques as RMI (Magnetic Resonance Image) which is the most sensitive imaging method to measure the response of neoadjuvant treatment in triple negative breast Cancer [217].

To date, it is necessary to identify molecular biomarkers in each oncological patient, this is in order to provide a more effective and selective chemotherapy regimen [218]. Within the margins of this personalized medicine, medical research suggests that for TNBC treatment, one of the most persecuted molecular targets is EGFR since it is positively expressed (around 60%) in TNBC [219].

It has been shown that neoadjuvant therapy improves the response rate in patients with TNBC compared to adjuvant therapy [213, 220] as the effectiveness of cisplatin in TNBC shown in preoperative phase II studies where there are deficiency of BRCA-1 expression. [221-223]. However, neoadjuvant systemic therapies should be individualized because tumors with a BRCA-1 mutation are basal, but not all basal Cancers express BRCA-1 mutation. Moreover cisplatin and bevacizumab-the latest as a molecular target of VEGF have been shown to be efficient drugs in neoadjuvant therapy against TNBC [213] [224] as researchers points out in a meta-analysis of three clinical trials (*E2100, AVADO, RIBBON-1*) [225].

Taxanes-resistance of malignant cells which express BRCA-1 mutation is reported in the *in vivo* studies [226], but a clinical trial called "*CALGB 9344 / INT1048",* concluded that the use of paclitaxel reduces by 17% the risk of recurrence and 18% the risk of death in patients with TNBC [227].

On the other hand, although the role of the AR pathway in TNBC remains uncertain, there is some evidence that indicates the efficacy of minimally toxic androgen blockade in advanced AR-positive TNBC, however more research is needed [228].

2.5.1.2 Adjuvant Therapy.

Adjuvant therapy also is critical to avoid the risk of metastases with rapid progression and tumor recurrence activity which leads to death approximately 3 years-survival [229]. Whereas many studies suggest that BRCA-1 associated TNBC may be less sensitive to anthracycline-based therapy (MA5 study) [230] [231] other studies show anthracyclines with encouraging results as adjuvant therapy [232]. The decision on the use of adjuvant therapy should be established under the clinical and histopathological staging of the patient and an adequate genomic and proteomic profile of the patient.

The ability of TNBC to produce metastasis has been mentioned above, therefore, it is very important to study chemotherapy regimen in a palliative state because it is a key for the clinician to understand which drug is more effective.

A large randomized phase III TNBC trial (TNT) in the UK is underway comparing carboplatin with docetaxel for metastatic TNBC [233]. Although different doses of taxane have been used in metastatic breast Cancer (MBC), there isn't evidence indicating an improvement in the treatment of TNBC [234]. Many studies are being done to evaluate the best treatment, the decision as to which type of chemotherapy should be given to patients with metastatic TNBC as first-line chemotherapy and therapy must be individualized according to the disease features (genomics, mirnomics, proteomics, co-morbility, etc). So then, scenario is ominous since there aren't specific guidelines for the management of TNBC still.

In the case of advanced stages (III C) having Anthracycline and Taxane resistance, Xeloda^{TM} (Capecitabine) 1,250 mg / m^2 can be started twice daily for 14 days followed by 7 days off, combined with Taxotere ^{TM} (Docetaxel) at a dose of 75 mg / m^2 in infusion intravenous, administered for 1 hour, every 3 weeks.

Another combination that has shown utility is Ixempra^{TM} (Ixabepilone) 40 mg/m^2 IV for 3 hours each 3 weeks plus Capecitabine, although Ixempra^{TM} can be used as monotherapy at the same dose.

Table 2: Conventional Treatment of Triple Negative Breast Cancer*

Conventional treatment	Drugs	Mechanism	Scheme/dose	References
Neoadjuvant treatment Early TNBC *(Gold standard)* **Advanced or Metastatic**	Anthracyclines + Taxanes **or** Capecitabine + Taxane Ixabepilone monotherapy or Ixabepilone + Capecitabine	Cytotoxicity** Stabilization microtubules	Doxorubicin 20mg/m^2 plus Cyclophospamide 600mg/m^2 4 weeks followed by Paclitaxel 80mg/m^2 12 weeks Capecitabine 1,250 mg / m^2 14 days + Docetaxel 75mg/m^2 Ixabepilone 40 mg/m^2 per 3 weeks	Lancet 2014. Palma et al Oncotarget 2015 [213]
New neoadjuvant agents (BRCA mutations)	Platinum (Carboplatin) Bevacizumab, Nab-paclitaxel.	Cytotoxicity and VEGF immunotherapy	Adding up standard scheme Abraxane 125 mg/m^2, Carboplatin AUC, Bevacizumab 10mg/kg	CALGB 40603 trial [216]
Adjuvant agents	Anthracyclines and Taxanes	Cytotoxicity	Cyclophosphamide 600mg/m^2 + Doxorubicin 20mg/m^2 + Docetaxel 75mg/$m^2$for q3 weeks 6 cycles.	[235]
Surgery is often the first treatment for stages I & II breast Cancer. Lumpectomy and a total mastectomy are two types of breast surgery used for stages I and II breast Cancer *(NCCN guidelines)*. However, In TNBC, the surgical treatment of choice is the preservation of the breast.				
Radiotherapy Radiation therapy is usually given after chemotherapy or surgery is finished or combined with chemotherapy. Probably benefit in BRCA mutations.				

***** *The conventional treatment presently prescribed in hospitals for TNBC. It pertinently depends on the clinical stage of the disease TNM, blood tests, imaging (mammography, ultrasound, CT-Scan, PET), tolerability to treatment, usually accompanied by corticosteroids (Dexamethasone) and drugs to control symptoms (Ondansetron, Filgrastim, etc.) to reduce adverse effects.* ***Cytotoxicity:*** *Inhibition of DNA and RNA synthesis. Inhibition of topoisomerase II enzyme, generation of free oxygen radicals, Induction of histone eviction from chromatin etc.*

2.5.1.3 Surgery.

Regarding surgical decision in TNBC, many studies are done to determine whether patient needs to choose mastectomy over lumpectomy [219]. In TNBC, the surgical treatment of choice is the preservation of the breast, this is because the choice of surgical treatment does not improve the prognosis or the local tumor recurrence so patients remain appropriate candidates for breast conservation [236]. A lumpectomy followed by radiation therapy could be an option and this is called breast-conserving therapy in women with stage I or II breast Cancer (NCCN guidelines). However, in TNBC, the gold standard is neoadjuvant therapy and is preferred before surgery.

2.5.1.4 Radiotherapy.

Radiotherapy is given in TNBC following mastectomy or conservative breast surgery (CBS). There is still controversy on this issue [237] but there is evidence that women with TNBCs harbor a pathogenic mutation in the BRCA-1 gene and tumors lacking functional BRCA-1 are deficient in double-strand DNA break repair via homologous recombination and are potentially highly radiosensitive [238].

TNBC is considered a pathological entity susceptible to radiotherapy. Because BRCA-1 is due to tumor detection, tumor cells can't repair the breakdown of DNA by homologous recombination. Indicative RT after mastectomy in the presence of risk factors (multiple positive lymph nodes, tumors> 5 cm, presence of lymph vascular invasion). Unfortunately, like the guidelines in the pharmacological treatment, the use of RT in TNBC does not have treatment guides [239, 240].

2.6 Advanced therapeutic: Nanomedicine, a targeted approach for treatment.

Chemoresistance is a significant problem in metastatic Cancer [241]. Moreover, the reduction of side effects in chemotherapy is a challenge for oncologists since most of these drugs are steroids that can be harmful to patients and cause a lot of immunological problems, constipation, anemia, leukopenia, thrombocytopenia, clotting problems, alopecia,

weight loss, etc. [242]. Moreover, non-steroidal anti-cancer drugs also possess many side-effects and they also exhibit severe toxicity towards normal cells apart from Cancer cells [243].

There are a number of examples of clinically approved nanomedicines used in hospitals around the world, e.g., liposomal doxorubicin (Doxil^{TM}) [244], albumin-bound paclitaxel or Nab-Paclitaxel (Abraxane^{TM}) [245] and PEG-1 Asparaginase (Oncaspar^{TM}) [246]. Additionally, many nanomaterials have been studied with functions such as: delivering drugs, aptamers or microRNA capable of inducing gene or immunological therapy [247]. Some examples of these delivery vehicles include micelles [248], ribonucleic acid (RNA) [249], nanodiamonds (NDs), carbon nanotubes (CNTs) [250] [251], Au-nano matryoshkas [252] as well as superparamagnetic iron oxide NPs (SPIONs) [253], quantum dots (QDs) etc.

It is imperative to synthesize nanoparticles with the correct properties for Cancer therapeutics. These properties are dependent on the method of synthesis and characterization employed. Obviously, nanomaterials for biomedical applications must be nontoxic and biocompatible. It is also necessary that the synthesis and purification methods for nanoparticles be reproducible. [254], providing uniformity in size and shape; characterization that can be verified through microscopy tools such as scanning electron microscope (SEM) and transmission electron microscopy (TEM). Applications in nanomedicine likewise require nanoparticles that are easy to metabolize by the human body via renal or hepatobiliary clearance [255, 256].

Nanomedicine provides a potential pathway to solve many of the problems of cytotoxicity and lack of specificity of conventional chemotherapies. For example, nanodiamonds (ND) can be used to transport doxorubicin and simultaneously anchor ligands that recognize tumor biomarkers conferring them greater selectivity and specificity [257, 258]. Nanoparticles (NPs) can avoid also minimize off-target effects, e.g., lonidamine is an inhibitor of aerobic glycolysis but has failed in clinical trials due to its intense hepatotoxic activity. However, recently NPs have been developed that incorporate lonidamine together

with a monoclonal antibody. In this way, it provides greater selectivity for malignant cells than for the healthy cells , reducing undesired systemic side effects [259].

Because there are several numbers of tumor markers different from the PR, ER and Her-2 neu hormone receptors expressed in TNBC, the NPs can be of help to achieve greater specificity and efficiency in the treatment, being able to pursue other molecular objectives.

There are two main types of strategies in which nanoparticles can exert the therapeutic effects.

1. A passive transport process called *"Enhanced Permeability and Retention"* (EPR) in which peripheral blood vessels to the tumor have leaky vasculature that increases nanoparticle permeability. However, the disadvantage of EPR is that not all tumors possess leaky vasculature . Therefore an adequate analysis of TNBC tumor biomarkers is required to load the nanoparticles with a ligand specialized in the search for receptors overexpressed like CXCR4 (folic acid receptor) [260].

2. Another approach used by researchers is active transport that is governed by using biomarkers miRNA (microRNA), proteins, antibodies, as well as therapeutic biomolecules as siRNA and aptamers, discussed below.

2.6.1 miRNA.

Nowadays, the importance of microRNA (miRNA / miR) related with Cancer treatment has increased due to the potential they have as diagnostic biomarkers [225]. It has been discovered in TNBC the presence of miRNA overexpressed miRNA558 [261]. Moreover, several TNBC miRNAs were founded in a metanalysis [262]. The miRNAs promise to be part of the arsenal of oncological studies that will soon be available in hospitals to provide better diagnosis and prognosis as powerful biomarkers.

Within some biomolecules we can also find some like siRNA (small interfering RNA) [263], for therapeutic approaches and aptamers for *theranostics.*

2.6.1.1Theranostics.

Even more promising, but not unrealistic, is the concept “Theranostics,” in which nanoparticles can diagnose and treat at the same time. The nanoparticles can be used to deliver drugs and generate *"Real-time images,"* [264]. In this work we are not going to use this application.

2.6.2 siRNA.

Since the discovery of the *Caenorhabditis elegans* plant’s properties, the siRNAs have supposed a revolution in the genesis and treatment of the diseases, the researchers use siRNA to switch off or change the tumor genes responsible for the drug resistance and in this way increase the efficacy in the treatments [265]. The siRNAs can be loaded in nanoparticles (non-viral) and in viral capsids or supramolecular complexes, they have already been used in animal models to fight TNBC getting gene silencing for proteins that reflect poor prognosis in oncological medical practice viability [266].

It is feasible to modify the cellular resistance of tumors using siRNA or other molecules that interfere with the survival response of malignant cells. Gold nanoparticles have been used to carry out siRNA against MDA-MB-231 cells (TNBC), so therefore researchers believe they could be useful for reducing tumoral activity [267]. Therefore it is now accepted that nanotechnologies are now part of the oncologist’s therapeutic arsenal [268, 269]. Since siRNA has shown therapeutic benefits in breast Cancer [270].

2.6.3 Aptamers.

Aptamers are molecules made up of nucleotides, generally in a range of 50 DNA or RNA nucleotides which makes them functional to reach molecular targets, therapeutic targets, protein complexes and Cancer cells [271].

Engineering of aptamers is based on a technique called systematic evolution of ligands by exponential enrichment (SELEX), its advantage over mAbs since it is easier and cheaper to produce them, but the degradation into the blood stream is a clear disadvantage [272]. However, scientists are developing “mirror aptamers” (Spiegelmers) enantiomers highly resistance to enzymatic degradation through synthetic biology to avoiding aptamer

degradation by nucleases [273]. SELEX consists in the amplification of RNA (oligoribonucleotides) or DNA (oligonucleotides) [274] using PCR (polymerase chain reaction) to subsequently incubate them with molecular targets (cells, protein complexes, etc.). After five rounds the maximum molecular affinity is obtained *"The maximum enrichment"*[275].

Various aptamers have been developed for therapy in TNBC; for example, the aptamer 5TR1 pursues the molecular target MUC1 which is a tumor protein in MDA-MB-231, the researchers have conjugated 5TR1 to Doxorubicin to make it more specific and avoid the known side effects such as cardiotoxicity [276]. But nanomedicine is advancing rapidly, and now researchers have focused on combining all the technologies mentioned above (siRNA, miRNA, aptamers) by loading them into nanoparticles that pursue the CD-44 receptor characteristic of TNBC pluripotent cells [277].

2.6.4 Novel nanoparticles and its molecular targets on TNBC.

Nanomedicine has promised to improve the specificity with which drugs and other molecules are transported using nanoparticles that maximize the therapeutic effect and decrease the systemic toxicity of conventional chemotherapies, but these nanocarriers must have adequate safety profile, the parameters of which must be known [278]. Therefore, understanding nano-pharmacokinetics and nanotoxicology is mandatory [279].

The functionalized nanoparticles for Cancer therapeutics and diagnosis can be made up of diverse materials such as gold, silver [280], platinum [281], diamonds [241], copper [282], among others. These materials are used due to their low cytotoxicity, for example, gold nanoparticles are not cytotoxic making them suitable candidates for nanomedicine [283]. Here there are other examples:

2.6.4.1 Quantum Dots (QD).

The matter at the nanoscale can be manipulated, which has made it possible to evaluate the unique properties of Quantum dots (QDs). QDs where discovered in 1982, they are semiconductor nanocrystals they have superior light absorbance and high fluorescent intensity [284]. QD-based nanotechnology possesses wider applications in Cancer molecule

imaging and quantitative detection [285]. Many studies signs QD technology could substitute immunohistochemistry (IHC) [286], because of its better fluorescent signaling, and performing even more accurate quantitative analyses for evaluating prognosis in TNBC [287]. Since QDs demonstrate, results of molecularly directed images, as well as better detection quantitative of Cancer molecules like Ki67 and EGFR, expressed on TNBC [288].

2.6.4.2 Fluorescent nano-diamonds (FNDs).

Current nuclear medicine uses radioisotopes such as Strontium-89, Iodine-131, Samarium-183 and Technetium-99. However, nanotechnology proposes the use of non-radioactive materials with improved sensitivity and specificity. In this technological revolution, we also can find materials such as fluorescent nano-diamonds (FNDs). Fluorescent nano-diamonds are biocompatible nanomaterials often used in MDA-MB-231 theranostics [289] [241].

2.6.4.3 Nano-matryoshkas.

Another singular design has been developed as thermal therapeutic, imaging and drug delivery nanoparticles. Nano-matryoskka, referred to as a multi-layer nanoparticle reminds of the Russian doll which can contain many other dolls inside, the application of the hollow nanoparticle capable of delivering multiple drug loads contained in multilayers that can be designed with different materials as suggest an MDA-MB-231 murine xenograft study [20].

2.6.4.4 Silver nanoparticles (AgNPs).

Silver NPs (AgNP) are another example of Nps that can act against tumor cells in TNBC that can induce DNA damage as in vivo studies suggest. Silver nanoparticles help in reduction of TNBC growth and augments radiation therapy. [280]. The mechanism of action is physical. However, it has not been specifically established. One possibility is that the reaction of silver in the cellular microenvironment will lead to the release of reactive oxygen species.

2.6.4.5 Iron Oxide Nano-particles (IONP).

The ability of iron oxide NPs to produce strong contrast images in RMI in T1(longitudinal relaxation – spin-lattice) and T2 (transversal relaxation – spin-spin) has given them a place in the theranostic of Cancer [67, 290]. This novel imaging system by using IONP has been used in several xenograft model [291] [292], for MRI diagnostic in TNBC [292].

2.7 Physical therapies- Hyperthermia, electric-based treatment.

Gold nanoparticles are photothermally tunable through this feature since gold atoms on the surface of nanoparticles upon illumination with light at the resonance wavelength evinces unique properties of matter at a nanoscale, these NPs are susceptible for producing heat bringing apoptosis through *Hyperthermia* [293]. Taking advantage of near-infrared (NIR) wavelength for medical applications, hyperthermia can kill cells because its enhanced optoelectronics.[294].

Hyperthermia has proven to be effective when combined with radiotherapy and chemotherapy [295]. Hyperthermia is aggressively considered Cancer treatment from last many years, currently, hyperthermia therapy continues to be the subject of research in Nanomedicine, because at less than 100 nm the electromagnetic properties of materials allow heat generation, this has prompted innovative treatments and diagnostics (theranostics) [296].

2.7.1 SPIONs (Superparamagnetic Iron Oxide Nanoparticles).

SPIONs have higher magnetic properties than paramagnetic materials due to their ability to spin alignment to an external magnetic field, SPIONs can generate heat inside the tumors producing apoptosis by hyperthermia [297].

2.7.2 Core-Shell Nanoparticles.

SPIONs core-shell are formed by layers: an iron oxide core and a therapeutic biocompatible coating [296] which can reduce toxic side effects [298]. Hayashi et al. [299] have shown in advantages of using SPION intravenously for Cancer theranostics. Also, SPIONs core-shell hyperthermia properties, have been the hallmark of this design. Researchers are using lasers

[300], ultrasound [301], radio frequencies [302] or alternating magnetic field [303] to generate apoptosis.

2.7.3 Nanocomposites.

The core-shell modality, however, has great disadvantages, the negative polarity and the amphipathic characteristic makes them an easy target for the immune system, so the alternatives in nanoengineering are the creation of nanocomposites [304] which consist of biphasic or multiphase materials, respecting the condition that at least one dimension of the material has less than 100 nm [305].

The improved optoelectronic properties allow nanocomposites to be useful candidates for drug delivery, food packaging [306], sensing devices and their antimicrobial properties are currently being studied [307]. Nanocomposites advantages over core shell design relies on colloidal easy synthesis and reproducibility [308]. Administration as colloids would guarantee an adequate renal clearance, and greater bioavailability in attack doses or standard treatment. Nevertheless, a clear disadvantage in contrast with core-shell design is the larger size (above 100 nm) which is characteristic of nanostructured materials [309] and could lead to a disaster in the human blood stream by creating blood clots.

2.8 Photodynamics PDT.

Current intrahospital photodynamic therapy (PDT) consists of administering porphyrins and phthalocyanines that have an affinity for malignant cells; then a laser can stimulate their chemistry structure and lead the release of reactive oxygen species (ROS). Nanotechnology takes PDT to a different enhanced level. PDT based on nanoparticles uses a photosensitizing agent to produce ROS and apoptosis avoiding healthy tissue damage [310]. Many other studies were carried out finding utility and efficacy in the joint use of NPS that act as a photosensitizer to produce PDT [311] [312] [313].

2.9 Immunotherapy.

Since they were described for the first time, the criteria of Hanahan and Weinberg have undergone constant modifications, continually adding more functions and properties that confer to the Cancer cells the capacity of proliferation and invasion to other tissues in

addition to having improved machinery for its survival. The hallmarks are described in **Figure 14** [314].

Researchers have focused their efforts on making immunological-portraits of the tumor microenvironment in TNBC [315] by using computational tools such as Cell-type Identification By Estimating Relative Subsets Of RNA Transcripts (CIBERSORT) [316] and Estimation of STromal and Immune cells in MAlignant Tumors using Expression data (ESTIMATE) [317] that allows the evaluation of gene expression in solid tumors, including those for immune response interest. Unfortunately, they confirmed TNBC has the worst outcome because of the metastasis-promoting genes higher expression as well as the depressed expression of metastasis-inhibiting genes. Finally, to make things more complicated, it has been documented in TNBC, higher expression of immuno-suppressor genes like TP-53 compared to other breast Cancer subtypes and normal tissue [315]. Altogether, this data allows to advance to the objective of seeking therapeutic targets and understanding TNBC microenvironment.

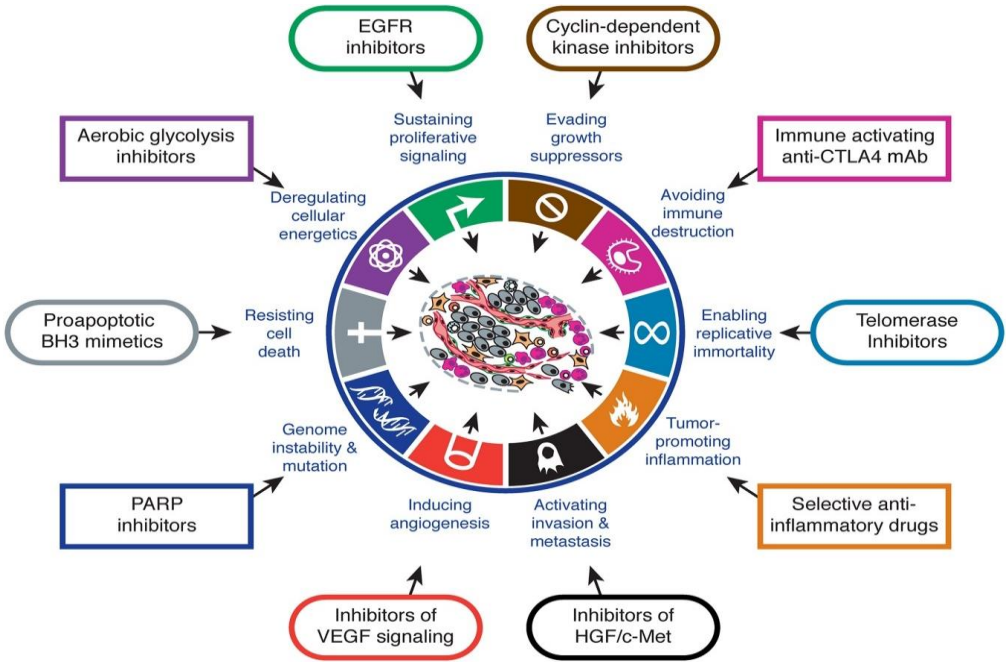

Figure. 14 Hanahan and Weinberg criteria.

But even when transcriptomics and genomics are giving insights on TNBC, it is hard to approach a therapeutic in such an aberrated environment. Within the TNBC tumor

microenvironment, there are latent T and B lymphocytes, antigen-presenting cells (APCs) which for some reason do not respond to the threat posed by tumor cells. Recently, strategies have been implemented to "wake up" these cells from their lethargic dream and initiate a response that slows the progression of the tumor [318] [319]. It is assumed Cytotoxic T-lymphocyte antigen-4 (CTLA-4) initiate the antitumor response [320]. So, the current efforts are directed to activate it by using CTLA-4 inhibitors such as ipilumab. The problem is they activate T-cell in an aggressive way generating different systemic side effects [321].

mAbs as rituximab (anti-CD20), cetuximab (anti-EGFR), trastuzumab (anti-HER2), bevacizumab (anti-VEGF-A), ipilimumab (anti-CTLA-4), and very recently pembrolizumab (anti-PD-1) have been approved for FDA. The programmed cell death-1 (PD-1) signal pathway has a ligand called 1 (PD-L1) [322] both can lead programmed death on malignant cells [323], especially for TNBC [324].

Two new PD-L1 inhibitors, mepolizumab and nivolumab, are running on an ongoing clinical trial. Unfortunately, 76% TNBC patients having PD-L1 expression haven't shown therapeutic response under mepolizumab therapy [325]. Medicine Nobel Prize (2018) was also given for both Anti-CTLA-4 and PD-1 discoveries and it is expected a new generation of immunotherapy-drugs are coming in the next years enhancing the outcome in Cancer patients.

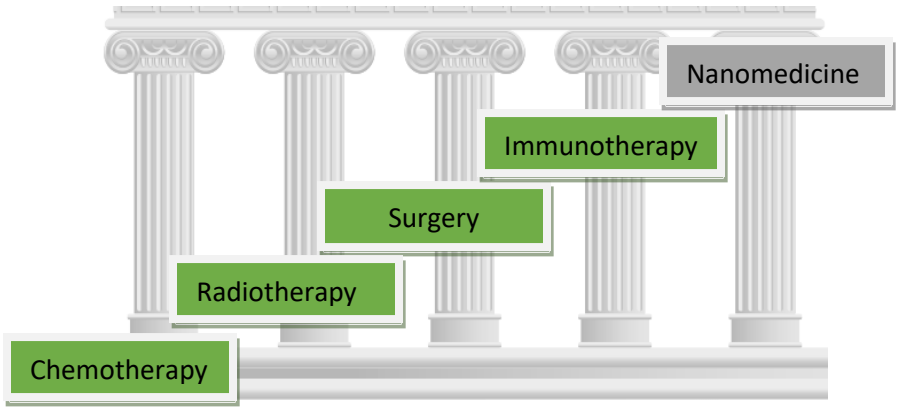

Fig. 15 The pillars of treatment in Cancer.

The 2018 Medicine Nobel Prize was given for insights on the so-called 4th pillar-Immunotherapy, yet, even when nanodrugs such as DaunoXome® or Doxil® are currently in use in oncology field, more research is needed to switch on the 5th pillar-Nanomedicine.

2.9.1 Artificial Intelligence.

It was in 1956 when Professor John McCarthy introduced the concept of artificial intelligence (AI). Currently, at the end of the second decade of the 21st century we can see the power of AI not as a science fiction anymore, but in real fields such as engineering, marketing, military industry and medicine [326]. In medicine, AI has an arsenal of complex statistical software-models that are based on learning and choosing the best therapeutic alternative through machine learning-AI. Some examples of these techniques are computer-aided detection (CADe), Case-Based Reasoning (CBR), OsteoDetect-Machine Learning, computer-aided and diagnosis (CADx), Explainable Artificial Intelligence (XAI) and rainbow boxes [327] [328] . In 2019, Jean-Baptiste Lamy et al. used XAI and CBR to create DESIREE (Decision Support and Information Management System for Breast Cancer) which can interpret and predict Breast Cancer disease by optimizing the treatment with metadata and confirmation from medical oncologists who validated the effectiveness of this AI in the service of oncology [329].

Metadata, also called metaheuristic data, are provided by real oncology-patient data banks, treatments and trends are analyzed qualitatively and quantitatively. It is hoped that in the future AIs can help physicians open up a faster and more accurate theranostics for building and elucidate extremely complex decision algorithm, as Cancer represents it [330].

Recently Fernández Martínez et al [331] published the idea to design an AI based on Machine-Learning able to help oncologist to detect different TNBC subtypes for optimizing therapeutics. In the near future, a sophisticated AI could feed back different databases such as TCGA (The Cancer Genome Atlas) [332] which contains SNP-based platforms, Reverse-phase protein array (RPPA), DNA and RNA sequencing among other useful-critical information working in conjunction with METABRIC (Molecular Taxonomy of the Breast Cancer International Consortium) [333] to study molecular heterogeneity in various molecular subtypes of breast Cancer including TNBC, they could provide valuable Bigdata

(clinical history, transcriptomic, tumor recurrence, prognosis, treatment, etc.) for the oncologist to bring personalized medicine to these patients in a reasonable time. Unfortunately, to date there are not many publications about it and more multidisciplinary research on AI in medicine is required.

Table 3. Nanomedicine for Triple Negative Breast Cancer Theranostics**

Nanoparticle	Unique properties	Application	Status	Evidence
Quantum Dots (QDs)	Semiconductor nanocrystals they have superior light absorbance and high fluorescent intensity [284].	QD-based nanotechnology possesses wider applications in Cancer molecule imaging and quantitative detection.	Experimental/clinical ongoing	Many studies signs QD technology could substitute immunohistochemistry (IHC) [286], because of its better fluorescent signaling, and performing even more accurate quantitative analyses for evaluating prognosis for TNBC [287].
Fluorescent nano-diamonds (FNDs)	Tunable-enhanced optoelectronics features allows fluorescent nano-diamonds (FNDs) issuing image signals [241] at low cost production.	Current nuclear medicine uses radioisotopes such as Strontium-89, Iodine-131, Samarium-183 and Technetium-99. FNDs proposes the use of non-radioactive materials for imagining applications enhancing sensitivity and specificity.	Experimental/clinical ongoing	Fluorescent nano-diamonds (FNDs) are biocompatible nanomaterials often used in MDA-MB-231 theranostics [289]
Nano-matryoshkas	Nano-matryoshka, referred to as a multi-layer nanoparticle, hollow nanoparticles can deliver multiple drug payloads.	Nano-matryoshka, singular design has been developed as thermal therapeutic, imaging and drug delivery nanoparticles.	Experimental/clinical ongoing	Designed by multilayers that can be designed with different materials, Nano-matryoshka can exert several drug medication payloads and inducing hyperthermia as suggest an MDA-MB-231 murine xenograft study [20].

Silver nanoparticles (AgNPs)	The mechanism of action is physical. However, it has not been specifically established. Ag affects cellular microenvironment will lead to the release of reactive oxygen species.	Therapeutics by using cytotoxicity.	Experimental/clinical ongoing	Silver NPs (AgNP) are another example of Nps that can act against tumor cells in TNBC that can induce DNA damage as in vivo studies suggest. Silver nanoparticles help in reduction of TNBC growth and augments radiation therapy. [280].
Iron Oxide Nano-particles (IONP)	Tunable-enhanced optoelectronics and magnetic features.	The ability of iron oxide NPs to produce strong contrast images in RMI in T1(longitudinal relaxation – spin-lattice) and T2 (transversal relaxation – spin-spin) has given them a place in the theranostic of Cancer [67, 290].	Experimental/clinical ongoing	This novel imaging system by using IONP has been used in several xenograft model [291] [292], for MRI diagnostic on TNBC [292].
SPIONs (Superparamagnetic Iron Oxide Nanoparticles)	SPIONs have higher magnetic properties than paramagnetic materials due to their ability to spin alignment to an external magnetic field	SPIONs can generate heat inside the tumors producing apoptosis by using hyperthermia [297] as well as real time images into the tumors [334].	Experimental/clinical ongoing	SPIONs are often use in human triple negative breast Cancer cells (TNBC) MDA-MB-231 therapeutics [335].
Core-Shell Nanoparticles	SPIONs core-shell are formed by layers: a magnetic iron oxide core and a therapeutic biocompatible coating [296] which can reduce toxic side effects [298].	Enhanced hyperthermia properties, by stimulation through lasers [300], ultrasound [301], radio frequencies [302] or alternating magnetic field [303] to generate apoptosis.	Experimental/clinical ongoing	Core shell design has been used for enhancing photodynamic, chemotherapy and gene therapy in TNBC [336]. Also Hayashi et al. [299] have shown in advantages of using SPION intravenously for Cancer theranostics.

Gold Nano-Stars	Enhanced optoelectronics specifically T1-signal for RMI.	Theranostics Gene Therapy Photodynamics Drug delivery Hyperthermia Drug Delivery	Experimental/clinical ongoing	RMI T1 -signal magnetic resonance imaging and photothermal therapy for TNBC [337].
Nanocages	Capacity to transport and deliver nucleic acids, peptides and drugs as well as PDT properties.	Theranostics Gene Therapy Immunotherapy Photodynamics Hyperthermia Imaging	Experimental/clinical ongoing	Immunogenic photodynamic therapy with gold nanocages on TNBC [338].
Nanorods	Enhanced magnetic-optoelectronics properties according to shape and size. Capacity to transport and deliver nucleic acids, peptides and drugs.	Theranostics Gene Therapy Immunotherapy Photodynamics Hyperthermia Imaging Drug Delivery	Experimental/clinical ongoing	Gold nanorods were developed for delivering cisplatin and producing photothermal therapy on TNBC. [339]
Nanocomposites	Enhanced magnetic optoelectronics including Resonance Plasmon Surface properties. Nucleic acids, peptides and drug releasing with enhanced specificity.	Theranostics Gene Therapy Immunotherapy Photodynamics Hyperthermia Imaging Drug Delivery	Experimental/clinical ongoing	Researchers are experimented on using immunotherapy nanocomposites vehicle on TNBC. [340]

CHAPTER 3

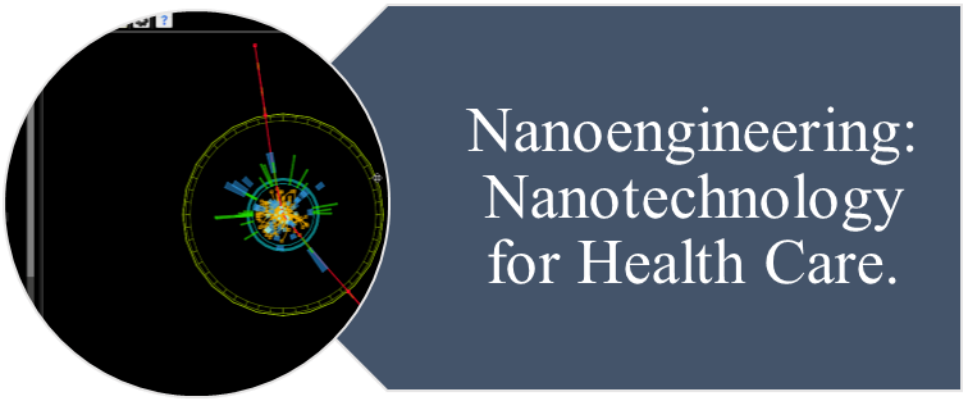

3. Justification.

Breast cancer continues to be a major public health problem. The incidence is increasing in most countries and is expected to increase further in the next 20 years despite current efforts to prevent the disease. Some risk factors for breast cancer are lower age of menarche, late age of first pregnancy, fewer pregnancies, having had dysfunctional or shorter lactation periods, late menopause, obesity, alcohol consumption, inactivity and therapy of hormone replacement (HRT). In addition to the known mutations of the BRCA-1 and BRCA-2 genes, the latter has quadrupled its presence in recent decades. Above all the molecular subtypes of breast cancer, the triple negative (TNBC) has the worst prognosis and the lowest response rate to treatment. In the present day, there is no specific oncological treatment for this type of cancer and the adverse effects of the current therapy are devastating for healthy cells, tissues and organs in these patients.

The superparamagnetic iron oxide nanoparticles (SPION) have been exploited as an important nanomaterial for the diagnosis and treatment of Cancer. These magnetic

nanoparticles (NPs) have a huge surface area for the union of biological structures, making them suitable candidates for the creation of contrast agents, drug transport (greater selectivity) and as hyperthermic-photodynamic agents. The doping of SPIONs with Cobalt Manganese and Zinc ions further improves its magnetic property, increasing the performance of materials for biomedical applications.

Active gold nanoparticles (Au) with surface plasmon resonance properties offer excellent potential in molecular imaging and Cancer therapy since they can act as multimodal contrast agents, they can be used for their use in computed tomography (CT), magnetic resonance imaging (MRI), positron emission tomography (PET) and its surface surfactants-free allows a versatile functionalization for the improvement in the selective therapy of Cancer and likewise allows the controlled release of drugs or act as a powerful agent of chemotaxis in the immune response by using hyperthermia.

Nanoparticles of sizes between 5 and 100 nm accumulate in tumors through the well-known permeability and enhanced retention (EPR) effect that originates in the permeable tumor vasculature. Although not all tumors present EPR, our research team has solved this problem through the study of personalized therapy aimed at specific molecular targets based on immunoproteomic studies and selective tumor markers.

The significant benefit of the gold nano-sphere is to provide complete protection to the internal magnetic core from a range of environmental factors, in addition to providing a platform for surface modifications, real-time images and drug transport loads. But the most important for medical purposes is the innocuous property of gold to be purified by renal clearance, which is defined as the volume of plasma that by renal action is free of a certain substance, measured in a unit of time.

From previous experiences we have optimized the synthesis of iron oxide nanoparticles with dopants, such as ***Cobalt, Manganese*** and ***Zinc*** together with the gold film to form a nucleus of nanoparticles with various biological functions, for example: drug delivery and cell diagnostic screening carcinogenic. These complexes were also used in *"In Vitro"* models for applications such as hyperthermia and contrast agents in MRI.

According to the National Cancer Institute (NCI), localized hyperthermia can be induced using microwaves, radiofrequency, ultrasound and even light. The disadvantage of traditional hyperthermia techniques using radiofrequency and microwaves are that they are invasive and lead to serious side effects. Another modality of hyperthermia is light that causes photothermal treatment using infra-red radiation, generating heat and inducing the necrosis or apoptosis of cancer cells. Again, the disadvantage of light is the lack of depth in its penetration into the tissues, thus proving to be futile for deep tumor therapy. Gold nanoparticles, especially gold nanospheres, gold nanostars , gold nanoshells and gold nanorods, single-walled carbon nanotubes, multiwalled carbon nanotubes, and polymers such as polyaniline can be used for photothermal cancer therapy as they can be injected and reach the local tumor area in a targeted manner and can be stimulated via near infra-red laser light to generate heat. There are magnetic nanoparticles such as iron oxide, doped iron oxide and superparamagnetic iron oxide nanoparticles that can be stimulated via alternating magnetic fields or microwaves to generate heat. Such magnetic nanoparticles can generate hyperthermia and increase the surrounding temperature to 42–45 °C. The mechanism of heat dissipation using MNPs involves a delay in the relaxation of the magnetic moments, either due to rotation within the particle (Néel) or due to rotation of the particle itself (Brownian) when an AC magnetic field is applied, in which the magnetic field reversal time is shorter than the magnetic moment relaxation of the nanoparticles.

The specific absorption rate (SAR) is the most important characteristic of any magnetic particle and can be defined as the rate of the electromagnetic energy absorption by a unit mass of biological material, with units of watts (W) per kilogram (kg). Moreover, the SAR is also proportional to the rate of the temperature rise (DT/Dt) due to energy absorption, when measurements are carried out in a short time and therefore the thermal conduction e_ects are minimal.

Hence:

SAR = [CeV] * (dT/dt) [341]

This relation is obtained from the Pennes bioheat equation. Using Equation (1), SAR is derived from P, which is the power absorbed by the material, and Ce, the specific heat capacity of the material, V is the volume of the sample, DT/dt is the change in temperature with respect to time.

3.1 OBJECTIVES.

Primary outcome

To evaluate super-paramagnetic iron oxide nanoparticles (SPIONs) therapeutic effect on triple-negative breast Cancer (TNBC) cell line MDA-MB-231.

Secondary outcomes

• To synthesize and characterize SPIONs that works as a drug carrier by using thermal decomposition method.

• Optimizing ferromagnetic core by doping with Co, Mn, Zn.

• In-vitro effects evaluation of nanoparticles by using several surfactants as PEG, CTAB, TX-100 and SDS.

• To test Docetaxel and Bicalutamide as well as CD-44 antibody as nanocargo in both negative control MRC-5 and positive control MDA-MB-231 TNBC cells.

• Analysis of the SPIONs chemo-hyperthermia effects over malignant cells MDA-MB-231.

3.1.1 HYPOTHESIS.

The Nano Magnetic Plasmonic platform is useful in the *"In Vitro"* therapeutic of the triple negative breast Cancer cell line (TNBC) MDA MB-231.

3.1.2 FLOWCHART.

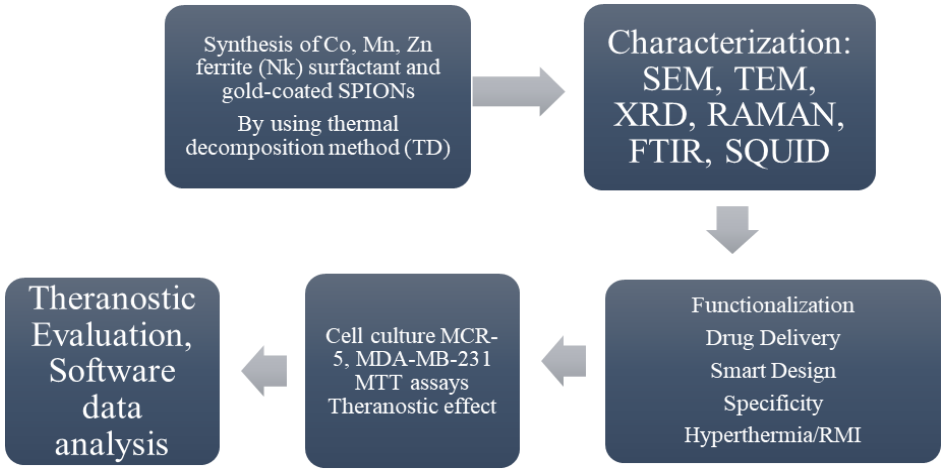

3.1.3 Type of design: Experimental.

Table 4. Operational variables definition

Variables	Conceptual definition	Operational definition	Dimensions	Indicators	Scale
Synthesis of SPIONs	Set of physical and chemical methods for the creation and manipulation of nanoscale materials between 1-100 nm	Its objective is the study, manipulation and design of nanoparticles capable of exercising theranostics in TNBC in vitro.	Size, shape, design, composition, monodispersity	In vitro cytotoxicity assays, confocal microscope, RMI, Hyper thermic behavior, HR-TEM, XRD, SQUID	Quantitative
Characterization of SPIONs	Set of techniques that allow to characterize nanomaterials, morphological structure, properties and chemical composition.	Its objective is the study of morphological as well as chemical and physical properties of nanoparticles capable of executing theranostics in TNBC in vitro.	Size, shape, design, composition, monodispersity	SEM, TEM, HR-TEM, RAMAN, XRD, FTIR, SQUID, UV-vis	Quantitative
Citotoxicity	A set of experimental techniques to analyze cell survival	Its objective is to analyze the therapeutic efficacy of nanoparticles in MDA-MB-231 and MRC-5 cell lines	Combined therapy (drugs-heat), theranostics	MTT Hyperthermia	Quantitative
Diagnostic	By using RMI analyzing NPs affinity for malignant cells MDA-MB-231	Its objective is to analyze the diagnostic efficacy of nanoparticles in MDA-MB-231 and MRC-5 cell lines	Combined therapy (drugs-heat), MRI theranostics.	MRI	Quantitative

3.1.4 Software for data processing: *IBM SPSS Statistics 21* and *OriginPro 9.0*

3.2 Synthesis methods in Nanotechnology.

The design and engineering of the nanoparticles depend on the application that is desired, the purpose in the field of application (semiconductors, medicine, fuels, etc.), thinking about the application the nanoparticle size, the chemical composition, the properties will be decided physical (electromagnetism, optics, etc.), crystallinity and shape (cubes, stars, spheres, rods, core-shell, etc.). All these variables can be controlled by temperature, pH value, concentration, chemical composition, nano-functionalization and standardization and reproducibility of the process.

There are two methods to produce nanoparticles: "Top down" and "Bottom up". The term "Top down" basically consists in the mechanical crushing “Mechanical milling” of the material using a grinding process. In the "Bottom-up" method, chemical processes such as precipitation processes, sol-gel processes, hydro-thermal processes, aerosol processes, spray hydrolysis etc.

3.2.1 Top Down: Mechanical grinding.

Mechanical grinding is used in the production of nanomaterials such as metal oxides that are pulverized using high energy ball mills. These mills are equipped with grinding media composed of wolfram carbide or steel.

The main disadvantage of the use of mills to crush particles, is that it produces powders with ranges of relatively large size, in addition the milling involves thermal stress that could contaminate the nanoparticles and requires a lot of energy. This method does not allow total control of the shape of the particle.

3.2.2 Bottom Up.

Bottom Up consists of physiochemical reactions of self-assembly and has the advantage of being able to produce more complex nanoparticles from atoms or molecules with better control of the nanoparticle size. The Bottom-Up processes are: 1.- Gas phase processes and 2.-Liquid phase processes.

3.2.2.1 Gas phase processes.

In these examples, the processes are carried out in flame (around 1500-2500 °K), plasma, laser and hot wall reactors. The nanoparticles are created by homogeneous nucleation, where at a certain temperature and after having traveled several phases with different free energies of Gibbs there is condensation (transition from the gaseous state to the liquid state of the aggregate) or coagulation (adhesion of two or more particles), as well as coalescence processes (particle fusion). The most used methods are aerosol and hydrolysis processes.

3.2.2.2 Liquid phase processes.

The hydro-thermal process, precipitation reactions, pyrolysis methods (using centrifugal forces, compressed air, ultrasonication, electrostatic forces) and sol-gel processes are the most used liquid phase processes at industrial level, however this work focuses on a process called *thermal decomposition*, so we are not going to delve into the rest.

3.2.3 Thermal Decomposition (TD).

Thermal decomposition synthesis is typically carried out at anaerobic conditions and temperatures well above the flash point of the organic vapors generated by the reaction mixture. One of the main advantages of this method is the enhanced shape and size control of the nanoparticles that the *Nanotechnologist* can get, the disadvantage for the applications in metallic oxides is the loss of the magnetic properties because the organometallic precursors in the absence of oxygen have yielded particles with mixed iron oxide phases, crystal defects, and poorer magnetic properties. To overcome this problem, Mythreyi Unni et al. propose the synthesis by using molecular oxygen injection, this research team reported having achieved single-crystalline iron oxide nanoparticles with few defects and enhanced magnetic properties [342].

3.3 Methodology: Magnetic core characterization.

Certainly, the morphological characteristics and structural properties of the SPIONs must be adequately verified before their administration in a biological model, be it cellular, animal or human. Clinical trials have shown that SPIONs can become very cytotoxic and

therefore to date the FDA has restricted its commercial use, since in the risk-benefit balance, the risks are even greater. However, clinical trials completed and reported by clinicaltrials.gov indicate that SPIONs are going to become a fundamental pillar in nanomedicine.

The iron oxide nucleus structure Fe_3O_4 (magnetite) must be characterized, since it is common that in physical-chemical processes, reactions that occur at high temperatures can lead to the formation of γ-Fe_2O_3 (maghemite) which isn't convenient to increase the control in the magnetic moment using an MRI system. Moreover, our working group decided to raise the bet in nanoengineering of these SPIONs using doping by substituting iron atoms for atoms of ***1.- Cobalt (Co), 2.- Manganese (Mn) and 3.- Zinc (Zn)***. Since in theory, the magnetic properties of iron oxides enhance when the addition of these elements take place.

In this work, Fe_3O_4 was used as a magnetic core to construct a SPION surfactant-coated nanoparticle. The surfactant that covers the magnetic core is essentially the only card we can play to evade the immune system, increase bioavailability, reduce toxicity in healthy cells and deliver the drug selectively to diseased tissue.

How do the nanoparticles escape from the immune system? The researchers responded by adding liposome layers, polyethylene glycol PEG coatings that reduce the recognition of macrophages (evacuation of the reticuloendothelial system), which increases the bioavailability and half-life of the drug [343]. Another useful coating could be SDS, CTAB or tween 20 [344].

Since much of the success of this nano design depends on the surfactant [304], our research group undertook the search for the ideal surfactant by exploring not only in the literature but in the laboratory.

The initial candidates were: 1.- Polyethylene glycol (PEG), 2.- Cetyl Trimethyl Ammonium Bromide (CTAB), 3.- Sodium Dodecyl Sulfate (SDS), 4.- Triton X-100.

3.3.1 Polyethylene glycol (PEG).

Polyethylene glycol (PEG) is a polyether compound which is currently/often used in medication as Nulytely™ (Asofarma labs) to evacuate intestine before to practice a

colonoscopy for example. PEG-coated is useful for avoiding immune response as a sort of disguise to nanoparticles (NPs). PEG was used as a coating at 3 different concentrations: 0.01 molar (M), 0.02 M and 0.03 M.

3.3.2 Cetyl Trimethyl Ammonium Bromide (CTAB).

The most celebrated useful quaternary ammonium surfactant has been used as an excellent stabilizer for synthesis of Gold nanoparticles. Many researchers have gotten different shapes as stars, nanorod, nanosphere, nano shell, etc.

Unfortunately, at higher concentrations, CTAB has shown teratogenic side effects. However, CTAB is one of the favorite surfactants for researchers still. We used 0.1 M, 0.2 M and 0.3 M to avoid undesirable side effects.

Example CTAB-Gold complex of reaction:

I.- $HAuCl_4$ + CTAB → CTA^+-$AuCl^-_4$ complex

II.- CTA^+-$AuCl^-_4$ complex + ascorbic acid → ascorbic acid radical + hydrochloric acid + $CTA\text{-}AuCl_3$

III.- The ascorbic acid radical and $CTA\text{-}AuCl_3$ react spontaneously to create metallic Au^0 nanoparticles.

3.3.3 Sodium Dodecyl Sulfate (SDS).

Anionic surfactant constituted by 12-carbon tail attached to a sulfate group, its amphiphilic properties allows SDS to be used in many cleaning and hygiene products and also genetic research. See Fig. 17. In the present work, we used 3 different concentrations (0.1 M, 0.2 M, 0.3 M) for coating $CoFe_2O_4$ NPs. **See Figure 17**

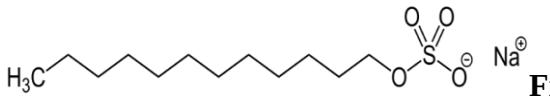

Fig 17. Representing SDS chemical structure

3.3.4 Triton X-100.

It is a nonionic surfactant that has a hydrophilic polyethylene oxide chain, on this work we used 0.1M, 0.2M and 0.3M concentrations. **See Fig. 18.**

Figure 18: Representing TX-100 chemical structure

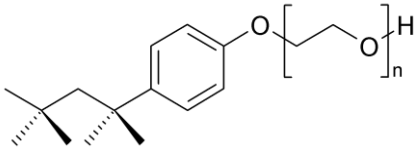

3.4 Material and methods: Synthesis of coated surfactant-nanoparticles.

The synthesis of nanoparticles of Fe_3O_4 magnetite doped with Cobalt was carried out by the process called ***Thermal Decomposition*** (TD), which consists of the reaction of a precursor compound that occurs by increasing the temperature (roughly 250-270°C) to produce two or more compounds. ***TD*** of this iron (III) acetyl acetonate 1 mmol (Sigma 97%) precursor plus Cobalt acetyl acetonate 0.5mmol (Sigma Aldrich 97%) plus an organic surfactant as polyethylene glycol (PEG) at 0.01, 0.02 and 0.03 Molar, Cetyl Trimethyl Ammonium Bromide (CTAB) at 0.1,0.2 and 0.3 Molar, Sodium Dodecyl Sulfate (SDS) at 0.1,0.2, 0.3 Molar and Triton X-100 (0.1,0.2,0.3 M), all the surfactants, each concentration separately onto 20 ml Benzyl-Ether (Sigma Aldrich 98%) solution. This leads the formation of monodisperse $CoFe_2O_4$.

$$\boldsymbol{AB \rightarrow C + D}$$

The mixture was placed in a volumetric flask connected to a cooling system driven by ice water and a pump to circulate the cold water inside a refrigerant tube and allow the reaction to be carried out for the required time. Under Nitrogen (N_2) atmosphere, during 10 minutes of exposure and a temperature of 260 °C, the solution was heated for 60 minutes until it acquires the characteristic dark color of magnetite.

The approximately 15 ml solution was left at room temperature for 24 hours and subsequently centrifuged in 5 cycles at 8,000 RPM, the first three adding 5ml of methanol 98% and the last two cycles adding 5ml water milli Q 800 Ohm.

Next, the milli Q water was distilled and 15 ml of bidistilled water was added. All solutions were standardized to physiological PH 7.35-7.45 using Mettler Toledo^{TM}. potentiometer. Finally, characterization showed the presence of $CoFe_2O_4$ nanoparticles of 5nm on average with superparamagnetic properties.

The coating is fundamental to get a uniform sample and enhanced biological capacities, otherwise $CoFe_2O_4$ would be toxic for *"In Vitro"* or animal model. Here, we discarded other surfactants as Tween-20, Tween-40, and in the end our best candidates were tested under different concentrations as mentioned above.

The same thermal decomposition technique with the respective calculations for Mn (Manganese acetyl acetonate 0.5mmol Sigma Aldrich technical grade) and Zn (Zinc acetyl acetonate 0.5mmol Alfa Aesar technical grade) was taken to engineer $MnFe_2O_4$ and $ZnFe_2O_4$ nanoparticles.

3.4.1 $CoFe_2O_4$ *In Vitro* and *In Vivo* cytotoxicity.

Cobalt alone is a genotoxic metal, has been shown to be carcinogenic in animal models and produces apoptosis by releasing ROS (reactive oxygen species). "*In Vitro"* cobalt toxicity is due to the presence of ionized cobalt [345]. However, cytotoxicity of $CoFe_2O_4$ particles has been published in different cell lines and vary from a range of between 15 to 50% decrease in viability [346]. Similar results were obtained for MDA-MB-231 ***(see chapter 4).*** Nevertheless, cobalt has been increasingly more important for researchers because it has been found to be essential in the cell metabolism, it is an important organo-metal in biological systems.

3.4.2 $MnFe_2O_4$ *In Vitro* and *In Vivo* cytotoxicity.

The human body requires Manganese to be able to perform the most basic vital functions such as the cellular respiration, in addition to the processes that protect the organism from oxidation as the reactions related to the superoxide dismutase path, which require Cobalt, Manganese and Zinc to work properly. Notwithstanding, "*In Vivo"*, manganese also is neurotoxic and competes with iron in the human body, it can cross the blood-brain barrier

and can reach the fetus through the placenta. The FDA states that the concentration in bottled water should not exceed 0.05 mg / L.

In animal model (rats) treated with high amounts of manganese alterations were observed in the kidney and urinary tract. "*In Vitro",* it produces stress and oxidative damage (ROS), alteration of energy metabolism and oxidative phosphorylation. Therefore, it is highly recommended to use a coated surfactant to avoid cytotoxicity of $MnFe_2O_4$ NPs [347].

3.4.3 $ZnFe_2O_4$ *In Vitro* and *In Vivo* cytotoxicity.

Zinc is an intracellular ion present in the cytoplasm and has great importance in cellular respiration, the elimination of free radicals, synthesis of DNA and RNA. The recommended intake of zinc for an adult is between 8 mg / day for women and 11 mg / day for men.

It has been demonstrated $ZnFe_2O_4$-NPs induced cellular and genetic damage *In Vitro* [348] due to the generation of ROS.

3.5 Core NPs characterization: Scanning Electron Microscopy (SEM), Transmission Electron Microscopy (TEM), X-Ray Diffraction, Raman Spectroscopy, FTIR.

The morphological characterization was performed using SEM and TEM microscopy, as well as XRD and Raman. SEM is just for external structure surface observation and surface characterization of inorganic and organic materials. However, delivery of morphological data was enough to ensure whether NPs synthesis was in the right direction.

An exploratory study was initiated to find the best surfactants and guarantee that we had indeed obtained magnetite. Fe_3O_4- PEG **(Figure 19)** surfactant was analyzed using SEM, XRD, Raman, FTIR, TEM at different concentrations.

3.5.1 Fe_3O_4 nanoparticles

Magnetite crystallizes in cubic form with the space group Fd3m and has 4 active modes of vibration belonging to the same species (T1u). The first one appears at 570 cm – 1 (Fe3 + td – O link) and the second one at 370 cm – 1 (Fe2 + link, 3 + oh – O). The energy at which the bands appear in this case is sensitive to the cation environment, with the highest energy appearing in the tetrahedral environment because it is subject to greater rigidity of the crystal lattice than in the octahedral environment. Characterization (SEM, XRD, Raman spectroscopy and IR) was performed on Fe_3O_4 nanoparticles coated with PEG at different concentrations **(Figures 19 and 20)**. Our results pointed out that magnetite is present in our samples for designing the nucleus as a first step towards to design core-shell nanoparticles.

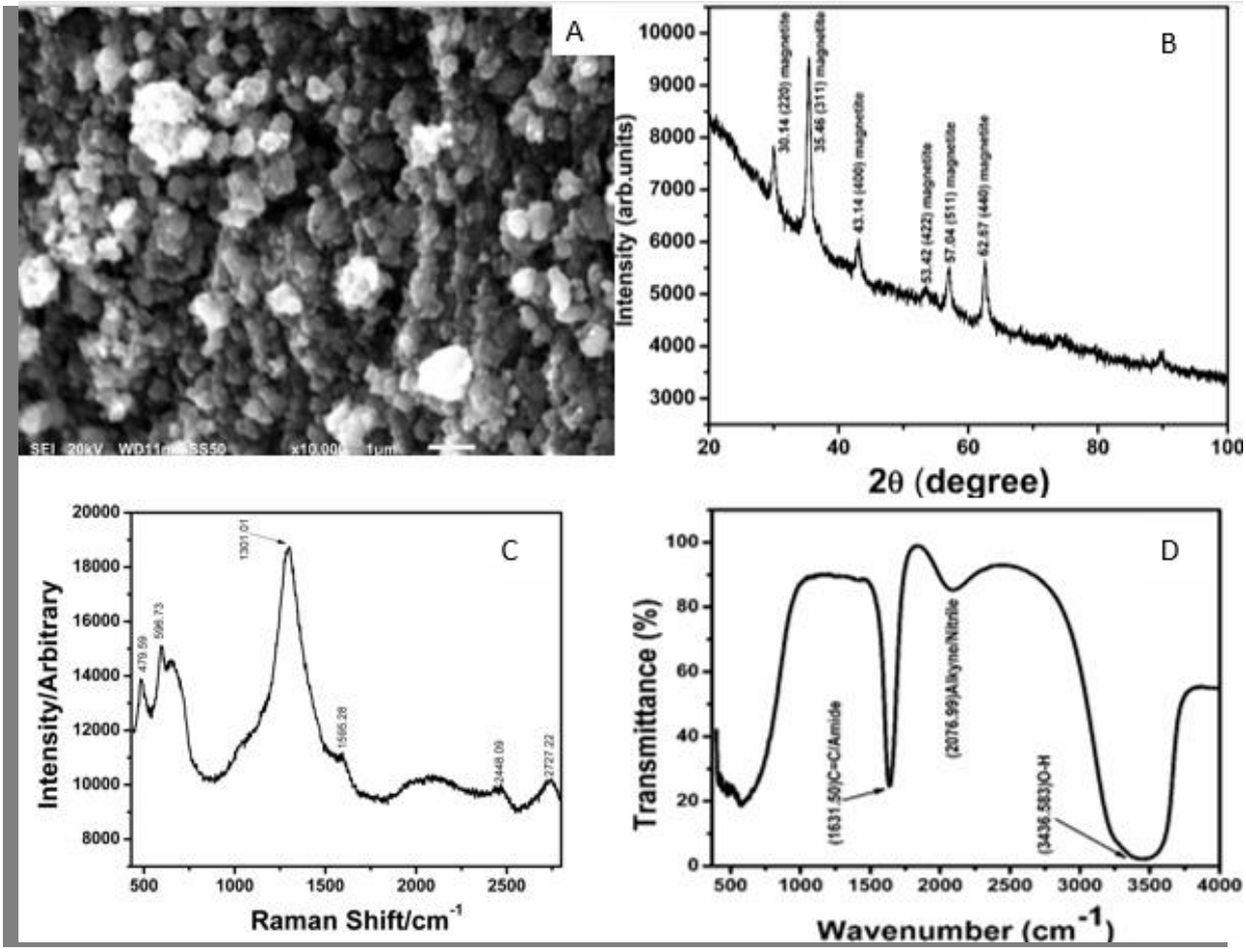

Figure 19: A) Morphological characterization of Fe_3O_4 PEG 0.01M Scanning Electron Microscope (SEM). B) Signaling of Fe_3O_4 PEG 0.01M XRD. C) Fe_3O_4 PEG 0.01M Raman spectroscopy. D) Fe_3O_4 PEG 0.01M IR. The presence of functional groups as O-H and NH_2 are revealed.

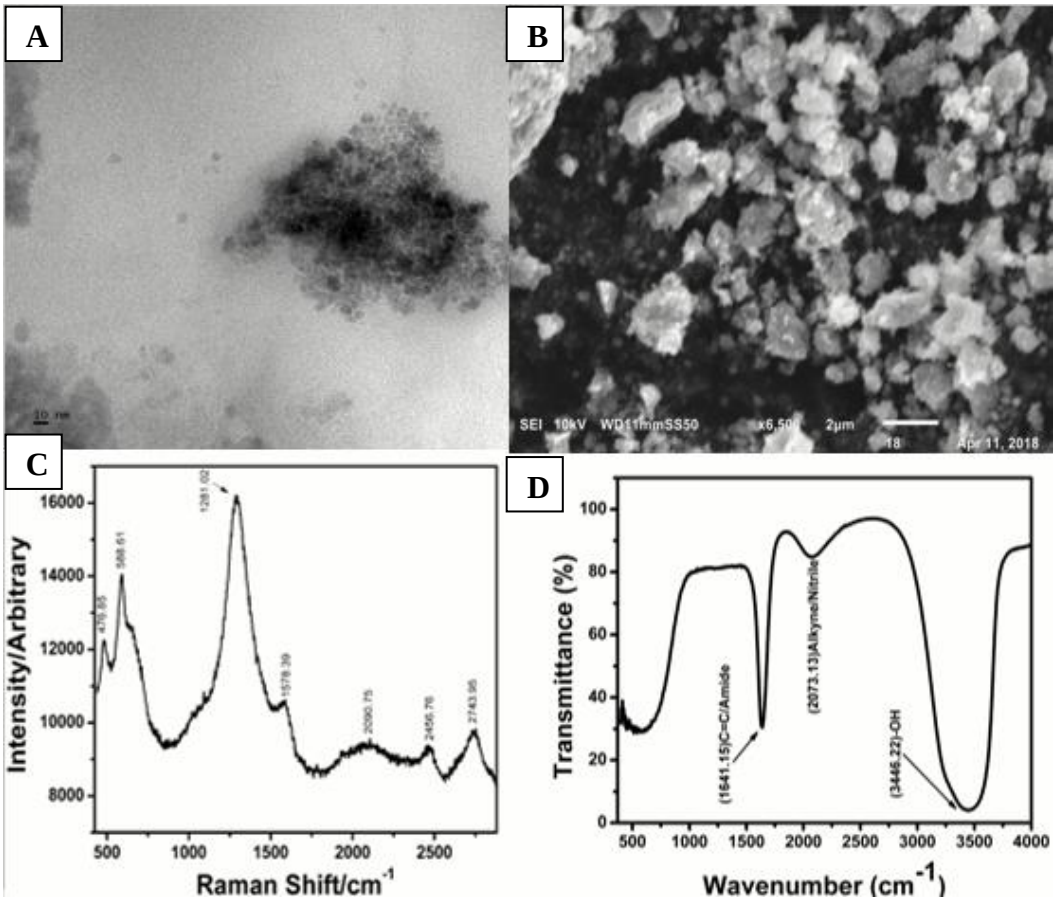

Figure 20: Fe_3O_4 PEG 0.02M. Representing characterization.

A) Fe_3O_4 PEG 0.02M Transmission Electron Microscopy (TEM)

B) Fe_3O_4 PEG 0.02M Scanning Electron Microscope (SEM)

C) Fe_3O_4 PEG 0.02M Raman Spectroscopy

D) Fe_3O_4 PEG 0.02M IR.

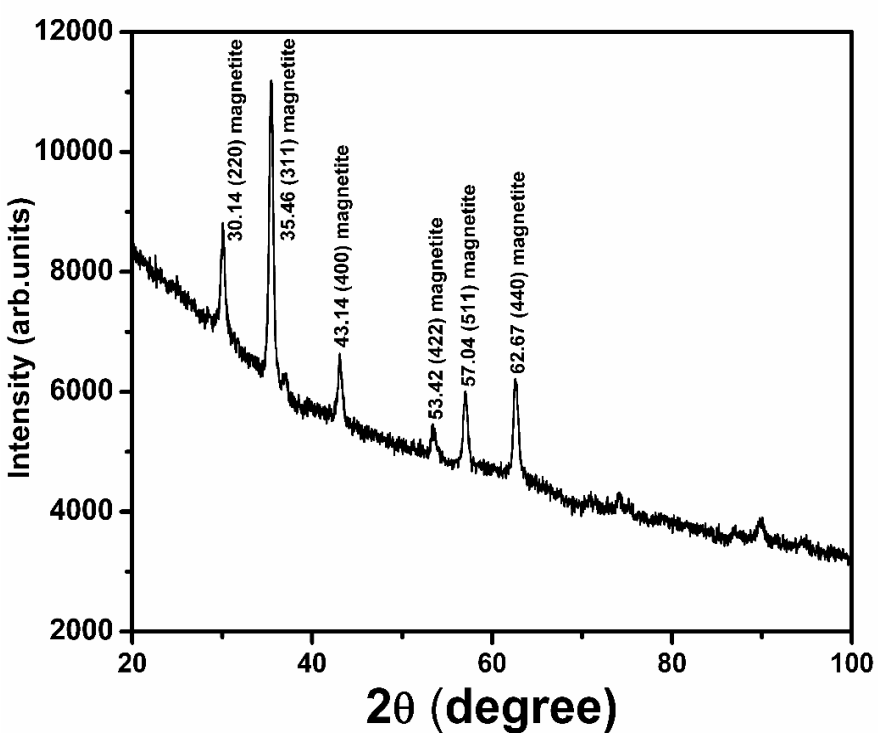

Figure 21. Fe_3O_4 PEG 0.02M XRD

The size and crystalline phase of the powdered iron oxide particles were identified by X-ray diffraction (XRD). Magnetite synthesis was carried out successfully. The image shows the peaks of data corresponding to magnetite.

Different concentrations of surfactants were tested. **Figure 22.**

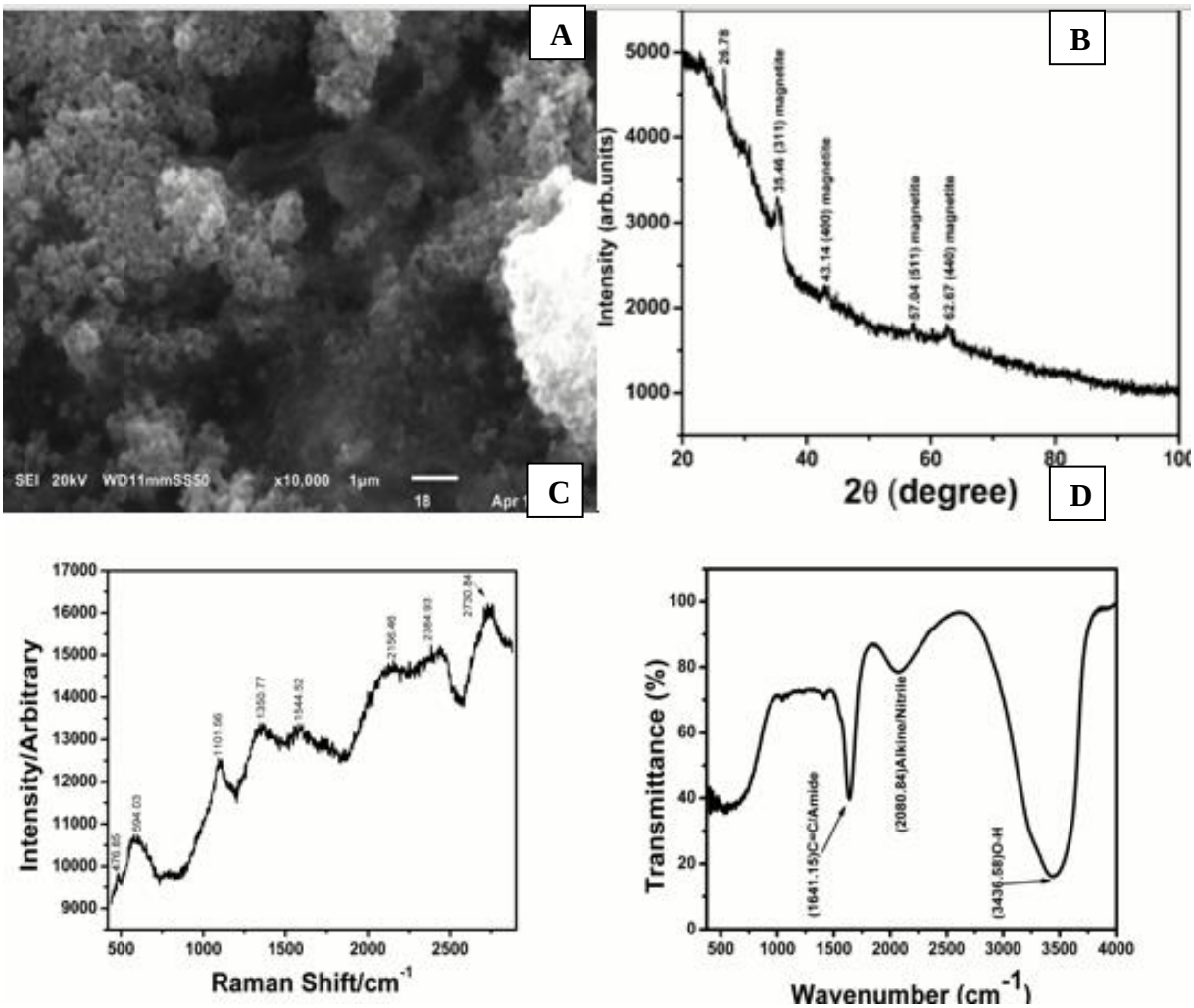

Figure 22: Fe_3O_4 PEG 0.03M characterization.

A) Fe_3O_4 PEG 0.03M Scanning Electron Microscope (SEM)

B) Fe_3O_4 PEG 0.03M XRD

C) Fe_3O_4 PEG 0.03M Raman Spectroscopy

D) Fe_3O_4 PEG 0.03M IR

In this way the different concentrations for the CTAB surfactant covering the magnetite were studied, confirming the presence of magnetite nanoparticles. However, the only suitable concentration turned out to be 0.1M. **Figure 23**.

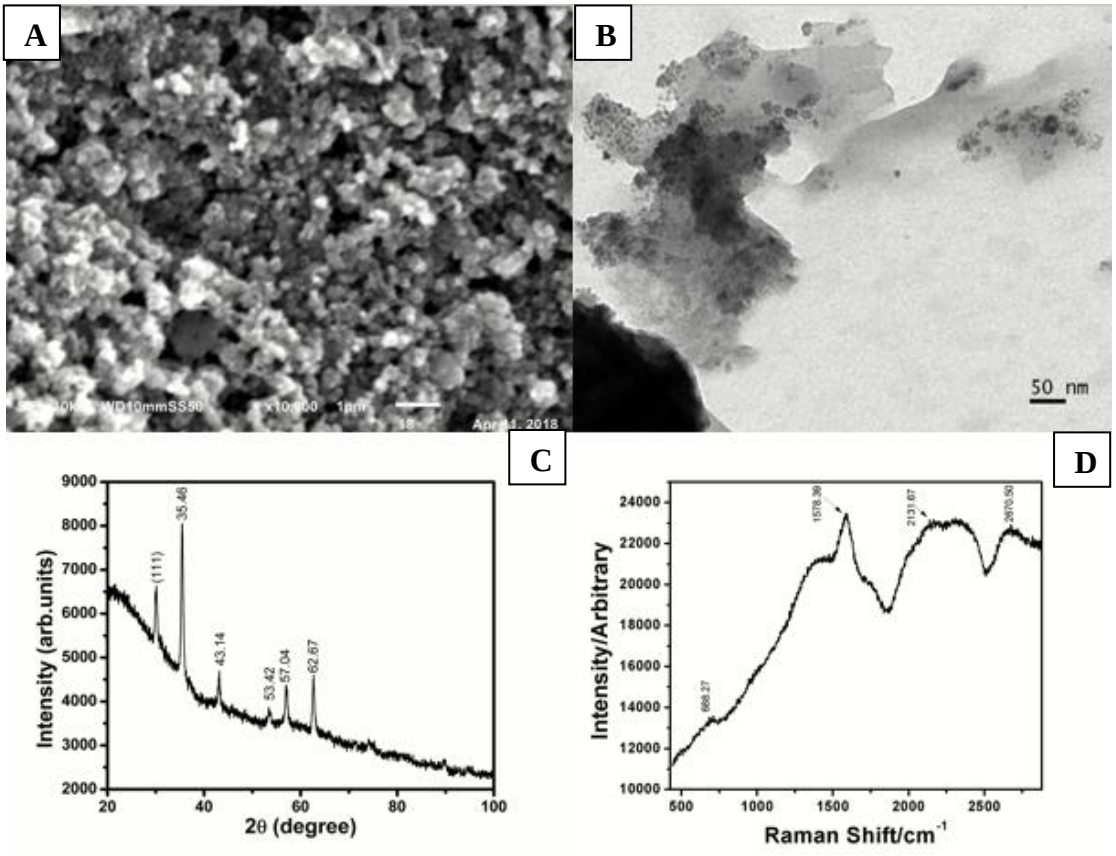

Figure 23. Fe_3O_4 CTAB 0.1M

A) Fe_3O_4 CTAB 0.1M SEM

B) Fe_3O_4 CTAB 0.1M TEM

C) Fe_3O_4 CTAB 0.1M XRD

D) Fe_3O_4 CTAB 0.1M Raman Spectroscopy

In the search for a third surfactant, our research group decided to use tween 20 at 0.3M, however this surfactant was discarded for its high cytotoxicity in normal cells and non-reproducible synthesis method. **Figure 24.**

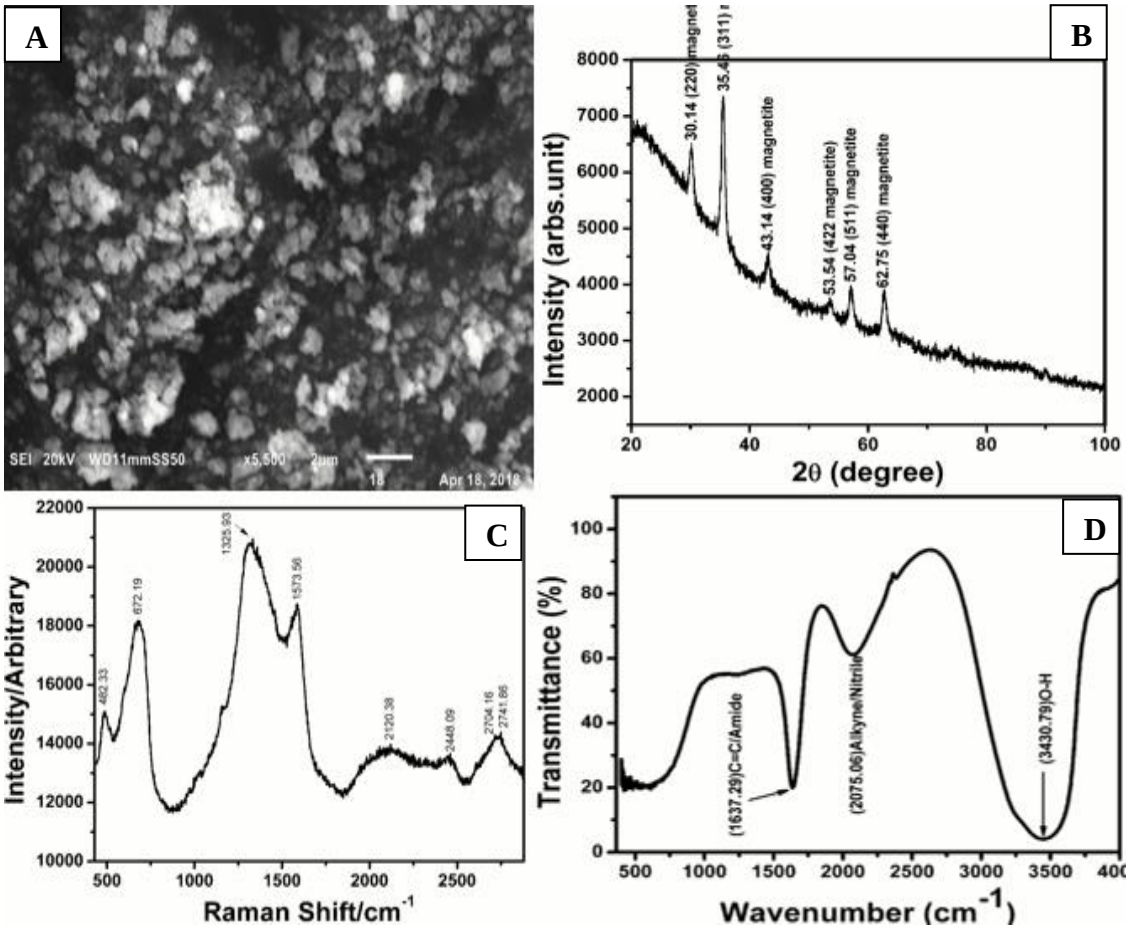

Figure 24. Fe_3O_4 Tween 20

A) Fe_3O_4 Tween 20 0.3M SEM

B) Fe_3O_4 Tween 20 0.3M XRD

C) Fe_3O_4 Tween 20 0.3M Raman Spectroscopy

D) Fe_3O_4 Tween 20 0.3M FTIR

Finally, our research group decided to explore the alternative of Triton-X-100 **(Fig.25)** and SDS **(Fig.26)** as a coating surfactant for Fe_3O_4 NPs by using the same surfactant concentrations (0.1 M, 0.2 M and 0.3 M).

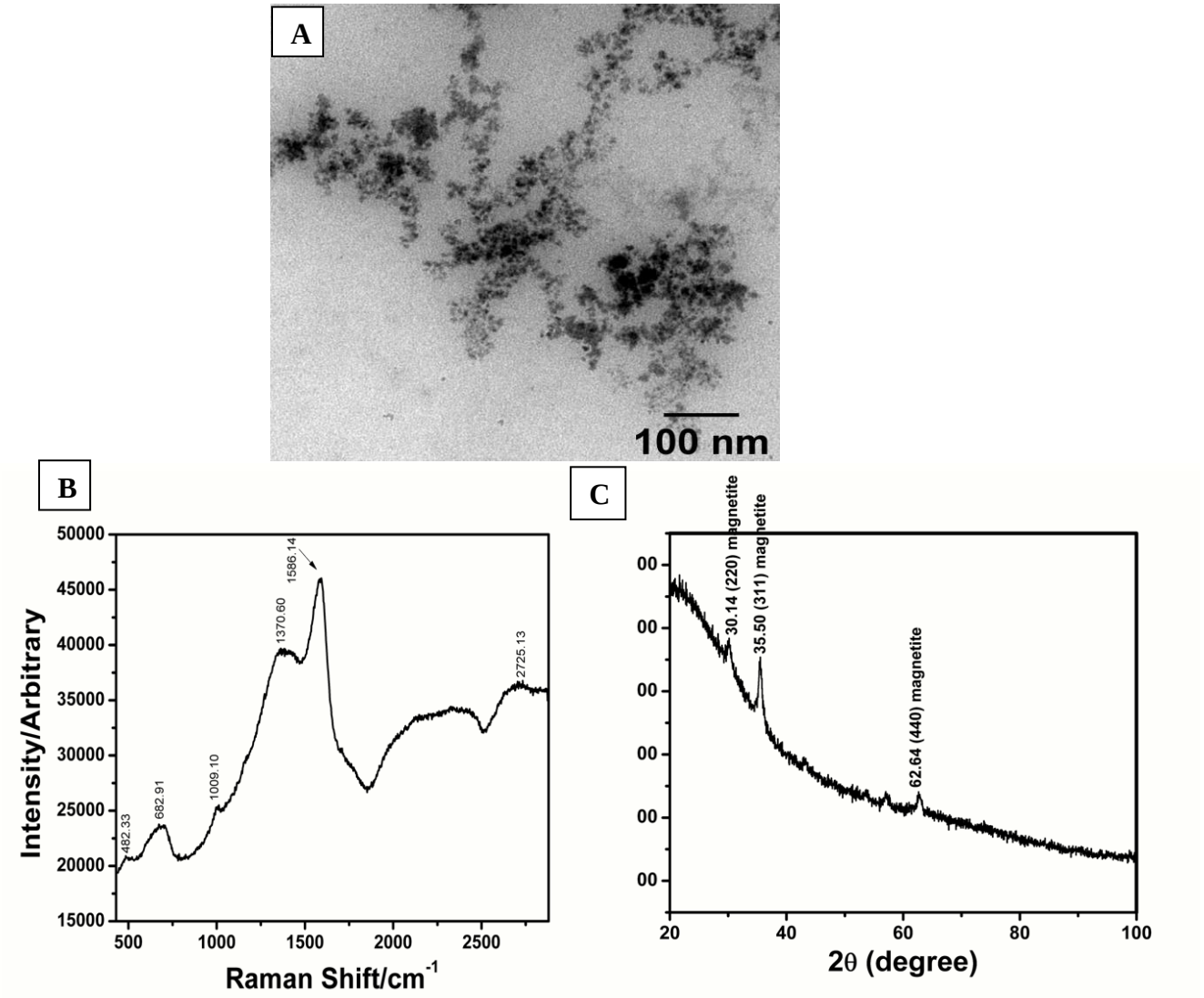

Fig. 25. Fe_3O_4 Triton-X-100 0.1M characterization.

A) Fe_3O_4 Triton-X-100 0.1M TEM (scale bar 100 nm)

B) Fe_3O_4 Triton-X-100 0.1M Raman

C) Fe_3O_4 Triton-X-100 0.1M XRD

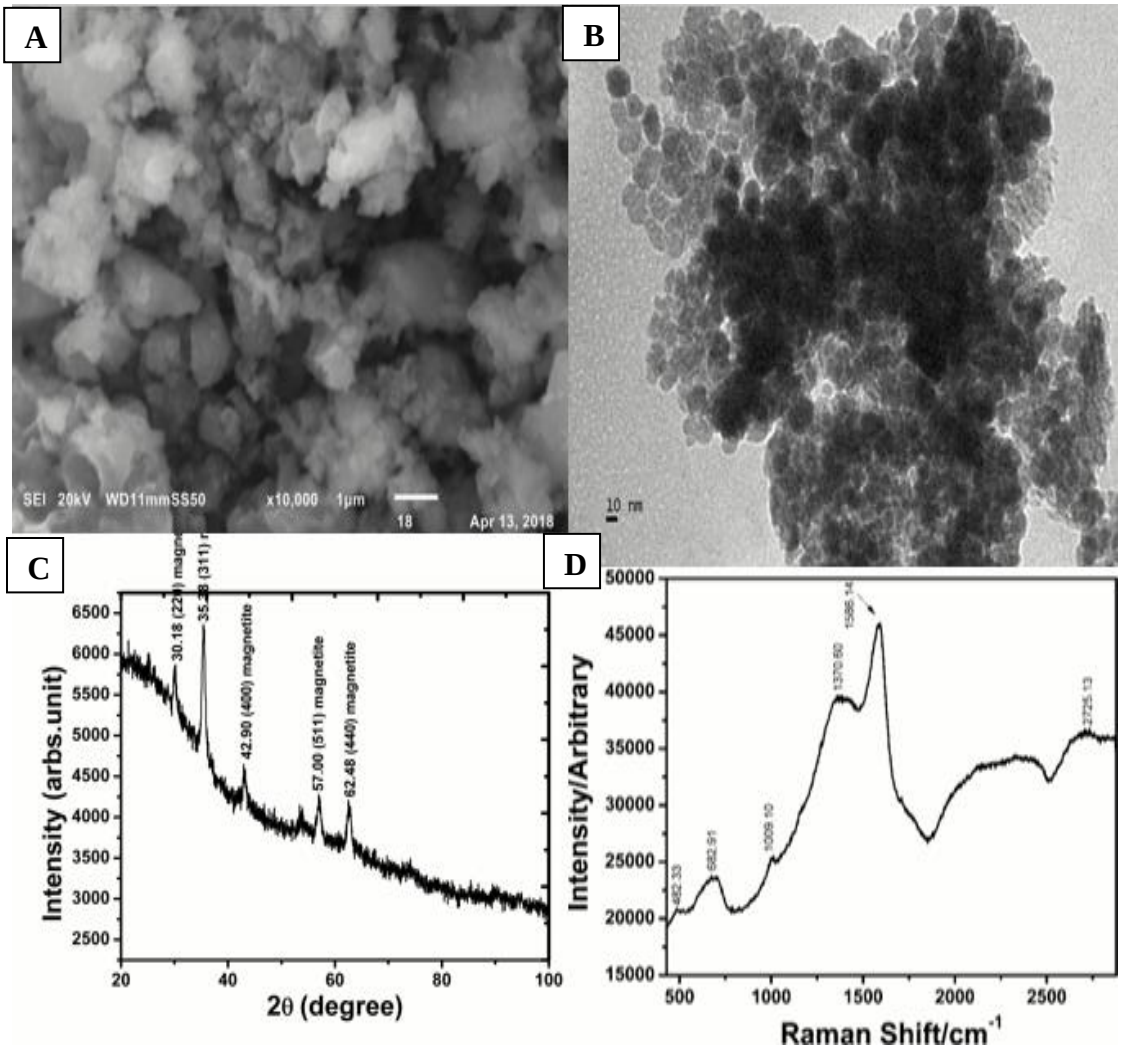

Figure 26: Fe_3O_4 SDS 0.1M characterization.

A) Fe_3O_4 SDS 0.1M SEM

B) Fe_3O_4 SDS 0.1M TEM (scale bar 10nm)

C) Fe_3O_4 SDS 0.1M XRD

D) Fe_3O_4 SDS 0.1M Raman Spectroscopy

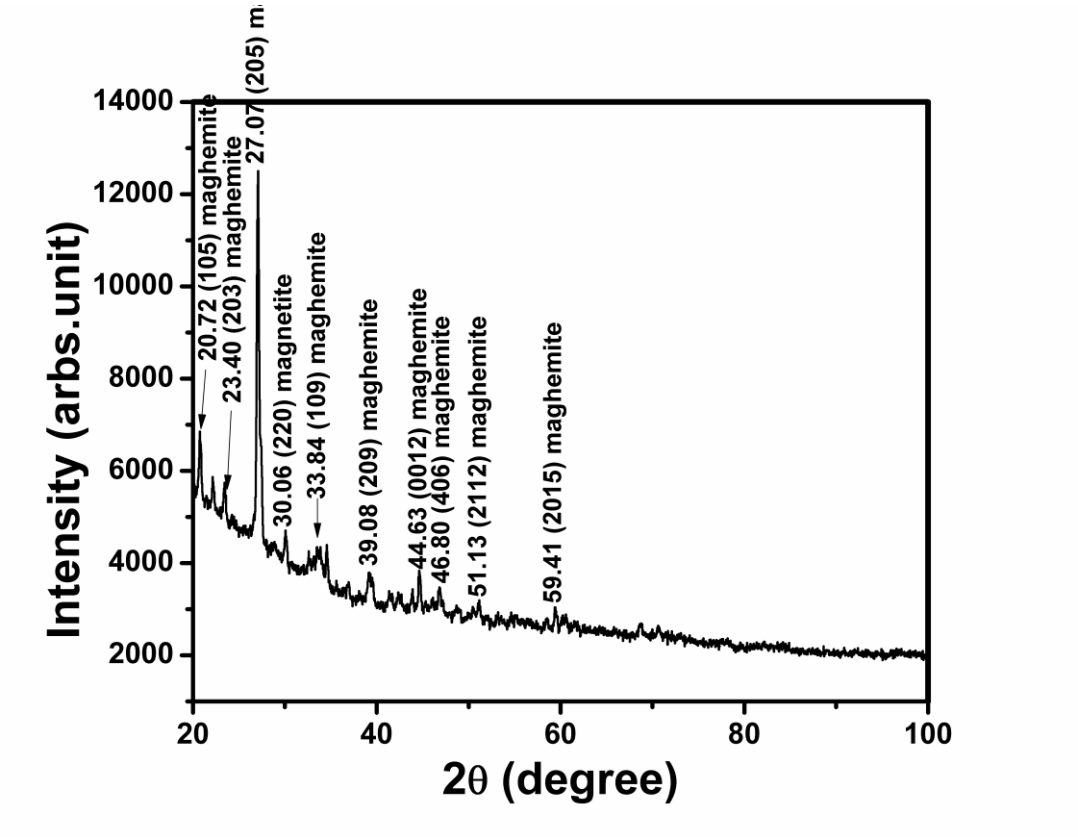

Figure 27. Fe_3O_4 SDS 0.4M XRD

After testing different NPs at different concentrations, we could discard those samples which are not reproducible. Here, a Fe_3O_4 SDS 0.4M XRD Sample showing maghemite instead magnetite. The presence of maghemite can be explained because during the oxidation of magnetite to maghemite there is a loss of symmetry elements when going from cubic to tetragonal, which allows the formation of γ-Fe2O3. Only the best reproducible samples were taken to move ahead with the project. Once the behavior of the surfactants with magnetite was identified, the next filter consisted of reproducibility. So, the work was continued using surfactants at specific concentrations, this time the magnetite was doped with Cobalt ($CoFe_2O_4$), Manganese ($MnFe_2O_4$) and Zinc ($ZnFe_2O_4$).

3.5.2 $CoFe_2O_4$ nanoparticles.

Based on morphology and cytotoxicity criteria (see next chapter), $CoFe_2O_4$ TX-100 0.1 M TEM nanoparticles were selected for the next step: Gold coated (core shell). Other several concentrations were characterized **Figure 28.**

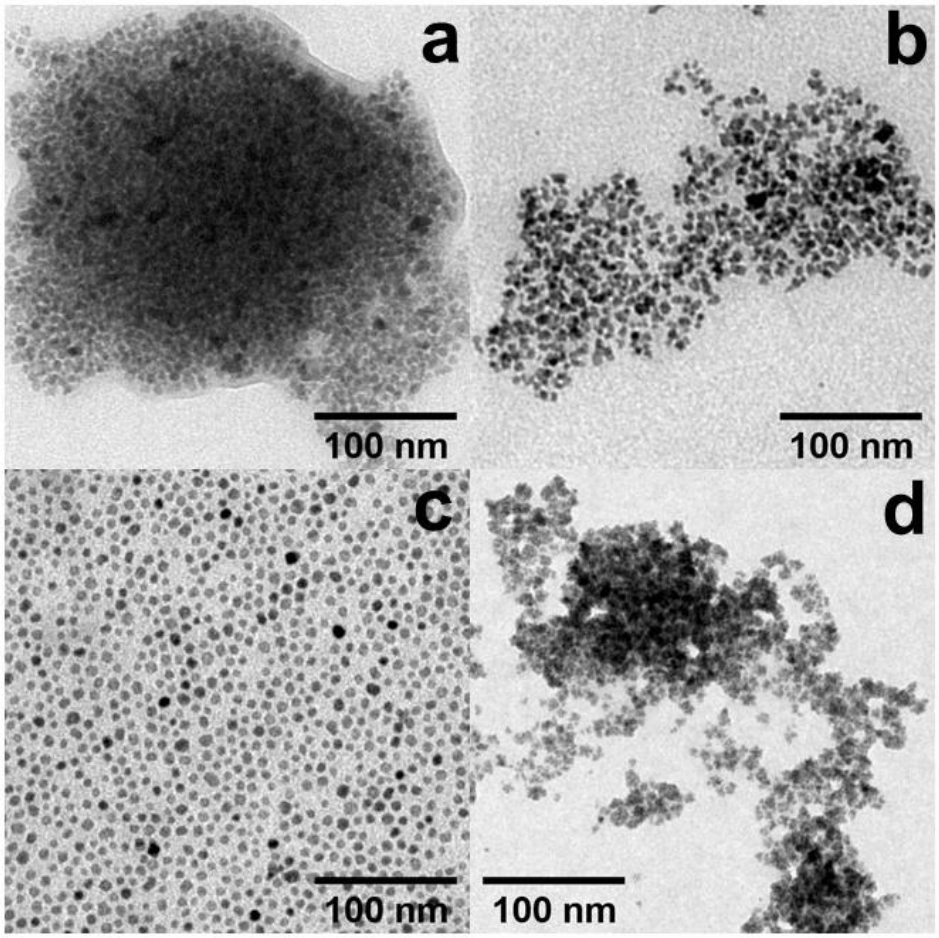

Figure 28. TEM microscopy of $CoFe_2O_4$ Nanoparticles

A) $CoFe_2O_4$ PEG 0.01 M TEM

B) $CoFe_2O_4$ CTAB 0.1 M TEM

C) $CoFe_2O_4$ TX-100 0.1 M TEM

D) $CoFe_2O_4$ SDS 0.1 M TEM

3.5.2.1 STEM-HAADF Sample $CoFe_2O_4$ PEG 0.02 M.

One of the various vantages of STEM-HAADF is to obtain images that allow us to see the morphology, size and elemental nature of different samples. In this case the electron microscopy statistical studies performed on a group of several NPs, reveled the formation of particles with a heterogeneous size distribution with average of 6.6 ± 2.92 nm as we can see in **Figure 29a**. **Figure 29b** at low magnification image, revels de heterogeneous sizes of NPs from 4 to 12 nm, differentness shapes and confirm no control in the size. **Figure 29c** shows an atomic resolution high-angle annular dark-field (STEM-HAADF) image. In this case, we found NPs which correspond to the Fe_3O_4 phase [110] zone axis. According to our analysis, we observe separate atomic positions in hexagonal arrangement: one bright spot in the center surrounded by ten atoms, in most cases. This arrangement suggests octahedral (FeB) and tetrahedral (FeA) atomic columns, shown in red and yellow, respectively.

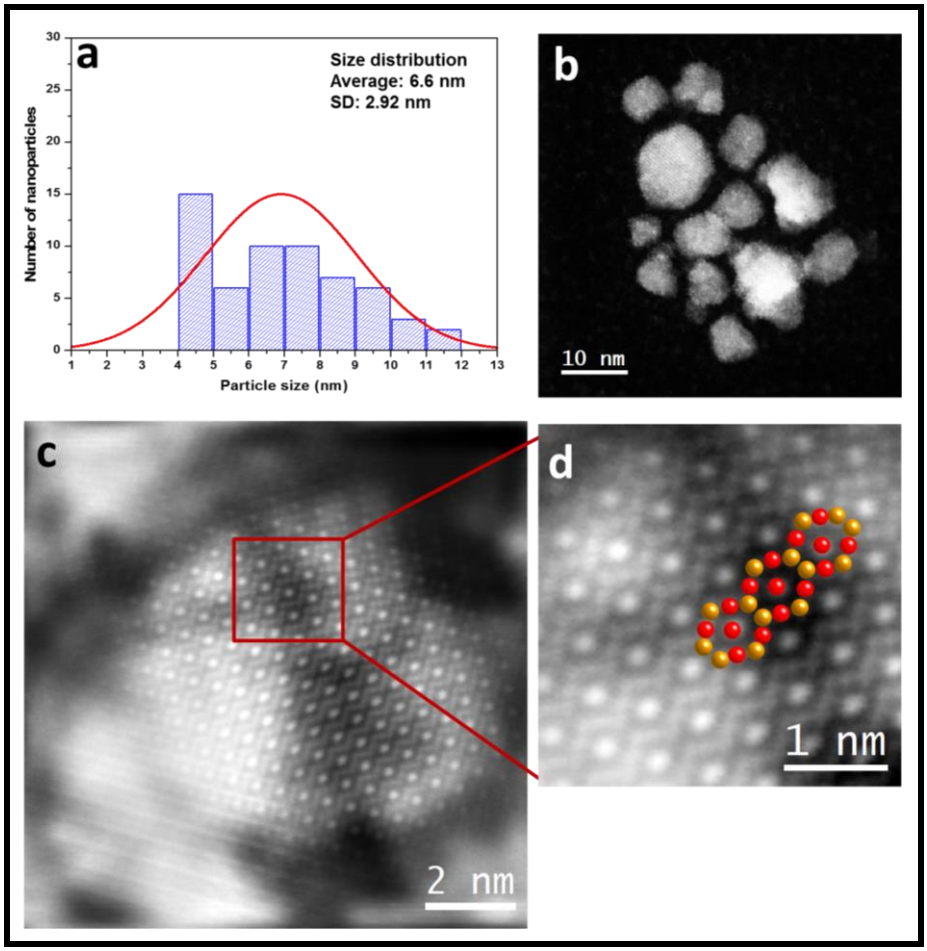

Figure 29. (a) Particle size distribution of $CoFe_2O_4$ PEG 0.02 M, (b) Low magnification Cs-corrected STEM-HAADF image of $CoFe_2O_4$ PEG 0.02 M showing differences sizes and morphology of NPs, (c) Cs-corrected STEM-HAADF image of $CoFe_2O_4$ PEG 0.02 M in this case the phase Fe_3O_4 is found, the white points represent atomic positions corresponding to Fe atoms, (d) High resolution of Fe_3O_4, octahedral (FeB) and tetrahedral (FeA) atomic columns are shown in red and yellow, respectively.

3.5.2.2 STEM-HAADF Sample $CoFe_2O_4$ CTAB 0.1 M.

The electron microscopy statistical studies performed on $CoFe_2O_4$ CTAB 0.1 M NPs are shown in the **Figure 30a**. The size distribution show average size of 5 ± 1.07 nm, as we can see the size is narrow between 3 to 9.5 nm, which means that we have homogeneous sizes and control during the NPs synthesis. The micrograph at low-magnification images showed in the **Figure 30b** illustrate good distribution, homogeneous sizes an agglomeration related with the magnetic moments of each NP. In the same zone, the **Figure 30c** was taken at high amplification, the zone marked in boxes show a square shape in the middle of an agglomeration of NPs, that kind of shape is frequently correlated with the precursors used during the synthesis. **Figure 30d**, shows the image taken by spherical aberration corrected (Cs-corrected) STEM-HAADF imaging. This NP corresponds to $CoFe_2O_4$ CTAB 0.1 M synthesis in which we can resolve atomic columns, Co and Fe atoms with planar distance of 0.442 nm. In the case of oxygen atoms when light atoms such as oxygen and heavy elements (Fe and Co) coexist in the same nanostructure, the contrast of the light elements is almost invisible in STEM-HAADF signal, in which the image is formed due to weak scattering when the scanning electron is transmitted through the sample. Due to the nature of STEM-HAADF measurements, the oxygen (atomic number 8) is very weak, compared to the high dispersion of the atomic number of Fe (26) and Co (27), for this reason it is difficult to identify the atomic position that corresponds to oxygen atoms. The substitution of the atoms for cobalt, takes advantage of the Fe – O movement of the tetrahedral and octahedral holes respectively.

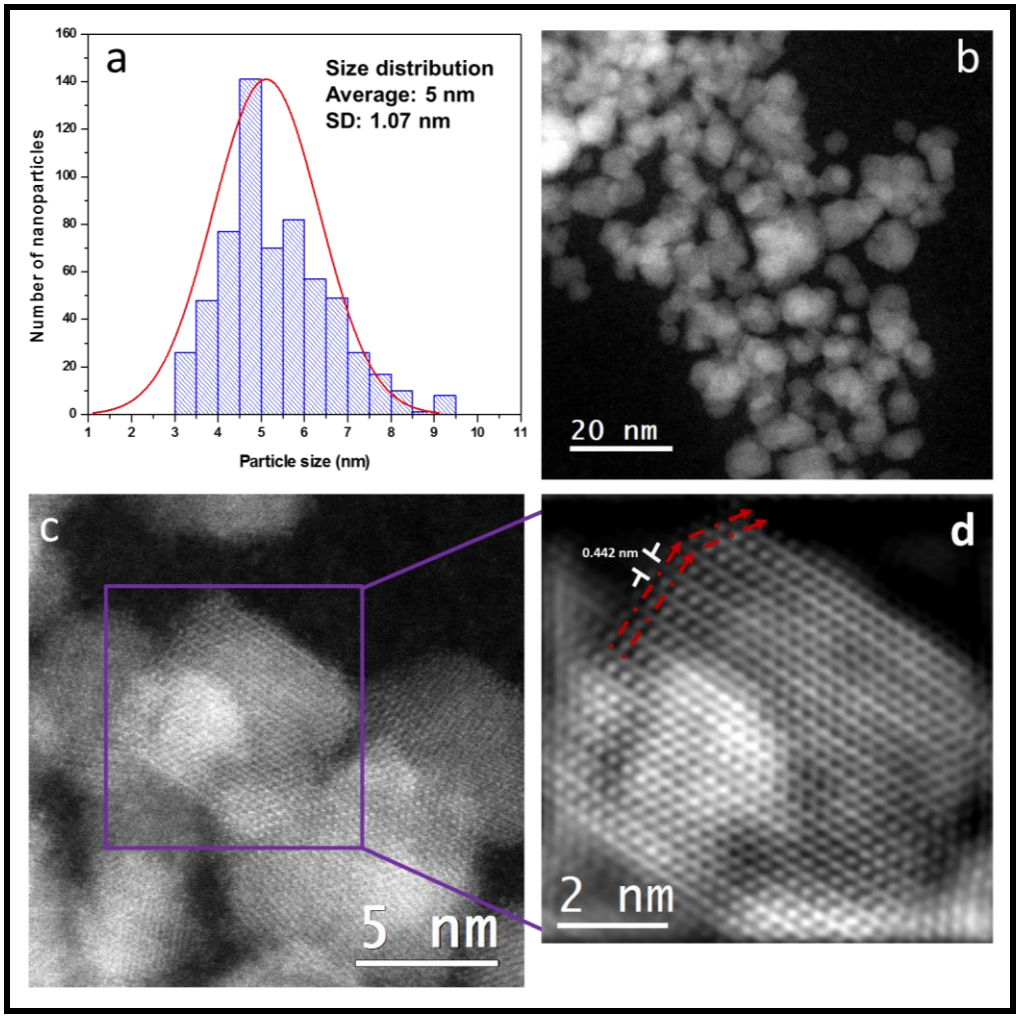

Figure 30. (a) Particle size distribution of $CoFe_2O_4$ CTAB 0.1 M, (b) Low magnification Cs-corrected STEM-HAADF image of $CoFe_2O_4$ CTAB 0.1 M showing a kind of agglomeration, with different sizes and morphologies of NPs, consistent with the LaMer and Dinegard theory where nucleation and growth processes are occurring at different times, promoting the growth of particles homogeneously. Operating in high conditions; temperature, stirring speed and dosing speed, the material suffers a decrease in size. (c) Cs-corrected STEM-HAADF image of $CoFe_2O_4$ CTAB 0.1 M, (d) Hight resolution of $CoFe_2O_4$ CTAB 0.1 M NPs showing atomic position, the white points representing atomic positions corresponding to Co and Fe atoms.

3.5.2.3 STEM-HAADF Sample $CoFe_2O_4$ TX-100 0.1 M.

Spherical aberration corrected (Cs-corrected) STEM-HAADF imaging technique was used for the statistical studies performed on several NPs, our analysis reveals very narrow sizes between 2 and 9 nm with average of 5.5 ± 1.2 nm of size as we can observe in the **Figure 31a. Figure 31b** revealed a very good NPs distribution, homogeneous sizes and spherical shapes, that allow us to say that we have a very good control in our synthesis. One of the important points is that we confirm the absence of smaller or larger NPs, due to control synthesis, reagent and precursors used during the synthesis. The chemical composition of the NPs was determined by spherical aberration corrected (Cs-corrected) STEM imaging. As we can observe in the **Figure 31c** $CoFe_2O_4$ NPs are formed with a spherical shape, the size of these NPs corresponds to 5 nm, the crystalline structure of these NPs can be described as a multi-twined NPs due to growing of atomic columns and defects in the nanostructure. An EDS profile spectrum performed along of these NPs are shown in the **Figure 31d**, the spectrum shows the elemental presence of Co, Fe and O correspond to NPs and C and Cu correspond to the grid.

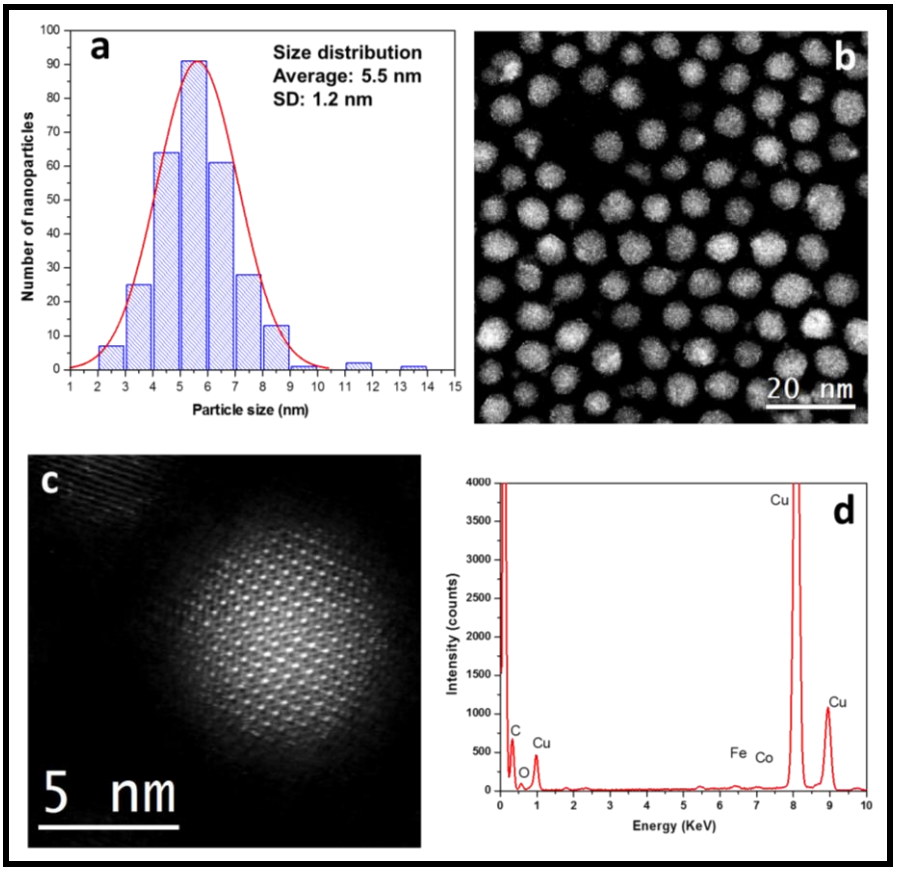

Figure 31. (a) Particle size distribution of $CoFe_2O_4$ TX100 0.1 M, (b) Low-magnification Cs-corrected STEM-HAADF image of $CoFe_2O_4$ TX100 0.1 M showing several NPs and a very narrow distribution, (c) Cs-corrected STEM-HAADF image of CoFe2O4 TX100 0.1 M showing very high resolution, the morphology correspond to spherical NP, (d) EDS profiles of $CoFe_2O_4$ TX100 0.1 M NPs, the spectrum show the elemental presence of Co, Fe, O correspond to NPs and C and Cu correspond to the grid.

Our material corresponds to a cubic spinel structure, it has octa and tetrahedral sites occupied by Fe + 2, Fe + 3 and O. The addition of Co, Mn and Zn atoms generate a substitution of octahedral tetrahedral iron. The addition of Co, Mn and Zn atoms does cause structural distortion but there is no change in the lattice parameter, because it is only a substitution for atoms. $CoFe_2O_4$ lattice parameter is preset, as shown in the following **table number 5**.

- Standard Formula: Fe_2CoO_4
- Alphabetic Formula: $CoFe_2O_4$
- Published Formula: $CoFe_2O_4$
- Refined Formula: $CoFe_2O_4$
- Wyckoff Sequence: 227,ecb
- Z Formula Units: 8

Published Data	**Standardized Data**		
	Unit Cell	**Niggli-Reduced Cell**	
Space Group	Fd-3m O2 (227)	Fd-3m O2 (227)	–
a	0.8413 nm	0.8413 nm	0.59489 nm
b	0.8413 nm	0.8413 nm	0.59489 nm
c	0.8413 nm	0.8413 nm	0.59489 nm
α	90°	90°	60.°
β	90°	90°	60.°
γ	90°	90°	60.°
a/b	1.000	1.000	1.000
b/c	1.000	1.000	1.000
c/a	1.000	1.000	1.000
V	0.59546 nm3	0.5955 nm3	0.14887 nm3

Source: https://materials.springer.com/isp/crystallographic/docs/sd_1821405

3.5.2.4 STEM-HAADF Sample $CoFe_2O_4$ SDS 0.1 M.

The electron microscopy statistical studies performed on several groups of NPs, obtained by a chemical synthesis, revealed the formation of agglomerated nanoparticles with a heterogeneous size distribution with average diameter of 4.5 ± 0.9 nm, the rage is between 2.5 to 9.5 nm as we can see in the **Figure 32a**. An image obtained in STEM-HAADF at low magnification shows the agglomeration of NPs **Figure 32b**, this phenomenon we correlated with the precursors used during the synthesis. **Figure 32c and 32d** shows an image with an interplanar distance of 0.256 nm corresponding to the $CoFe_2O_4$ phase. In this image, we can observe some sub-nanoparticles that formed 5 nm NPs. Finally, these results are showing that we do not have control and dispersion regarding this synthesis.

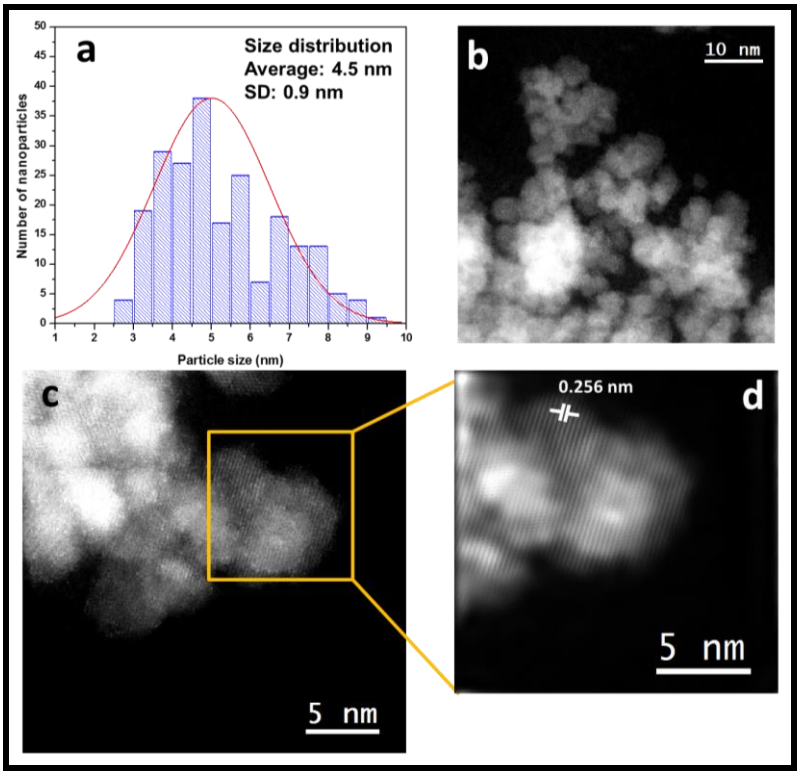

Figure 32. (a) Particle size distribution of $CoFe_2O_4$ SDS 0.1 M, (b) Low magnification Cs-corrected STEM-HAADF image of $CoFe_2O_4$ SDS 0.1 M showing agglomeration of NPs, (c) Cs-corrected STEM-HAADF image of $CoFe_2O_4$ SDS 0.1 M, (d) Hight resolution of $CoFe_2O_4$ SDS 0.1 M NPs showing interplanar distance.

3.5.3 STEM-HAADF $MnFe_2O_4$ nanoparticles.

TD of iron (III) acetyl acetonate 1 mmol (Sigma 97%) precursor plus Mn (Manganese acetyl acetonate 0.5mmol Sigma Aldrich technical grade) plus an organic surfactant as polyethylene glycol (PEG) at 0.01, 0.02 and 0.03 Molar, Cetyl Trimethyl Ammonium Bromide (CTAB) at 0.1, 0.2 and 0.3 Molar, Sodium Dodecyl Sulfate (SDS) at 0.1, 0.2, 0.3 Molar and Triton X-100 (0.1, 0.2, 0.3 M), all the surfactants, each concentration separately onto 20 ml Benzyl-Ether (Sigma Aldrich 98%) solution. This leads the formation of monodisperse iron oxide doped nanoparticles ($MnFe_2O_4$). The mixture was placed in a volumetric flask connected to a cooling system driven by ice water and a pump to circulate the cold water inside a refrigerant tube and allow the reaction to be carried out for the required time. Under Nitrogen (N_2) atmosphere, during 10 minutes of exposure and a temperature of 260 ° C, the solution was heated for 60 minutes until it acquires the characteristic dark color of magnetite. The approximately 15 ml solution was left at room temperature for 24 hours and subsequently centrifuged in 5 cycles at 8,000 RPM, the first three adding 5ml of methanol 98% and the last two cycles adding 5ml water milli Q 800 Ohm. Finally, the milli Q water was distilled and 15 ml of bidistilled water was added. All solutions were standardized to physiological PH 7.35-7.45 using Mettler Toledo^{TM}. potentiometer. The next step, characterization showed the presence of $MnFe_2O_4$ nanoparticles of 5 nm on average with superparamagnetic properties.

The use of a technic of STEM-HAADF like state-of-the-art means to do an atomic characterization, in this context the micrographics obtained allow us to see the morphology, size and elemental nature of different samples. In this study the electron microscopy statistical studies performed on a group of several NPs revealed a very good formation of spherical nanoparticles as we can observe in the **Figure 33a** with a heterogeneous size distribution with average of 5.24 ± 1.54 nm shows in the **Figure 33b**.

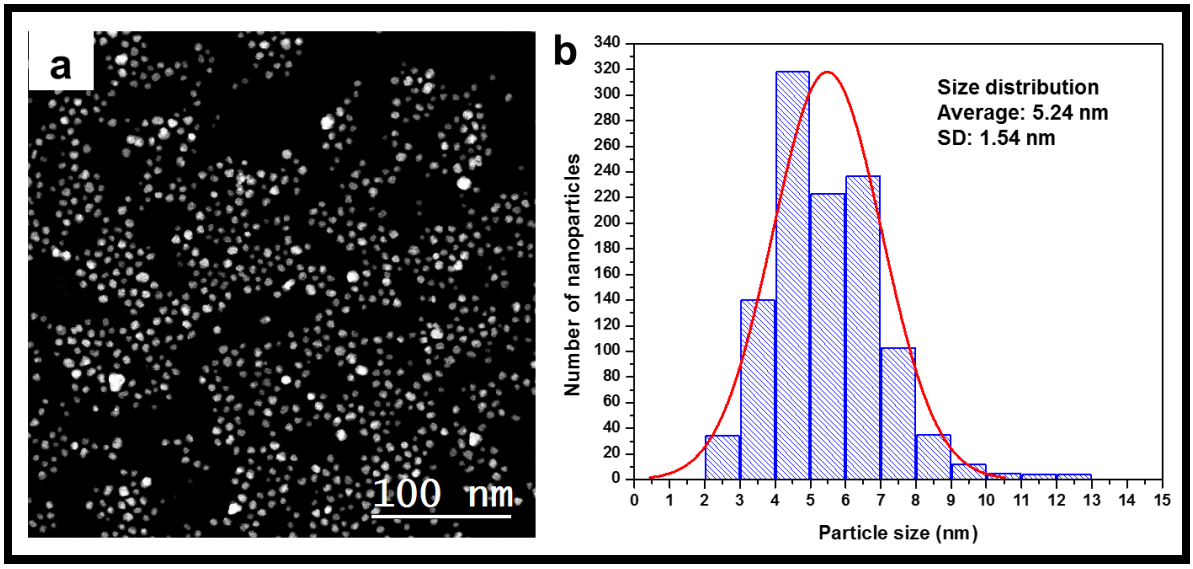

Figure 33. Nanoparticles were mono-disperse with spherical shape (a) Low magnification Cs-corrected STEM-HAADF image of $MnFe_2O_4$ PEG 0.02 M showing differences in sizes and morphology of NPs, (b) Particle size distribution of $MnFe_2O_4$ PEG 0.02 M. The average particles size is 5.2 nm.

A group of NPs (**Figure 34a)** at high magnification image reveals the heterogeneous sizes of NPs. The uniform 5 nm spherical shapes confirm our control in this synthesis. **Figure 34b** shows the FFT of a single NP with (311) and (220) and **Figure 34c** shows an image of a particle of $MnFe_2O_4$ PEG 0.02 M taking in high resolution Cs-corrected STEM-HAADF mode.

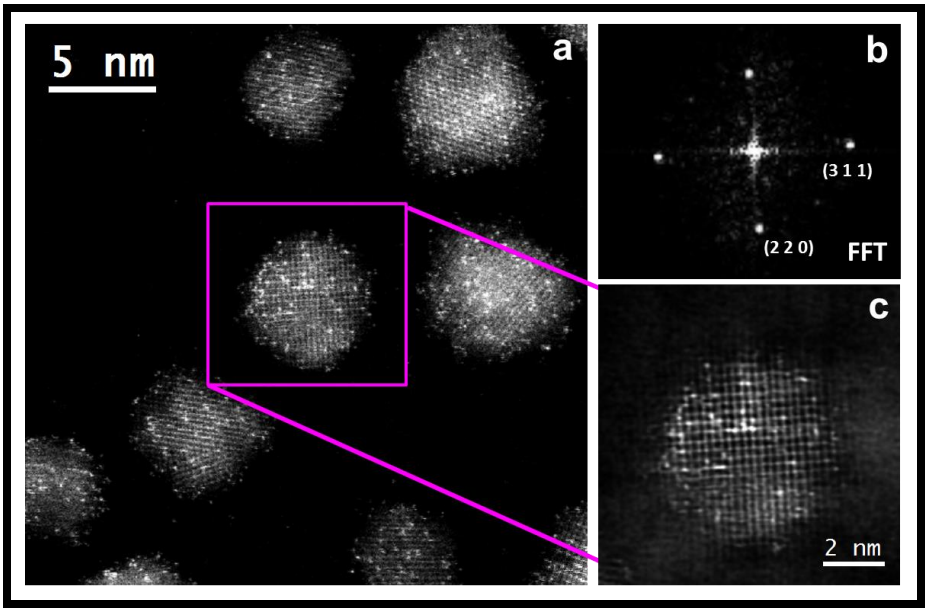

Figure 34. (a) Image of particle distribution of $MnFe_2O_4$ PEG 0.02 M showing a spherical shape in high resolution Cs-corrected STEM-HAADF mode, (b) FFT image of a single $MnFe_2O_4$ PEG 0.02 M nanoparticle and (c) image of a single NPs in high resolution taking in Cs-corrected STEM-HAADF mode.

3.5.3.1 Sample $MnFe_2O_4$ CTAB 0.1 M.

The conventional high-resolution transmission electron microscopy (HRTEM) studies performed on $MnFe_2O_4$ CTAB 0.1 M are shown in the **Figure 35.** The NPs size distribution corresponds to a 5 nm average as we can see in the **Figure 35a**. The HRTEM analysis allowed us to observe a spherical shape and morphology. The micrograph at high-magnification images showed good distribution, homogeneous sizes agglomeration related with the magnetic moments of each NP. In the **Figure 35b** taking at high amplification, showed a NP with size of 10 nm with an irregular shape correlated with an agglomeration of NPs, those kind of shapes in most of the cases are correlated with some of the precursors used during the synthesis process.

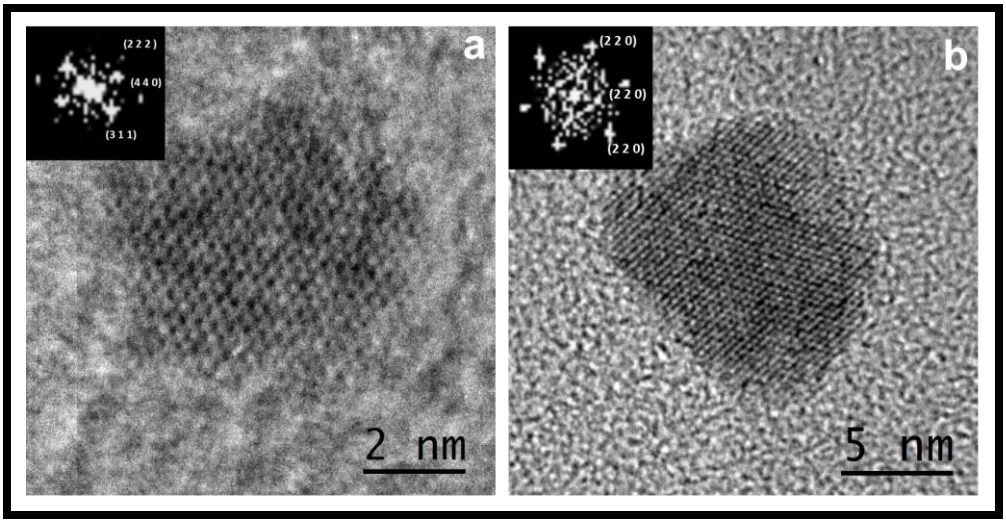

Figure 35. (a) Single NP of $MnFe_2O_4$ CTAB 0.1 M taking in HRTEM, FFT insert in the left position and (b) Irregular NP at high magnification HRTEM image of $MnFe_2O_4$ CTAB 0.1 M showing high resolution, FFT insert in top left position.

3.5.3.2 Sample $MnFe_2O_4$ TX100 0.1 M

The use of a technic of HRTEM allowed us to do an atomic characterization, in this context the micrographics obtained allowed us to see the morphology, size and distribution of different samples. In this study, the electron microscopy statistical studies performed on a group of several NPs revealed a very good formation of spherical nanoparticles and excellent distribution as we can observe in the **Figure 36** having a heterogeneous size distribution of 5.24 ± 1.54 nm average.

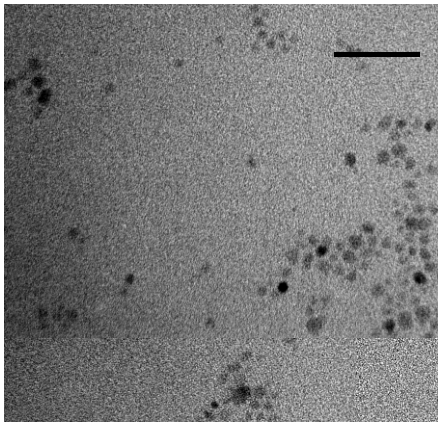

Figure 36. HRTEM image of $MnFe_2O_4$ TX100 0.1 M showing good distribution and spherical NP-morphology.

In order to confirm the particle size and morphology of the $MnFe_2O_4$ TX-100 0.1 M NPs, conventional high-resolution transmission electron microscopy (HRTEM) studies were carried out. **Figure 37** shows an image at high magnification, as we can observe most of the NPS showing a kind of agglomeration that is correlated with the strong magnetic moments between the NPs, the size of the agglomerations is in the range of 2 to 5 nm. To use a HR-TEM technic allow us to confirm the formation of NPs like morphology agglomeration with smaller size, the FFT is insert showing the (220) planes.

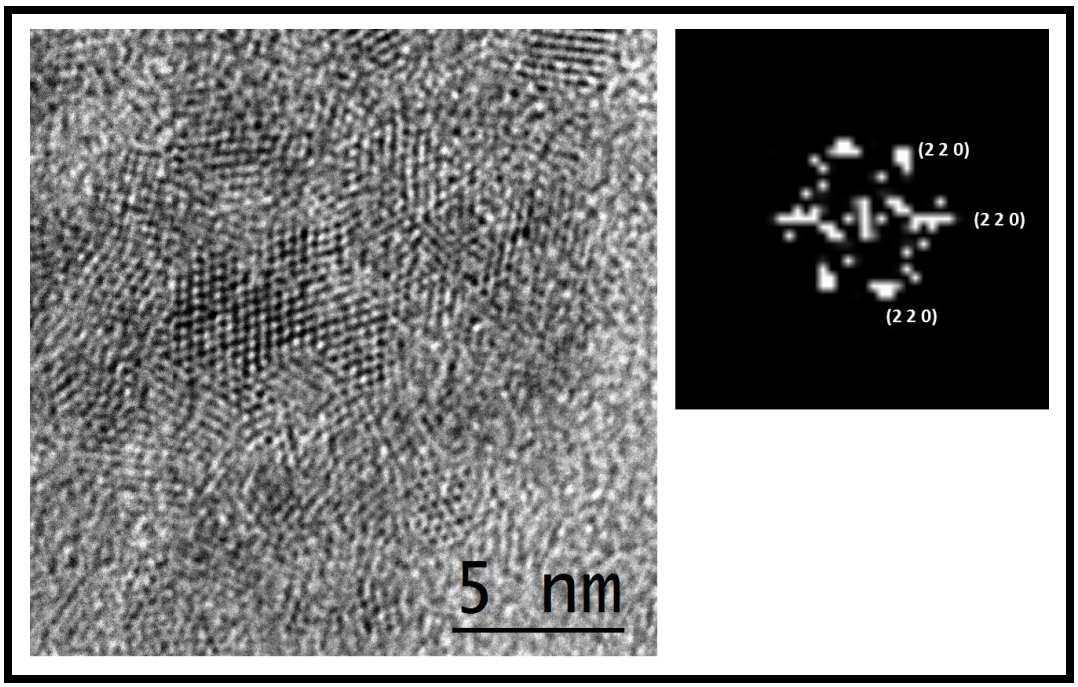

Figure 37. Image reveals a group of TX-100 0.1 M NPs, high magnification image reveals the heterogeneous sizes of NPs which size correspond at 2 nm with spherical shapes and the FFT of a single NP with (200) planes correspond to PEG 0.02 M NPs.

$MnFe_2O_4$ lattice parameter is showing in the next **table No. 6.**

- Standard Formula: $MnFe_2O_4$
- Alphabetic Formula: Fe_2MnO_4
- Published Formula: $MnFe_2O_4$
- Refined Formula: –
- Wyckoff Sequence: –
- Z Formula Units: 8
- Density: $\rho = 4.96\ Mg \cdot m^{-3}$

Published Data	Standardized Data		
	Unit Cell	Niggli-Reduced Cell	
Space Group	Fd-3m O2 (227)	Fd-3m O2 (227)	–
a	0.8515 nm	0.8515 nm	0.6021 nm
b	0.8515 nm	0.8515 nm	0.6021 nm
c	0.8515 nm	0.8515 nm	0.6021 nm
α	90°	90°	60.°
β	90°	90°	60.°
γ	90°	90°	60.°
a/b	1.000	1.000	1.000
b/c	1.000	1.000	1.000
c/a	1.000	1.000	1.000
V	0.61738 nm3	0.6174 nm3	0.15434 nm3

3.5.4 $ZnFe_2O_4$ Nanoparticles

The size and morphology of a series of $ZnFe_2O_4$ using different surfactants such as PEG, CTAB and TX-100 were investigated using both TEM **(Figure 38)** and High-Resolution Transmission Electron Microscope (HRTEM) TEM JEM2010 FEG JEOL. **Figure 39**.

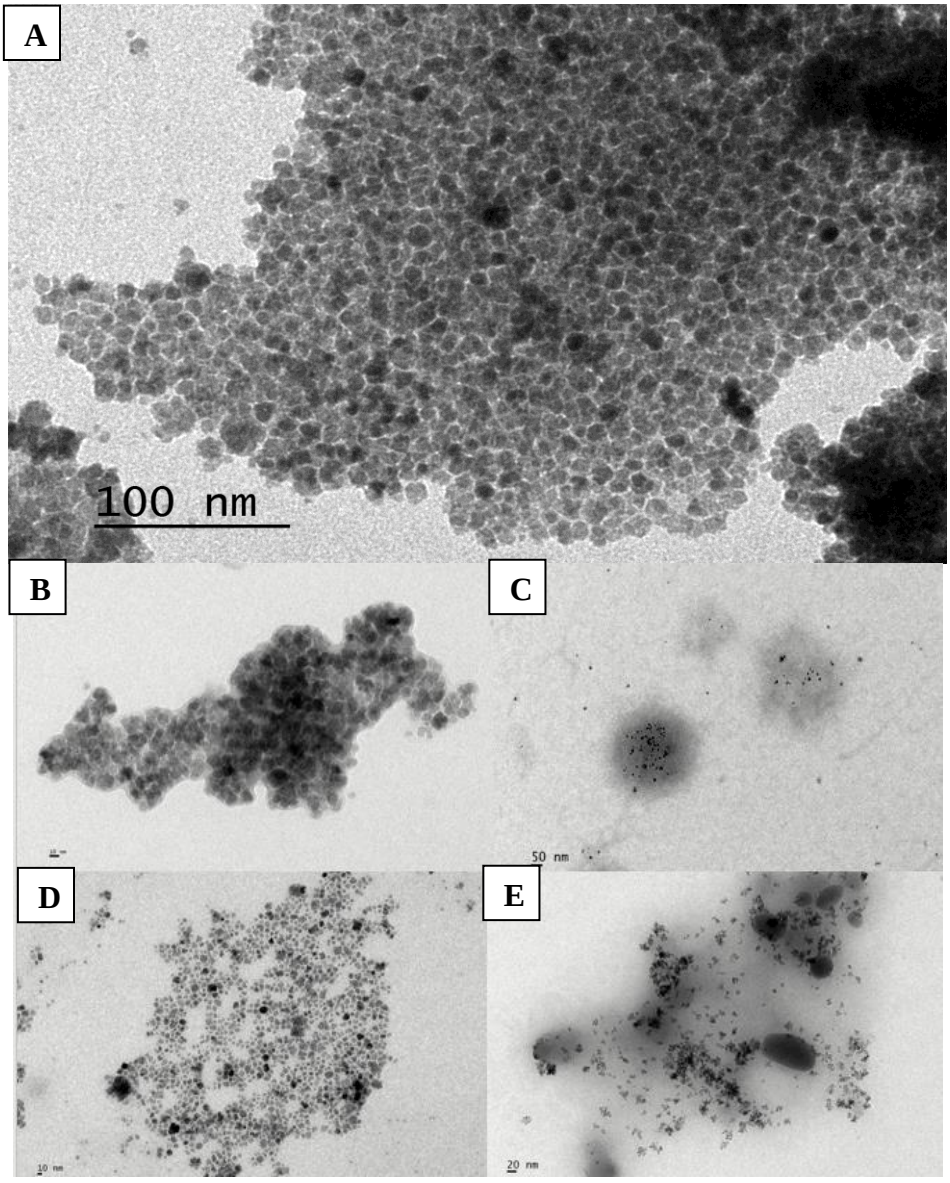

Figure 38. $ZnFe_2O_4$ PEG NPs at different concentrations.

A) $ZnFe_2O_4$ PEG 0.02M TEM (100 nm scale), B) $ZnFe_2O_4$ PEG 0.03M TEM (10 nm scale), C) $ZnFe_2O_4$ CTAB 0.2 M TEM (50 nm scale), D) $ZnFe_2O_4$ Triton X-100 0.1 M TEM (10 nm scale), E) $ZnFe_2O_4$ SDS 0.2 M TEM (20 nm scale). **See in appendix.**

$ZnFe_2O_4$ PEG 0.02 M sample was analyzed by using HRTEM **(Figure 39)**. This image was obtained by bright field dimension allocation. According to our analysis, the shapes are quasi-spherical, however, particle size distribution is difficult to obtain due to agglomerated nanoparticles and high magnetic moment of $ZnFe_2O_4$ NPs. The size distribution for the synthesized sample is found to be in the range of 5 to 10 nm. **Figure 39b** shows a high-resolution nanoparticle, these NPs show columns clearly defined with different contrasts. This demonstrates that an alloy of $ZnFe_2O_4$ forms only when the growth rate is lower than the nucleation rate and the atmosphere is under control. **Figure 39c**, shows the profile obtained in an atom column were the spacing correspond to 0.270 nm.

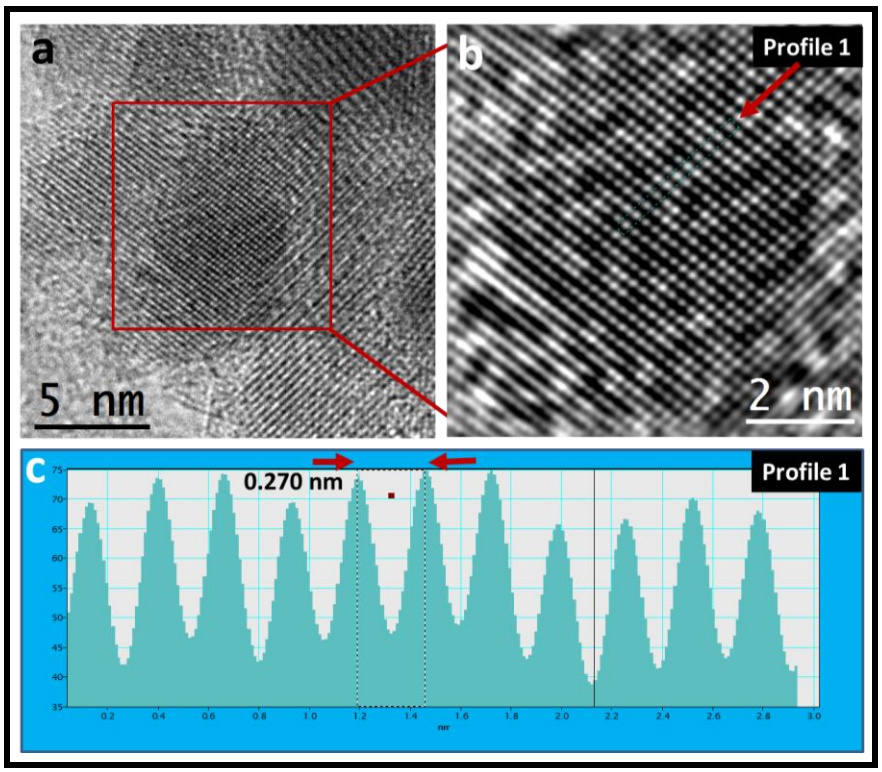

Figure 39. (a) Particle size distribution of $ZnFe_2O_4$ PEG 0.02 M, (b) High resolution image of $ZnFe_2O_4$ PEG 0.02 M and (c) Image profile of a $ZnoFe_2O_4$ PEG 0.02 M atom columns.

The morphology and structure of $ZnFe_2O_4$ CTAB 0.1 M NPs have been characterized by HRTEM (High resolution TEM). **Fig. 40 (a)** revels that the synthesized samples were composed of well-dispersed NPs with a spherical shape with diameter in the range of 5 to 10 nm approx. **Figure 40 (b)** show a high resolution $ZnFe_2O_4$ CTAB 0.01 M NP, differences in the contrast of each point and columns of the atoms is because we use a bright field TEM mode, and we thought that this contrast reveals differences because of the presence of Zn and Fe atoms. The interplanar distances are 0.204 nm and 0.294 nm according with the measure and Card No. PDF 00-001-1108. The single spherical NPs show clear lattice fringes, suggesting their crystalline nature of $ZnFe_2O_4$ NPs.

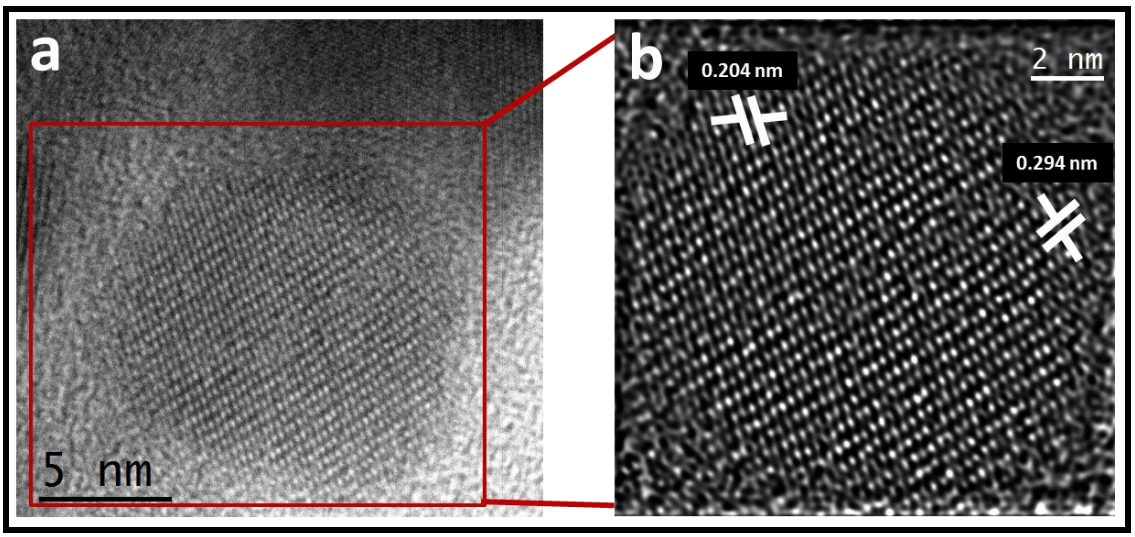

Figure 40. (a) Particle size distribution of $ZnFe_2O_4$ CTAB 0.1 M, (b) High resolution image of $ZnFe_2O_4$ CTAB 0.1 M.

3.5.4.1 HR-TEM Sample $ZnFe_2O_4$ TX-100 0.1 M.

In order to confirm the particle size and morphology of the $ZnFe_2O_4$ TX-100 0.1 M NPs, conventional high-resolution transmission electron microscopy (HRTEM) studies were carried out. First, **Figure 41a**, shows an image in low magnification, as we can observe, this is a kind of agglomeration which is correlated with the strong magnetic moments between the NPs, the size of the agglomerations is in the order of 2 to 15 nm. To use a HRTEM technic allow us to confirm the formation of NPs like morphology agglomeration with smaller size. **Figure 41b** reveals an atoms column in an agglomeration of NPs, the profiles 1 and 2 **(Figure 41c)** show distances of 0.295 and 0.505 nm respectively according

to the data Card No. PDF 00-001-1108 its correspond to $ZnFe_2O_4$ NPs system, the system shows that the sample are good crystalline, particle size small and higher crystalline in nature.

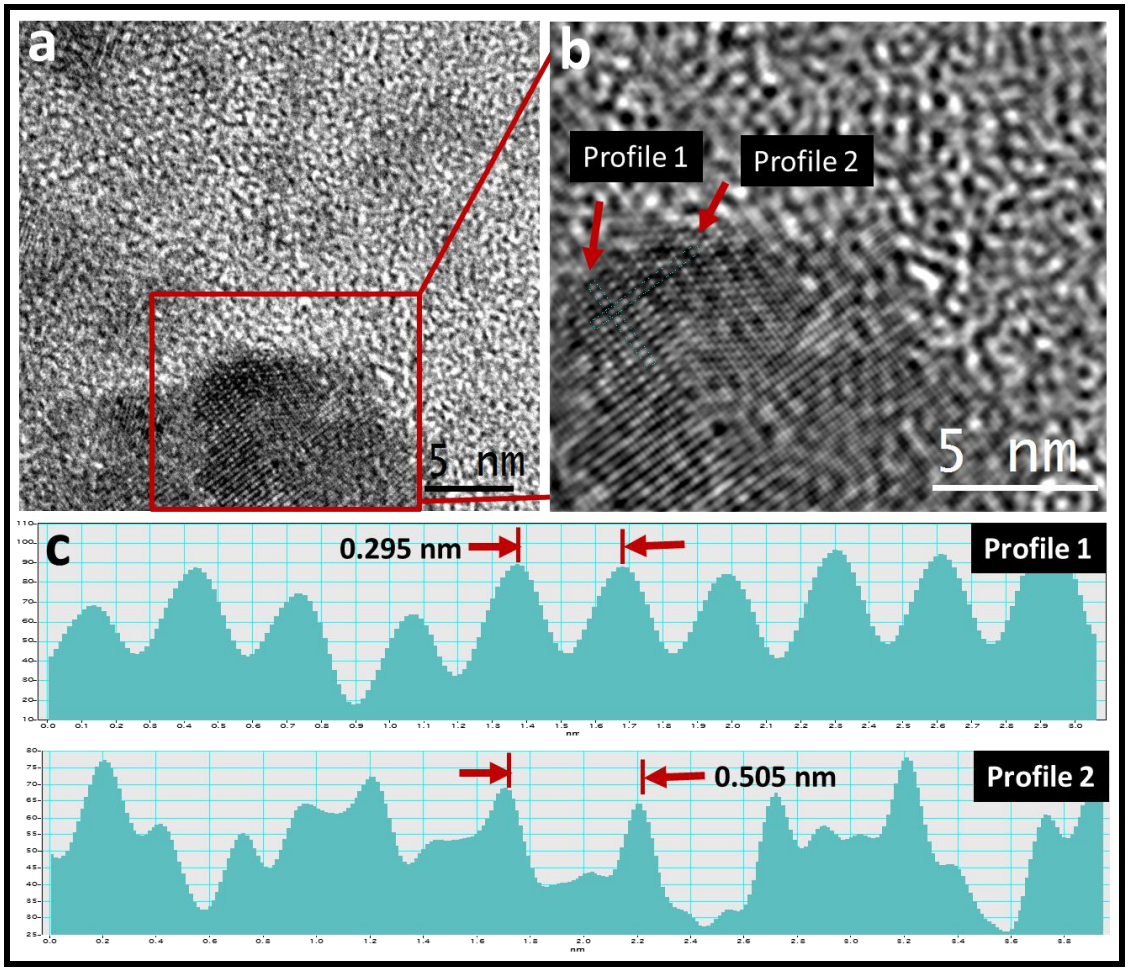

Figure 41. (a) Particle size distribution of $ZnFe_2O_4$ TX-100 0.1 M, (b) High resolution image of $ZnFe_2O_4$ TX-100 0.01 M and (c) Image profile of a $ZnFe_2O_4$ TX-100 0.1 M atom columns.

$ZnFe_2O_4$ a lattice parameter is shown in the next **table number 7**:

- Standard Formula: $ZnFe_2O_4$
- Alphabetic Formula: Fe_2O_4Zn
- Published Formula: $ZnFe_2O_4$
- Refined Formula: –
- Wyckoff Sequence: –
- Z Formula Units: 8

- Density: $\rho = 5.38\ \mathrm{Mg \cdot m^{-3}}$

Published Data	Standardized Data		
	Unit Cell	Niggli-Reduced Cell	
Space Group	Fd-3m O2 (227)	Fd-3m O2 (227)	–
a	0.8413 nm	0.8413 nm	0.59489 nm
b	0.8413 nm	0.8413 nm	0.59489 nm
c	0.8413 nm	0.8413 nm	0.59489 nm
α	90°	90°	60.°
β	90°	90°	60.°
γ	90°	90°	60.°
a/b	1.000	1.000	1.000
b/c	1.000	1.000	1.000
c/a	1.000	1.000	1.000
V	0.59546 nm3	0.5955 nm3	0.14887 nm3

Source: https://materials.springer.com/isp/crystallographic/docs/sd_0306408

3.6 Superconducting Quantum Interference Device (SQUID) results.

Superconducting Quantum Interference Device (SQUID) was performed on these NPS, the result showed great magnetization for hyperthermia purposes.

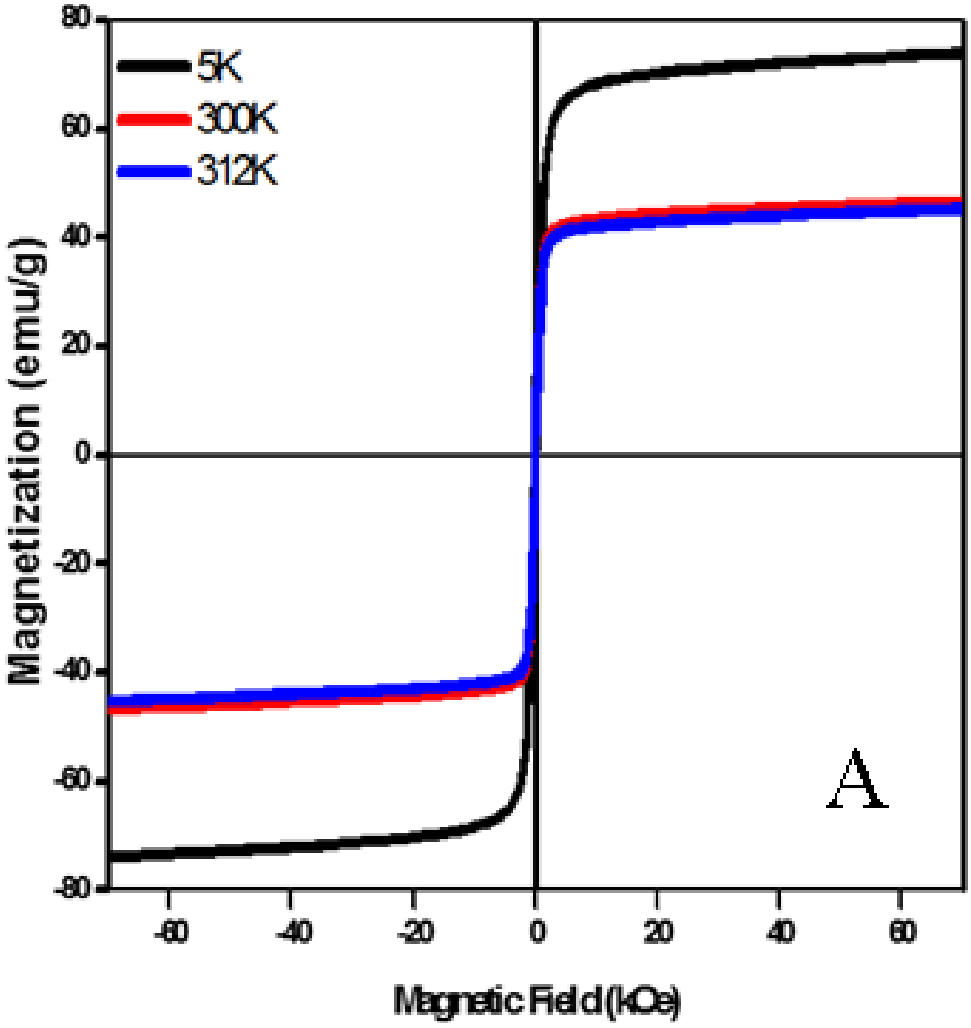

Figure 42. Superconducting Quantum Interference Device (SQUID). Physics Department SQUID IFUNAM.

$CoFe_2O_4$ nanoparticles are required to have a narrow size distribution, high magnetization values, a uniform spherical shape, and superparamagnetic behavior at room temperature.This property of reversible magnetization and hysteresis-free allows for quick "on-off" switching capability that can be controlled by the presence of an external magnet. For this reason, it is necessary to study the coercive field, which is the intensity of the magnetic field that must be applied to that material to reduce its magnetization to zero after the sample has been magnetized to saturation. In the presence of a magnetic field, the $CoFe_2O_4$ will be added, but when the field is removed, the magnetization drops quickly to zero, allowing the particles to redisperse. It is of great interest that the $CoFe_2O_4$ nanoparticles can be reused, however our results after 2 uses point to a lower response in the hyperthermia-time relationship [39].

The magnetic anisotropy constant *K* of the samples as-prepared can be calculated by the followed formula

$$K = 25 k_B T_B V^{-1}$$

where k_B is the Boltzman constant, T_B is the blocking temperature of the samples, and *V* is the volume of a single particle. The calculated magnetic anisotropy constant *K* of our samples is 3.8×10^6 ergs/cm^3, which is slightly larger than that of the *K* values of bulk $CoFe_2O_4$ [$(1.8–3.0) \times 10^6$ ergs/cm^3].

The distribution function of the magnetic anisotropy energy barriers *f*(*T*) can be obtained through the following equation.

$$f(T) = \frac{d}{dT}\left(\frac{M_{ZFC}}{M_{FC}}\right)$$

where M_{FC} (FC magnetization) involves the total magnetization from the contribution of all particles, M_{ZFC} (ZFC magnetization) is determined by the magnetization from only the contribution of the nanoparticles whose energy barriers are overcome by the thermal energy (k_BT) at the measuring temperature, and *f*(*T*) reflects a quantitative characterization for superparamagnetism of the magnetic nanoparticles [349]

Generally, the volume and shape distribution of the samples determine the magnetic anisotropy energy distribution. Therefore, the result implies that the thermal energies of most particles have exceeded the energy barriers beyond T_B(about 240 K). So, the as-synthesized samples display superparamagnetic behavior at room temperature. In addition, the narrow magnetic anisotropy energy distribution reveals that the as-prepared $CoFe_2O_4$ nanoparticles possess uniform sizes.

3.6.1 SQUID of $COFe_2O_4$

Figure 43A shows the zero-field cooling (ZFC)‑field cooling (FC) curves of Cobalt ferrite nanoparticles (CFNPs) samples measured from 10 K to 400 K. The blocking temperature is the temperature where ZFC and FC curves join together, TB, above which the hysteresis coercivity reduces to zero and superparamagnetic behavior begins. For monodispersed non-interacting samples, this temperature region evidences a transition between irreversible and reversible regimes. CFNPs showed a TB = 360 K denoted by the inflection point of the rapid magnetization rise in the FC curve up to its thermodynamic equilibrium value (when the thermal energy k_BT_B is nearly proportional to the anisotropy energy barrier KV of the particles). Higher TB indicates higher magnetocrystalline anisotropy (K). FC curve is flatter at lower temperatures, as depicted in Figure 43A, suggesting the existence of strong dipolar interactions among the particles, which can cause the ferrite nanoparticles to have higher anisotropy values and may increase their blocking temperatures. Figure 43B‑D show the hysteresis loops for CFNPs at 300 K and 312 K. In both cases, CFNPs presented similar behaviors when dispersed in Triton X (higher saturation values). The effective moment values indicated the contribution of two magnetic sublattices coupled antiferromagnetically, as expected for cobalt ferrites with two different Co(II) and Fe(III) sites. Moreover, CFNPs displayed magnetic moments reported in emu/g for Co0.37Fe2.63O4 and Co0.19Fe2.81O4 ferrites. No evident traces of FeO or CoO were detected, as no exchange bias was noticed in Figure 4C,D. CFNPs displayed the higher coercive field (HC) at 20 K, exhibiting a value around 1.349 T (Figure 43B), thus confirming the presence of highly crystalline CoxFe3-xO4- δ nanoparticles prepared by thermal decomposition. The reduced remnant magnetization (M_R/M_S) of CFNP is 0.86, a signature value for a system with cubic anisotropy.

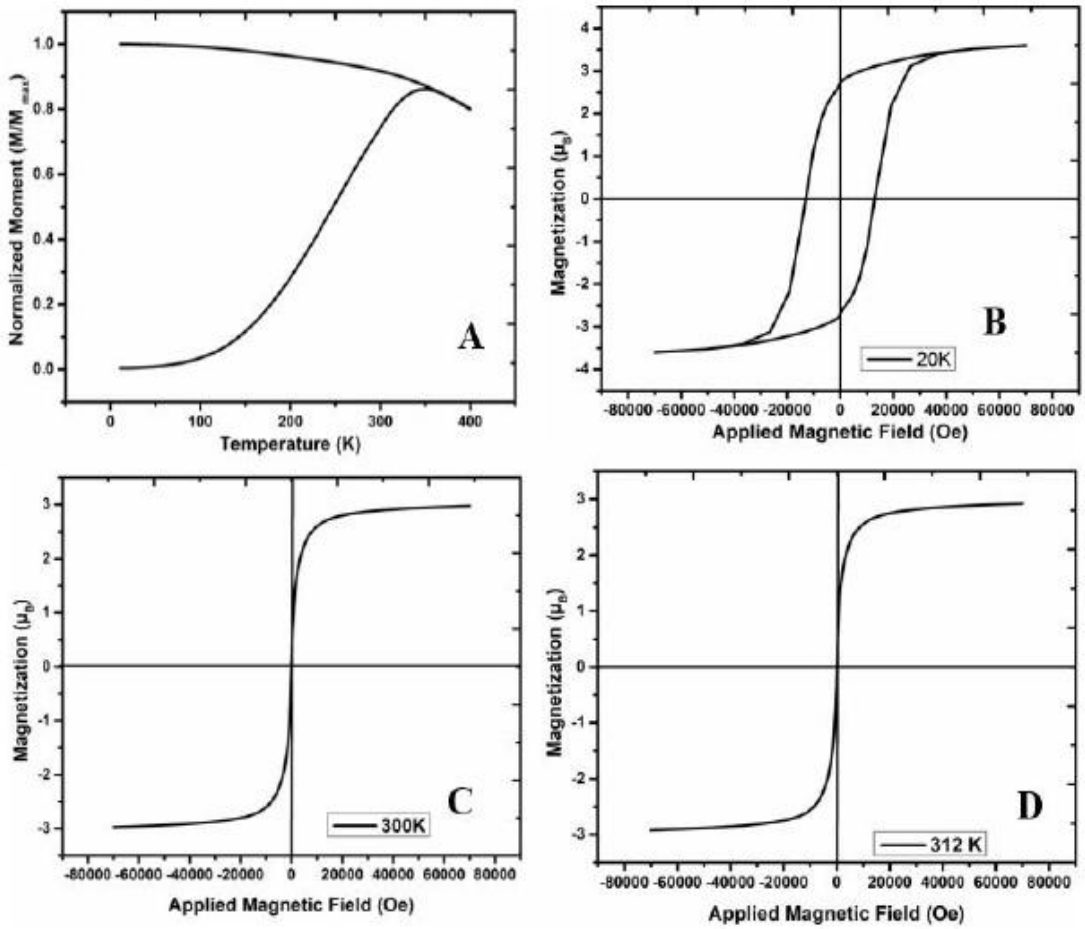

Figure 43. (A) Field cooling and zero-field cooling curves for CFNPs. Changes in magnetization as a function of applied magnetic field at different temperatures (B) 20 K, (C) 300 K and (D) 312K.

3.6.2 SQUID of $MnFe_2O_4$

At low temperature (4K), $MnFe_2O_4$ showed hysteresis curves, revealing a standard ferrimagnetic character. Mn ferrite MNPs displayed an Ms of 90 emu/g and 95 emu/g, which was significantly higher than the Ms of Fe_3O_4 MNPs synthesized in EG (75 emu/g) [35].

Large MNPs are generally expected to display an Ms close to the value obtained for the bulk material (for magnetite 92 emu/g), but in this case, the significantly lower Ms might be attributed to the cation vacancies resulting from synthesis during the aggregation of

multiple crystallites. However, Mn ferrite MNPs presented high saturation magnetization values at 4 K, which were close to the bulk values. These observations are an indication, on one hand, of excellent crystallinity, and on the other hand, they are an indication that the cationic substitutions of Fe2+ with Mn2+ led to an increase in the magnetization of the MNPs, as expected.

The lowest coercive field (26 kA/m) at 4 K was obtained for the Mn ferrites, a result that was in agreement with the well-known "softness" of manganese ferrites.

At 300 K, there was a normal decrease in both Ms and Hc for all samples. For the Mn ferrites, the Ms value at 300 K was 76 emu/g.

The ratios of Mr/Ms were smaller than 1:2 for all the ferrites both at low and high temperatures, thus indicating uniaxial anisotropy. Therefore, the anisotropy constants were calculated as Ke_ = _0HcMs/0.96 [48], with the saturation magnetization and the coercive field values measured at 4 K. The effective anisotropy constant at low temperatures was very close to the bulk magnetite values (11–13 kJ/m3) for the ferrous ferrite, indicating the good quality of our MNPs. A slightly smaller value of the effective anisotropy constant was obtained for the Mn ferrites, a behavior that was consistent with the lower anisotropic constant in the case of bulk Mn ferrite. However, the behaviors of ferrite MNPs were not superparamagnetic at room temperature, as can be clearly seen in the zero-field-cooled/field-cooled (ZFC/FC) magnetization curves (Figure S1). In both cases, the ZFC and FC curves started to join around 300 K. In addition, the maximum of the ZFC curves was located at the same temperature and was broadened. This behavior suggests a gradual transition from the ferromagnetic to the superparamagnetic state, with the majority of the MNPs being in a blocked state at 300 K, the temperature range where the hyperthermia experiments were conducted. It should be noted that the M(T) values of the FC curves for the Mn ferrite MNPs were 37 emu/g, which suggests that both types of ferrite MNPs can exhibit similar interparticle interactions that can influence SAR values.

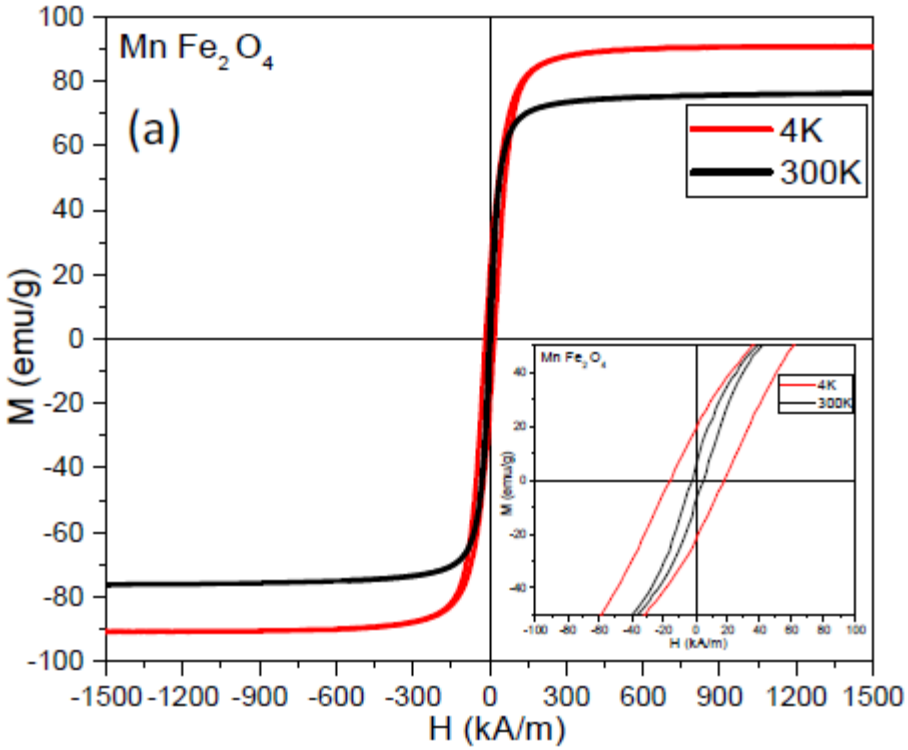

Fig. 44 SQUID of $MnFe_2O_4$ at 4K and 300K. Inset shows zoomed SQUID results of $MnFe_2O_4$

3.6.3 SQUID of $ZnFe_2O_4$

At low temperature (4K), $ZnFe_2O_4$ also showed hysteresis curve, thus revealing a standard ferrimagnetic character similar to $MnFe_2O_4$. Zn ferrite MNPs dislayed an Ms of 95 emu/g. Large MNPs are generally expected to display an Ms close to the value obtained for the bulk material (for magnetite 92 emu/g), but in this case, the significantly lower Ms might be attributed to the cation vacancies resulting from synthesis during the aggregation of multiple crystallites. Zn ferrite MNPs presented high saturation magnetization values at 4 K, which were close to the bulk values. These observations are an indication, on one hand, of excellent crystallinity, and on the other hand, they are an indication that the cationic substitutions of Fe2+ with Zn2+, thus led to an increase in the magnetization of the MNPs, as expected. At 300 K, there was a normal decrease in both Ms and Hc for $ZnFe_2O_4$

samples. The largest decrease in the Ms was measured for the Zn ferrites, with a value of 58 emu/g at 300 K. The stable phase of $ZnFe_2O_4$ possesses a normal spinel structure in which diamagnetic Zn2+ and magnetic Fe3+ ions are located in the (A)- and (B)-sites, respectively. Due to the negative superexchange interaction between Fe3+ ions only at (B)-sites, $ZnFe_2O_4$ with a normal spinel structure behaves as an antiferromagnet below 10 K and is paramagnetic above this temperature.

However, our $ZnFe_2O_4$ MNPs exhibited ferrimagnetic properties with a nonzero coercive field and high magnetization even at room temperature. This result can be explained only by considering a different crystal structure from the normal spinel for the zinc ferrites.

The random distribution of Zn2+ and Fe3+ ions in the (A)-sites as well as the (B)-sites and the presence of a strong superexchange interaction between them (giving rise to high magnetization at low temperatures and also at room temperature) were also observed for sputtered $ZnFe_2O_4$ films [46]. According to our XRD data, in the case of Zn ferrites, some of the Zn2+ ions were found in a ZnO phase, meaning that the Zn ferrite was not stoichiometric, and this fact could also explain the high Ms of these MNPs. As the temperature increased, the Zn2+ ions might have migrated in the (A) sites, thus reducing the saturation magnetization to 58 emu/g.

The ratios of Mr/Ms were smaller than 1:2 for the Zn ferrites both at low and high temperatures, thus indicating uniaxial anisotropy. The effective anisotropy constant at low temperatures was very close to the bulk magnetite values (11–13 kJ/m3) for the ferrous ferrite, indicating the good quality of our MNPs. For the Zn ferrites, the effective anisotropy constant of 17 kJ/m3 was high compared to the value for magnetite, showing that the substitution of Fe2+ ions with Zn2+ ions led to an increase in the anisotropy, which was in agreement with values reported by other groups [47].

As can be clearly seen in the zero-field-cooled/field-cooled (ZFC/FC) magnetization curves both the ZFC and FC curves started to join around 300 K. In addition, the maximum of the ZFC curves was located at the same temperature and was broadened. This behavior suggests a gradual transition from the ferromagnetic to the superparamagnetic state, with the majority of the MNPs being in a blocked state at 300 K, the temperature range where the hyperthermia experiments were conducted. It should be noted that the M(T) values of

the FC curves for the Zn ferrite MNPs was 34 emu/g, which suggests that Zn ferrite MNPs can exhibit similar interparticle interactions that can influence SAR values.

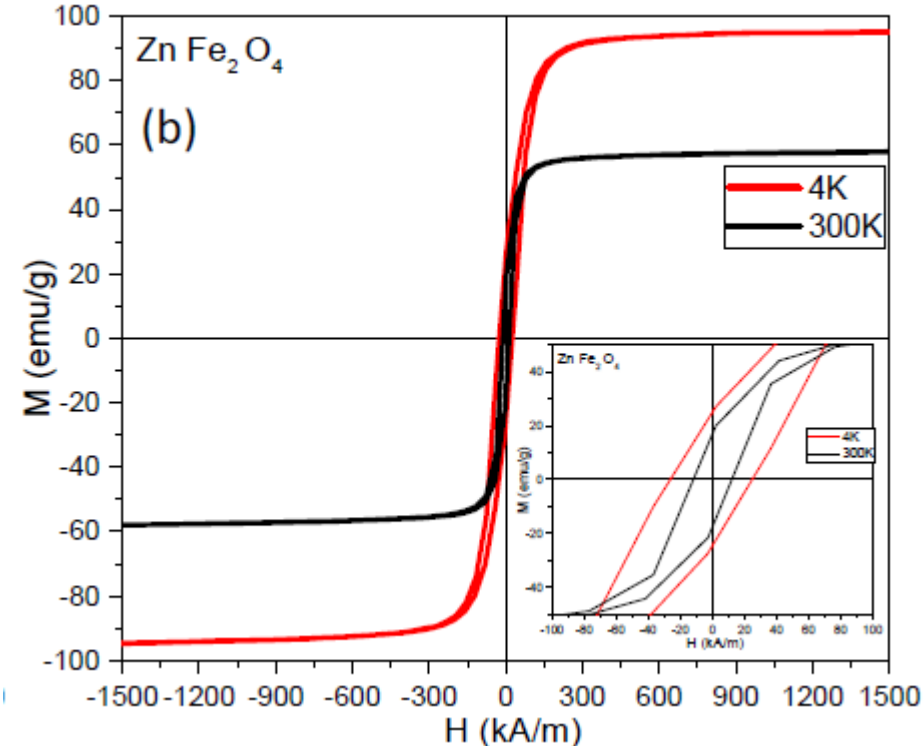

Fig.44 SQUID of $ZnFe_2O_4$ and inset shows the zoomed $ZnFe_2O_4$ results at 4K and 300K.

Table 8. Magnetic properties of $MnFe_2O_4$ and $ZnFe_2O_4$

Sample	300K			
	Ms (emu/g)	Hc (kA/m)	Mr (emu/g)	Mr/Ms
$MnFe_2O_4$	76	5	6	0.08
$ZnFe_2O_4$	58	12	16	0.28

CHAPTER 4

4. Triple Negative Breast Cancer: In Vitro studies.

As we studied in chapter 2, there are several ongoing clinical trials regarding TNBC. In the present chapter, we are going to define our experimental model regarding the TNBC MDA/MB/231 cell strain.

4.1 MDA-MB-231 cell strain.

In vitro studies at TNBC are becoming more relevant in the field of nanotechnology [350]. Recently the cell lines of TNBC such as MDA-MB-231 and MDA-MB-468 have been studied for the creation of nanoparticles in drug delivery against breast Cancer. In this work we use the cell line MDA-MB-231, one of the most used in research. The first vial was isolated from the pleural effusion of a patient diagnosed with metastatic adenocarcinoma at Anderson Houston TX Hospital in 1973. ATCC (**American Type Culture Collection)** highly recommends the use of protective gloves and clothing as well as full-face mask since MDA-MB-231 is a biosafety level 1 hazard (www.atcc.org).

4.1.1 MDA-MB-231 cell culture method.

To cultivate MDA-MB-231 the same protocol was used as in MRC-5, however, with the difference that they use RPMII1640 culture medium, antibiotic streptomycin-penicillin (100 mg/ ml), 10% fetal bovine serum and must not contain amino acids.

Another difference is that in this case in the Bauer chamber there are larger numbers of cells, because these cells are too aggressive and grow in environments where there are few nutrients. In this case the populations were diluted with culture medium. Finally, cell lines were incubated at 37° C under an atmosphere of 5% CO2 and 99% humidity.

4.2 MRC-5 fibroblast cell strain negative control.

It was used MRC-5 human diploid cell line fibroblast-like morphology as a negative control since they maintain a normal diploid karyotype over long in vitro expansion [351]. Although the tissue is lung fibroblast type and non-breast tissue, it is ideal as a negative control because it represents a normal parameter of human tissue.

4.2.1 MRC-5 cell culture method.

1.- Culture medium was removed by using vacuum with pipette or suction.

2.- Two washes were made with PBS, applying approximately 5 ml to each plate.

3.- Then 0.5ml of trypsin was applied for each box

4.- Subsequently, 10% Dulbecco's Modified Eagle Medium (DMEM) culture medium, fetal bovine serum, L-glutamine and amino acids, 4ml were suspended. DMEN, fetal bovine serum (FBS), and streptomycin were obtained from Life Technologies.

5.- Deposit in the plate of new Bauer 10 µl

6.- Since this type of cells cannot be reduced in its population below 50%, 2 million cells per box were needed.

7.- The populations in the new Bauer chamber were analyzed, this has 4 quadrants and each of these has 16 squares, the cell count is done, the sum of all squares is divided by 4 and we obtain an average. The result of the average is multiplied by X 10,000. For example:

In 10 µl there are 260,000 cells, then:

In 1,300,000 -------- 5 ml

1,000,000 ------- X = 3.8 ml

Because 2 million cells are required to work

3.8 ml was diluted in culture medium and then 1 ml was added to the 24-well multi-plate, bone 1 ml per well.

4.3 Cytotoxicity Assay MTT

The cell viability can be measured by means of a colorimetry test called MTT assay 3- (4,5-dimethylthiazol-2-yl) -2,5-diphenyltetrazolium bromide which is soluble in formazan giving it the typical purple color. This compound is reduced by the metabolic activity of the cell enzymes, so it is an index of survival or cellular activity **Figure 43**. The absorbance of this colored solution can be quantified by measuring at a certain wavelength (usually between 500 and 600 nm) by a spectrophotometer.

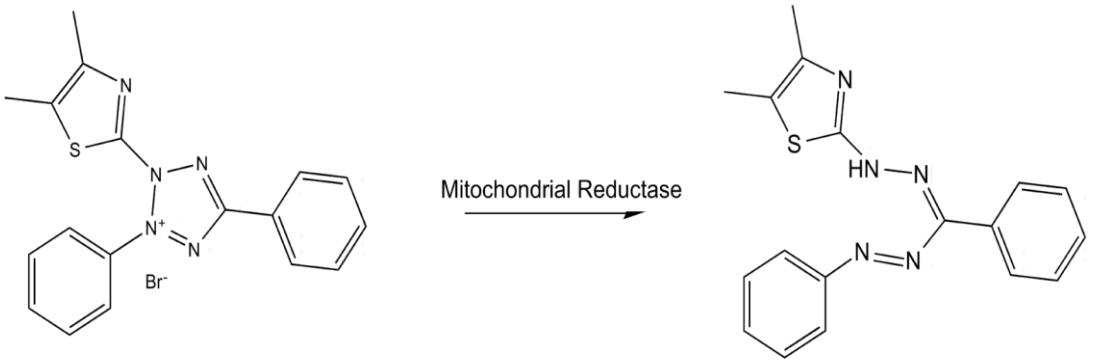

Figure 43. The tetrazolium reduction (MTT assay) is the *Gold standard* for measuring metabolism as a marker of viable cells.

4.3.1 Viability protocol by using MTT.

1. Harvest the cells in suspension (MRC-5 or MDA-MB-231) by means of centrifugation. The adherent cells must be detached by trypsinization or scraping.

2. Carry out the cell count

3. Re-suspend the cells so that 50,000 cells of MRC-5 or MDA-MB-231 are deposited in each well.

4. Deposit in triplicate, 100 µl of the dilutions in the wells of a microtiter plate.

5. Include medium control wells only to provide the target readings for absorbance

6. Incubate the cells under appropriate conditions for the cell line for 6 to 48 hours (to recover from handling).

7. Add the nanoparticles and allow to incubate for 24 hours.

8. Remove the medium and NPs. For MRC-5 or MDA-MB-231 cells, centrifugation must be performed in order to remove the culture medium.

9.- Proceed with the steps to add the MTT

10.-MTT tests in 24 well plates. **Figure 44.**

11.-Remove the supernatant from the wells of the plate.

12.- Wash each of the wells with 0.5 ml of 1X PBS (in triplicate) and eliminate the washing solution.

13.- Add 100 µl of culture medium for HeLa cells to each of the 24 wells.

14.- Add 10 µl of MTT to each of the wells (the MTT is 100% and is used at 10%, so 10 µl is used for the 100 µl posts of culture medium).

15.- Incubate the plate at 37ºC for 3 hours

NOTE: the MTT must be sterile, it can be stored at -20ºC when it is in solution and it must be protected from light.

What follows can be worked in non-sterile conditions:

16.- Add 300 µL of isopropanol to each well. Stir for 5-10 minutes at room temperature.

17.-Help dissolving the crystals by pipetting 15 times with the 1 µl micropipette and placing 100 µL in triplicate in wells of the 96-well plate.

18.- Sample is ready for measurement in synergy. See **Figure 44.**

4.3.1.2 MATERIALS AND METHODS.

They were inoculated in MRC-5 cells of healthy fibroblasts and in triple negative breast Cancer tumor cells MDA-MB-231, various concentrations of iron oxide nanoparticles Fe_3O_4 magnetite alone and covered with surfactants such as SDS, PEG, Triton X 100 and CTAB at different molar (M) concentrations, in addition iron oxides doped with Manganese, Cobalt and Zinc ($CoFe_2O_4$, $MnFe_2O_4$, $ZnFe_2O_4$) were also used to improve the super-paramagnetic properties of the nanoparticles, this class of nanoparticles are called SPIONs by its acronym Super -Paramagnetic Iron Oxide Nanoparticles.

After leaving incubated 24 hours, the nanoparticles were removed from the wells by using vacuum, to then make 3 washes with PBS, after each wash was performed again and finally the cells were allowed to incubate for 3 hours with 100 µl of MTT prepared together with the corresponding culture medium for each cell line.

Subsequently, after three hours had elapsed, 300 microliters of Isopropanol were added and the wells containing the cell lines were shaken for 15 minutes.

Finally, the content was deposited in duplicate in a 96-well grade for further evaluation in the spectrophotometer to measure cell survival.

Figure 44. MTT process.

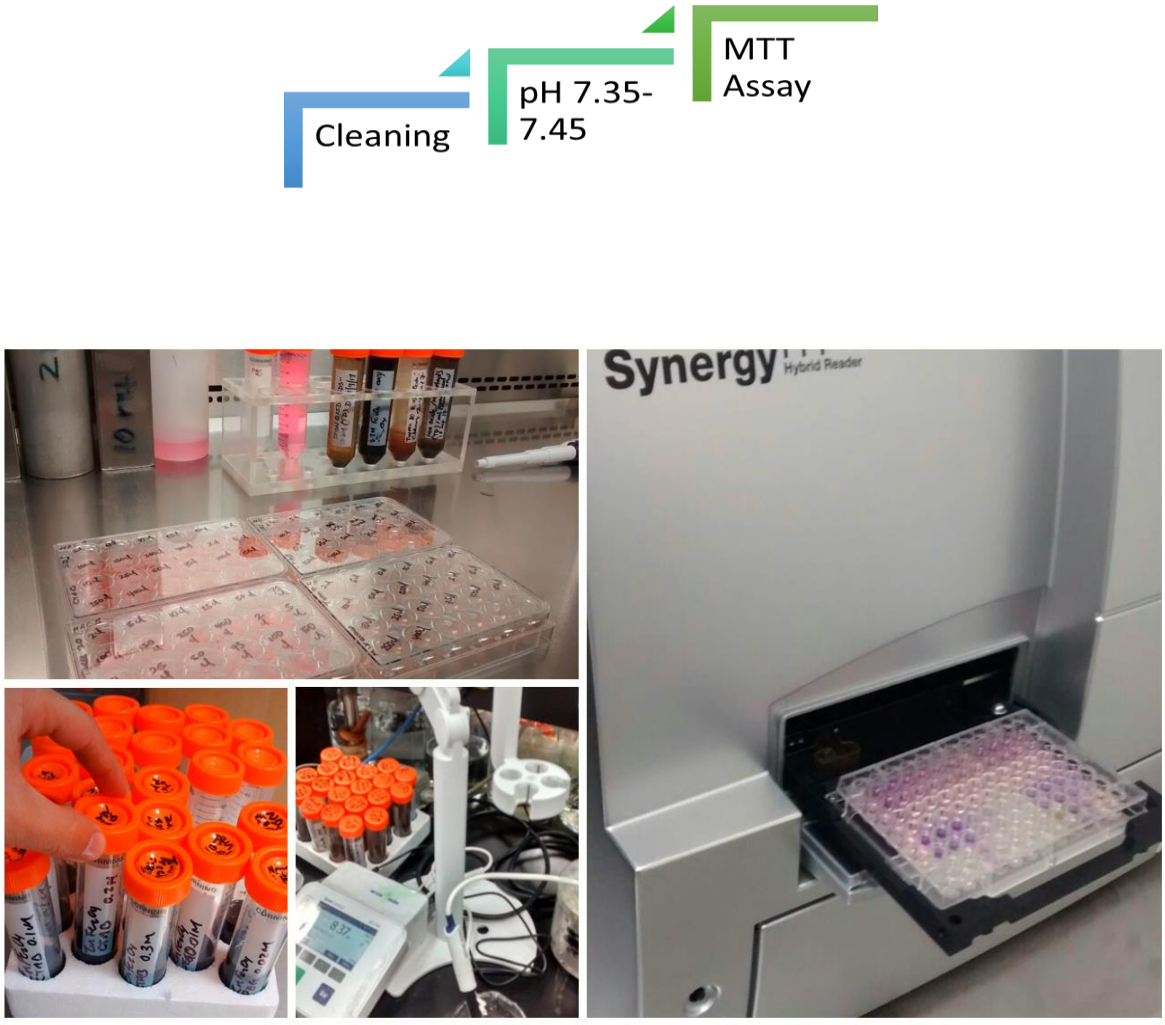

4.3.2 MTT Surfactants alone without Magnetite.

It was expected PEG alone at minimum concentration increasing cell viability since PEG is a biodegradable, biocompatible and non-toxic surfactant. Widely used on medical industry field as well as 3D cell culture scaffold [352]. Our results indicate this surfactant is safe to use as SPIONs coat design, improving monodispersing as well as avoiding an overdose of iron (over 3.5mg/kg) on humans. See **Figure 45 (A).**

The Cetyl Trimethyl Ammonium Bromide demands an adequate and rigorous method of purification when coating NPs **Figure 45 (B)**. It is an antiseptic and detergent also used as a cationic surfactant. It has been incorporated in the synthesis of NPs of iron oxide, because of its mono-dispersive properties. However, we believe that its use as a surfactant in nanomedicine is overvalued, since its cytotoxic activity can be easily detected by the immune system (there are exceptions like CTAB-gold nanorods under strict purification parameters), reducing its bioavailability in bloodserum. This has been the reason why researchers use gold to diminish CTAB nanotoxicity effects [353]. Although our designs at the minimum molarity allow us to obtain spherical, morphologically aesthetic nanoparticles using TD method, we do not consider it a long-term strong candidate for living systems.
It has been widely described TX-100 applications; it is a nonionic surfactant detergent, so we expected cell survival diminished. What was unexpected was the reversed pattern where the MDA-MB-231 cells (which are more aggressive than the fragile MRC-5 fibroblasts) were more susceptible. This information was interesting for our research group, and it was decided to take it as a candidate for the next stage as Fe_3O_4-coated surfactant **Figure 45 (C).** For stoichiometry reasons, cytotoxic surfactants continue to be used as detergents that help to bind electrical charges when gold NPs synthesis is taking place. This is the case of CTAB, TX-100 and it is also the case of SDS **(Figure 45D)**, an anionic surfactant a bit controversial for causing skin irritations and dermatological problems within the cosmetic industry context where is widely used. We do not think that this surfactant is promising in the long term, but we decided to use it to encapsulate magnetite and test its bad reputation.

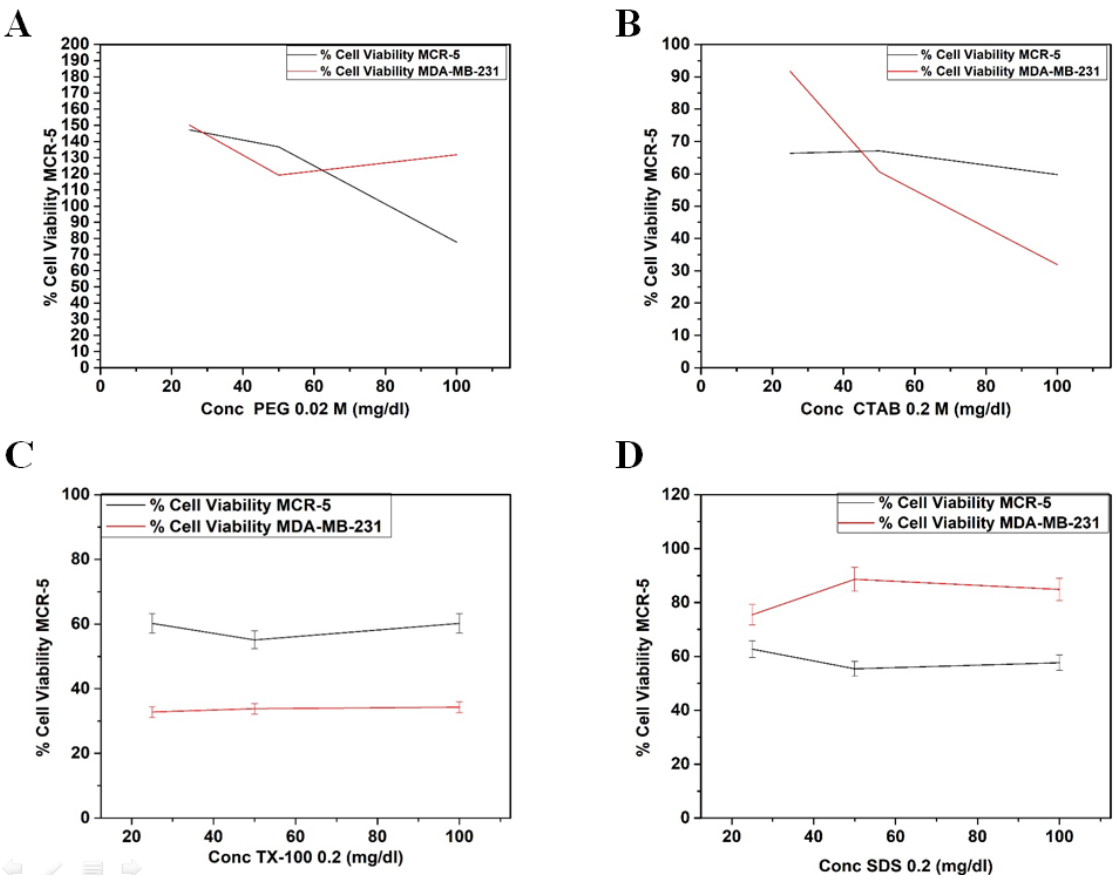

Figure 45. MTT Surfactants alone without Magnetite.

4.3.3 Selecting the best surfactant at the best concentration.

At this point we cannot conclude which surfactant is more convenient, for example the TX-100 pattern seems to be useful but once coupled to the magnetite it could change its cytotoxic behavior. Therefore, these measurements can only give a vague idea of which are the most cytotoxic surfactants, but it does not tell us if they are useful for a specific nanoparticle configuration, since the NPs have different shapes, sizes and chemical residues which are the product of the synthesis method used as well as purification methods and monodispersing techniques.

4.3.4 MTT Fe_3O_4 alone

Controversially and contrary to the pre-established in the literature, our research group found out the Fe_3O_4 magnetite (created under the TD protocol described in Chapter 3) doesn't have effect over TNBC MDA-MB-231 cell viability as well as MRC-5 cell viability. The results were verified, and we hypothesized that iron oxides at physiological pH, duly purified and free of alkylating reagents, could act to improve both cell strains energy metabolism. However, when our magnetite was stimulated through an electromagnetic field, cell viability decreased dramatically due to the hyperthermia effects. **Figure 46.**

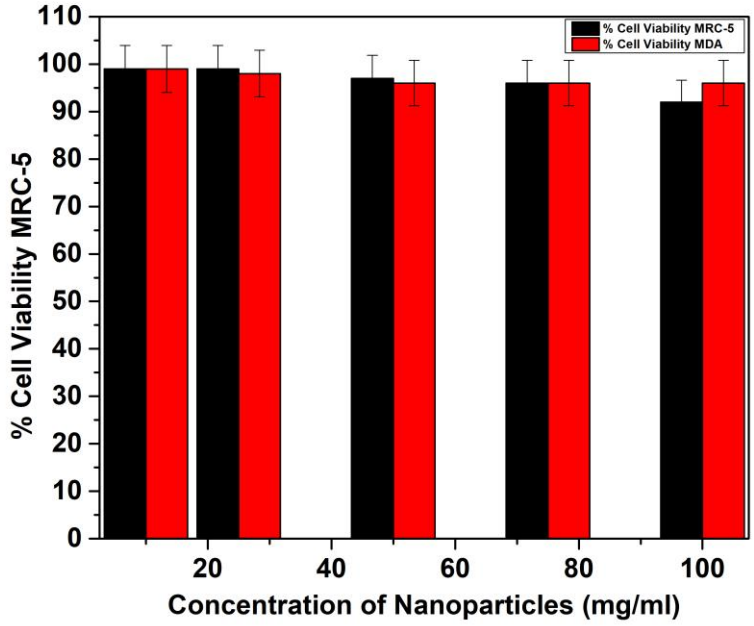

Figure 46. MTT Fe_3O_4 without surfactant showing minimal effect on cells.

4.3.4.1 MTT Fe_3O_4 -PEG at different concentrations.

A synthesis of Fe_3O_4 NPs was carried out by using the latest TD synthesis protocol. We decided to perform this synthesis with PEG-surfactant at 0.001 M, 0.02 M and 0.03 M. Every experiment was performed 3 times. **See figure 47.**

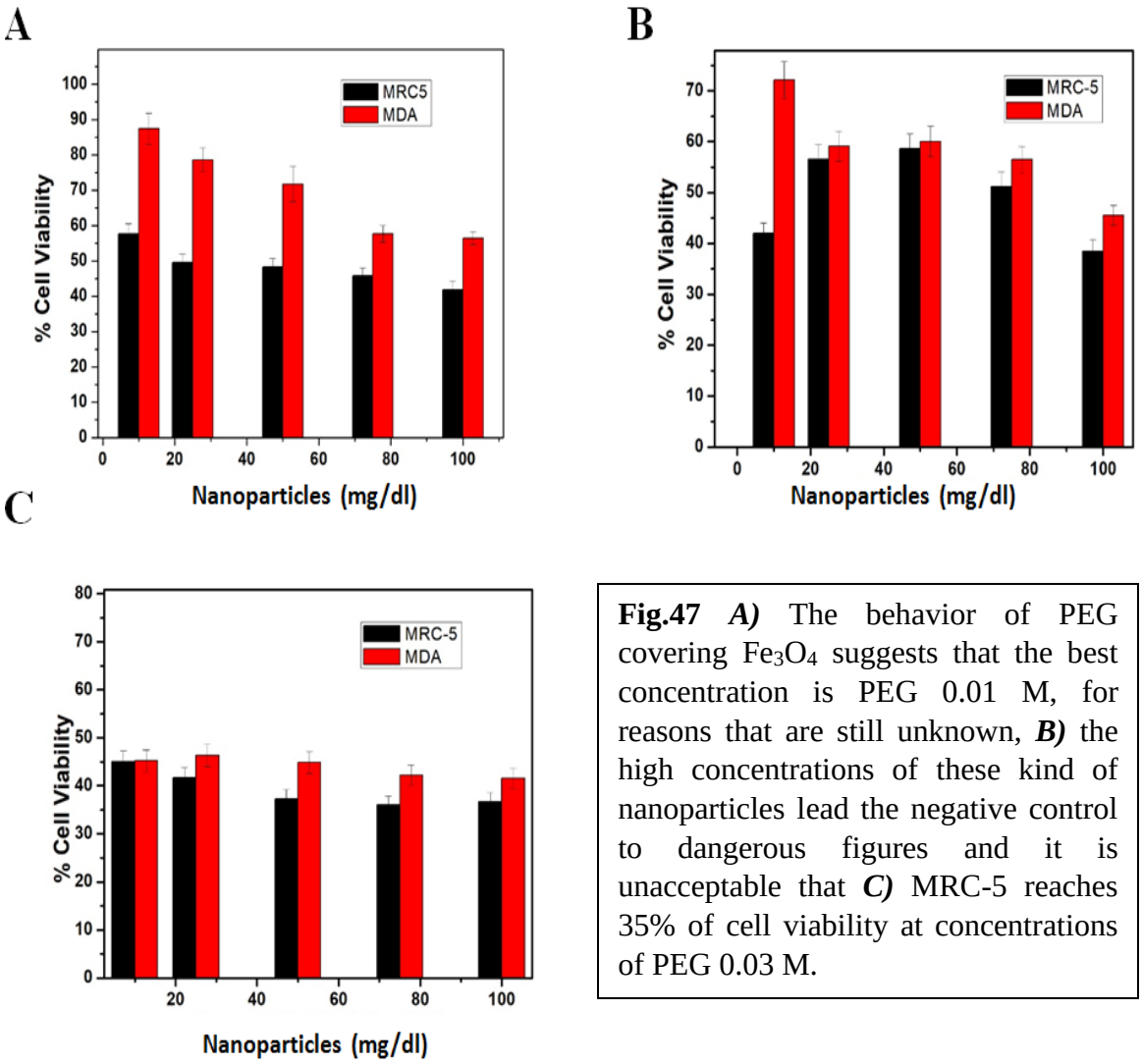

Fig.47 ***A)*** The behavior of PEG covering Fe_3O_4 suggests that the best concentration is PEG 0.01 M, for reasons that are still unknown, ***B)*** the high concentrations of these kind of nanoparticles lead the negative control to dangerous figures and it is unacceptable that ***C)*** MRC-5 reaches 35% of cell viability at concentrations of PEG 0.03 M.

4.3.4.2 MTT Fe_3O_4 -CTAB at 0.1 M.

Due to the poor morphological Fe_3O_4 CTAB quality NPs achieved at 0.2 and 0.3 M, we decided to evaluate MTT only at 0.1M **(Figure 48)**. However, cell viability at 0.1 M is not consistent or related to our interests. Cytotoxicity is present at low concentrations and stoichiometry without gold makes this detergent dangerous.

In this work, a good design Fe_3O_4-CTAB synthesis using TD method was not achieved. The disadvantages continue to outweigh the possible advantages if gold is not used over these nanoparticles yet. Thus, iron oxide-CTAB NPs design remains as a threat to any living cell so we considered at high concentration would be risky in animal or human model.

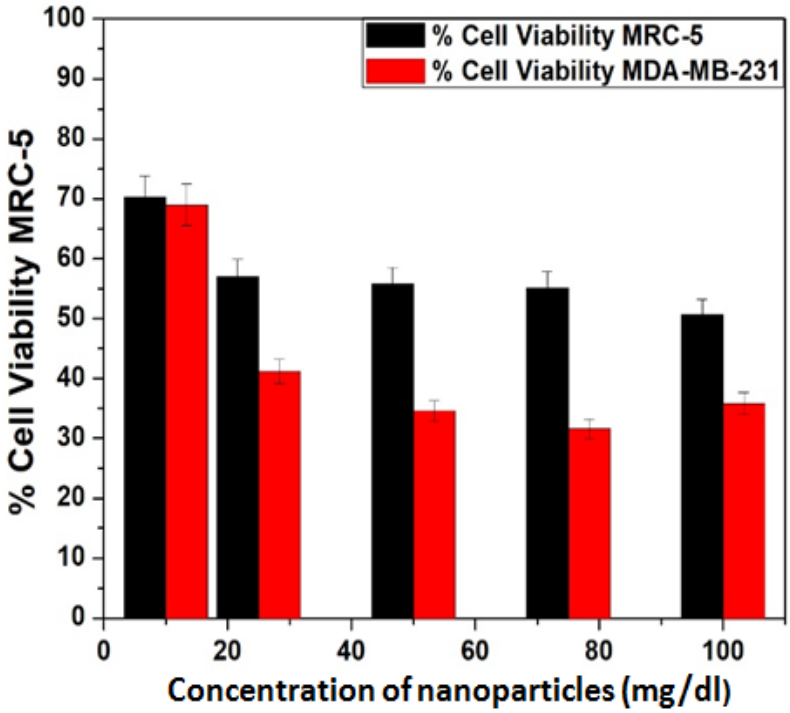

Figure 48: MTT Fe_3O_4 -CTAB at 0.1 M.

4.3.4.3 MTT Fe_3O_4 Triton-X-100 0.2M at different concentrations.

Due to the control over synthesis evidenced by the previous characterization of NPs Fe_3O_4 TX-100, we decided to continue running MTT studies at 0.2 M concentration of TX-100. Our research group found that at low doses such as 20 mg / dl (0.1 M), the use of TX-100 may be viable because MRC-5-MDA-MB-231 pattern is reversed, conferring a therapeutic window between doses of 20 to 50 mg / dl. **Figure 49.**

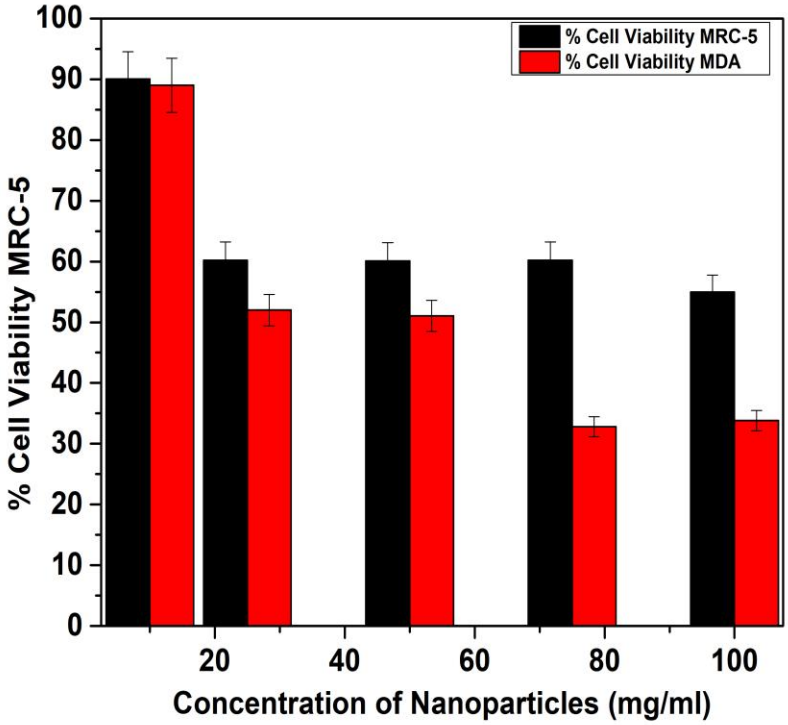

Figure 49. MTT Fe_3O_4 Triton-X-100 0.2M at different concentrations.

4.3.4.4 MTT Fe_3O_4 SDS 0.2 M at different concentrations.

Another unexpected therapeutic window was found with 0.2M SDS surfactant. It seems that at a dose of 50 mg/dl we get the desired pattern where fibroblasts MRC-5 survive more than aggressive malignant MDA-MB-231 cells. Optimistically, we decided to continue working on this surfactant in the next stage of doping Fe_3O_4 iron oxides by using Co, Mn and Zn. **Figure 50.**

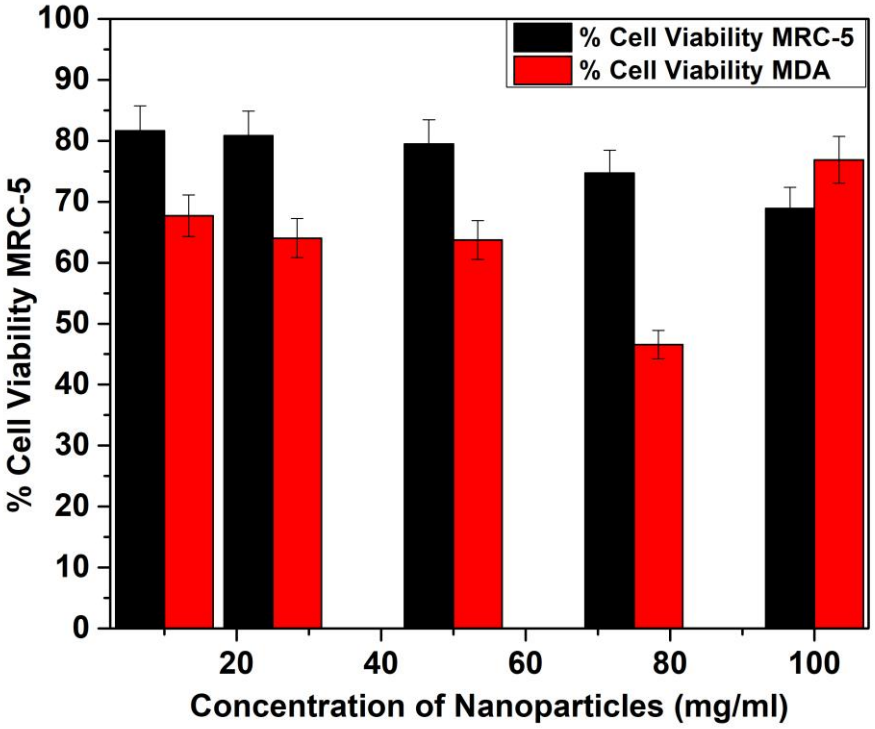

Figure 50. MTT Fe_3O_4 SDS 0.2 M at different concentrations.

4.3.5 MTT $CoFe_2O_4$-PEG at different concentrations.

It is not clear why the use of **$CoFe_2O_4$ PEG 0.01 M** (**Figure 51A)** stresses the MRC-5 negative control cells as the concentration increases, probably due to higher cobalt toxicity in cells **Figure 51B** $CoFe_2O_4$ PEG 0.02 M and **Figure 51C** $CoFe_2O_4$ PEG 0.03 M. What is clear is that the resistance of MDA-MB-231 is greater in this nanoparticle configuration. Cobalt is toxic to cells in high concentrations, but vitamin-enriched bovine serum specifically enriched with vitamin B-12 (Cobalamin) can optimize this metal as a cofactor that accelerates the rate of cellular replication, because cobalt participates in protein reactions that improve the synthesis of DNA and RNA, so it improves mitochondrial and ribosomal metabolism.

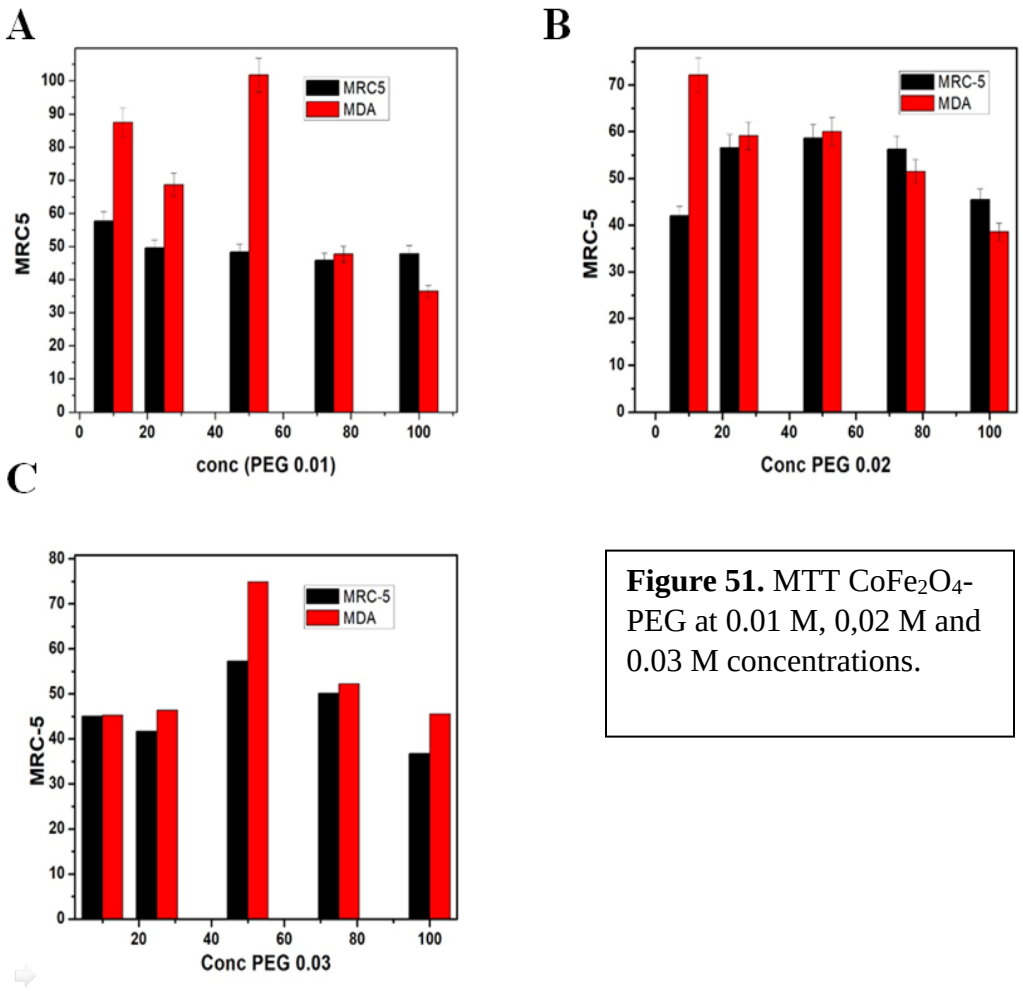

Figure 51. MTT $CoFe_2O_4$-PEG at 0.01 M, 0,02 M and 0.03 M concentrations.

4.3.5.1 MTT $CoFe_2O_4$ CTAB at different concentrations.

The concentrations of $CoFe_2O_4$ CTAB 0.1 M seem to be ideal to be used as a scaffold for delivery of drugs at a dose of 50 mg / dl, a uniform cellular viability is observed in both MRC-5 and MDA-MB-231 **Figure 52A**. As the $CoFe_2O_4$ CTAB 0.2 M concentrations increase at this Molarity, the MRC-5 cell line begins to suffer **Figure 52B**. The behavior of $CoFe_2O_4$ CTAB 0.3 M also indicates a lower viability in MRC-5, but the characterization of these nanoparticles indicates a large amount of free surfactant not suitable for use in the next phase of the project **Figure 52C**.

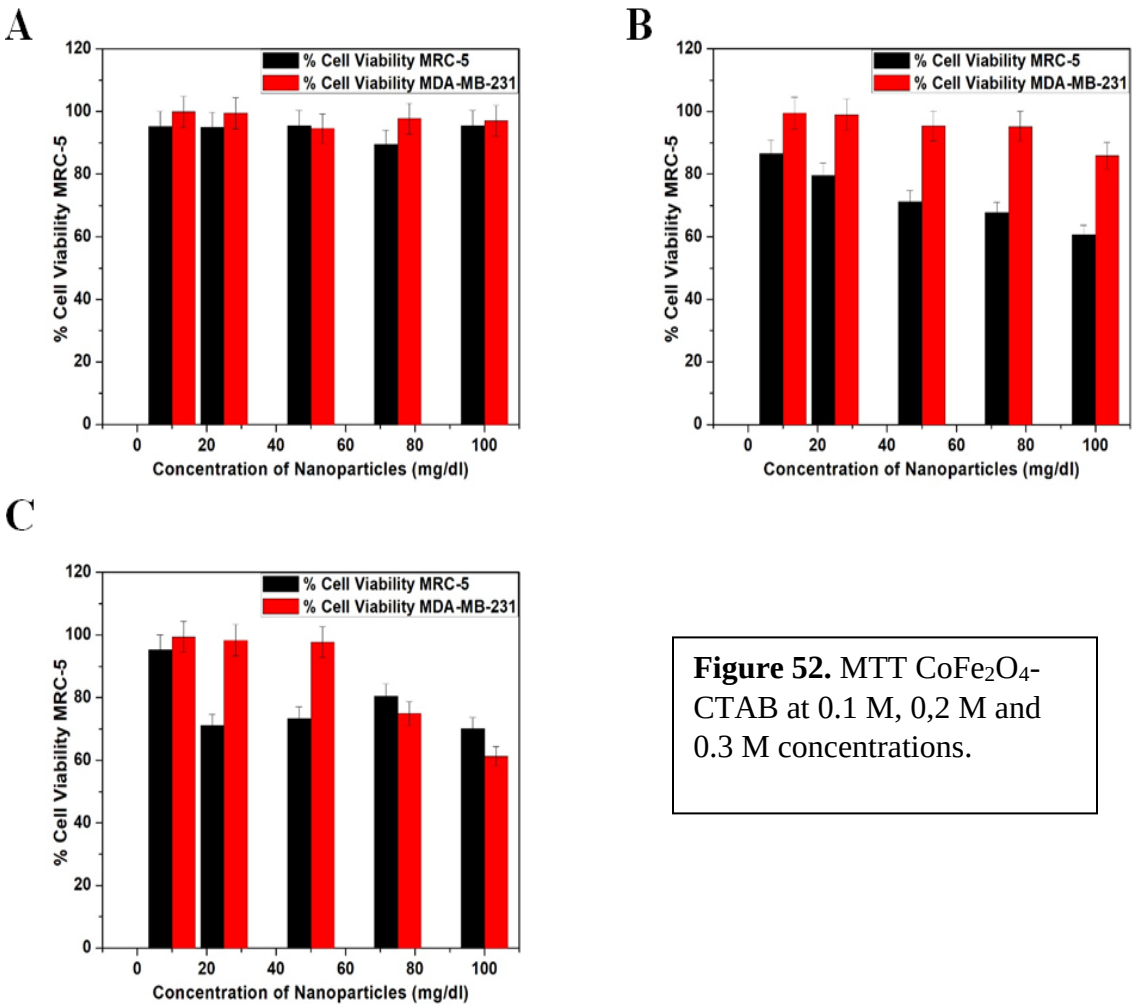

Figure 52. MTT $CoFe_2O_4$-CTAB at 0.1 M, 0,2 M and 0.3 M concentrations.

4.3.5.2 MTT $CoFe_2O_4$ Triton-X-100 at different concentrations.

The synthesis of $CoFe_2O_4$ Triton-X-100 0.1 M NPs was performed by using the TD method and then tested on both cell strains through MTT assay, **Figure 53 A**. Our research group achieved an adequate design, morphological structure and composition. In addition, there is a therapeutic window from 10 mg / dl to 50 mg / dl, so this configuration is a candidate to continue in the design of core shell gold-coating and nano-functionalization. **Figure 53 B**, $CoFe_2O_4$ Triton-X-100 0.2 M The transition metals such as Co, Mn, Zn can be toxic at higher concentrations or they can enhancing the rate of cellular replication, however when a detergent such as TX-100 is added, it seems that the high concentration at this molarity begins to decrease the cell viability of both MDA-MB-231 as of MRC-5. **Figure 53 C** $CoFe_2O_4$ Triton-X-100 0.3 M showing a favorable behavior again, however, the nanoparticles obtained were characterized and do not denote an adequate morphology and structure, this candidate was discarded for the next stage.

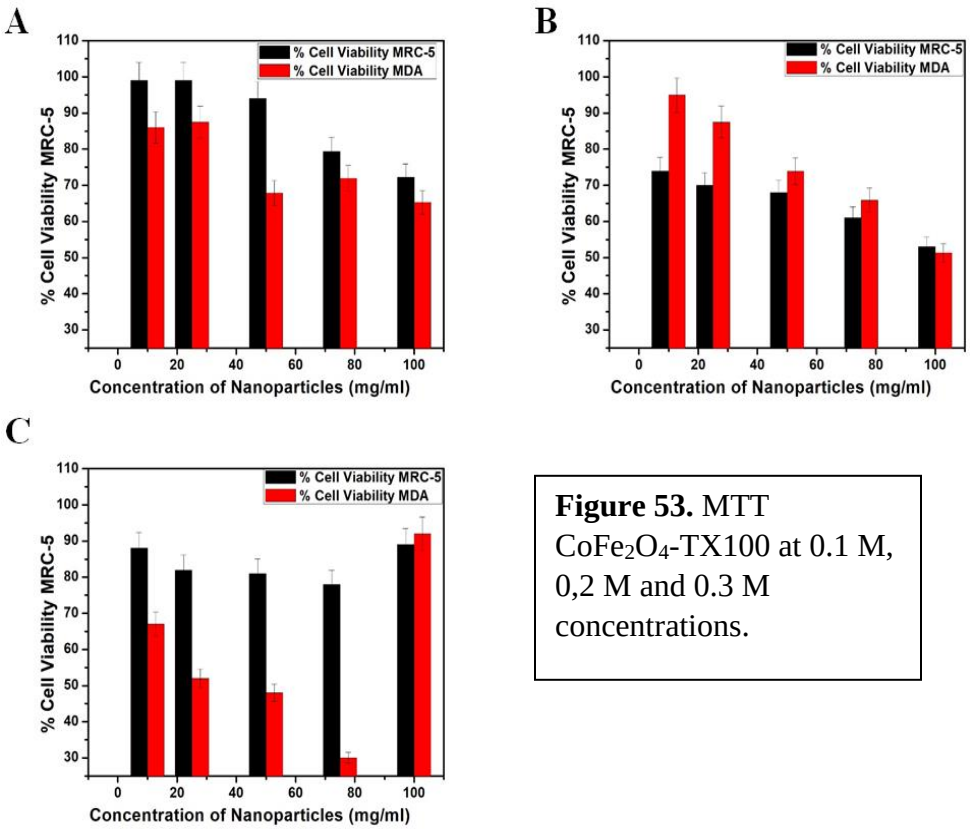

Figure 53. MTT $CoFe_2O_4$-TX100 at 0.1 M, 0,2 M and 0.3 M concentrations.

4.3.5.3 MTT $CoFe_2O_4$ SDS at different concentrations.

The SDS under this configuration $CoFe_2O_4$ SDS 0.1 M (**Fig 54. A**) has no cytotoxic effects for both MRC-5 or MDA-MB-231 at any concentration, there are some reports of SDS nanocomposites having the same behavior [354], but as long as the concentrations increase **Fig 54. B**, $CoFe_2O_4$ SDS 0.2 M and **Fig 54. C,** $CoFe_2O_4$ SDS 0.3 M), the cell viability decreases, at this point we can only hypothesize that it is due to the increase of SDS detergent not properly fixed to the cobalt ferrite core. However, we discarded SDS 0.2 and 0.3 M concentrations for next NPs generation.

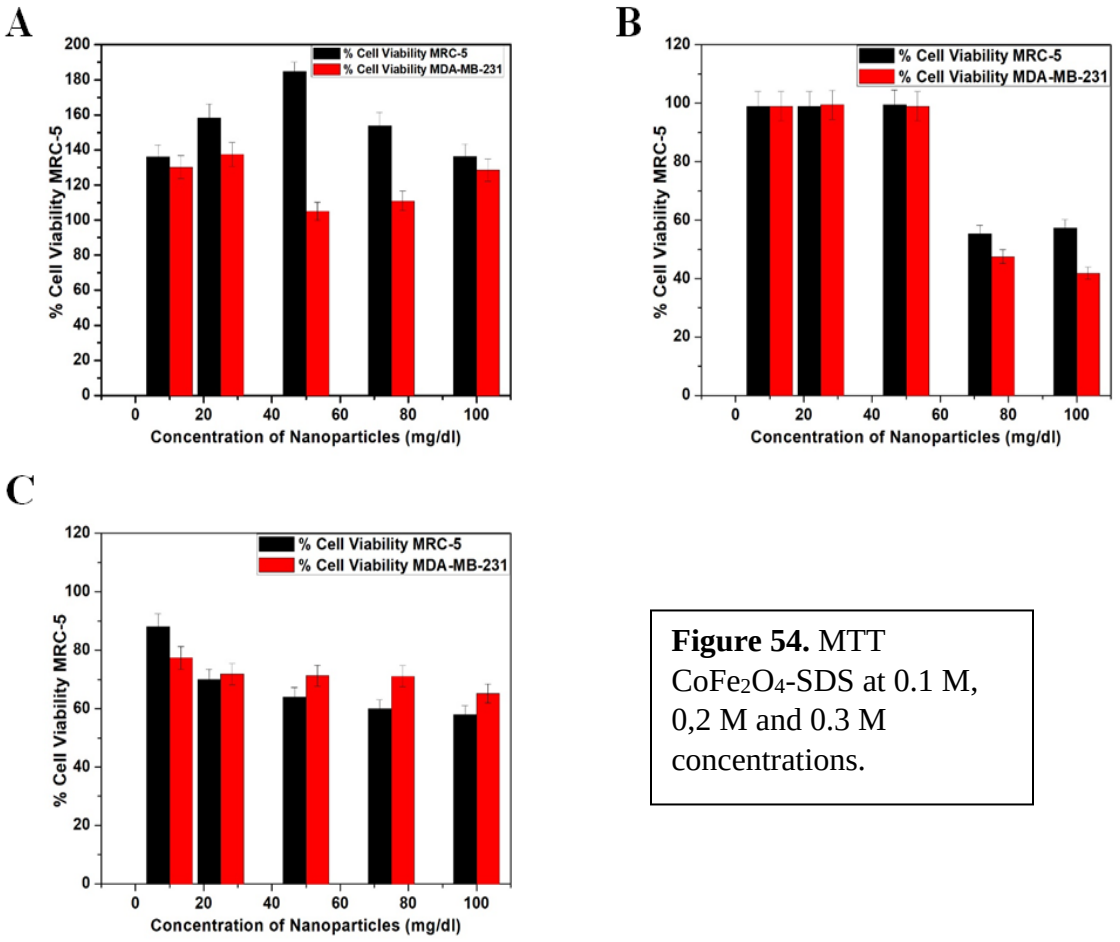

Figure 54. MTT $CoFe_2O_4$-SDS at 0.1 M, 0,2 M and 0.3 M concentrations.

4.3.6 MTT $MnFe_2O_4$ PEG at different concentrations.

$MnFe_2O_4$ PEG 0.01 M NPs are not affecting MDA-MB-231. However, it is a good candidate since homogenous behavior is present and remains contradictory 100 mg/dl seems to be a therapeutic window. **Figure 55 A.** The $MnFe_2O_4$ PEG 0.02 M. The more PEG molar concentration is adding to more decrease cell viability for both MDA-MB-231 and MRC-5 presumably due to NPs morphological reasons (**Figure 55 B).** $MnFe_2O_4$ PEG 0.03 (**Figure 55 C)** is not a good candidate, the synthesis at higher molarity in TD generates free manganese that is maintained in PEG irrigated as satellites, the high concentrations of manganese are toxic for the cells.

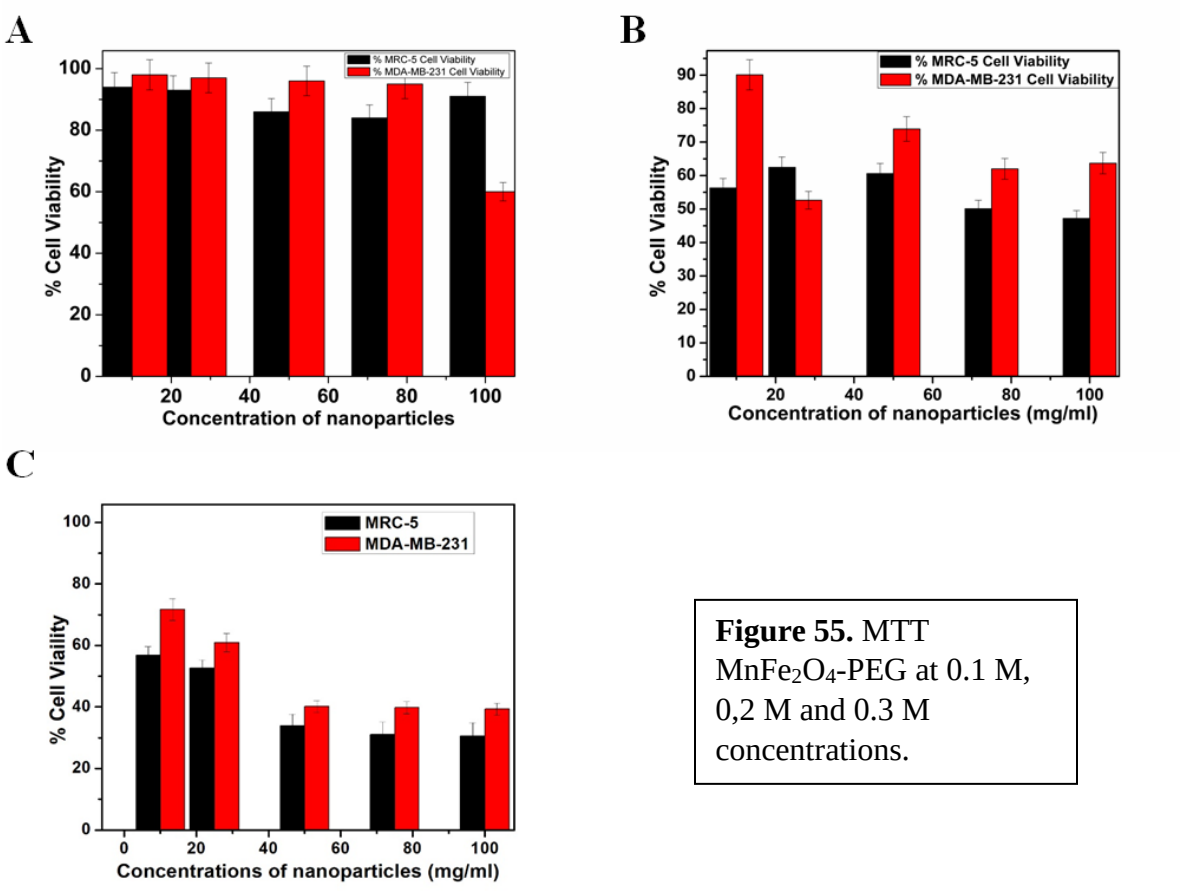

Figure 55. MTT $MnFe_2O_4$-PEG at 0.1 M, 0,2 M and 0.3 M concentrations.

4.3.6.1 MTT $MnFe_2O_4$ CTAB at different concentrations.

The MTT assay was performed also 3 times. **Figure 56 A.** $MnFe_2O_4$ CTAB 0.1 M. NPs seems to be a good candidate at least until 50 mg/dl dose. **Figure 56 B,** $MnFe_2O_4$ CTAB 0.2 M. It could be useful till 20 mg/dl dose. **Figure 56 C** $MnFe_2O_4$ CTAB 0.3 M**.** made by using TD synthesis is affecting in a negative way both MRC-5 and MDA-MB-231 cell strains.

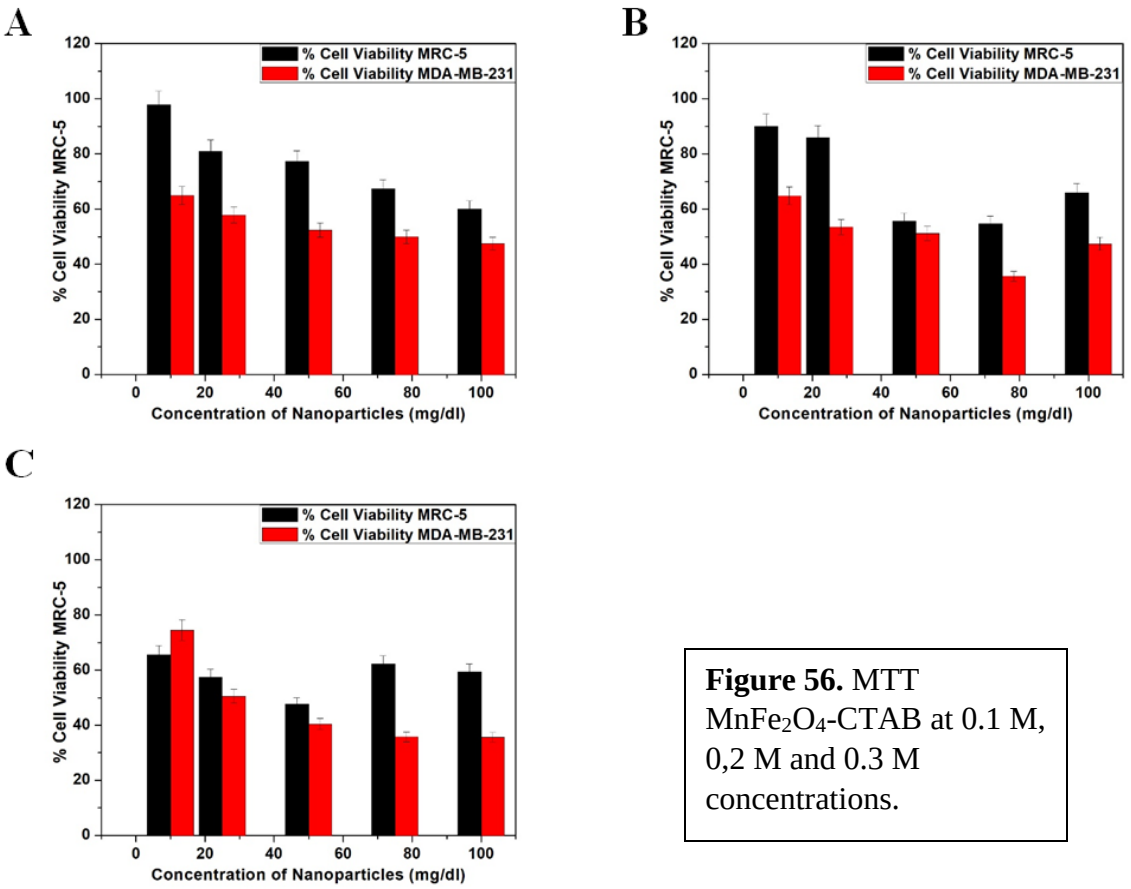

Figure 56. MTT $MnFe_2O_4$-CTAB at 0.1 M, 0,2 M and 0.3 M concentrations.

4.3.6.2 MTT $MnFe_2O_4$ Triton-X-100 at different concentrations.

Figure 57A, $MnFe_2O_4$ Triton-X-100 0.1 M. showing an excellent candidate due to composition, size and morphology, seems to have an excellent behavior at low doses. **Figure 57 B,** $MnFe_2O_4$ Triton-X-100 0.2 M. TX-100 detergent is creating cell toxicity. **Figure 57 C** $MnFe_2O_4$ Triton-X-100 0.3 M It is unacceptable the cytotoxicity is producing even at low doses over MRC-5.

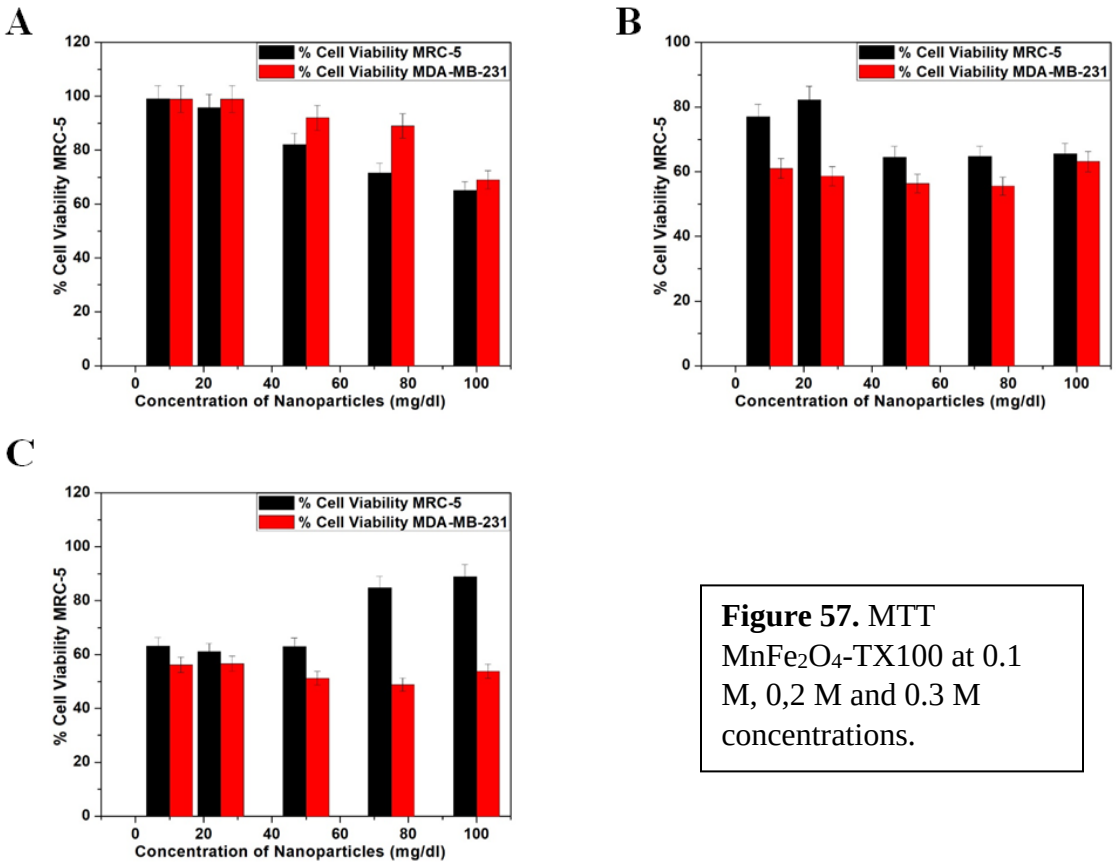

Figure 57. MTT $MnFe_2O_4$-TX100 at 0.1 M, 0,2 M and 0.3 M concentrations.

4.3.6.3 MTT $MnFe_2O_4$ SDS at different concentrations.

We cannot ignore **Figure 58 A** $MnFe_2O_4$ SDS 0.1 M, this nanoparticle configuration, it is increasing or not affecting cell-viability neither when high molarity concentrations are being applied. **Figure 58 B,** $MnFe_2O_4$ SDS 0.2 M and **Figure 58 C** $MnFe_2O_4$ SDS 0.3 M are behaving in the same way, that's why we decided to proceed with these for the next gold coated step having in mind that $MnFe_2O_4$ SDS 0.1 M was one of the best candidates.

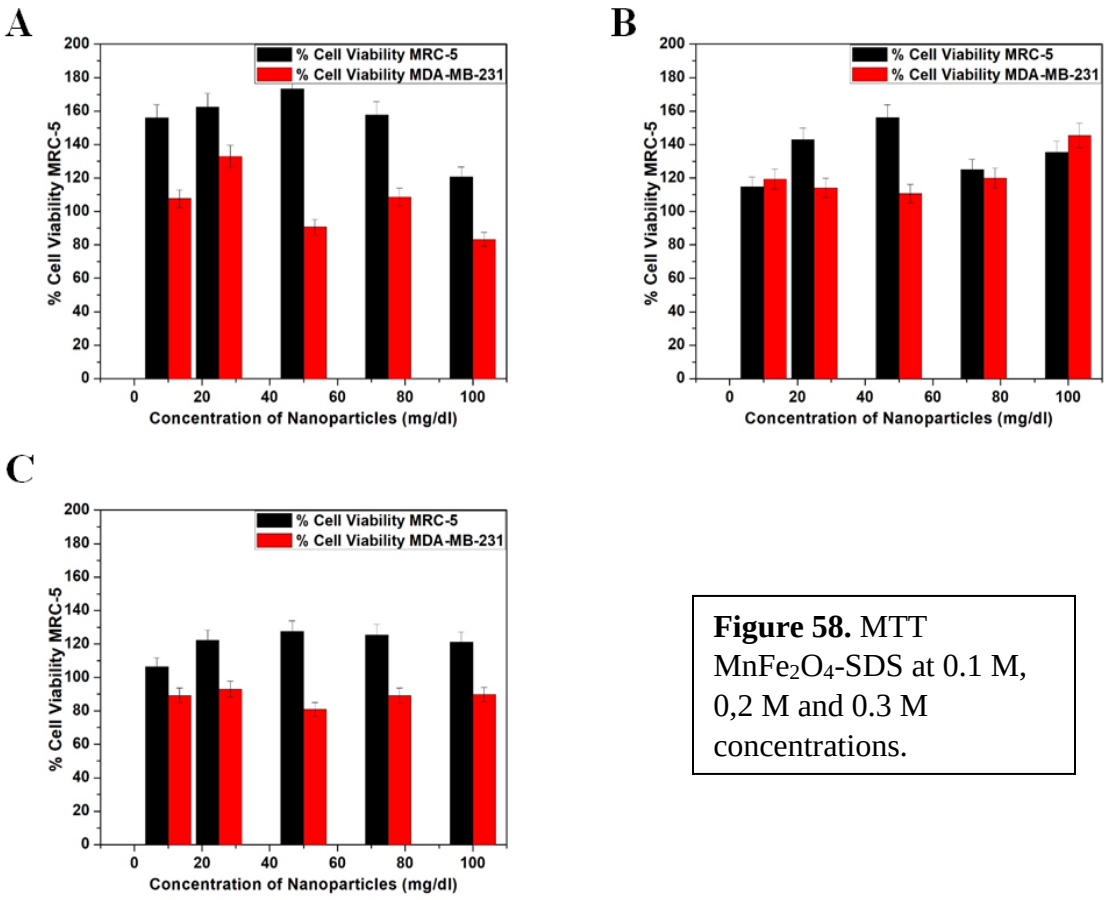

Figure 58. MTT $MnFe_2O_4$-SDS at 0.1 M, 0,2 M and 0.3 M concentrations.

4.3.7 MTT $ZnFe_2O_4$ PEG at different concentrations.

Zinc is an intracellular ion found mostly in the cytosol. Its amount in the adult human body ranges between 1 and 2.5 g, therefore, it is the second trace element in relation to the total amount in the organism, because the first is iron.

It was decided to study zinc ferrite cytotoxicity effects. Although zinc is related to enzymatic processes of cellular respiration, and is a cofactor of enzymes such as aldolases, dehydrogenases, peptidases, alkaline phosphatase, carbonic anhydrase, superoxide dismutase and DNA and RNA polymerases which are involved in energy metabolism, here you can see a decrease in cell viability that we do not like , since the MRC-5 cell line is mostly negatively affected in comparison with MDA-MB-231. However, **Figure 59 A) $ZnFe_2O_4$ PEG 0.01 M** seems to be promising unlike **B) $ZnFe_2O_4$ PEG 0.02 and C) $ZnFe_2O_4$ PEG 0.03 M**.

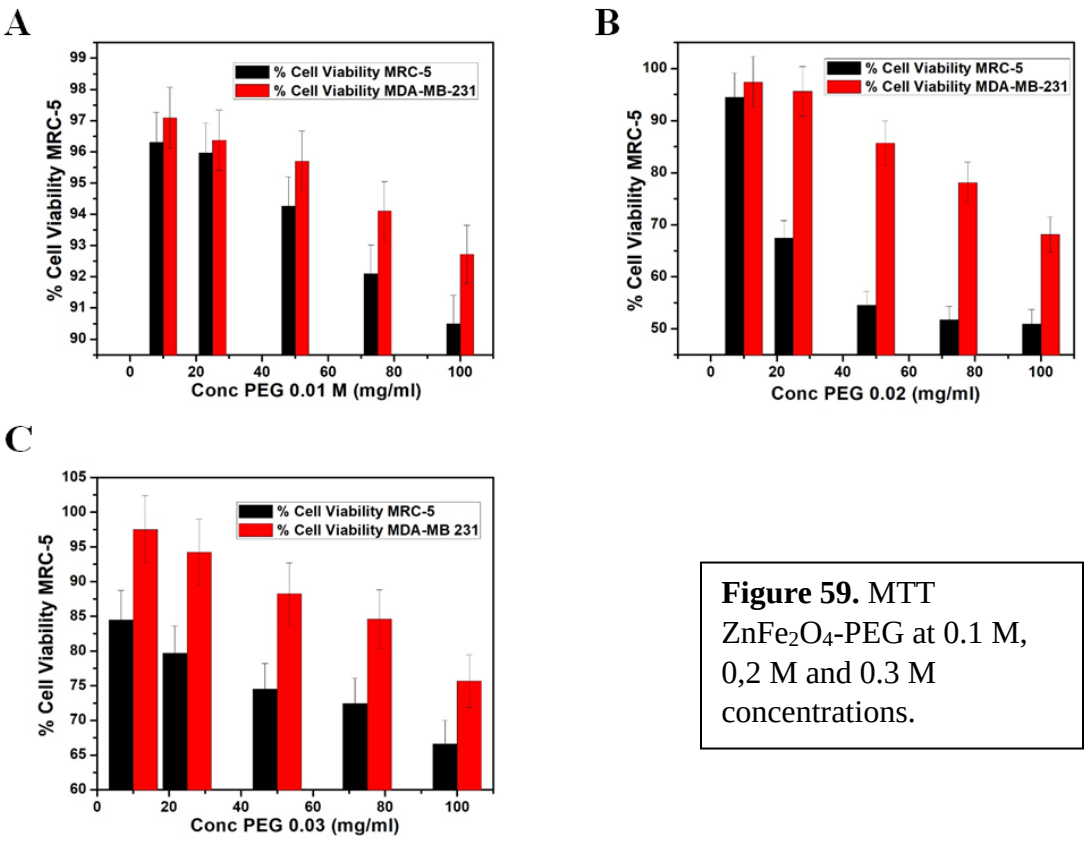

Figure 59. MTT $ZnFe_2O_4$-PEG at 0.1 M, 0,2 M and 0.3 M concentrations.

4.3.7.1 MTT $ZnFe_2O_4$ CTAB at different concentrations.

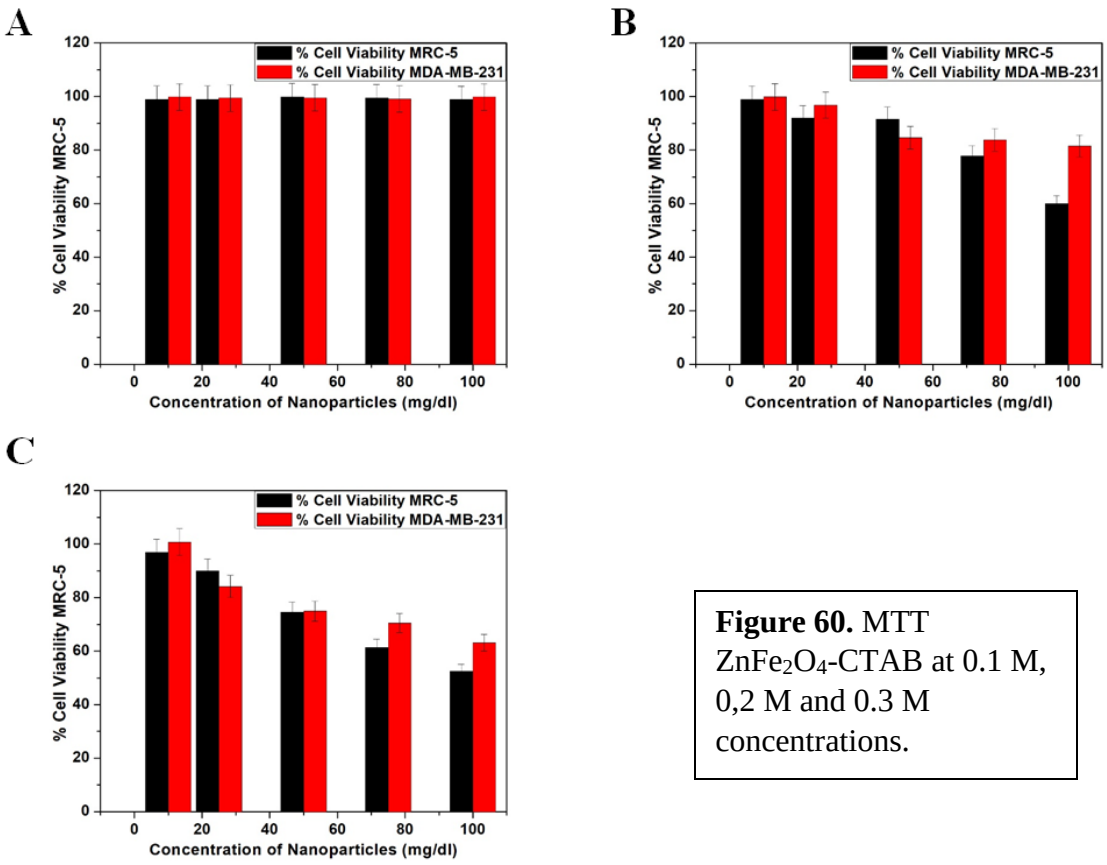

Figure 60. MTT $ZnFe_2O_4$-CTAB at 0.1 M, 0,2 M and 0.3 M concentrations.

The MTT assay run with $ZnFe_2O_4$ CTAB 0.1 M **(Figure 60A)** is showing that, *"In vitro"*, Zn produces cytotoxicity due to an increase in reactive oxygen species (ROS) and activation of the MAP-kinase cascade. However, the low concentration of 0.1 M CTAB covering provides adequate prevention against cytotoxicity. **Figure 60 B**, $ZnFe_2O_4$ CTAB 0.2 M. A non-homogeneous microscopic structure observed in these NPs may be the explanation of why cytotoxicity increases as CTAB concentration increases. **Figure 60 C,** $ZnFe_2O_4$ CTAB 0.3 M. This configuration is the worst, as TEM has demonstrated. The CTAB formed an amorphous mixture with agglomerated $ZnFe_2O_4$ NPs and free iron NPs, instead of coating individual NPs, leading to cytotoxicity for both MRC-5 and MDA-MB-231.

4.3.7.2 MTT $ZnFe_2O_4$ Triton-X-100 at different concentrations.

$ZnFe_2O_4$ Triton-X-100 0.1 M. "*In Vitro"*, zinc also reduces levels of reduced glutathione and an increase in the levels of the oxidized form of glutathione which leads to cytotoxicity. This suggests that this design should be adequately covered with non-detergent type surfactant. Although possibly in a living model zinc promotes replication by the presence of enzymes that reduce its cytotoxicity. See **Figure 61 A**.

Figure 61 B. $ZnFe_2O_4$ Triton-X-100 0.2 M In this concentration of TX-100 0.2M, cell survival improves, but it is not a candidate that we can take seriously in the long term.

Figure 61 C. $ZnFe_2O_4$ Triton-X-100 0.3 M Finally, cell survival is decreased in both cell lines, our hypothesis is that it is due to the presence of TX-100 at high concentration and a broken structure of zinc ferrite that produces metal cytotoxicity.

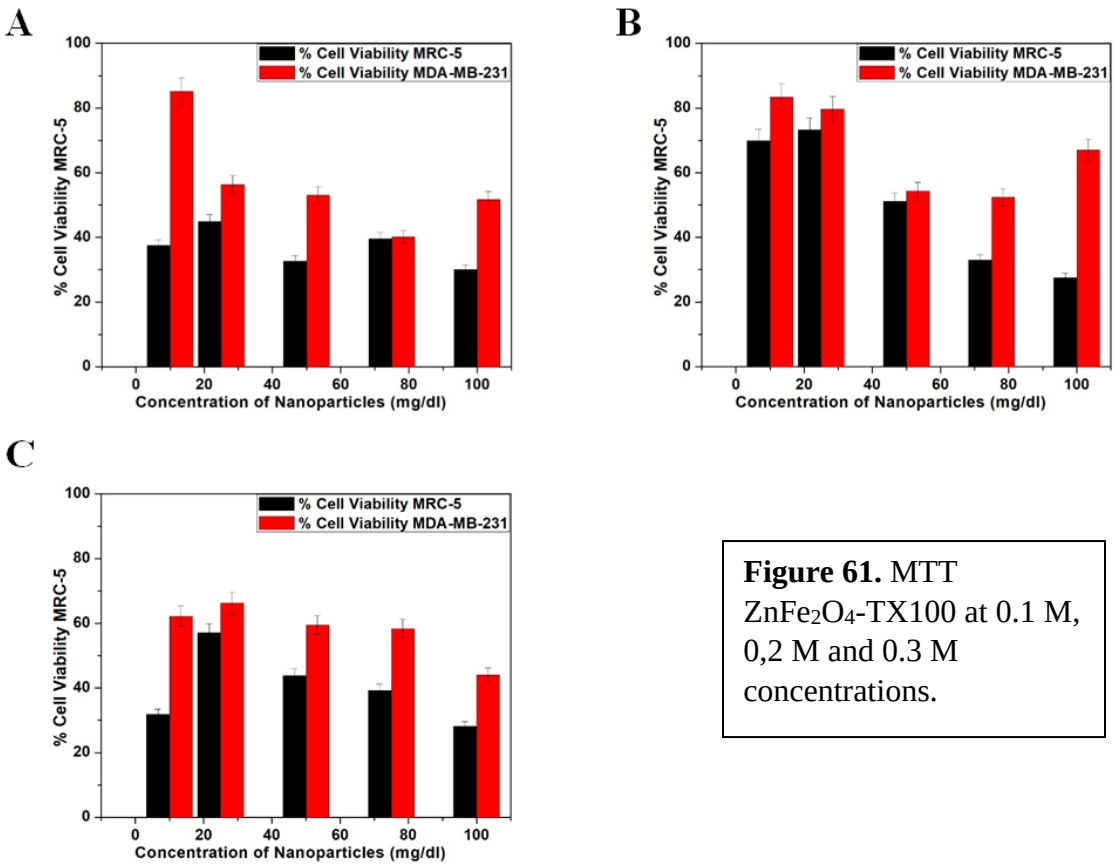

Figure 61. MTT $ZnFe_2O_4$-TX100 at 0.1 M, 0,2 M and 0.3 M concentrations.

4.3.7.3 MTT $ZnFe_2O_4$ SDS at different concentrations.

The effects of Zn added to those of SDS are not desirable *In Vitro*, possibly it is worth using the minimum concentration of SDS. Although morphologically, these NPs seem to have a pattern in bunches of flowers, their properties remain unknown. See **Figure 62 A.** The $ZnFe_2O_4$ SDS 0.2 M NPs. It is worth analyzing the behavior of these nanoparticles in the range of 10 and 20 mg / dl. See **Figure 62 B.** $ZnFe_2O_4$ SDS 0.1M.

In **Figure 62 C.** $ZnFe_2O_4$ SDS 0.3 M. we can appreciate in chapter 3, that the morphology of these nanoparticles obeys to nano-flowers, they did not prove to be useful in the MTT tests at a high SDS concentration.

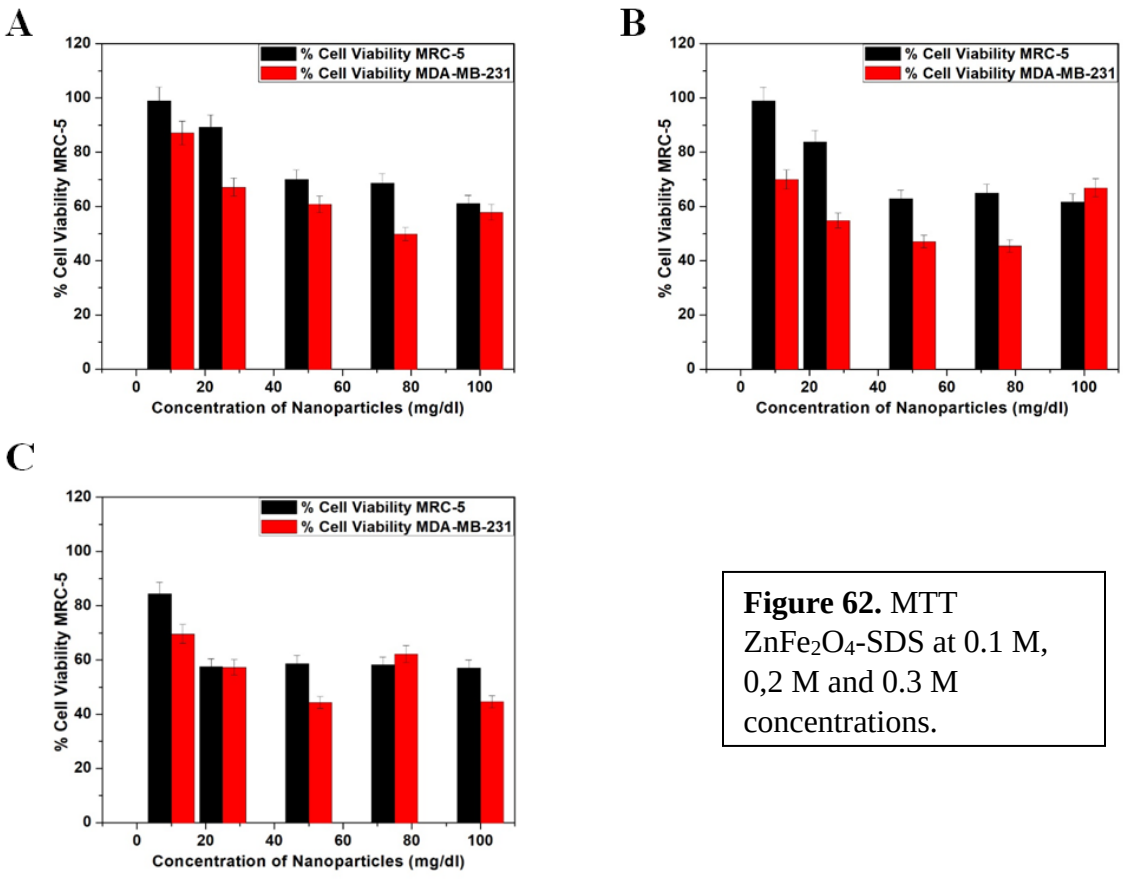

Figure 62. MTT $ZnFe_2O_4$-SDS at 0.1 M, 0,2 M and 0.3 M concentrations.

4.4 Selecting drugs.

The literature highlights that the efficacy of Doxorubicin can reach 80% in vitro, however the high rate of resistance both in vitro and in vivo pushes researchers to nanofunctionalize this type of drug, but resistance mechanisms are widely known, and we decided not to nanofunctionalize this drug on this occasion. The cytotoxic value found was only 70% in the best of cases and mostly compromised MRC-5 negative control **Figure 63.**

On the other hand, for Docetaxel and Bicalutamide, the calculation at 10 micromolar established a safe and comfortable way to adjust the drug in the cells, at a dose of 2000 nM the cell viability of MDA-MB-231 for Bicalutamide was 49%, which was a surprise since Bicalutamide was superior in therapeutic effect, presumably due to the presence of androgenic receptors in MDA-MB-231. However, similar results were found in Docetaxel concentrations.

4.4.1 MTT Doxorubicin alone at different concentrations.

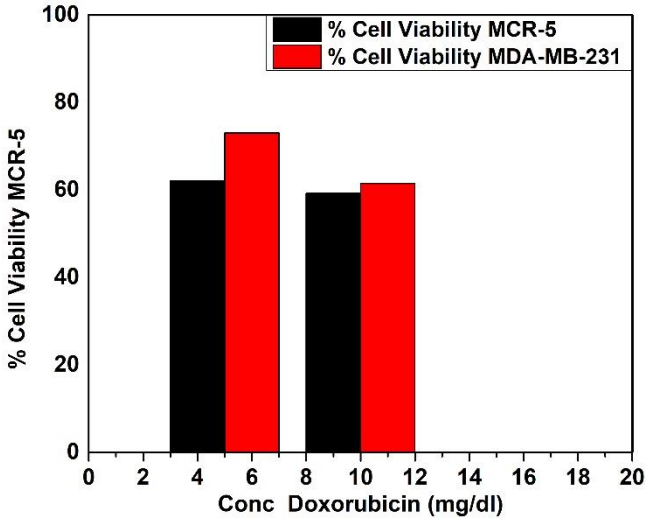

Figure 63. MTT Doxorubicin alone at different concentrations.

4.4.2 MTT Docetaxel alone at different concentrations.

Docetaxel has cytotoxic activity against breast Cancer, its action mechanism relies in the microtubule dynamic assembly and disassembly leading to apoptosis. Here, we found Docetaxel alone at 2000 nM is affecting MRC-5 (60% cell viability) in comparison with MDA-MB-231 (70% cell viability) **Figure 64**.

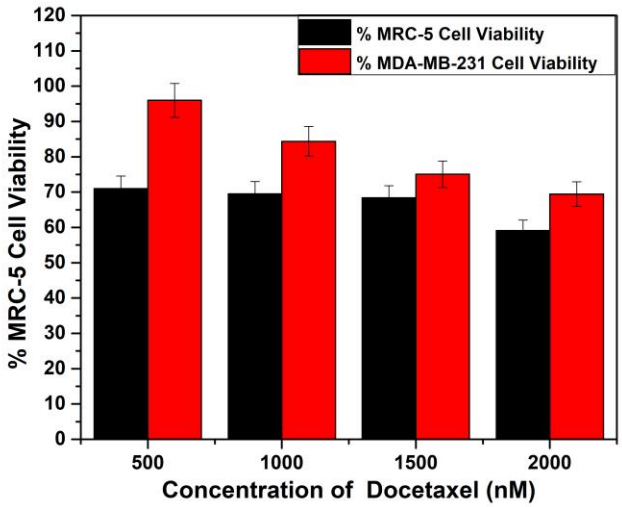

Figure 64. MTT Docetaxel alone at different concentrations.

4.4.3 MTT Bicalutamide alone at different concentrations.

We found Bicalutamide alone at 2000 nM is not affecting MRC-5 (90% cell viability) **(Figure 65)** in comparison with MDA-MB-231 (50% cell viability). Our research group theorize that it is due to the presence of the androgenic receptor in this model, because Bicalutamide works by blocking the androgen receptor (AR). So then, our research group decided moving forward with both Docetaxel and Bicalutamide for next step: Nano-functionalization.

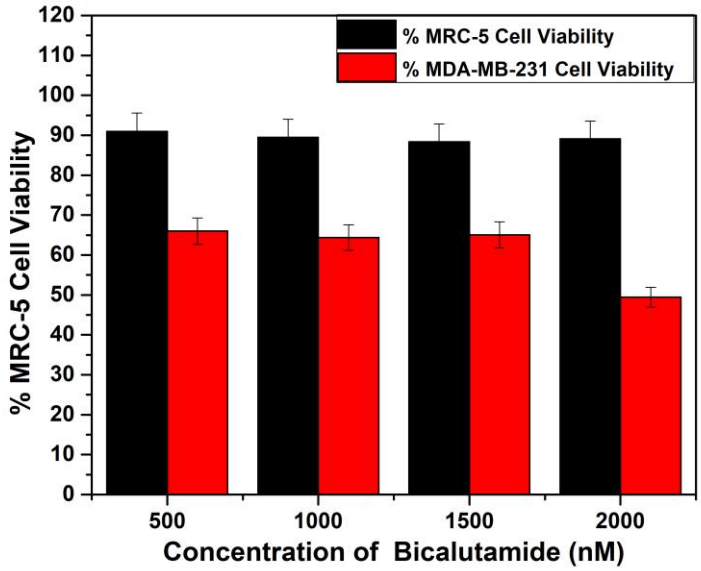

Figure 65. MTT Bicalutamide alone at different concentrations.

4.5 Core-shell UV-Visible Spectroscopy.

The absorption in the UV-Vis spectrum reflects the resonant oscillation frequency of the collective free electrons in the nanocrystal that is intended to be studied, in this case Au. The details of the UV-Vis technique were explained in Chapter 1. The UV-Vis spectra were performed using the UV-Vis UV-2401PC spectrometer from Shimadzu Corporation. The protocol used is the same as Ravichandran et al [355].The samples were dispersed in a polar solvent such as DI water. The baseline was obtained using a standard solution and was measured in the range of 200-1000 nm at a sensitivity of 1 nm.

The experiment aims to recreate the process of drug release (absorption, distribution, metabolism and excretion) and its pharmacological activity. The release of the Au @ $CoFe_2O_4$ Bicalutamide Docetaxel drug was studied using a dialysis method. The dialysis bags were soaked before use in DI water at room temperature for 12 h to remove the preservative, followed by thorough rinsing with distilled water. The in vitro release of Au @ $CoFe_2O_4$ Bicalutamide Docetaxel was performed by dialysis in a dialysis bag with 50 ml

of PBS. Three sacks were prepared to contain Au @ $CoFe_2O_4$ Bicalutamide Docetaxel for cumulative release (pH 5.3, 6.8 and 7.4) with continuous agitation to simulate the intercellular, intracellular and external environment of cancer cells. To carry out this study, 2 ml of dialyzed Au @ $CoFe_2O_4$ Bicalutamide Docetaxel complex was used. Two ends of the dialysis bag were tightly bound with threads. The bag was hung inside a beaker with the help of a glass rod so that the portion of the dialysis bag with the formulation was immersed in the buffer solution. The flask was kept on a magnetic stirrer and the stirring was maintained at 100 rpm at 37 ° C with a thermostatic control. Then, 1 ml of sample was taken from the system in a known period of time to determine the content of the drug. To compensate for the PBS solution as soon as 1 ml was extracted, it was replaced with the same equivalent volume. The amount of Au @ $CoFe_2O_4$ Bicalutamide Docetaxel released was determined using a UV-Vis spectrophotometer. This drug release study was also explained with different models of drug kinetics to explain the mechanism of release.

4.5.1 Drug kinetics models: Dialysis membrane.

Exactly as in previous studies, the loading efficiency of the drug has to be evaluated until an acceptable percentage above 90% is achieved. Then, the "*In Vitro"* drug release performance of the Gold NPs was investigated using 3 different pHs of PBS buffers (5.4, 6.8 and 7.4) at room temperature for 24 h. Cancer cells work at an acidic pH due to the formation of lactic acid due to the lower oxygen content and high metabolic capacity. The mechanism of drug release was studied using in vitro release models at various pHs. The various kinetic models are as follows: 1.- Zero order (cumulative amount of drug released versus time), 2.- First order (cumulative percentage of drug remaining versus time), 3.- Higuchi model (cumulative percentage of drug released versus square root of time) and 4.- Hixson-Crowell model (cumulative percentage of drug release versus square root of time). **Figure 66** shows the different equations of every single model.

Model	Equation	β_0	β_1
Zero order	$Q_t = Q_0 + k_0 t$	Q_0	k_0
First order	$\ln Q_t = \ln Q_0 + k_1 t$	$\ln Q_0$	k_1
Higuchi	$Q_t = Q_0 + k_H t^{1/2}$	Q_0	k_H
Hixson-Crowell	$Q_0^{1/3} - Q_t^{1/3} = k_w t$	$Q_0^{1/3}$	k_W
Weibull	$\log[-\ln(1-m)] = \beta\log(t - T_i) - \log\alpha$	$-\log\alpha$	β

Q_t: amount of drug released in time t; Q_0: initial amount of drug in dissolution media; k_0, k_1, k_H, k_W: release rate constants; m: accumulated fraction of the drug; α: scale parameter; β: shape parameter; T_i: location parameter.

Figure 66. Drug kinetic Model. *Source: André Lima de Oliveira Costa, In vitro dissolution kinetic for mycophenolic acid derivatives tablets, Braz. J. Pharm. Sci. vol.49 no.2 São Paulo Apr./June 2013*

4.6 Hyperthermia experiment setup.

Hyperthermia is one of the most celebrated features for Cancer therapeutics. It has been demonstrated that solid tumors are more susceptible to enter in apoptosis when chemotherapy and radiotherapy are being used combined with hyperthermia. The main advantage and difference of hyperthermia with respect to thermoablation is that the former does not cause damage to normal tissues and comprises a temperature range of 41-50 ° C, while a temperature above 50 °C is considered thermoablation [67]. In the present work, microwave technology was used to stimulate the effects of hyperthermia of $CoFe_2O_4$ nanoparticles as well as electromagnetic bovine heating **(Figure 67).**

Microwave (MW) experiment setup: The setup used to apply the MW electromagnetic field to perform the experiments consisted of a generator (SML 03, Rhode & Schwarz, Germany) set to a frequency of 2.45 GHz. This signal was then amplified using an RF & MW module power amplifier (1164-BBM3Q6AHM, Empower, USA). The output power was then monitored by using a dual direct coupler (DC7154M, Amplifier Research, USA) and a power meter (PM2002, Amplifier Research, USA) to ensure an output power of 10 W and to monitor the reflected power of the system. To adjust the standing wave ratio (SWR) to an optimal value, a coaxial stub tuner (1878C, Maury Microwave Corp., USA) was used along a network analyzer (E5071B, Agilent Technologies, USA) to measure and reduce the SWR to a minimum prior to each experiment.

Temperature Measurements: Non electromagnetic interfering optical fiber probes temperature sensors (M3300, Luxtron, USA) were used to record temperature increment. The temperature was measured inside the phantom which simulated the tumor. Each tests lasted 200 sec in order to study the temperature response as a function of time. The temperatures were recorded every second during the experiments using True Temp software (Luxtron, USA).

The following are the measurement conditions used in microwave heating:

1.- Adjustment of the signal generator at the frequency of 2.45 GHz

2.- Power adjustment to -13.2 dBm (to have 3 watts)

3.- One-slot microwave applicator (antenna), 1.2 mm in diameter

4.- Fixed 50-watt amplifier module

5.- Temperature of the thermal bath at 30 ° C

6.- Three fiber optic sensors are used to measure the temperature, they are placed in the middle of the slot of the applicator and separated by capillaries.

7.- Thermal insulation material for houses is used to avoid heat loss during the experiment

8.- The distance of the applicator to the bottom of the test tube is kept constant for all samples.

9.- The measurement time is 3 minutes and is measured with a stopwatch.

10.- The amount of material for the tests is 2 ml

11.- It adjusts the bandwidth of the network analyzer from 2.4 GHz to 2.5 GHz and is measured at 2.45 GHz

12.- The STUB is adjusted for each measurement (if there is a change in the dielectric properties of the material, a change in the reflected wave is seen).

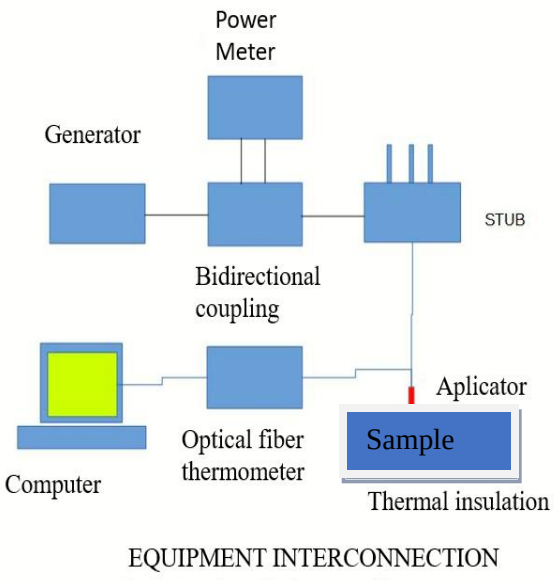

Figure 67. Hyperthermia experiment setup.

4.6.1 Hyperthermia measurement protocol.

1.- The sample is kept at a temperature of 30 ° C in the thermal bath for a minimum of 5 minutes to the stabilization of temperature **(Figure 68)**.

2.- The sample is shaken with a vortex machine for about 6 seconds.

3.- The sample is placed inside a thermal insulation material containe.r

4.- The STUB is adjusted to obtain a SWR of 1.01 or 1.02 with the antenna inside the sample.

5.- Apply 3 watts (34.77 dBm) for 3 minutes.

6.- As temperature increases, data were obtained every 5 seconds * by means of optical fiber measuring equipment at different distances from the applicator.

7.- The amplifier is turned off to continue with the next measurement, but the fan is left over the applicator and then is dried with absorbent paper.

8.- The liquid inside the capillaries is extracted.

A typical measurement of SWR at the end of the experiment is 34.77 dBm of direct wave and 18.0 dBm of reflected wave.

If necessary, the applicator can be rinsed with double-distilled water and then dried.

* Command to adjust to 5 seconds:

ESC MU = 5 RETURN [1] By means of the network analyzer the depth of the antenna is sought so that the SRW approaches 1 in a sample with water.

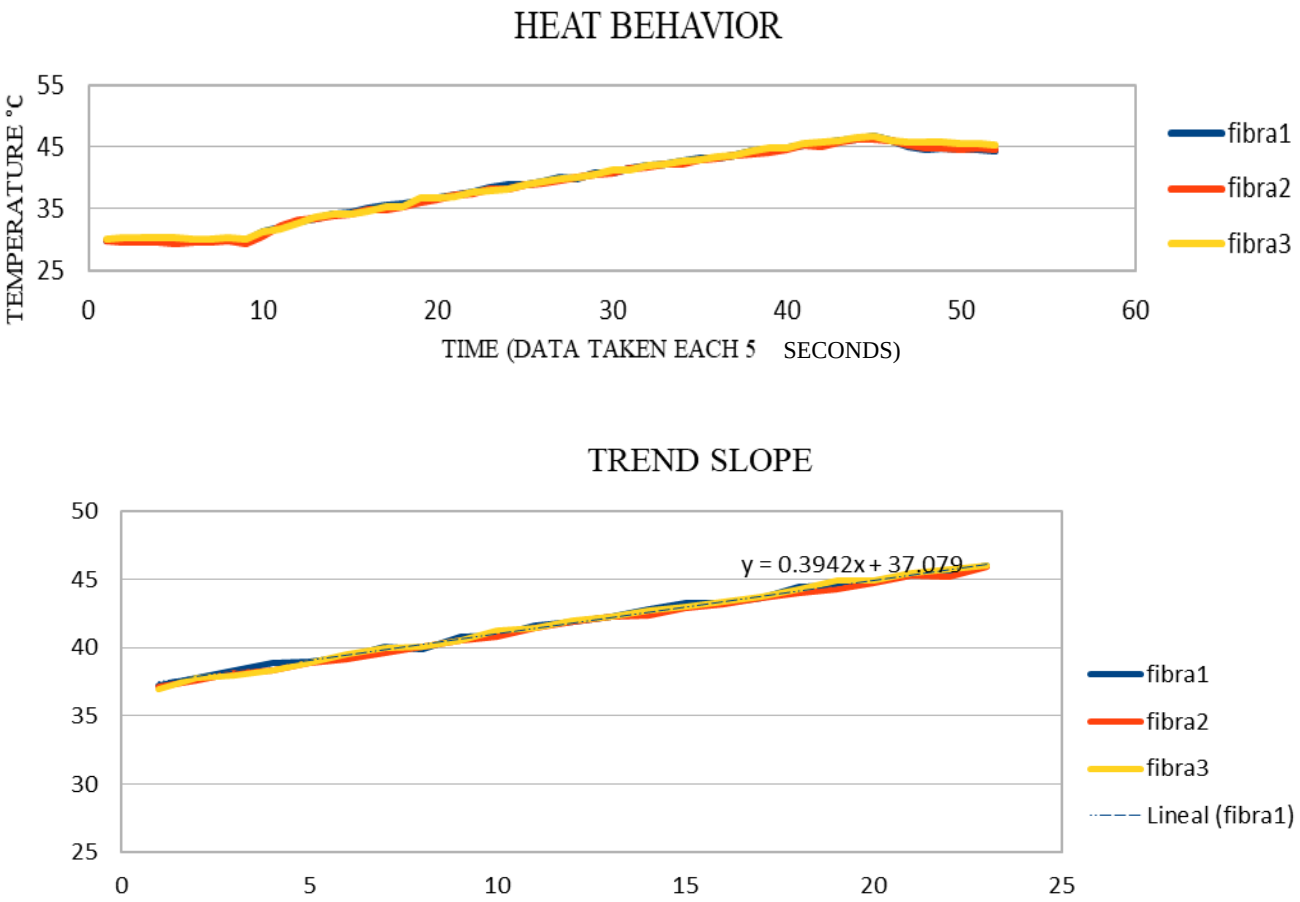

Figure 68. Hyperthermia measurement protocol.

4.6.2 Hyperthermia TX-100/CTAB Au@$CoFe_2O_4$ measurement protocol.

The thermal enhancement of the drug cytotoxicity was first tested using MNPs@Au Gold coated magnetic nanoparticles drug complex (Bicalutamide and Docetaxel) with drug concentrations that varied from 25µg/ mL to 100 ug per ml with a Au@$CoFe_2O_4$TX-100/CTAB 0.1M concentration fixed at 300 nM. The cytotoxicity was then determined using an MTT assay. Briefly, MRC-5 or MDA/MB/231 cells were seeded at a density of 5 × 104 cells into 24-well plates and were cultured in DMEM and RPMI medium in an incubator with a humidified 5% CO_2 atmosphere at 37 °C. After 24 h of incubation, various

concentrations of core-shell complexed with drug, without drug and drug alone was added to the cells, and the samples were incubated for 2 hours with an additional set of the same set of samples kept as controls. The samples were divided into two groups: one where hyperthermia was applied by switching on microwave hyperthermia and control groups where hyperthermia was not applied. After the hyperthermia treatment on all samples, fresh media was added and incubated in a 24-well plate again in an incubator with a humidified 5% CO_2 environment at 37°. After 1 day, 50µl of MTT reagent (Promega, USA) were added to each of the wells, and the plate was incubated for an additional 4 hours, and the absorbance at 490 nm was then measured using a microplate reader.

4.6.3 Hyperthermia "In Vitro" $CoFe_2O_4$ Tx-100 coated magnetic nanoparticles measurement protocol.

A micro-antenna was used that works at 2.45 GHz and was set to give a SWR of 1.1 in a sample of double-distilled water. The power used was 10 watts with duty cycles of 50% to 10%. The objective of the experiment was to heat the samples to 50 ° C in a time of 20 s and maintain that temperature for 50 seconds.

The duty cycle was determined using a sample of double distilled water. The 100% corresponds to 10 ms, so 50% corresponds to 5 ms on and 5 ms off. The temperature measurement was performed with an optical fiber placed in the antenna slot.

The antenna is attached to the antenna by means of Teflon tape.

Process:

The samples are kept in a thermal bath at 37 ° C. Then, samples were placed in a thermal chamber for microwave application. Next, the antenna was placed to the bottom of the test tube. After that, when the system reaches 47 ° C it changes to 40% and when it reaches 50 ° C, system changed to 10% and it was kept for 50 seconds at 50 ° C. Finally, the sample was removed. When changing cell types, the antenna is washed in double-distilled water.

Hyperthermia is a treatment strategy that involves the exposure of magnetic nanoparticles to an alternating magnetic field to increase temperature and induce apoptosis in cells or tissues. In this work, microwaves were used to irradiate CFNPs with a microcoaxial

double-slot antenna as an applicator, which was placed inside the tube containing the nanoparticles in physiological saline. In this case, 2.45 GHz was used as an Industrial, Scientific and Medical (ISM)-approved frequency for localized hyperthermia induction. **Figure 69** depicts the temperature profiles in correspondence to the microwave irradiation time for water and different concentrations of cobalt ferrite nanoparticles in physiological-saline water. The microwave absorption rate of physiological saline (3.3*10-3) is higher compared to water ($1*10^{-3}$). Upon the absorption of microwaves (2.45 GHz), the rotational motion of the electric dipole of water molecules gets excited and the average phase of this motion is delayed compared to the microwave electric field. The microwave energy leads to an increase in kinetic as well as intermolecular energies of water. The kinetic energy is responsible to increase the temperature of water, while the intermolecular energy leads to internal rearrangements in the water molecules. Physiological saline suspension (diluted salt solution) is heated drastically and rapidly compared to water since salt ions tend to heat up faster, specifically Cl- ions. The chloride ions in the presence of a microwave electric field tend to undergo motion and the microwave energy transfer leads to higher collision between salt ions and water molecules. The specific heat capacity of 0.13 molal of physiological saline suspension is 4184 J/gram K. In physiological saline, SAR was calculated as **68.28W/g.** SAR value for cobalt ferrite was found to be 68.28 W/g and we need to find out SAR values for TX-100-CTAB-Au@$CoFe_2O_4$. This is our future perspective. Heat generation is possible when magnetic nanoparticles dispersed in physiological saline leads to the excitation of unpaired electron of cobalt and Fe ions to a higher-energy state when microwaves are absorbed. When the excited electron alters its spin direction and returns back to its ground state, then it emits phonons. The microwave fields and the magnetic dipoles are coupled to convert the energy of radiation to heat. When CFNPs present in the saline suspension are exposed to microwave radiation, then the collision between nanoparticles, salt ions and water molecules tend to increase thus leading to higher heat generation. One of the parameters to determine the efficacy of hyperthermia is the specific absorption rate, (SAR). As mentioned earlier, SAR is defined as the amount of energy absorbed per unit mass and can be determined from the bio-heating equation which, under certain experimental conditions, can be determined by the relation between the increase in temperature and time, multiplied by the specific heat capacity. This

relationship of changed ratios is represented by the slope of the equation described by each of the lines in **Figure 69**. Considering 0.5 mg/mL as the base concentration at which all samples possess same specific heat capacity, the percentage increase in SAR for the 1.0 mg/mL, 1.5 mg/mL and 2.0 mg/mL concentrations are 3.5%, 10.7% and 30.6% respectively. As we can see, there is a non-linear increase in SAR at different concentrations. Considering that the biological effects in tissues depend on the increase in temperature and that they are also correlated with the Arrhenius equation, the increases that we obtained are significant. The Arrhenius relationship has been used to define the temperature dependence on the rate of cell killing, which can then be used as a method for thermal dosimetry in which a change in temperature of 1C will double the rate of cell killing, above which is known as the "break point". Thus, the temperature increases for the different concentrations obtained are significant in relation to the biological effects.

For SAR calculations, we need to find the slope of each concentration which is DT/dt. Later we need to draw the graph of DT/dt versus concentration. After getting slope from this graph, we can get DT/dt value for SAR calculations. SAR as mentioned above is this slope multiplied by the heat capacity of solvent, which in our case is physiological saline.

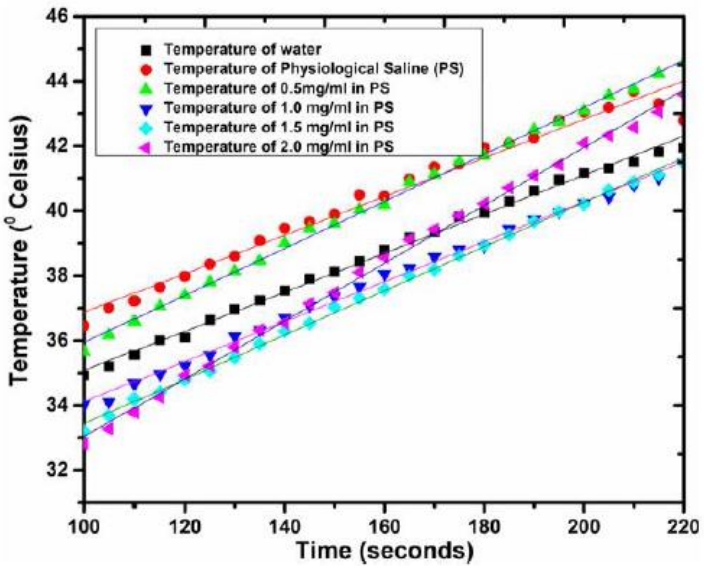

Figure 69. Temperature versus microwave (2.45 GHz) radiation time for water, physiological saline and different concentrations of cobalt ferrite nanoparticles in physiological saline.

4.6.4 In Vitro Hyperthermia Studies on TNBC Cell Lines

Thermal exposition of the cells through microwave irradiation of the CFNPs lead to higher cytotoxicity and mortality of cells compared to the absence of microwave irradiation. In the absence of microwaves, the inherent cytotoxicity of CFNPs was less in both types of cell lines, but as soon as the cells were exposed to microwave irradiation, the viability decreased tremendously. The microwave-exposed cells also showed increasing cell mortality with increasing concentrations of CFNPs. In the presence of alternating electromagnetic radiation, the magnetic nanoparticles lead to localized hyperthermia, thus causing the degradation of the cell organelles and the fragmentation of their DNA. In **Figure 70**, the cell viability results of both MRC-5 and MDA-MB-231 cell lines as a function of CFNP concentrations with and without microwave irradiation are shown. Au@$CoFe_2O4$ will be study in future.

Our research group found a therapeutic window of CFNPs from 5 mg/mL to 40 mg/mL in which the cell viability of MDA-MB-231 decreases to 55% in contrast to the cell viability of MRC-5 cells, showing 70% on exposure to microwave irradiation at the same CFNP concentration of 40 mg/mL. Hyperthermia can be induced in cells above 43 °C. Hence, in this study, localized hyperthermia is induced in cells using microwave irradiation, maintaining the exposure time for 50 s. There is a relationship between the microwave power output and the temperature rise in the tube containing physiological saline with cells and nanoparticles. The power output was adjusted in such a way that the temperature was maintained at 50 °C for 50 s. This optimized power output was relevant to kill cells in the presence of nanoparticles with a lower exposure time. CFNPs absorb microwaves that induce hyperthermia in the cells, thus leading to their death. In the control cell studies, the cell viability of MRC-5 upon exposure to microwaves for 50 s, but without nanoparticles, was 98%, while that of MDA-MB-231 was 94%. Cancer cells are found to be more vulnerable upon exposure to microwaves compared to the normal ones. Furthermore, when both MDA-MB 231 (triple negative breast cancer cell lines) and MRC-5 (fibroblast normal cell lines) are exposed to the same increasing concentration of the CFNPs, cancer cells are found to have more mortality compared to the normal ones upon exposure to microwaves

which can be corroborated from **Figure 70**. The reason for this vulnerability is still not known.

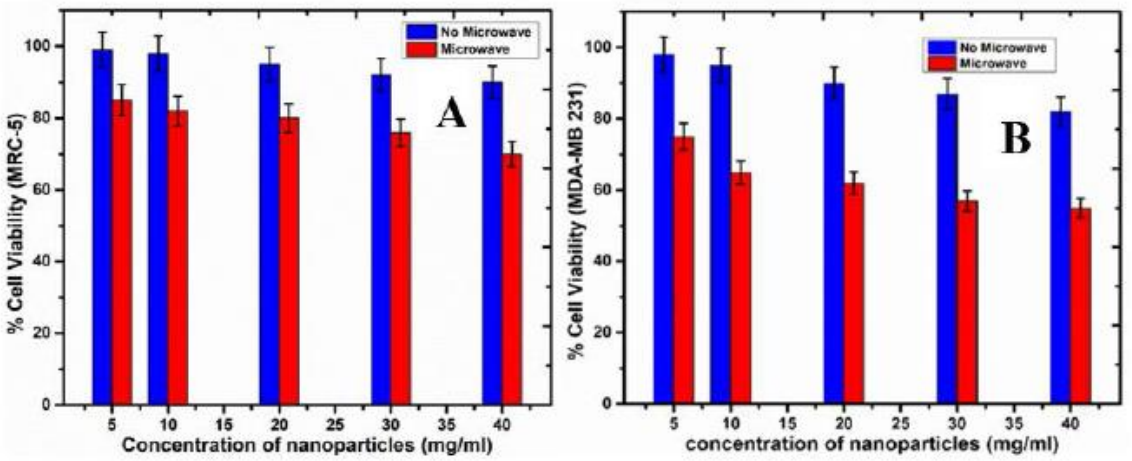

Figure 70. Cell viability of (A) MRC-5 and (B) MDA-MB-231 as a function of CFNP concentration with and without microwave (MW) irradiation.

4.7 Synthesis of Gold Core/shells: Materials and methods.

4.7.1 Iron oxide nanoparticles seed preparation.

400ul of Iron oxide were dispersed in 1ml of DI water, then 0.5 ml of Triton X 100 and the mixture was stirred continuously under N_2 atmosphere at 75 °C for 3 h to reduce the aggregation of NPs.

4.7.1.1 Gold seed solution.

An aliquot of gold seed solution was prepared freshly by mixing 0.5 ml of triton X 100, 1 ml (50 mM) of ascorbic acid, and 75 µl (1M) of HAuCl4 solution. This solution complex mixture was sonicated for 120 mins.

4.7.1.2 Au-Fe_3O_4 core-shell nanoparticles.

The seed solution of Iron oxide and gold were used to synthesize core-shell. Initially, 1 part of gold seed solution was added dropwise to the faint brown-colored seed solution. This solution mixture was stirred for 3 h continuously until there is color change. Then, these core-shell nanoparticles were magnetically separated by magnetic separation

technique and they were washed twice with a mixture of hexane and ethanol to obtain high purity NPs excluding excess gold NPs. The washed NPs were centrifuged again twice to remove excess Triton X 100 from the solution.

4.7.1.3 CD-44, activation and attachment onto core-shell nanoparticles.

The lack of therapeutic specificity in Cancer is remarkable in breast Cancers, specifically in the triple negative molecular subtype. Recently, glycoprotein CD-44 has been reported to be present on the surface of carcinogenic cells in TNBC being correlated with a poor outcome [356]. CD-44 is a molecule related with leukocyte attachment, it remains into peripheral lymphoid organs, inflammation sites, and leukocyte aggregation. More interestingly, in vivo and in vitro studies have shown encouraging results of CD-44 as a therapeutic target due to overexpression of CD-44 in Cancer stem cells [357].

In this work, two strategies were used to provide specificity to nanoparticles, the first was to provide an humanized ligand of CD-44 coating to the coreshell nanoparticles to pursue their CD-44 receptor overexpressed in Cancer stem cells and the second was to use Bicalutamide as a therapeutic option since the androgen receptor (AR) is present in more than 70% of breast Cancers and has been shown to have therapeutic effects in TNBC [358]. The therapeutic characteristics of bicalutamide are discussed in detail in the drug section.

4.7.1.3.1 Flow cytometry.

In 1968, Wolfgang Göhde, unveiled the first patented fluorescence-flow cytometry device. This device allows measuring physical properties of the cells [359] and it is widely used in health sciences research, since it allows studying a wide range of fluorophores linked to specific antibodies that are useful for the diagnosis and treatment of diseases that present overexpression of biomarkers or proteins. Its working consist on the light scattering features of the cells [360]. In this work, flow cytometry measurements were made to corroborate the presence of receptors and proteins that are overexpressed to find a therapeutic target specific for TNBC. It was very interesting to evaluate our negative control MRC-5 and the malignant cell line MDA-MB-231 for human TNBC. The two receptors evaluated were the folic acid and CD-44 receptors.

Our research team used Alexa Fluor 488 Molecular Probes (Thermo Fisher Scientific) and PE/Cy7 anti-mouse/human CD44 Antibody for distinguish antibodies cell signal in fluorescence microscopy within the visible and infrared spectrum. Here the results below **Figures 71-74**:

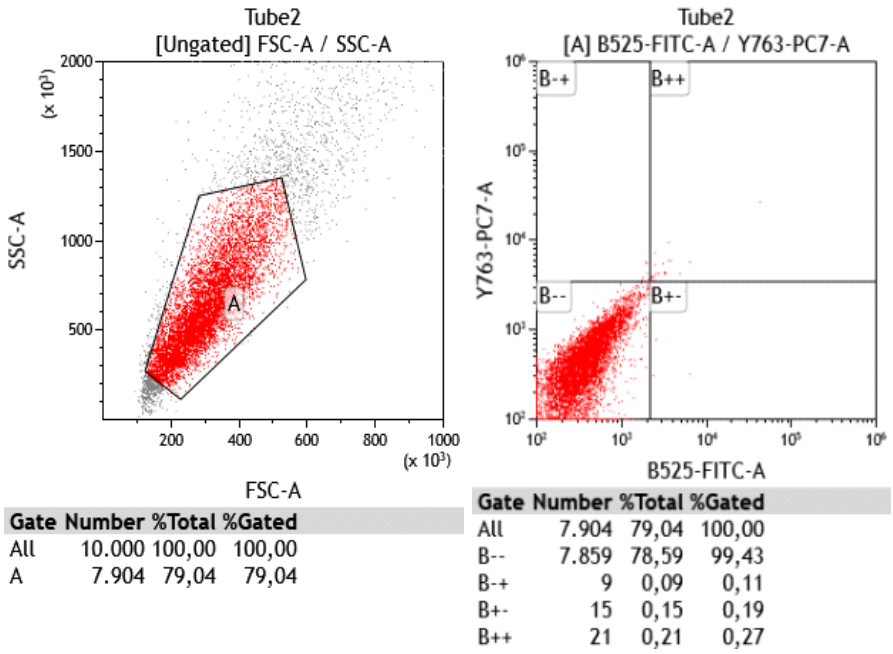

Gate	Number	%Total	%Gated
All	10.000	100,00	100,00
A	7.904	79,04	79,04

Gate	Number	%Total	%Gated
All	7.904	79,04	100,00
B--	7.859	78,59	99,43
B-+	9	0,09	0,11
B+-	15	0,15	0,19
B++	21	0,21	0,27

Figure 71. Flow cytometry of the MRC-5 cell line was done without including antibodies.

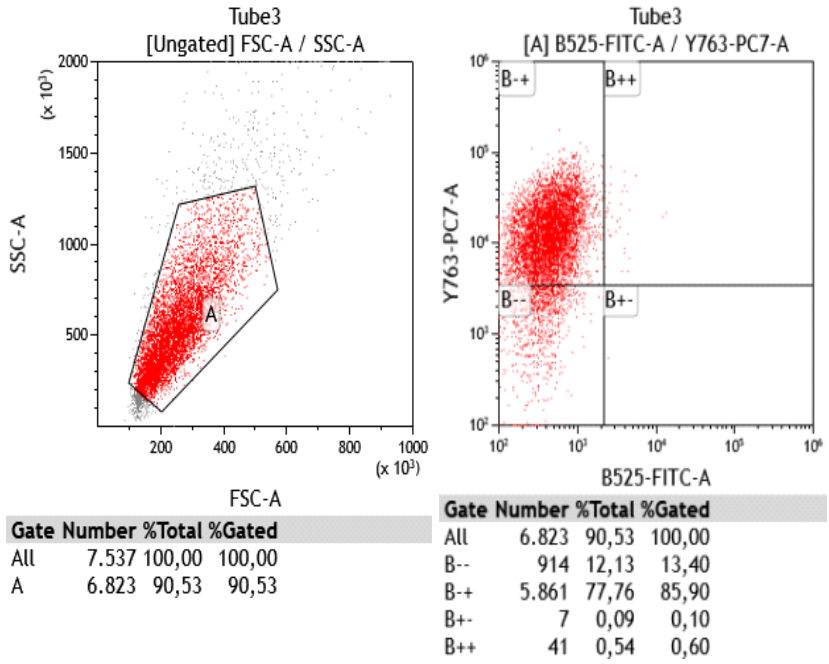

Gate	Number	%Total	%Gated
All	7.537	100,00	100,00
A	6.823	90,53	90,53

Gate	Number	%Total	%Gated
All	6.823	90,53	100,00
B--	914	12,13	13,40
B-+	5.861	77,76	85,90
B+-	7	0,09	0,10
B++	41	0,54	0,60

Figure 72. Flow cytometry of the MRC-5 cell line was done, this time including antibodies MRC5+ FOLR-AF488 + CD44-PECy7. Overexpression of folic acid was found in 85% of the cells but there is no overexpression of CD-44.

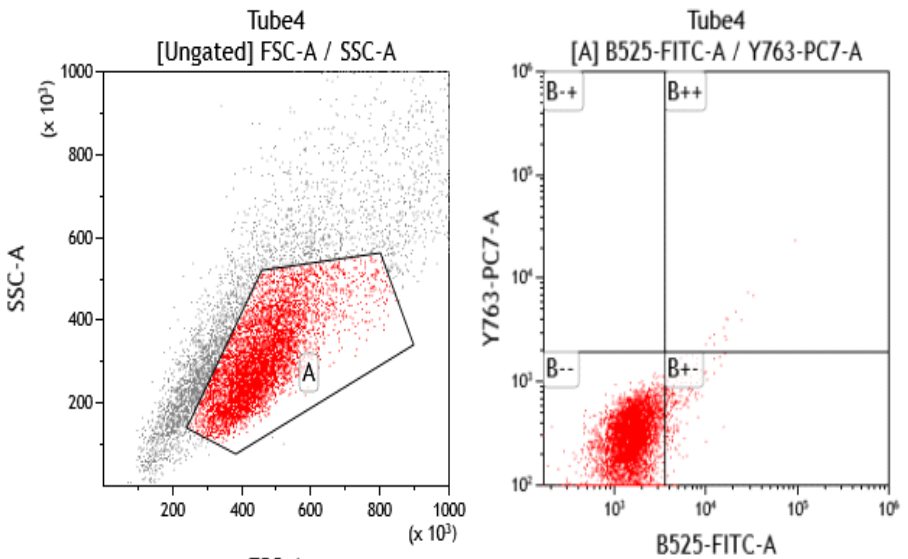

Gate	Number	%Total	%Gated
All	10.000	100,00	100,00
A	6.163	61,63	61,63

Gate	Number	%Total	%Gated
All	6.163	61,63	100,00
B--	5.957	59,57	96,66
B-+	0	0,00	0,00
B+-	191	1,91	3,10
B++	15	0,15	0,24

Figure 73. Analysis of MDA-MB-231 control without antibodies yielded expected results, there is no signal for folic acid and CD-44 (B-+, B++).

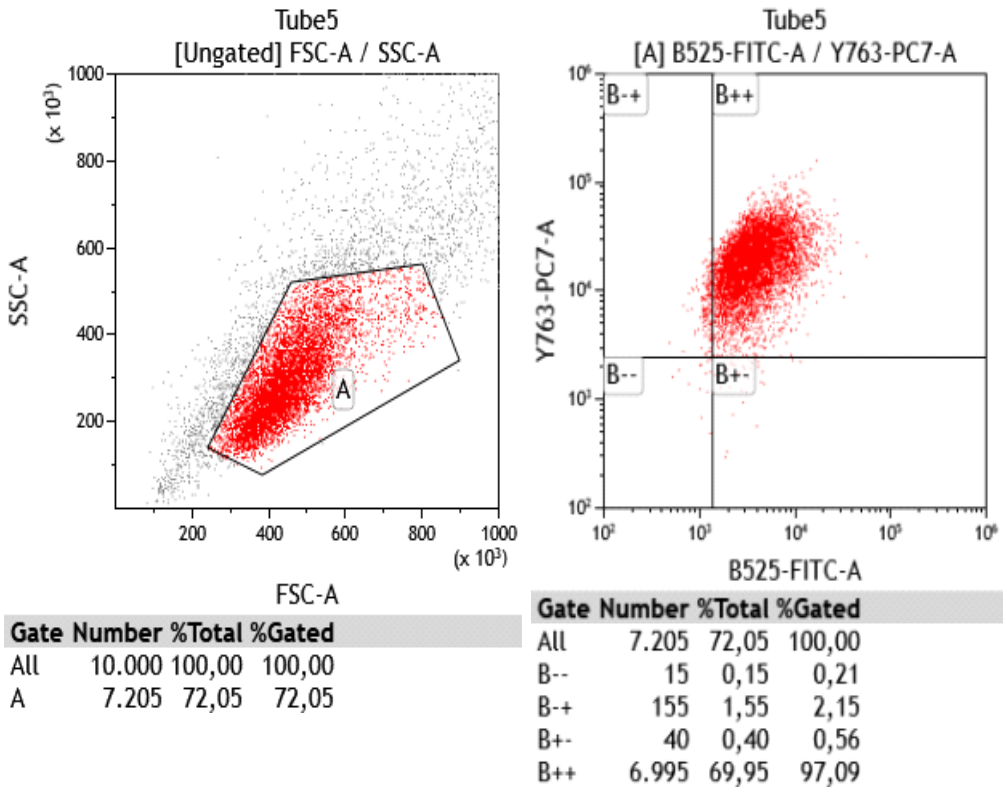

Gate	Number	%Total	%Gated
All	10.000	100,00	100,00
A	7.205	72,05	72,05

Gate	Number	%Total	%Gated
All	7.205	72,05	100,00
B--	15	0,15	0,21
B-+	155	1,55	2,15
B+-	40	0,40	0,56
B++	6.995	69,95	97,09

Figure 74. Unlike the previous graph, MDA-MB-231 + FOLR-AF488 + CD44-PECy7 antibodies they resulted in no expression of folic acid (B- +) but an enormous expression (B ++) 96.6% of the cells are signaling for CD-44 receptor. With this valuable information in mind, it was decided to wrap the nanoparticles with ***Human Antibody CD-44*** to improve TNBC-treatment specificity.

4.7.1.3.2 Protocol for Attachment humanized CD-44 antibody (Nano-functionalization) on Core-shell.

1.- 0.25 ml of core-shell NPs was dissolved in 10 mL of (methanol water 1:1)

2.- 30 mM of cysteamine solution (30ml)

3.- Ultrasonication for 3 hours

4.- Centrifugation at 1500 RPM for 15 minutes

5.- Supernatant decanted and pellet was suspended in DMSO.

Process:

> 0.5ml of coreshell-cisteamine complex will be mixed with 5 microliters (0.2mg/ml) CD44 antibodies. Subsequently 5 microliters of 0.2M EDC and 10 microliter 0.2M of NHS was added to the reaction mixture to activate antibody.

The mixture was stirred for one hour at room temperature. The resulting particle suspension was diluted four times and then used further.

4.7.1.3.3 Surface functionalization of Bicalutamide.

The role of androgenic hormones in TNBC is not yet known with certainty, but it is known that the expression of the androgen receptor is greater than that of estrogen receptors and this is the reason why it recently became in a matter of interest for researchers seeking AR to use it as a therapeutic target since until now there is no effective treatment for TNBC. AR is expressed in 12–55% of cases of TNBC [358].

Bicalutamide is an antiandrogen drug that competes for androgenic receptors, inhibits transcription of AR-regulated genes by assembling corepressors [361]. Conventionally it is used in the treatment of prostate Cancer in combination with leuprolide, an analogue of the luteinizing releasing hormone. Typically, prostate Cancer presents overexpression of androgenic receptors (AR). However, given the latest findings in TNBC, it is being studied in clinical trials to assess its therapeutic efficacy. Therefore, in this work it was decided to nanofunctionalize $CoFe_2O_4$ nanoparticles with Bicalutamide at an *In Vitro* adjusted-dosage

for increasing the specificity to track down MDA-MB-231 malignant cells and respect the healthy cells. Currently, there is another drug called enzalutamide, with a more potent anti-androgenic effect [362], but for reasons of stoichiometry is not used in this work.

4.7.1.3.4 Protocol for Bicalutamide Core-shell Nano-functionalization.

Synthesis of AuPEG NPs.Thiolate-mPEG (Mw=550mg;55mg,0.1mmol) was dissolved in 10mL MeOH, and this solution added into a solution of core-shell (0.25ml) in 10mL (MeOH:H_2O 1:1) stir the solution for 24 hours. Subsequently, bicalutamide (0.45 ml), methanol (5 ml) and high-grade water (5 ml) were added to the solution with constant stirring for 1 h at 70 °C. The BMP were separated from the electrolytes remaining in solution with a magnet, and then washed. The density of the solution became 0.0801 g/ml when the magnetic nanoparticles precipitated. This indicated that the nanoparticles had been successfully loaded with Eg-bicalutamide for stabilization under various physiological conditions. Centrifuge the complex at 8000 rpm for 15 minutes the crude product was dissolved in 3mL high grade water followed by dialysis.

4.7.2 Surface functionalization of Docetaxel.

Docetaxel acts at the level of the microtubules, specifically the assembly of tubulin in stable microtubules inhibiting its polymerization, which alters tubulin, the cytoskeleton of the cells that is essential for the functions at the cellular interface. A taxane scheme accompanied by bicalutamide was decided with improved specificity by using nanotechnology **Figure 75**. The objective of these combined drugs is to improve cytotoxicity in the malignant cell line and reduce adverse effects.

4.7.2.1 Protocol for Docetaxel Core-shell Nano-functionalization.

Synthesis of AuPEGNPs.Thiolate-mPEG (Mw=550mg;55mg,0.1mmol) was dissolved in 10mL MeOH, and this solution added into a solution of core-shell (0.25ml) in 10mL (MeOH:H_2O 1:1) stir the solution for 24 hours. Subsequently, Docetaxel (0.45 ml), methanol (5 ml) and high-grade water (5 ml) were added to the solution with constant stirring for 1 h at 70 °C. The Docetaxel complex was separated from the electrolytes remaining in solution with a magnet, and then washed. The density of the solution became

0.0801 g/ml when the magnetic nanoparticles precipitated. This indicated that the nanoparticles had been successfully loaded with Eg-Docetaxel for stabilization under various physiological conditions. Centrifuge the complex at 8000 rpm for 15 minutes the crude product was dissolved in 3mL high grade water followed by dialysis.

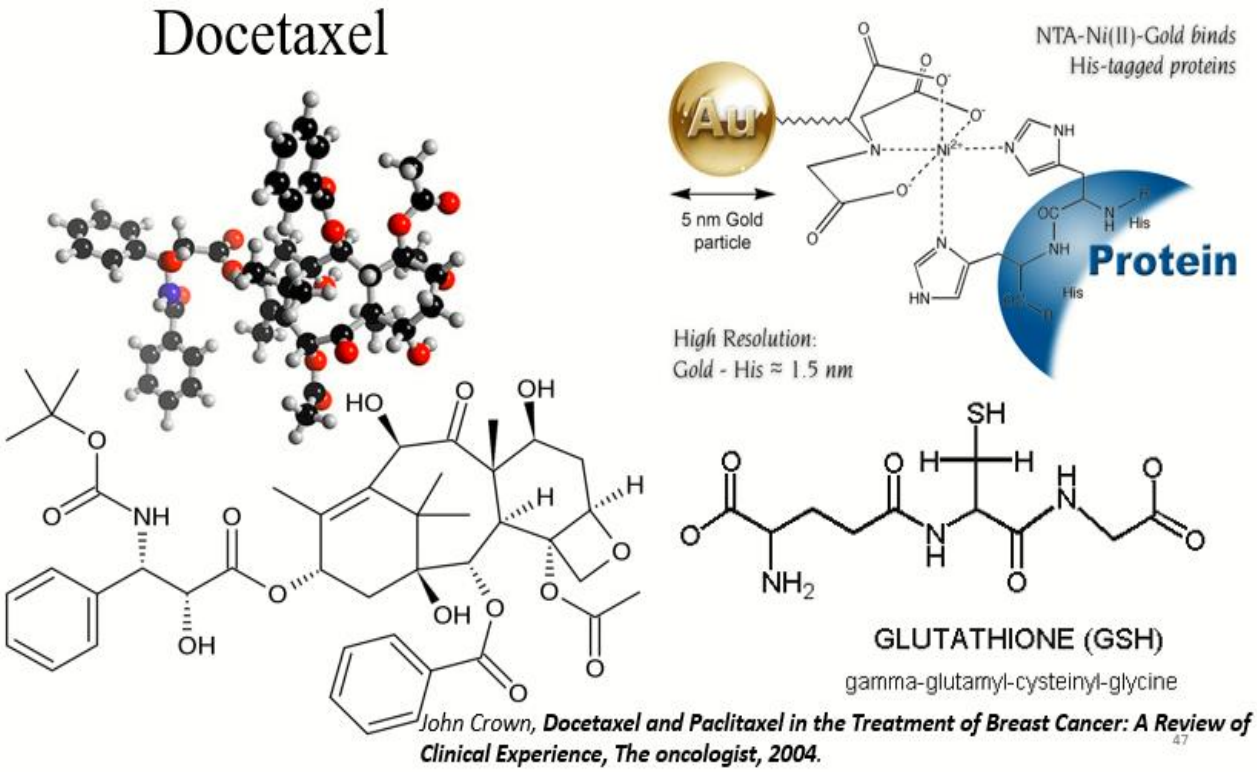

Figure 75. Scheme representing functionalization with Docetaxel through functional groups onto Au nanoparticles.

4.8 Complex characterization: Coreshell characterization.

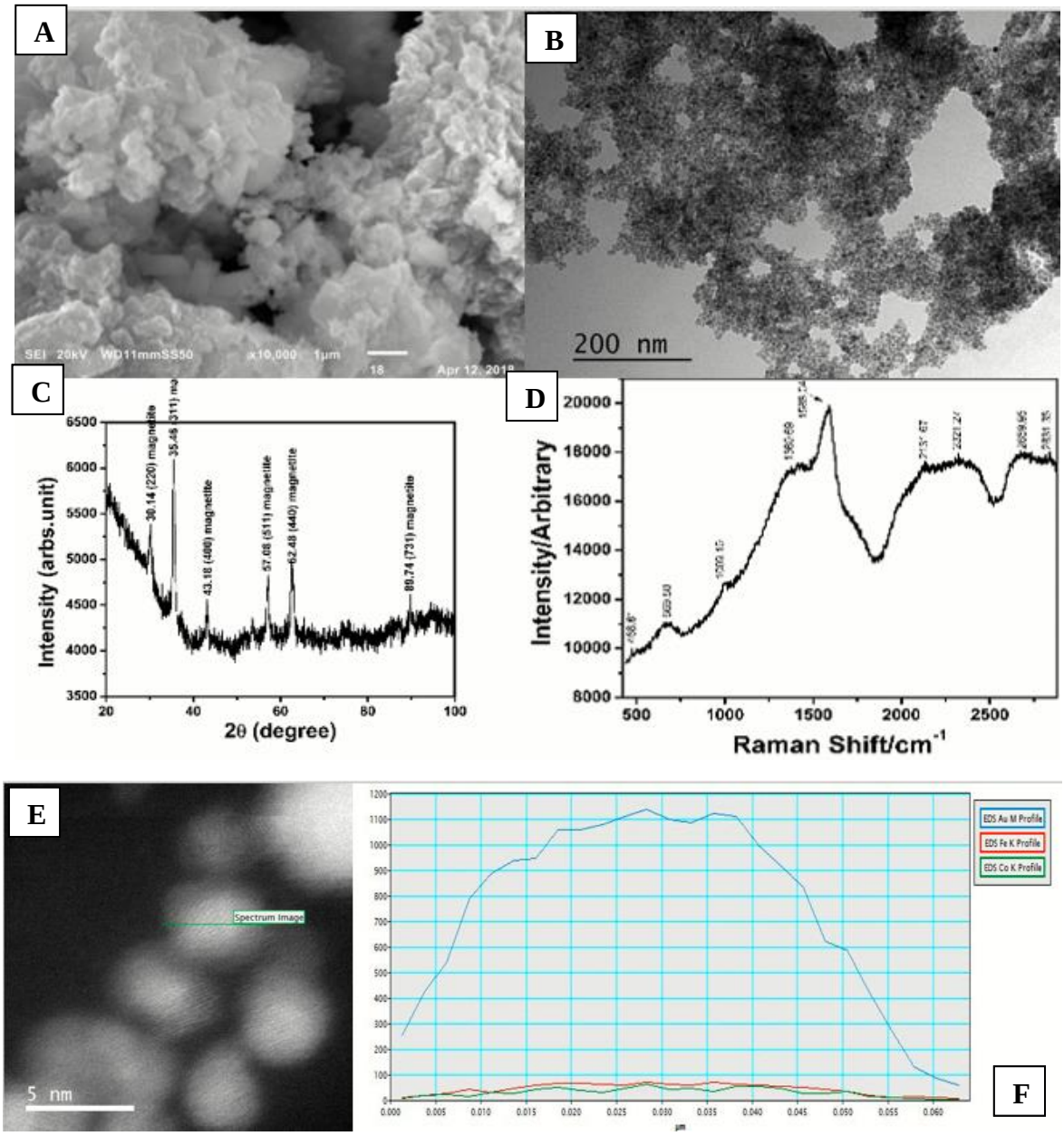

Figure 76. A) SEM and B) TEM morphological characterization of core-shell. C) XRD and D) Raman spectroscopy E) Scan mapping for compositional characterization reveals $CoFe_2O_4$ as a nucleus and Gold as a shell. Taken with a Jeol JEM-ARM200CF at the center of Micro and Nanotechnology of the National Polytechnic Institute, Mexico City.

4.8.1 Zeta potential Analysis.

The colloidal particles dispersed in a solution are charged electrically due to their ionic properties and bipolar characteristics. The Z potential analysis describes the intensity of the electric field of the nanoparticles in the interface between the grain and the fluid [363].In order to characterize and guarantee the electronegativity of the nanoparticles we need for theranostics purposes, Z potential studies were performed on the $AuCoFe_2O_4$ nanoparticles.

The erythrocyte membrane contains proteins and sialylated glycoproteins in the membrane that are responsible for a negative surface that creates a potential repulsive electric zeta potential between cells **Figure 77.** [364]. These charges help prevent the interaction between red blood cells and other cells and especially with each other. Using an electrophoretic mobility assay, we found that the mean ZP of human erythrocyte was −15.7 mV [365]. The Z potential was performed at CINVESTAV toxicology department with a Malvern Panalytical device. The results indicate -11.4 for $Au@CoFe_2O_4$ nanoparticles which is ideal for our applications in nanomedicine. **Figure 77.**

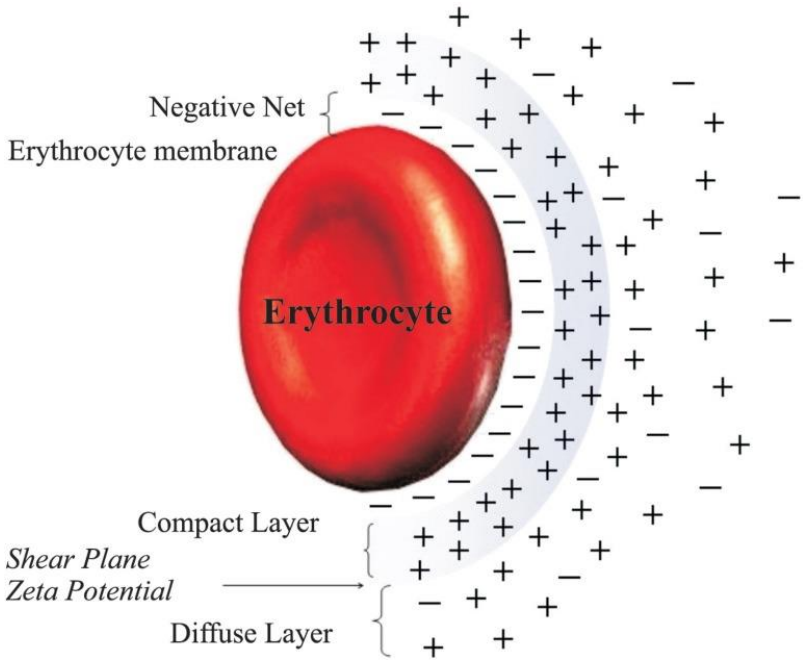

Figure 77. The erythrocyte membrane helps to prevent the interaction between red blood cells and other cells and especially with each other.

Sample Name:	AuCoFe2O4 tx100 ctab en agua 3		
SOP Name:	AuCoFe2O4 PEG en agua.sop		
File Name:	AuCoFe2O4.dts	**Dispersant Name:**	Water
Record Number:	17	**Dispersant RI:**	1.330
Date and Time:	viernes, 10 de mayo de 2019 12:26:01 p...	**Viscosity (cP):**	0.8872
		Dispersant Dielectric Constant:	78.5

Temperature (°C):	25.0	**Zeta Runs:**	12
Count Rate (kcps):	147.3	**Measurement Position (mm):**	4.50
Cell Description:	Zeta dip cell	**Attenuator:**	6

			Mean (mV)	**Area (%)**	**St Dev (mV)**
Zeta Potential (mV):	-11.4	**Peak 1:**	-11.4	100.0	6.65
Zeta Deviation (mV):	6.65	**Peak 2:**	0.00	0.0	0.00
Conductivity (mS/cm):	0.0201	**Peak 3:**	0.00	0.0	0.00

Result quality : Good

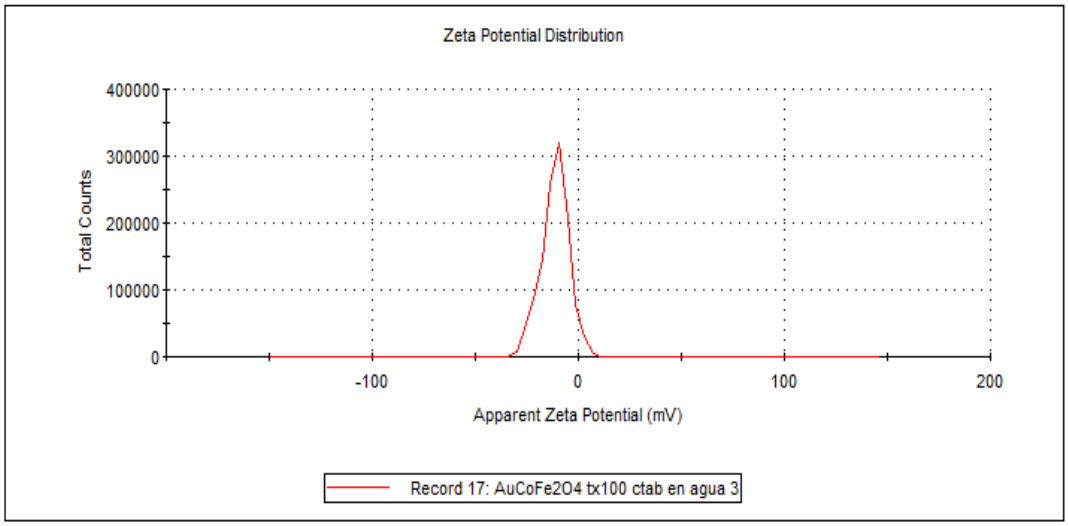

Figure 78. Z potential was performed at CINVESTAV toxicology department with a *Malvern* Panalytical device. The results indicated a Z-potential of -11.4 mV for Au@$CoFe_2O_4$ nanoparticles, compatible with the charges of erythrocytes.

4.8.2Thermogravimetric Analysis (TGA).

Thermogravimetric Analysis (TGA) is a method of thermal analysis capable of measuring physical changes, chemical reactions and stoichiometric processes depending on the temperature of a given material [366]. The information is used to determine thermal stability of the materials and their stoichiometric behavior. In this work, TGA-DSC was used to measure the physical and chemical changes of Au @ $CoFe_2O_4$ alone, with docetaxel and with bicalutamide. **Figure 79.**

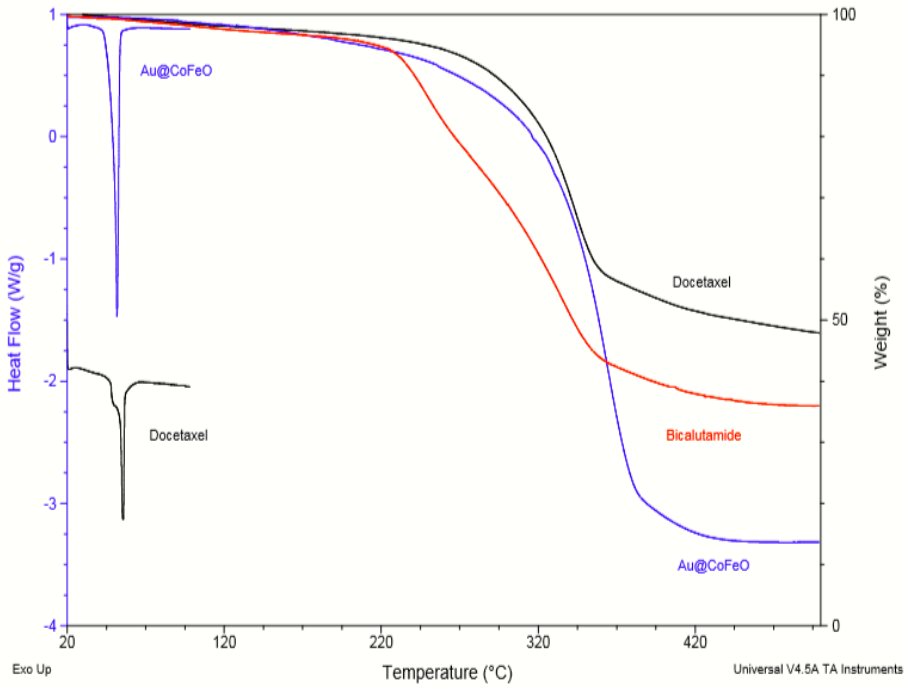

DSC = Differential Scanning Calorimetry

Figure 79. Thermogravimetric Analysis (TGA) taken by DSC, showing our NPs are safe and stable at physiological temperatures.

4.8.3 HPLC High-performance liquid chromatography.

High-performance liquid chromatography (HPLC) is a column chromatography device that pumps a sample in a high-pressure solvent through a column with a chromatographic filler material. The system has the ability to determine the retention time of the samples or how quickly they pass through the column [367]. There are materials with long and short retention times, these materials pass through a detection module, such as a fluorimeter or a UV absorbance detector, this signal is subsequently recorded by an HPLC control computer program and provides adequate sample analysis. Currently, there are novel techniques which can be used to enhance HPLC like HPLC to tandem mass spectrometry (LC-MS/MS) or matrix-assisted laser desorption/ionization–time-of-flight (MALDI-TOF) analysis for improved detection of the messenger molecules [367].

4.8.4 ICP-AES Inductively coupled plasma atomic emission spectroscopy.

ICP-AES is an analytical tool which uses inductively coupled plasma to produce electromagnetic radiation at wavelengths characteristic for a given element. The values measured from the nucleus of these NPs was 23.3 mg Fe per g of particles and 9.3 mg Na per g of particles. Interesting to note, converting these values into molarity is a 1: 1 ratio between Fe and Na.

It takes sixty-five thousand errors before you are qualified to make a rocket.

—Wernher von Braun

CHAPTER 5

5. RESULTS & DISCUSSION.

In this work, the synthesis and structural characterization of a series of $CoFe_2O_4$, $MnFe_2O_4$, $ZnFe_2O_4$ NPs using different precursors like **PEG 0.01 M**, **CTAB 0.1 M**, **TX-100 0.1 M** and **SDS 0.1 M** are presented. All this NPs were synthesized by a general solid-liquid solution process prepared by a novel and efficient method chemist called Thermal decomposition (Chapter 3), then, a thorough exploration and several repetition of experiments and comparisons allowed us to stablish a security profile of these nanoparticles **(Table 9)**.

Table 9. Properties of different nanoparticles*.

MATERIAL AND SURFACTANT	TOXICITY TO NORMAL CELLS (1-5*)	TOXICITY TO MALIGNANT CELLS (1-5*)	HYPERTHERMIA EFFICACY (1-5*)	REPRODUCIBILITY, NANOPARTICLE CHARACTERIZATION (1-5*)
PEG 0.01 M $CoFe_2O_4$	*	*	***	***
PEG 0.02 M $CoFe_2O_4$	*	*	**	***
PEG 0.03 M $CoFe_2O_4$	**	*	*	*
CTAB 0.1 M $CoFe_2O_4$	**	*	***	***
CTAB 0.2 M $CoFe_2O_4$	***	**	*	*
CTAB 0.3 M $CoFe_2O_4$	****	**	*	*
TX100 0.1 M $CoFe_2O_4$	**	**	****	*****
TX100 0.2 M $CoFe_2O_4$	**	**	****	****
TX100 0.3 M $CoFe_2O_4$	***	***	***	**
SDS 0.1 M $CoFe_2O_4$	****	***	**	**
SDS 0.2 M $CoFe_2O_4$	****	***	**	*
SDS 0.3 M $CoFe_2O_4$	****	***	**	*
PEG 0.01 M $MnFe_2O_4$	**	*	*	***
PEG 0.02 M $MnFe_2O_4$	**	*	*	**
PEG 0.03 M $MnFe_2O_4$	***	**	*	*
CTAB 0.1 M $MnFe_2O_4$	**	**	***	**
CTAB 0.2 M $MnFe_2O_4$	**	**	*	*
CTAB 0.3 M $MnFe_2O_4$	****	**	*	*
TX100 0.1 M $MnFe_2O_4$	**	***	**	****
TX100 0.2 M $MnFe_2O_4$	**	***	*	***
TX100 0.3 M $MnFe_2O_4$	***	***	*	*
SDS 0.1 M $MnFe_2O_4$	*	*	***	**
SDS 0.2 M $MnFe_2O_4$	*	*	***	*
SDS 0.3 M $MnFe_2O_4$	***	**	**	*
PEG 0.01 M $ZnFe_2O_4$	*	*	*	***
PEG 0.02 M	*	***	*	**

$ZnFe_2O_4$				
PEG 0.03 M $ZnFe_2O_4$	*	***	*	*
CTAB 0.1 M $ZnFe_2O_4$	*	*	*	**
CTAB 0.2 M $ZnFe_2O_4$	*	*	*	*
CTAB 0.3 M $ZnFe_2O_4$	**	**	*	**
TX100 0.1 M $ZnFe_2O_4$	****	**	***	*
TX100 0.2 M $ZnFe_2O_4$	***	**	**	*
TX100 0.3 M $ZnFe_2O_4$	***	***	*	*
SDS 0.1 M $ZnFe_2O_4$	**	*	**	*
SDS 0.2 M $ZnFe_2O_4$	***	**	*	*
SDS 0.3 M $ZnFe_2O_4$	****	***	*	*
PEG 0.01 M $Au@CoFe_2O_4$	*	*	****	**
CTAB 0.1 M $Au@CoFe_2O_4$	*	*	**	**
TX-100 0.1 M $Au@CoFe_2O_4$	*	***	****	***
Dandelion extract Fe_3O_4	**	**	**	***
CTAB TX/100 0.1 M $Au@CoFe_2O_4$	**	*****	*****	****

*Security profile based on MTT experiments. Highlighted in green color suggests deeper exploration in future research.

The best candidate ($CoFe_2O_4$) was chosen for its functionalization with antibody CD-44 and drugs such as Docetaxel and Bicalutamide (chapter 4). Next, scanning transmission electron microscopy (STEM) in the mode high-angle annular dark-field (HAADF) technique was used for the structural characterization and several other techniques for the compositional characterizations (chapter 3 and chapter 4). The HAADF like state of the art allow us to see the morphology, to obtain the size distribution, to identify the structure and atomic positions corresponding to $CoFe_2O_4$ in the different series of the samples. In order to obtain the elemental chemical composition, measurements were carried out using the STEM-Energy-dispersive X-ray spectroscopy (STEM-EDS) that showed the presence of Co, Fe, and O.

In order to study of the structural characterization of the series of $CoFe_2O_4$ NPs was carried out by scanning transmission electron microscopy (STEM), firs able a drop of solution of each sample was deposited in the copper grids with a carbon film, then the samples we analyzed by using an equipment Jeol JEMARM-200F STEM/TEM microscope, 200 keV of acceleration voltage, equipped with a CEOS Cs-corrector as probe-corrector for STEM. Using this condition in the equipment then all the images were obtained using the mode high-angle annular dark-field (HAADF)-STEM with a collection angle of 50-180 mrad. The best candidate to continue with the core-shell design was $CoFe_2O_4$ **TX-100 0.1 M. Figure. 80.** Some points that are worth considering about the synthesis of these nanoparticles are: a) Free energy b) Saturation and supersaturation (LaMer) to obtain nanoparticles. and (c) Influence of the medium and conditions including pH for the mentioned methods that we will discuss below.

(a) Free energy to form particles.

As many authors refer, nanostructured systems can be obtained by techniques such as bottom-up whose focus is the self-assembly of atoms to generate a larger nanoparticle. In this study NPs of $CoFe_2O_4$ were obtained by thermal decomposition method. The generation of NPs is a function of the type of precursor to initiate the reaction and in some cases a stabilizer because phenomena of mass and energy transfer occur on the surface of the nanoparticle during its growth. In our case we believe that the active tensile Triton X-100 controls the surface energy necessary for the formation of $CoFe_2O_4$ nanoparticles.

(b) Saturation and supersaturation (LaMer) to obtain nanoparticles.

According to the concepts transferred by Lamer's, the growth of $CoFe_2O_4$ metallic nanoparticles due to saturation and supersaturation involves three main prisoners as a function of time; the first process is the amount of Co and Fe atoms due to the reduction process in synthesis, the second corresponds to rapid nucleation due to the saturation effect that promotes the formation of the first clusters and finally the nucleation-growth process occurs to NP formation of stable $CoFe_2O_4$. We believe that the saturation speed, due to the reducing agent, was the key to obtaining dispersed and homogeneous NPs.

(c) Influence of the medium and conditions including pH for the mentioned methods.

The effect of pH on the stability, behavior and aggregation of the $CoFe_2O_4$ nanoparticles were carried out in a controlled environment. The temperature of 260 ° C and the environment controlled by the flow of nitrogen were essential for the generation of the NP oxides. During the formation of NPs according to the LaMer processes, the first atoms during the reduction are of vital importance since if the environment contains excess oxygen, it can oxidize and take part in the reduction reaction, nucleation and formation of NPs, no modification of pH was required to allow the stabilization of the reduction reactions during the formation of NPs. On the other hand, the pH of 7.4 standardized at the end of the synthesis, allowed us to work for our goal in TNBC cells.

However, to obtain a better stability in the Au (shell) and $CoFe_2O_4$ Tx-100 0.1 M (core) ratios, we consult the literature and added CTAB 0.1M, to the complex. In this way our research group successfully obtained the core-shell design confirmed with scan mapping **Figure 81.**

Previously, characterizations were performed on Au@ $CoFe_2O_4$ with XRD, Raman, IR, XPS, EDS, HR-TEM. However, we had to repeat the combinations with all surfactants. We should know what the winning combination was, and in this way, we performed core-shell experiments with the 4 surfactants PEG, CTAB, TX100 and SDS.

We found out that Au@$CoFe_2O_4$ PEG 0.01M is a good candidate. The safety profile of these nanoparticles is adequate for the purposes of this investigation **Figure 82A.** Nevertheless, we could not solve the reproducibility problem, Au @ $CoFe_2O_4$ PEG 0.01M and SDS **Figure 82D** creates a lot of agglutination and we obtained irregular nanoparticles, cages, rollers, cylinders. This was the main reason we ruled them out and we just continued the work with TX-100 + CTAB.

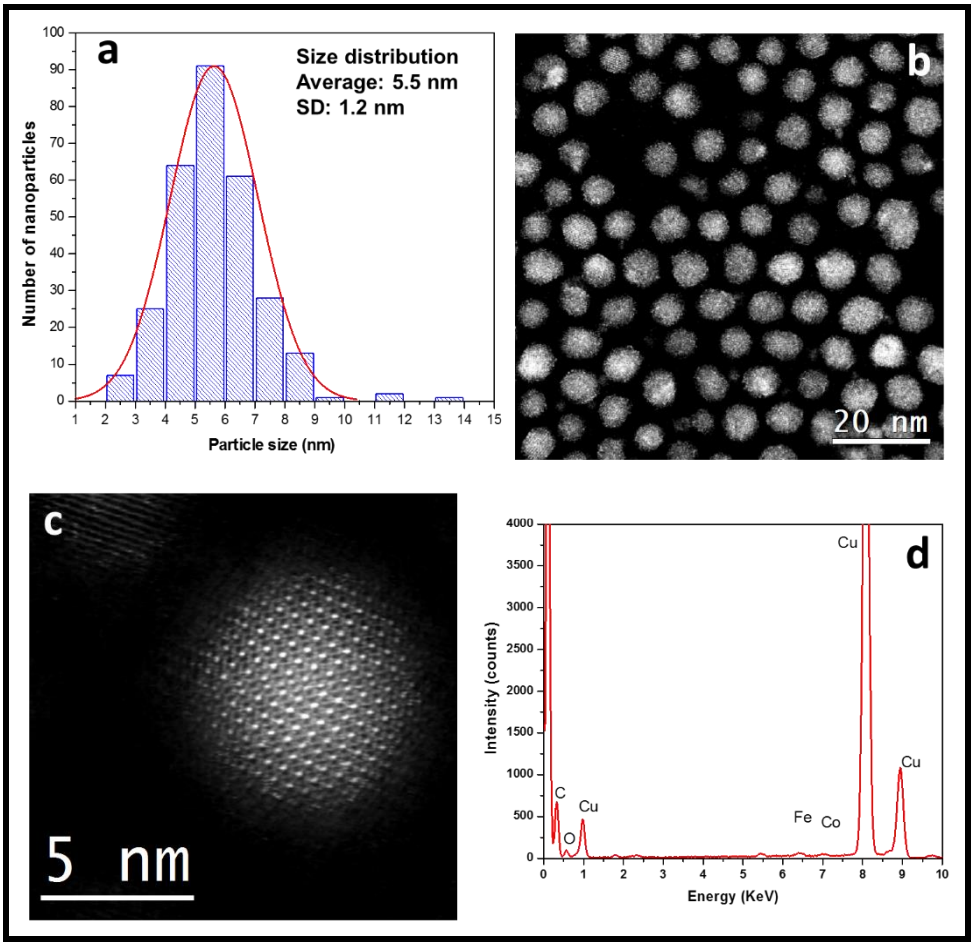

Figure 80. (a) Particle size distribution of $CoFe_2O_4$ TX-100 0.1 M, (b) Low-magnification Cs-corrected STEM-HAADF image of $CoFe_2O_4$ TX-100 0.1 M showing several NPs and a very narrow distribution, (c) Cs-corrected STEM-HAADF image of $CoFe_2O_4$ TX-100 0.1 M showing very high resolution, the morphology correspond to spherical NP, (d) EDS profiles of $CoFe_2O_4$ TX-100 0.1 M NPs, the spectrum show the elemental presence of Co, Fe, O correspond to NPs and C and Cu correspond to the grid.

The safety profiles of the core candidates were evaluated with MTT trials as well as hyperthermia features. Once the safety profile for the MRC-5 negative control was confirmed, the preparation of core-shell, proportion 1: 1 was carried out.

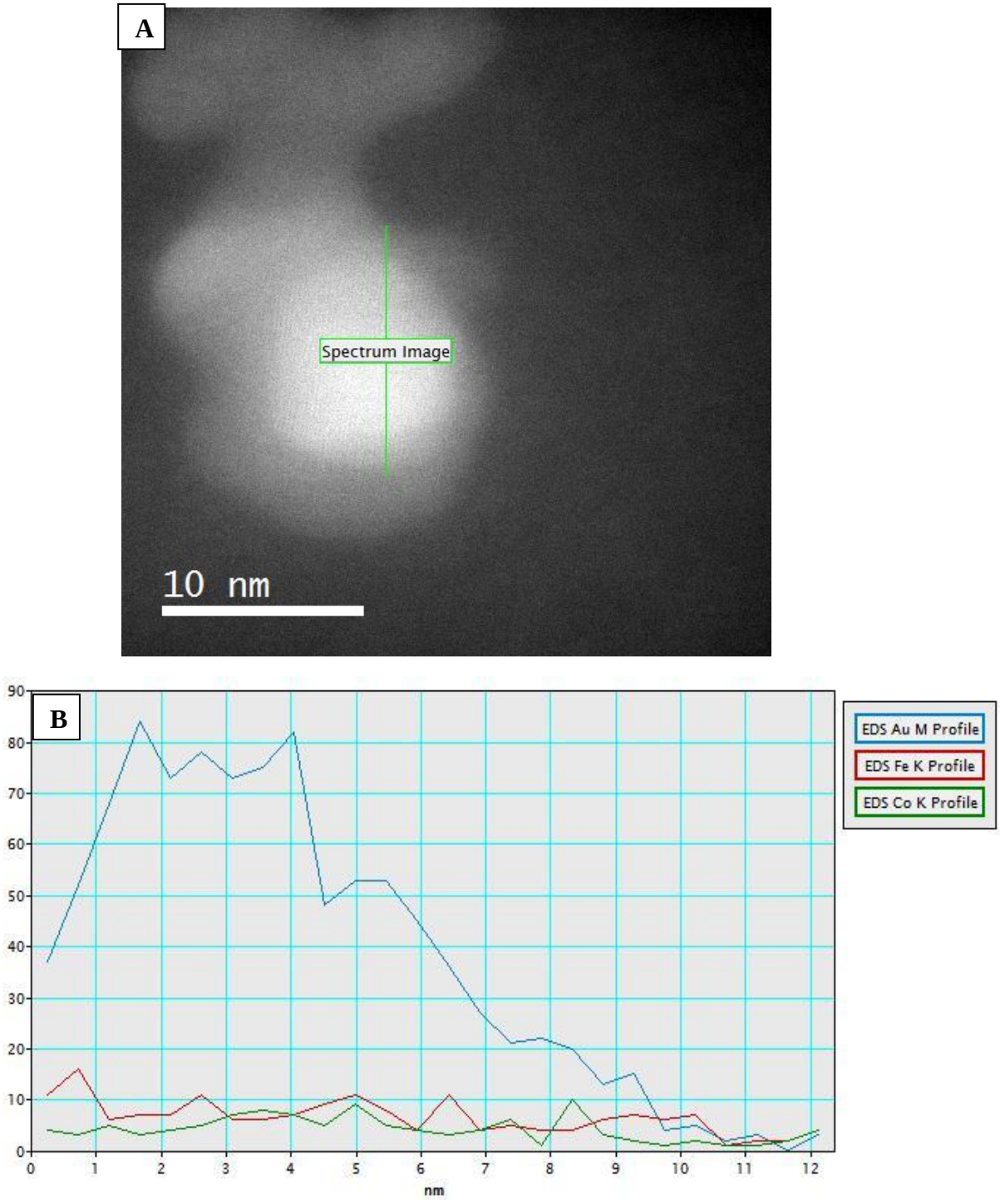

Figure 81. Au@$CoFe_2O_4$ TX-100 0.1 M CTAB 0.1M Core-shell scan mapping revealing a Core-shell nanoparticle Au shell of 5nm and Co Fe as a Core**.** Jeol JEM-ARM200CF at the center of Micro y Nanotecnologías, Instituto Politécnico Nacional, Mexico City.

5.1 Coreshell MTT citotoxicity evaluation.

Fig. 80. Au@$CoFe_2O_4$ using different surfactants.

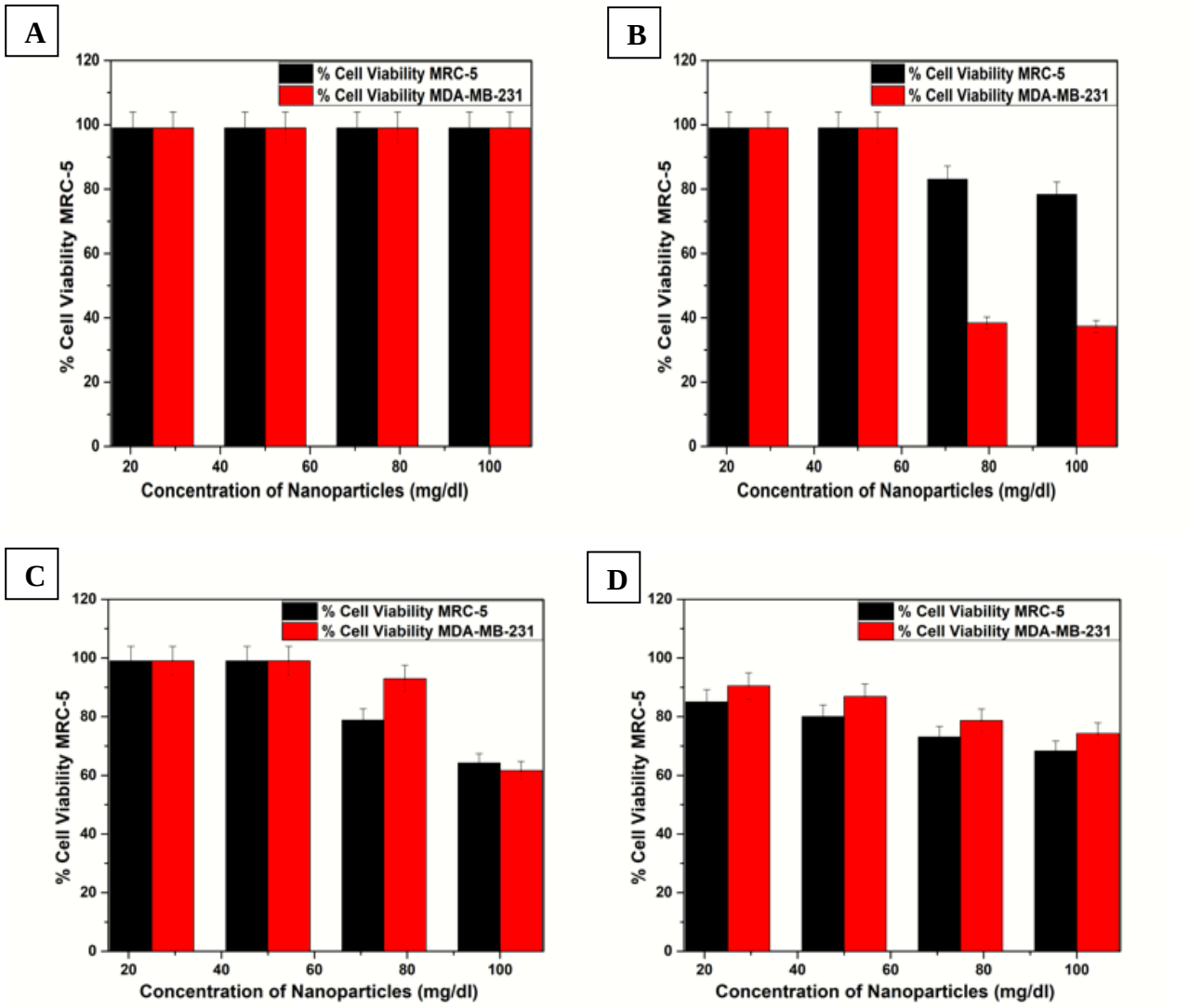

Fig. 82A. Au@$CoFe_2O_4$ PEG 0.01M is a good candidate to scale for nano-functionalization since it is evidently biocompatible, we also made adjustments to the protocol, to skip some chemicals which were acting as a cytotoxic substance such as oleic acid or oleylamine. **Figure 82B.** Au@$CoFe_2O_4$TX-100/CTAB 0.1M is also an excellent candidate for nano-functionalization, specially at 50 mg/dl it looks like a beautiful upside-down pattern where we can see MRC-5 viability much higher than MDA-MB-231. **Figure 82C.** Au@$CoFe_2O_4$ TX-100 0.1M promises to be a good candidate based on cell viability, we had to add CTAB to obtain a better stability when nanoparticles containing Au. **Figure 82D**.Our work team had to discard Au@$CoFe_2O_4$ SDS 0.1M to functionalize with drugs due to the inferior cell viability results for the MRC-5 cell strain.

5.2 Coreshell Hyperthermia evaluation.

$Au@CoFe_2O_4$ nanoparticles have different properties compared to those of bulk materials, including magnetic behavior. That is, in the absence of an external magnetic field, the $Au@CoFe_2O_4$ spins can orient randomly resulting in zero magnetic moment. However, in the presence of a magnetic field, a high magnetic response is induced. Superparamagnetism appears in ferromagnetic nanoparticles with sizes ranging from a few nanometers to several tenths of a nanometer. This characteristic largely depends on the size, material, temperature, and surface modification of the nanoparticle.

5.2.1 Maximized Gold Armada: CD44-Bicalutamide-Docetaxel $Au@CoFe_2O_4$.

Finally, as explained in the previous chapter, the candidates were functionalized with CD-44 Bicalutamide and Docetaxel. Then, the complex was evaluated again with MTT after hyperthermia therapy.

5.2.1.2 Protocol for CD-44 Gold Armada Hyperthermia: Cell assays.

The objective of the experiment was to heat 1 ml of cell suspension samples. Nanoparticles with Gold Nanocomposite Armada were exposed to a temperature of 50 ° C in a time of 20 s and then kept the sample at that temperature for 50 seconds to lead apoptosis.

5.2.1.3 Microwave Heating Conditions.

The signal generator was adjusted to the frequency of 2.45 GHz. The generator output was adjusted to - 8.2 DBm a to have 10 watts at the amplifier output (40DBm) of power at a load of 50 ohms. The signal generator was set in pulse mode with a 10 ms period and pulse width of 5 ms 100% corresponds to 10 ms, so 50% corresponds to 5 ms on and 5 ms off.

It uses a micro-antenna, with a groove, 1.2 mm in diameter that was designed to work at 2.45 GHz. The STUB was adjusted to obtain a SWR <1.1 in a sample of 1.2 ml of water double distilled. The temperature measurement was performed with an optical fiber placed in the middle of the groove of the antenna. The optical fiber was attached to the antenna by means of Teflon tape and a marker is placed on the antenna to immerse it at the same depth in all samples. The temperature capture time was adjusted to 1 s to have better control of it.

5.2.1.4 Hyperthermia final experiment process.

The samples are kept in a thermal bath at 37 ° C for at least 5 minutes. The sample was placed in a container with thermal insulating material walls for the application of the microwaves. Then, the antenna was placed in the sample until the indication of the mark. Next, the temperature control was done manually. The radiofrequency was applied starting with a 50% duty cycle, when it reaches 48 ° C it changes to 40% and when it reaches 50 ° C it changes to 10% and stays for 50 seconds at 50 ° C. When changing cell types, the antenna was washed in double-distilled water.

5.3 Armada complex final functionalization MTT In vitro test.

The MTT results were surprising, it seems that in this experimental model MDA-MB-231 is susceptible to Bicalutamide armada CD44 Au@$CoFe_2O_4$ complex. The novelty is when the gold nanoparticles plus Bicalutamide and the human antibody CD-44 are combined, the cellular viability of MRC-5 remains in safe profiles (90%). On the contrary, the cell viability for MDA-MB-231 falls to dangerous limits (35%) **Figure 83**. It is theorized that in addition to the expression confirmed by flow cytometry of the CD-44 receptor, there is possibly also an important expression of the androgenic receptor since when we test Bicalutamide without nanoparticles, we observe a similar pattern (Chapter 4).

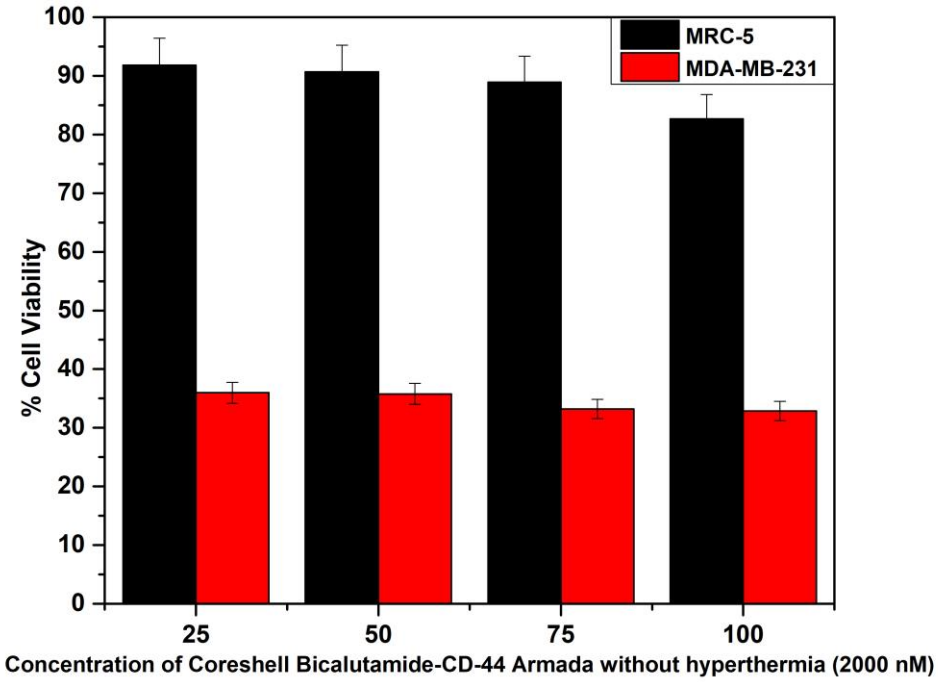

Figure 83. Concentration of Core-shell Bicalutamide-CD-44 NPs without hyperthermia C.I 95% (Condifence interval 95%).

The same combination, but this time adding hyperthermia demonstrates subtle better results attacking MDA-MB-231. However, this occasion, MRC-5 is compromised for the hyperthermia treatment reducing cell viability to 80%. **Figure 84.**

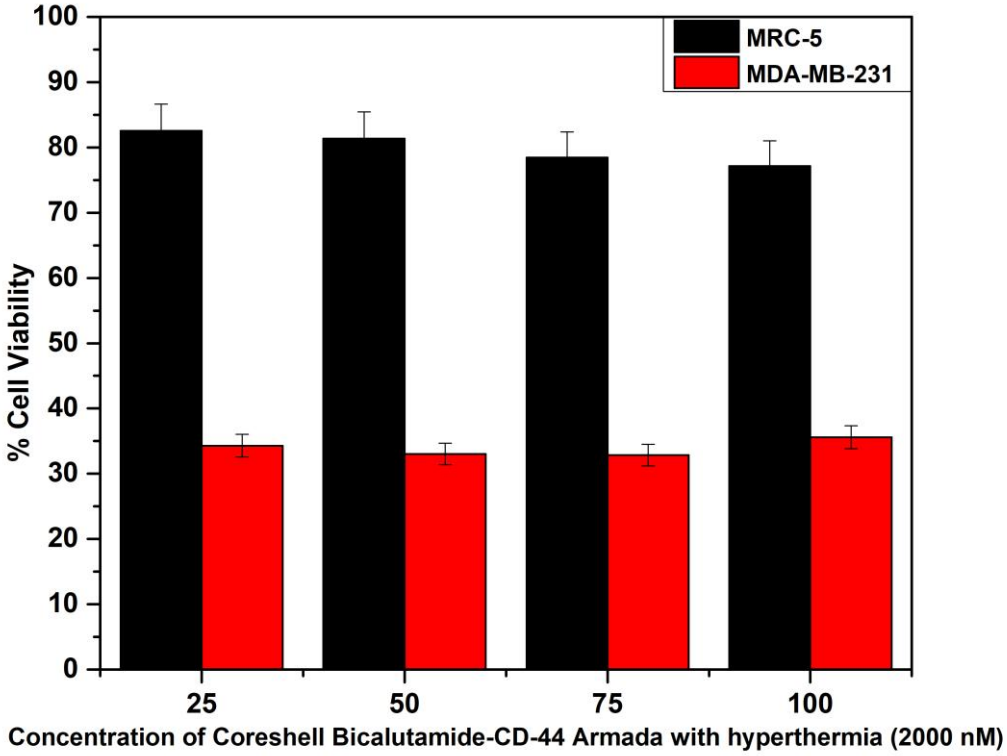

Figure 84. Core-shell Bicalutamide-CD-44 armada with hyperthermia. C.I 95%

The core-shell Docetaxel CD-44 Au@$CoFe_2O_4$ TX100-CTAB 0.1M (Armada) also was tested without hyperthermia. Results pointed out at 100 microliters of 2000nM cell viability of MRC-5 is 75% versus 33% of MDA-MB-231 (C.I 95%). **Figure 85.**

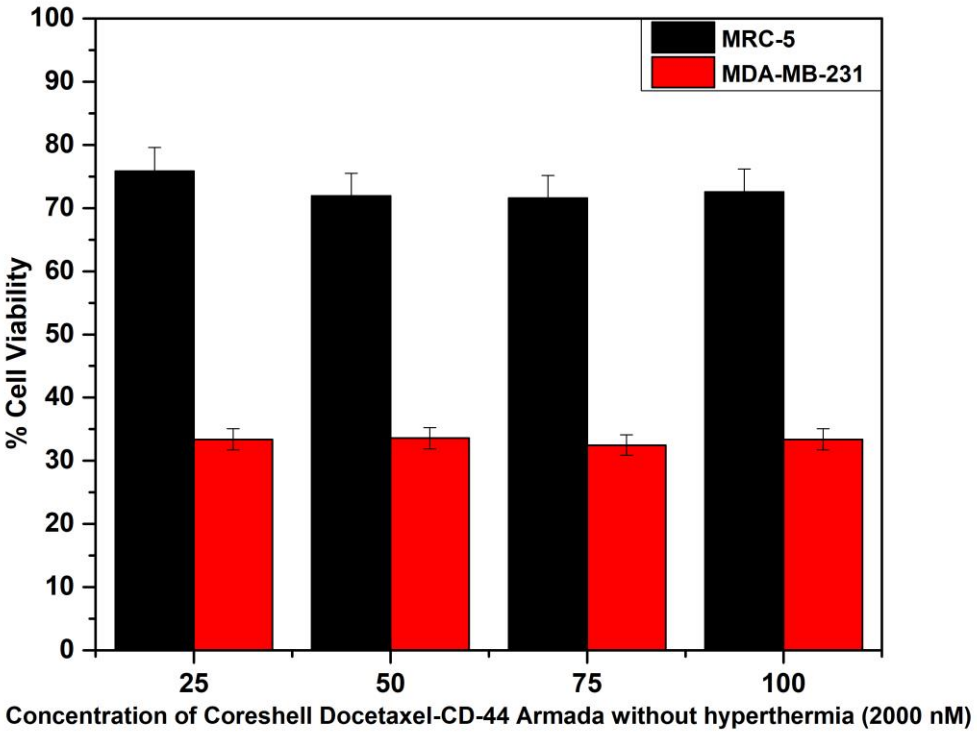

Figure 85. Core-shell- Docetaxel CD-44 armada complex without hyperthermia.

The same complex, this occasion using hyperthermia reveals 68% cell viability to MRC-5 and 31% for MDA-MB-231. Then, we can say that the improvement in treatment with hyperthermia is in the order of 2 to 4% but affecting normal cells in the same percentage in comparison with non-hyperthermia treatment (C.I 95%). **Figure 86.**

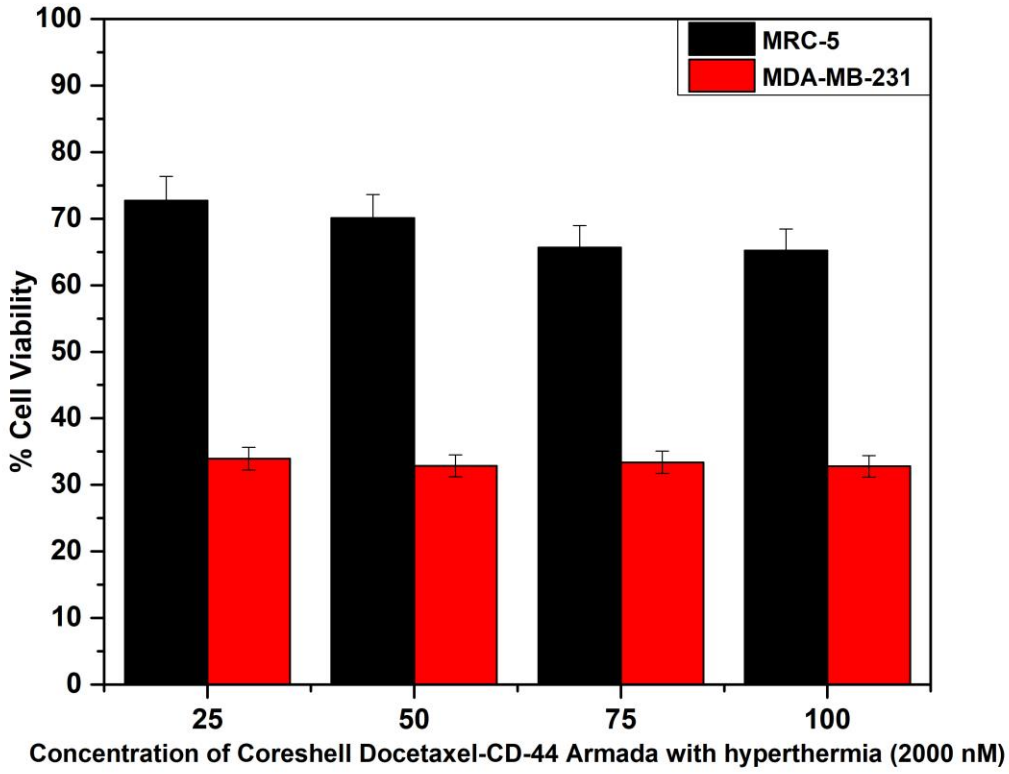

Figure 86. Core-shell- Docetaxel CD-44 armada complex using hyperthermia.

Next, a synergy effect was found (80% MRC-5 vs. 22% MDA-MB-231), when both complexes were evaluated. Using 75 microliter of $Au@CoFe_2O_4$ CD-44 TX-100-CTAB 0.1M Docetaxel and 75 microliter of $Au@CoFe_2O_4$ CD-44 TX-100-CTAB 0.1M Bicalutamide at 2000 nM. (C.I 95%) **Figure 87.**

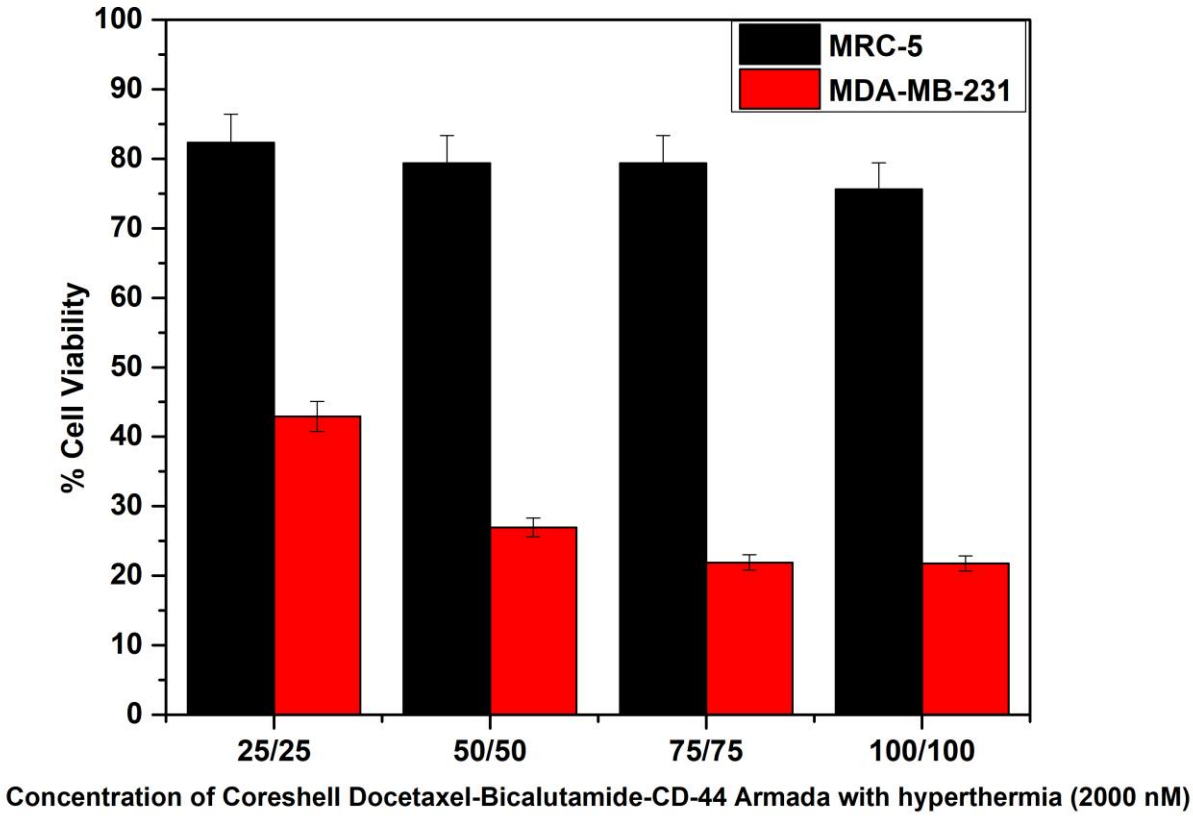

Figure 87. Core-shell- Docetaxel Bicalutamide CD-44 armada complex using hyperthermia showing a synergistic effect reducing MDA-MB 231 cell viability to 21.79%.

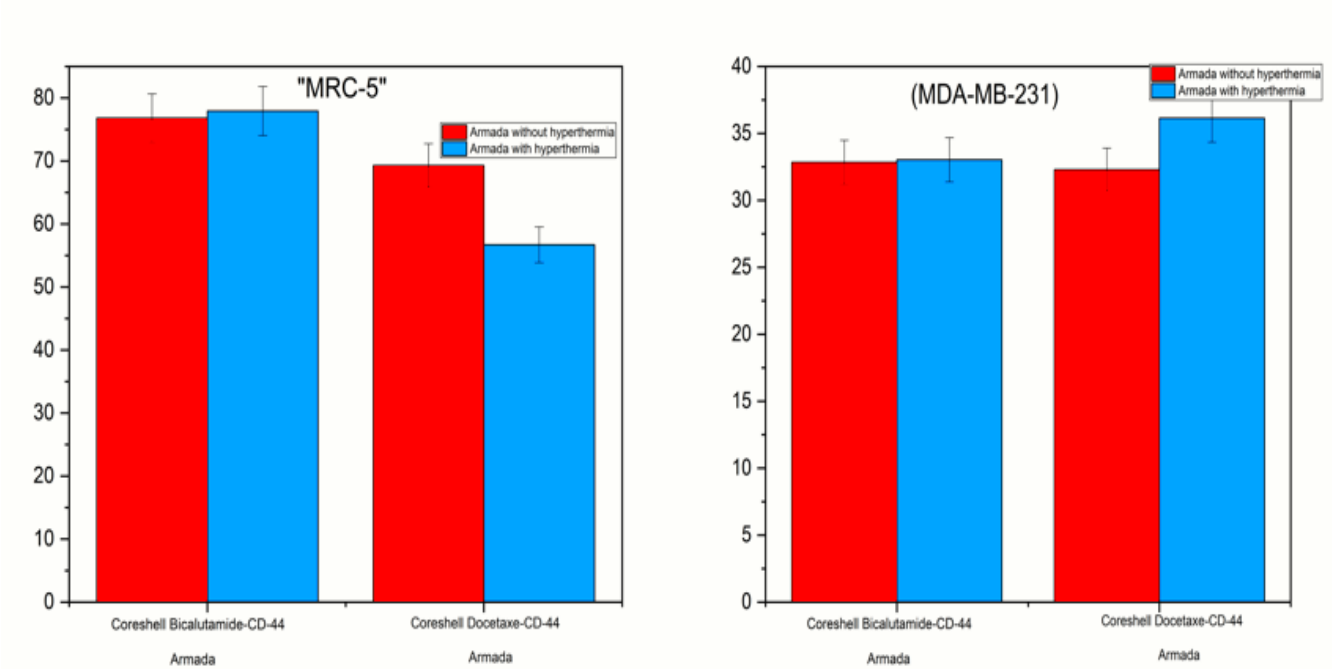

Figure 88. Nanotechnology as the future of personalized medicine demonstrates in our results the great selectivity of Gold armed nanoparticles to reduce cell viability (33%) on malignant cells while MRC-5 cells are keeping above 70% cell viability.

5.4 CONCLUSION.

The present work has consisted of synthesizing nanoparticles with an iron oxide core and a gold-coated surface, together with the functionalization of said surface, in order to use it in Cancer therapy applications. The main advantage of this nanoparticle nucleus-envelope is that it is constituted by two different nanomaterials, which can be effectively used for treatment multifunctionality (drug delivery and hyperthermia). The gold coating provides a versatile functional surface platform as well as improving bioavailability and enhancing liver and kidney clearance metabolism. The surface was functionalized with the drugs Docetaxel and Bicalutamide for the effective treatment of triple negative breast cancer (TNBC) in vitro MDA-MB-231 cell line. The gold-plated complex with surface functionality, as well as the ferromagnetic core was characterized using techniques such as IR, TGA, Potential Z, SQUID, XRD, Raman, TEM, HR-TEM line mapping, SEM, Inductively coupled plasma atomic emission spectroscopy (ICP-AES), and was also evaluated for *"In Vitro"* cytotoxicity studies to ensure that the nanoparticle complex does

not show toxic effects on normal cells. Subsequently, drug release was studied by dialysis membrane technique at different pH. Then the model was adapted to a different mathematical drug kinetic models, in this case drug-release was carried out at 3 different pH like 5.4, 6.8 & 7.4 and found that at pH 5.4 the release is maximum which is favorable for Cancer cell treatment. to find the right release adjustment. Finally, under an alternating magnetic field, the amount of heat produced by the nanoparticles to induce apoptosis in Cancer cell lines *"In Vitro"* was quantified. This combined therapy was shown to produce enough damage to the malignant cells (21.79% cell viability) respecting the benign cells (80% cell viability), but this was achieved using the humanized antibody CD-44 and possibly blocking androgen receptor using Bicalutamide, both have been demonstrated to have enhanced selectivity to our core-shell design. **Figure 88:**

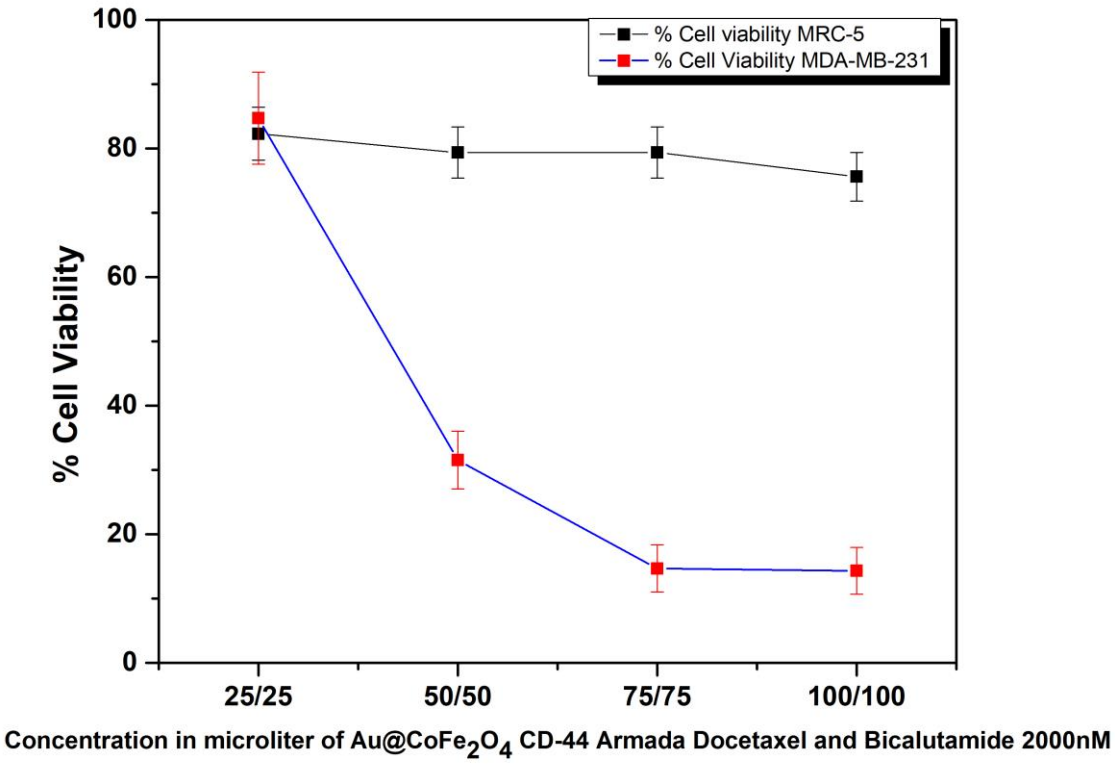

Figure 89. Concentration in microliter of $Au@CoFe_2O_4$ Armada Docetaxel and Bicalutamide 2000 nM (I.C 95%). The blue line shows superior damage of the malignant cells (21.79% cell viability).

Finally, we have demonstrated the death cell- mechanism of these NPs over MDA-MB-231 by using Flow cytometry **(Figure 90)**. Representing CFNP-CD44-Docetaxel over MDA-MB-231. It seems to be that ***Necrosis*** is happening over these unfortunate malignant cells.

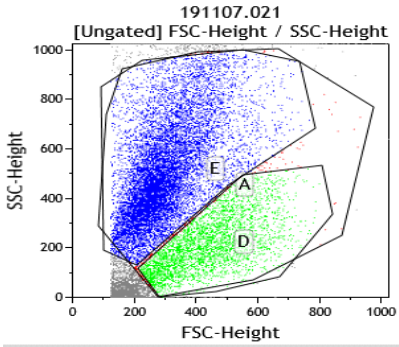

Gate	Number	%Total	%Gated
All	20.000	100,00	100,00
A	14.302	71,51	71,51
D	3.458	17,29	17,29
E	10.654	53,27	53,27

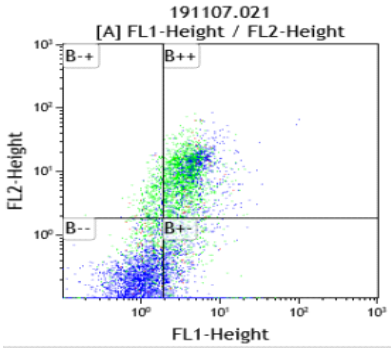

Gate	Number	%Total	%Gated
All	14.302	71,51	100,00
B--	7.925	39,63	55,41
B-+	296	1,48	2,07
B+-	3.771	18,86	26,37
B++	2.310	11,55	16,15

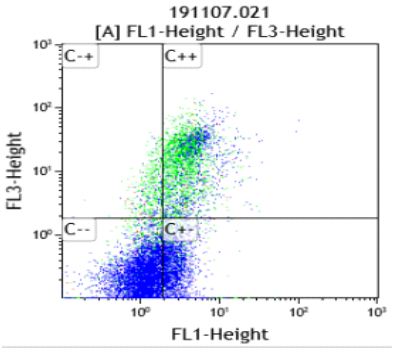

Gate	Number	%Total	%Gated
All	14.302	71,51	100,00
C--	7.905	39,53	55,27
C-+	521	2,61	3,64
C+-	3.070	15,35	21,47
C++	2.806	14,03	19,62

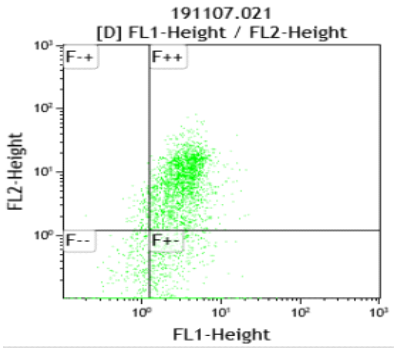

Gate	Number	%Total	%Gated
All	3.458	17,29	100,00
F--	454	2,27	13,13
F-+	93	0,47	2,69
F+-	949	4,75	27,44
F++	1.962	9,81	56,74

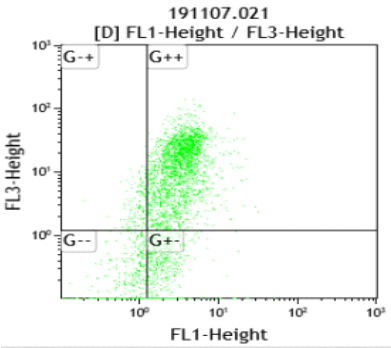

Gate	Number	%Total	%Gated
All	3.458	17,29	100,00
G--	393	1,97	11,36
G-+	154	0,77	4,45
G+-	596	2,98	17,24
G++	2.315	11,58	66,95

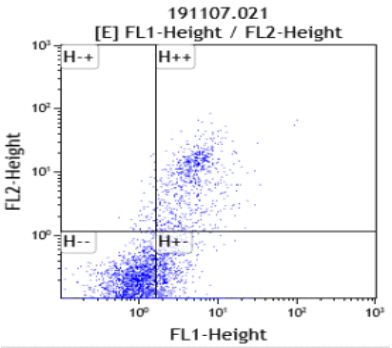

Gate	Number	%Total	%Gated
All	10.654	53,27	100,00
H--	6.255	31,28	58,71
H-+	51	0,26	0,48
H+-	3.652	18,26	34,28
H++	696	3,48	6,53

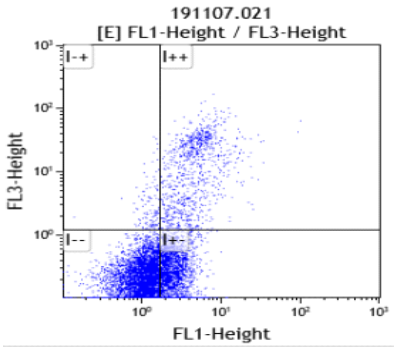

Gate	Number	%Total	%Gated
All	10.654	53,27	100,00
I--	6.430	32,15	60,35
I-+	116	0,58	1,09
I+-	3.202	16,01	30,05
I++	906	4,53	8,50

Conclusions can be summarized in the following points:

*A reproducible protocol of synthesis and optimization of nanomaterials (cobalt, manganese, and zinc ferrite nucleus) by using thermal decomposition method (TD) was successfully carried out to improve their magnetic properties.

*Cobalt and Manganese NPS have demonstrated to be the best candidates compared to Zinc NPs.

*Triton X-100 and CTAB were tested as the best surfactants to create the core-shell design.

*Reproducible Au-NPs were optimized for surface functionalization.

*The anchoring of specific ligands (therapeutic missile or magic bullet effect) to receptors (molecular keys to reach the desired site) such as humanized antibody CD-44 was optimized.

*The multi-functionalization of nanoparticles for the coupling of drugs such as Docetaxel / Bicalutamide and humanized antibody CD-44 was successfully performed.

*The therapeutic efficacy was demonstrated by using this complex of drug-carrying *"In Vitro"* magnetic nanoparticles studies in MDA-MB 231 cell line of triple negative breast Cancer (TNBC). All experiments were repeated three times for all samples.

*The TNBC model used is vulnerable to the use of Bicalutamide possibly due to the presence of androgen receptor.

*Individually or combined, Bicalutamide and Docetaxel have less cytotoxic effect on MDA-MB-231 cells in comparison with the Bicalutamide-Docetaxel Gold core-shell complex.

*Bicalutamide and Docetaxel combined have a synergistic effect.

*In combination with coreshell-CD-44 humanized antibody, both drugs have been demonstrated a better therapeutic effect in MDA-MB-231 reaching 80% malignant cell mortality, possibly the lack of expression of CD-44 plays an important role in the 20% which are showing resistance.

*The highest efficiency and selectivity in the therapeutic against TNBC in vitro were achieved when the complex Au@$CoFe_2O_4$-CD-44-Bicalutamide -Docetaxel was combined with hyperthermia (50°C).

* Au@$CoFe_2O_4$-CD-44-Bicalutamide -Docetaxel death cell mechanism is due to Necrosis.

5.5 Future prospects

In the present document, the significant benefit of the gold core-shell design has been demonstrated. Core-shell design provides complete protection to the inner magnetic core from a range of environmental factors, in addition to providing a platform for surface modifications, real-time imaging, and drug transport loads. These NPs expectations are to go through renal clearance, which is defined as the volume of plasma that is freed of a certain substance through renal action, measured in unit time. Therefore, *"In vivo"* models are the next step to test them. Also, doping super-paramagnetic iron oxide nanoparticles (SPIONs) further enhances its magnetic property, increasing the performance of materials for biomedical applications. In this work, we also have optimized the synthesis of SPIONs with dopants, such as Cobalt, Zinc and Manganese together with the gold film to form a nucleus of nanoparticles with various biological functions, for example: 1.-Drug delivery (Docetaxel and Bicalutamide) 2.- Hyperthermia, 3.-Functionalization, since these magnetic NPs have an enormous surface area for the union of biological structures, making them suitable candidates for the creation of non-radioactive novel contrast agents.

As a sustainer of this thesis, my suggestion to enhance this technology will be to consider cytotoxicity in animal model, but also, testing these NPs in the most possible real tumor micro-environment by using Lab-on-a-chip and Micro-Electro-Mechanical Systems (MEMs). The concept is called Cancer-on-a-chip, and serious research leader group teams across the globe are currently working on it. Subsequently, NPs can be studied when interacting with stroma, lymphocytes, interleukins, thromboxane's, tumor cytokines, etc.

Nanomedicine is in its infancy, but future trends are described in the next chapter.

CHAPTER 6

For someone who was never meant for this world, I must confess I'm suddenly having a hard time leaving it. Of course, they say every atom in our bodies was once part of a star.

Maybe I'm not leaving

Maybe I'm going home.

—Jerome, Gattaca movie 1997

6. Synthetic Biology

Synthetic biology is the branch of engineering that design synthetic-artificial biological microorganism through several simulation tools, and novel biology cell tools as genome and epigenome edition. Thus, allows engineering of synthetic systems and biological circuits by simulating cells and micro-organisms functions. However, engineering eukaryotic cells is primitive still [368] since this technology remains limited to using logarithmic locks to emulate intracellular functions, but the complexity of biological systems continues to exceed current technology. Soon, synthetic biology will be an important complement not only for molecular cell biology but ***Nanotechnology***, true programmed nanobots could be the alternative to materialize the commands and algorithms offered by synthetic biology.

On the other hand, epigenetic editing tools seem exceptional for the treatment and study of the underlying molecular epigenetic mechanisms in diseases such as Cancer, chronic diseases of the Central Nervous System (CNS) or imprinting defects; for example, DNA methylation has already been used to silence overexpressed oncogenes [369] and it could be used to repress even more factors inducible by hypoxia, which can lead to Cancer regression. Also, silenced tumor suppressor genes can be reactivated by demethylation of the target DNA, since it has been demonstrated that hypermethylation could be considered as an inactivating mechanism for BRCA1 expression in TNBC [370].

6.1 Synthetic epigenetics

The human genome comprises approximately three billion base pairs. The fact that different cells contain basically the same DNA but show very different phenotypes indicates that regulated access to this information is key to the understanding of human development and health.

The term epigenetics refers to the branch of biology that studies all those non-genetic factors that intervene in the development of an organism [371]. That is, factors such as quality of life, food, environment and climate. These factors act on genes and influence their functioning, e.g. an identical twin born in the fast food western environment will have more predisposition to obesity and metabolic syndrome than one born in China, where the

feeding is different and this due to alterations in the replication of their DNA, motivated by external factors. In other words, epigenetics studies the interactions of DNA with the *Epigenome*, which is made up of molecules that do not belong to DNA and that are capable of interfering with the expression of genes or their non-expression, since they can methylate or acetylate them.

Two processes are fundamental in epigenetics, methylation and acetylation of histones, are reversible processes that are responsible for the activation or silencing of transcription. The degree of acetylation of histones is maintained by the enzyme histone acetylase or HAT, as well as by the enzyme histone deacetylase or HDAC [372].These processes are involved with functions such as: Control of cell differentiation, gene expression during embryonic development, inactivation of the X chromosome, silencing of endogenous retroviruses, and genetic imprinting (errors in imprinting manifest themselves clinically as genetic diseases such as Prader-Willi, Angelman syndrome, Beckwith-Wiedamann, Rusell-Silver syndrome, Wilm's tumor and retinoblastoma) [373].

Epigenetic editing involves an adjustment of the epigenome and offers the possibility that the corresponding change to the epigenetic signal in the expression state of the gene is hereditably maintained by the cellular machinery through multiple cell divisions, even after the construction of the initial epigenetic edition is removed from the cells. What this technology supposes is the ability to edit the errors in the epigenome that code for the diseases and in this way correct the anomalous signaling that translates into clinical pathologies including TNBC (Triple Negative Breast Cancer) and other types of Cancer [372, 374].

It was thought that epigenetic marks were more related to diseases of imprinting than Cancer, but it has been mentioned that environmental factors, diet, sedentary lifestyle, smoking, among other factors, could be implicated; because they affect the disease states in the epigenome, and it is known that some types of Cancer are the product of the aforementioned habits. Then we could attack Cancer by modifying the epigenome, perhaps by inserting methylation or acetylation factors that suppress oncogenes, editing the genome, we will call this concept *"synthetic epigenetics"*.

If epigenetics determines not only the appearance of diseases, but also the way in which we age, epigenetics could be used in anti-aging medicine. Most of the chronic-degenerative diseases and certain types of Cancer appear at older ages. Synthetic epigenetics can be the solution to the polypharmacy problems of geriatric patients, and it can also be the solution to prolong our lives, which supposes an essential advance for humanity, increasing lifespan from 80 to 120 years and improving the quality of life by "switching off" the genes responsible for certain diseases. It is possible that in the future, *nanocomposites or nano-cargos* (colloidal nanoparticles) can edit the epigenome with higher selectivity.

6.2 Advanced Preventive Medicine and Cancer (Anti-Age Medicine).

Despite breakthroughs epigenetic-signaling pathways, as well as the characterization of epigenetic marks (DNA and histone modifications) and the enzymatic machinery that can be written, read and eliminated [374]. At this point we are still far away to delete oncogenes or increasing lifespan considerably.

However, the implications of epigenetics are unprecedented, the diet of a great-grandmother of one person could affect the current state of illness of a great-grandchild, the fact that the father or mother of someone is a smoker will alter the epigenome of the children; this has discarded the old idea that the genetic load with which people were born could not be changed, some protective factors such as diet and exercise can significantly improving people lineage quality of life. Thus, *Anti-Age Medicine* studies all these processes which are related with Cancer and other metabolic diseases.

Anti-age medicine is the branch of medical science and applied medicine which studies underlying causes of aging to extend the healthy lifespan of humans having youthful characteristics. To reach this goal, this discipline focuses on strategies such as hormone replacement therapy to reach levels similar to individuals of 20-30 years old, manage physical exercise, promotes the consumption of antioxidants, vitamins and minerals and correct diet.

Although the rise of this discipline has increased, and in principle serves in a preventive way the triggers of some types of Cancer and other chronic diseases, it has not yet been recognizing/accredited by the American Medical Association [375].

6.3 Immortality

It was described that Cancers result in the immortality of telomerase activation, but it has been shown that this is not enough to produce immortalization, it also requires specific karyotypes [376]. Immortality is operationally defined by growth more than the *Hayflick limit*, which is about 50 generations in vitro [377]. It is still unclear how immortal Cancers originate from malignant somatic cells and why these diseases are immortal. To explore that idea scientist are researching on spontaneous mutations of genes chromosomes not only human but other species [376].

6.3.1 Exploring immortality capacities.

An aneuploid is an individual whose chromosome number differs from the wild type or euploid in part of its chromosomal endowment, due to an extra or absent chromosome, which is always associated with a deficiency in physical or mental development or both. Aneuploidy can often be seen in Cancer cells, especially random aneuploidy. In humans, all aneuploidies produce disease, however they are closely related to cell immortality, which is why they are of scientific interest to develop immortal cell strains. The idea would be to control the aneuploidies but for this the scientists are wondering if tumorigenicity and immortality are also karyotypically united in independent tumorigenic clones [376]. There is a theory which explain the last paradox, aneuploidy impairs normal growth and development. But, what if the "aneuploidies" of Cancers are karyotypes of new species? So then mystery would be solved [109].

However, it seems there are species which can live many years overcoming the problem of the paradox (perhaps tumorigenesis and immortalization are simultaneous clonal events), having an incredible specialization and control not only telomerases but other mechanism implicated on immortality such as random aneuploidy, for example, the eastern box turtle "*Terrapene carolina*" [378] can live 130 years, the red sea urchin "*Strongylocentrotus franciscanus"* (200 years) [379], ocean quahog "*Arctica islándica"* (507 years) [380], the Greenland shark "*Somniosus microcephalus* "(400 years) [381] and some amazing life forms as the great basin bristlecone pine "*Pinus longaeva*" (4.713 years) [382] and Hydra "*H. oligactis"* which has stem cells continuously self-

renewing so then it has not been possible to calculate their longevity, which has created the idea that they are immortal [383]. The fact that there are long-lived species may provide some insight that cell immortality is not necessarily linked to the same code as malignancy and the appearance of tumors, some novel studies suggest that the transfection of genes by means of viruses into normal cells could offer them immortality without necessarily to transmit malignity (Cancer) [384].

6.4 The possible origin of Panacea and the reverse engineering utilizing synthetic biology.

A multidisciplinary approach is necessary to land visionary ideas, for example, we have more powerful quantum computers, graphene will replace silicon in microprocessors. If history has taught us anything, mass extinctions occur each million years naturally, so we are a young species and privileged. If we want to cling to life, we will have to take a quantum leap by finding a cure for all diseases, something that heals everything; this term is called "*Panacea"* and can only be possible through a multidisciplinary approach.

In Greek mythology Πανάκεια Panákeia, (Panacea) which means that heals everything, was the granddaughter of Helios. In modern medicine the panacea is a utopic drug which can cure everything without side effects, however, panacea has not been possible indeed, almost all drugs have side effects, thus the difference between poison and medicine is in the dose.

Currently researchers believe that the panacea could be found in the CRISPR-Cas9 system [385].Genome edition requires the Cas9 nuclease and an engineered single-guide RNA (sgRNA). Next, the guide portion of the sgRNA recognizes complementary DNA sequences outflanked by a protospacer-adjacent motif (PAM), and Cas9 cleaves the identified DNA. The modification of the target region takes place by the breakage of the double chain that is subsequently repaired by non-homologous (NHEJ) and homologous (HDR) junctions [386]. Although CRISPR/Cas 9 biotechnologies could improve immune response against fungi and other microorganism, enhancing microbiome and reducing antibiotic resistance [385], the system is currently being enhanced through Nanotechnology

by using nanoparticles as a vehicle to transport CRISPR/Cas9 complex [386] since, *Non-viral treatment* by using nanoparticles could be safer than conventional viral therapy,

The personalized medicine of the future will use all the tools of molecular cell biology as the edition of the epigenome to solve chronic degenerative diseases and will use programmed nanorobots made by synthetic circuits (synthetic biology) to solve problems such as traumatisms and wounds. The old procedures used for all patients will be replaced by individualized protocols that will provide instead of only 6 vital variables (bicarbonate, oxygen, heart rate, respiratory rate, number of leukocytes, carbon dioxide), more than 1800 variables (Big Data) [387] in 60 seconds through *nano-sensors* including the best pharmacogenomic treatment, genomic profile, social and medical history, short, medium and long term outcome.

In this quest to alleviate pain and eradicate disease a discipline of biology called epigenetics emerged, like a branch of engineering called synthetic biology, together, working for playing at being gods, the first artificial synthetic cell was produced in a laboratory *"Mycoplasma Laboratorium"* patent number 20070122826 [388], said synthetic cell could be programmed to eradicate, for example, tumor cells, if the immune system fails, a pluripotential artificial cell could theoretically be programmed to produce apoptosis in the malignant cells, specifically *Natural Killer cells* (NK). The implications for these discoveries are enormous, since it could be the panacea as well as a threat if the technology goes out of control or falls into the wrong hands.

6.5 Quantum Chemistry for Nanomedicine.

Quantum chemistry (also called molecular quantum mechanics) is the branch of chemistry that studies and understands the application of quantum mechanics in chemical system experiments allowing a better understanding on the study of intermolecular networks (equation-of-motion) [389].

The physical models of computational quantum chemistry, which applies the principles of quantum mechanics of molecular and condensed systems that make it possible to understand the interactions of helical peptides and DNA complexes such as polyketide-

based pharmaceuticals (PKSs), which are some of the most critical drugs in the pharmaceutical industry.

The recent development of direct space structure solution methods has allowed the study of crystalline organic materials, by using powder diffraction data. These methods of direct space are based on simulated genetic algorithms such as the so-called *Monte Carlo* (MC) which offers great modeling flexibility and potential for adherence to reality [390]. The simulations are determinant to improve understanding about underlying interactomics. Current technology, such as MALDI-TOF *(Matrix Assisted Laser Desorption Ionization-Time Of Flight Mass Spectrometry)* [391] allows for the understanding of interaction between metabolites, proteins and molecules associated with Cancer. This is important because the high expression of cell markers, telomerases, and proteins interact, facilitating or disabling the therapeutic effect of the nanodrugs. However, these technologies could be dramatically enhanced using simulation-modeling through MC or another quantum modeling like IBMqX4 which is being used to simulate quantum artificial life [392]. Nowadays, it is feasible MC can increase the chances of success regarding effectiveness and safety of nanoparticles through simulating Cancer microenvironment since interactomes will be unveiled.

Studying *"In vivo"* systems demands understanding of a complex interactive network, e.g., artery pressure, pH, metabolism, bioavailability, pharmacogenomics, blood viscosity, the lethal, therapeutic and minimum dose of a drug, etc. Consequently, it is highly recommendable for the nanotechnologist of the future and for nanomedicine discipline to implement simulation and experimentation systems simultaneously. Currently, *The Human Connectome Project* (Characterization and mapping of the microstructural environment in the human brain) is using tools such as MC simulations, RMI and Big Data [393].

6.5.1 Quantum Computation: Valleytronics.

A quantum computer is a device able to simulate all the physical processes which include living systems by using the so-called *Deutsch-Church-Turing principle* [392].The era of quantum computers is a fact [394], as there are currently storage systems operating with qubits. The logical capacity of the processors will allow deciphering of complex networks

of interactions in biological systems, helping to decode the molecular problems that underlie complex diseases such as heart disease, immunological diseases, metabolic syndrome, Parkinson's, Alzheimer's and of course more than 100 diseases called “Cancer”.

While spintronics-based devices, where the charge of the electron and its spin are taken, manifest as a state of weak magnetic energy that can take only two values, *Valleytronics* can read the extreme multiple of the band structure, this means it can process 1 and 0 simultaneously instead of 1 and 0 at different times. The quantum information processing is coherent and adiabatic; it has been pursued using internal degrees of freedom encoded in *uαk*, such as spin or valley pseudospin [395].

Quantum computing will allow for evaluation reactions that occur in femtoseconds (10^{-15})[396], attoseconds (10^{-18}) [395] and yocto-seconds (Ys, one septillionth of a second 10^{-24}), as well as modeling of the whole Fluxomics and molecular quantum chemistry behind diseases, as a reverse engineering process. Future physicians will know which points to attack through *Nanomedicine* with extreme accuracy by combining all mentioned disciplines and sending nano-vectors to silence genes or blocking specific reactions within the cytosol or cell-nucleus by interfering chemical processes which take place in nanoseconds e.g. interference RNA (RNAi), the implications of those technologies will be essential in this emerging era of *Nanomedicine*.

Currently, for instance, the MERIT (Systematic Analysis and Characterization of Mutational Effect on RNA Interactome Topology) system does not yet work by using quantum computing, however, it has already provided valuable information to establish interactions between RNA-binding proteins (RBPs) and RNA in Cancer [397]. Thus, the potential of qubits of information working on novel Cancer disease models (transcriptomics, proteomics, metabolomics micro-environment behavior, capacity for metastasis, mutations, prognosis, treatment) is unimaginable.

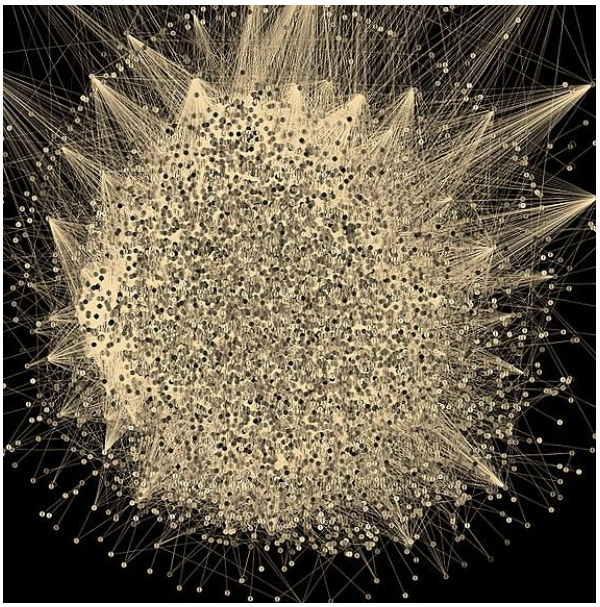

The genomic, transcriptomic, proteomic and metabolomic connections (Interactomics) will provide an individualized scheme of each type and subtype of Cancer, allowing the clinician to attack the most vulnerable points, anticipating the behavior of the disease and blocking tumor functions by using nanoparticles with specific molecular objectives.

On the left, an illustrative scheme where each point in the figure represents proteins, genes, metabolites and other signals interacting, establishing communication and therefore cell-function.

6.6 Transhumanism.

At the pinnacle of human fulfilment, *Transhumanism* is a current quasi-medical ideology [398], a cultural, socio-political and intellectual trend that supports not only the use of present technologies to improve beauty, lifespan and resistance to disease, but also new and emerging technologies, such as *Nanotechnology*, genetic engineering [399], robotics [400, 401], cybernetics (brain-machine interfaces) [402], quantum computation and synthetic biology to radically modify the human organism [398].

However, what initially emerged as a science fiction idea, now turns out to be an idea of overwhelming importance for researchers and academics. Because transhumanism is promoted culturally, bioethically, scientifically and politically by a number of technological advances such as artificial human organs [403], robotic arms and legs [404], and neurological chips that allow linking human brains to computers.

Numerous articles begin to talk about this techno-progressive trend, *The Journal of Medicine and Philosophy* has published on transhumanism as a topic to consider in the debate between bio-conservatives and transhumanists about ethics in genetic engineering, transfection of memories, transfection of thoughts, mental control, as well as privacy and respect for personality or identity.

The social problems expected as a result of transhumanism is that it will undoubtedly increase inequalities between the rich and the poor. The rich can afford to use transhumanism, but the poor will not be able to do it. The last group will suffer the consequences in health and well-being, an example of this happens with modern plastic surgery: the people who can afford a surgical procedure to look more beautiful or healthy could increase the odds for getting a job opportunity. Another modern example is the use of SNPs which can act as biological markers that may help predict an individual's risk of developing congenital or heart disease [405], susceptibility to environmental factors such as toxins, and response to medications and drugs bringing the user advantage to avoid illness compared to those who cannot pay. In future transhumanism, rich people could secure an artificial heart [406] or an artificial lung [407] and exoskeletons [408] for physical therapy or human body replacement while a poor person would die before being able to afford the price of this technology.

We are already living the benefits and consequences of transhumanism, for example the use of robotic prosthesis or a pacemaker in a patient who needs it or the use of exoskeleton for the rehabilitation of patients [408].

6.6.1 Regenerative Medicine by using synthetic-artificial organs.

3D printing as well as the 3D scanner are two of the most notable advances in the materialization of designs created in software or taken from reality. However, the current organ replacement technology is based on robotics, cybernetics, regenerative medicine and cell replacement therapy for stimulation of pluripotent stem cells. Currently, the enormous size of salamander genomes had been object of study for researchers for the biological process of limb regeneration these animals have, for example the *Axolotl* [409].

Researchers have also managed to guide pluripotent stem cells to generate specialized cells that take the shape of a mold in the form of the desired organ and thus build a human organ by using 3D tissue-cell printer [410]. The other alternative of organ replacement is by artificial organs [411]. At the moment, there is in process the development of synthetic heart [412], synthetic kidneys [413], artificial pancreas [414], artificial retina [415], artificial lungs [407] and exoskeleton-assisted walking in patients with spinal cord injury

[416]. Recently, *Dr. Anthony Atala* and his team from *Harvard University* have already performed a successful transplant of bladder cultivated with the patient's cells. All the previous advances in regenerative medicine and 3D cell-tissue-printer-technology can become the solution for the lack of organs in patients that require an organ transplant *"Regenerative Surgery"*, which is currently a public health problem [417, 418].

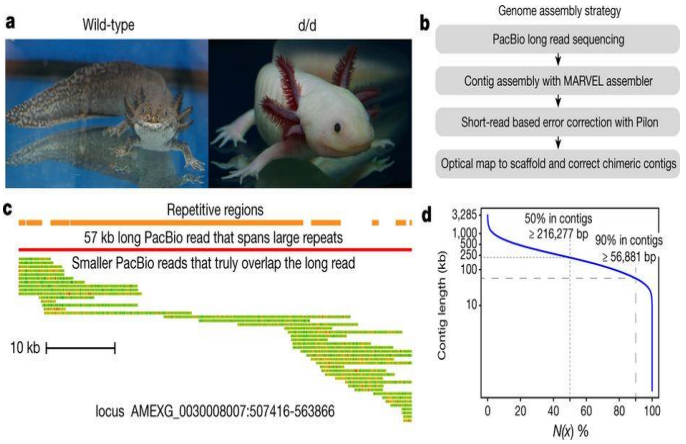

The Axolotls genome is currently being studied to find the genes involved in its capacity for regeneration of lost limbs. The editing of human genes using recombinant technology, could generate gene therapy by means to regenerate lost limbs in patients who have suffered trauma or accident.

6.6.2 Organ-on-a-chip.

Organ-on-a-chip is a novel technology that simulates the physiological conditions (pH, temperature, cationic proteins, function, homeostasis, metabolism), mechanics and biochemistry of a specific organ (heart, kidney, pancreas) on a chip. The applications for this technology are ideal for the study and evaluation of drug medication [419], pharmacokinetics (PK), *Dose-Limiting Toxicity* (DLT) and *Maximal Tolerated Dose* (MTD), *Median Lethal Dose*, etc. [420]

The chips can simulate the cellular microenvironment [421] factors such as cytokines, metabolites, biological molecules, hormones, the extracellular matrix and intercellular junctions [422]. The chips can connect to each other building *Multi-organ-on-a-chip* (for example lung organ-on-a-chip connected to heart organ-on-a-chip) and in this way dispense with the *"In Vitro"* models (unreal compared to an *"In Vivo"* system) and likewise distribute with animal models for the experimental study of drugs or metabolic studies.

Currently, researchers are working with integrated carbon electrodes to offer an accurate controllable physiological mechanical condition to create cardiac patches for both replacement of cardiac tissues and the creation of *Heart-on-a-chip* [423] . Other organ-on-

a-chip models available are: vessel-on-a-chip, liver-on-a-chip, kidney-on-a-chip and a novel microfluidic device fabricated by Shamloo and coworkers called: *Neuron-on-a-chip* [424]. Chiefly organ-on-a-chip advantages are: 1.-They allow emulation of accurate conditions similar to the real living beings (presence of macrophages, nutrients, hormones, myeloperoxidases, hydrolases, drug permeability, etc.) 2.- Dispense the necessity to sacrifice animals, which do not correctly simulate human organisms. The main disadvantage is that they are currently expensive.

These chips can be MEMS [425], NEMS, or biomimetic 3D tissue structures made by printer [426]. Despite the research about organ-on-a-chip being in its infancy, it is expected that in the future, experimental medicine researchers and cell biology scientists will base their models on these devices and perhaps physicians will begin replacing human organs at hospitals implementing these technologies.

6.6.3 Lab-on-a-chip.

Lab-on-a-chip technology can simulate several lab conditions on a single chip [10]. These are biomolecular detection systems based on microfluidics [427] and its role as a novel model is currently being used in many labs of the world.

The creation of integrated circuits by Top-down technique has allowed the formation of Micro-Electro Mechanical Systems (MEMS) and subsequently miniaturization to nanometers (NEMS), which perfectly simulate 3-D conditions and physical mechanisms mediated by fluidic microchannels, the concept is also called Microfluidic-lab-on-a-chip (Loc) [428].

The operation by means of valves, external or internal pumps, and integrated circuits, allows MEMS to emulate precise biological situations [429]. The applications range from cardiovascular disease medical research [430] to the food industry and agriculture [431], thus, this technology has evolved dramatically to the point where the variables of a whole laboratory are inside a chip, but, How?

High-precision bioanalytical applications allow scientists to analyze molecules [432], amplify them and even study the interactions between the molecules. For example

researchers have gone through the analysis of protein-protein interactions in *S. pneumonia*, [433] or finding biomarkers for prostate Cancer [434]. Instead of having a device to perform RT-PCR, the user can use a portable lab-on-a-chip that fits in the pocket of the gown or the trouser, transport it to run a given experiment and analyze the data in a computer connecting the chip to a USB storage.

More amazing still, is the fact that lab-on-a-chip can connect to "N" number other Loc´s and generate powerful and complex laboratories [435]. Hence, lab-on-a-chip must be free from contamination and its versatile features allow emulating almost any lab-condition, but the problem remains they are costly still.

6.7 Insights about nanotechnology for the food industry.

As the Hippocrates quote *"Let food be thy medicine and medicine be thy food"*. Recent studies indicate that food daily choices as well as the emotions we are feeling might be influenced by the *Microbiome* [436]. That we have, as well as microbiome has an enormous impact on the life of the host, and the diet plays a fundamental role in shaping microbiome composition and function [437]. Food is one of the pillars to the well-being of the human body, and Microbiome feeds on that food. It has been demonstrated that altered Microbiome (dysbiosis) is associated with the pathogenesis of many inflammatory diseases and infections [438] like *Clostridium Difficile*, since microbiota is necessary to eradicate and control higher rate-proliferation of harmful bacteria. Currently, a fecal microbiota transplant (FMT) is the solution [439] for attending patients who have *Clostridium Difficile*.

Moreover, it is possible that many other diseases like Cancer and other long-term diseases are involved in the deregulation of the microbiota. The recent concern for the industrialization of food has resulted in trends such as veganism and the consumption of organic products. Following this trend induces a worthy debate: the idea that transgenic or processed foods may be a health problem or a solution to world hunger. However, the food industry generates huge profits, according with *USDA 2012 Census of agriculture* in the United States, farm operations generate nearly $ 400 billion in sales and more than $ 100 billion in net farm income in 2013.

Given the importance of food in the impact of health, it is still unclear if some of the consumer products available in supermarkets are the source of Cancer. There are no studies about it, but what has been shown is that sausages, bacon, ham and processed food can predispose to Cancer [440], that is why researchers are trying implementing the use of anthocyanin-rich foods to decrease the incidence of colorectal Cancer [441]. Anthocyanins are potent antioxidant flavonoids which have diverse biological functions once ingested, including immunomodulatory, anti-inflammatory and antitumor functions. Thus, the enrichment of the food with vitamins and amino acids at micro and nanoscale will require better food regulation for the safety and tranquility of consumers.

The natural nanostructures found in food are produced by some proteins and carbohydrates, i.e. for generations, consumers have been eating foods with nanoscale raw materials which undergo structural changes at the nanometer and micrometer scales during the normal processing of food. The dairy industry uses casein micelles, fat globules, whey proteins to build all kinds of emulsions such as butter, ice cream, cream and smoothies, milk, yogurt and cheese, whose components are assembled at the nanoscale, forming solids, liquids, foams and gels [442]. Then, the dairy technology is not only microtechnology but also nanotechnology and has supported food industry applications for several decades.

The current nanotechnology is developing self-assembled nanotubes of α-lactalbumin hydrolyzed milk protein, whose main application is the nanoencapsulation of nutrients, supplements and pharmaceutical products [442]. Similarly, nanostructured food is applied to improve the flavor, texture and consistency of foods, such as yogurt that incorporates titanium dioxide to ensure natural color, or low-fat nanostructured mayonnaise and creamy ice cream due to nanoparticles, that provide better texture. Nanotechnology also intends to make a difference in processing of meat. Soon, researchers will try to create intelligent packaging of meat and meat products from bioactive peptides and the inclusion of pro and prebiotics in processed meat products. Nano food packaging materials may extend food life by releasing preservatives to extend the life of the food in the package, improve food safety and alert consumers that food is contaminated or spoiled [443]. However, there may be concerns about biosecurity-nanotechnology and the use of nanomaterials for food industry.

The chief reason this novel technology is considered as a possible danger, is that the nanoparticles do not have proper bio-security regulations yet [444].

For this purpose, *Nanotoxicology* must review at the toxicological level and the risks not only regarding food but to establish a regulation for the use of these materials for the benefit of human beings as well as adverse effects on the *environment, ecosystems and the potential occupational exposure for workers and researchers***.** Therefore, there is growing interest in assessing the risk of nanomaterials [445].

In summary, *Nanotechnology* could benefit human beings to a large extent with adequate regulation and scientific evaluation. The establishment of a regulatory system for manufacturers that use nanomaterials or nanotechnology is necessary, as these regulations would provide greater ethical transparency regarding the contributions of nanotechnology for food industry, cosmetics industry, scientific research, etc. Transparency allows consumers and industry-workers to develop optimistic confidence in nanotechnology and primary education about this technology. Moreover, more research is needed on nanoparticles in water, air and food, since Cancer is known to be a group of diseases related to genes and the environment. However, food, due to its daily importance represents a priority objective to establish standards of security about preservatives, micro, and nanoparticles used as artificial flavorings and artificial colors, since these could be serious components for the development of Cancer.

6.8 Nano-Biosecurity.

It was in 1959 when Dr. Richard Feynman (Nobel Prize in Physics 1965) suggested the possible manipulation of objects atom by atom. Currently, such manipulation is a fact; Nanotechnology can be defined as the study, design, synthesis, manipulation and application of materials, devices and functional systems through the control of matter at the nanoscale. However, this great power of manipulation of the nanoscale brings infinite possibilities of social impact for good and for ill. Applications in Nanotechnology, specifically in Nanomedicine, should be an opportunity to improve the quality of life of many people, yet some radical people and groups fear for the destruction of humanity by alteration of the environment (nanotoxicity) [446], bio-terrorism, warfare applications (spy

devices as biomimetic hexapod robot) [400], etc. Thus, this is the reason that the term ***Nano-bioethics*** is currently used (Buxó, Casado, 2010) to indicate the importance of risk assessment, not only in the work-environment context, but also in biosecurity.

The same way, *"In Vivo"* clinical trials ongoing in Nanomedicine require a robust strategy in biosecurity, the characteristic of the materials, nanoparticles must be evaluated *"In Vitro"* (pre-clinics) and therefore twice in animal model so then stablishing Phase I human clinical trials, *Dose-Limiting Toxicity* (DLT) and *Maximal Tolerated Dose* (MTD) suitable for next phase II human clinical trials. Then the comparison to standard or no therapy takes place in phase III where the test-drug must have reversible non-life-threatening side effects. Responses must translate on *overall survival, time to progression* and *quality of life*.

Except for the current lack of safety margins both for the scientists who produce nanomaterials and for the rest of the people exposed to environmental contamination, nanodrugs seem to be a promising solution not only for Cancer-treatment but serious diseases of high molecular complexity. Nevertheless, it is clear previous technologies described above need subsequent phases of research and scrutiny.

6.9 Nanotechnology Future Trends.

It is expected that the 4^{th} industrial revolution will modify the protocols in medicine, changing paradigms, finding solutions to the problems we face as humanity in this century, the climatic deterioration, air, water and soil pollution by implementing nano-photocatalysis [447] and the definitive resolution of the *war against Cancer* and other terrible diseases that for years have killed more people than all wars combined known to man.

The use, synthesis, characterization, manipulation and application of nanomaterials for several disciplines must be legislated and regulated by organizations such as FDA, OMS, OECD (The Organization for Economic Co-operation and Development) UNESCO (United Nations Educational, Scientific and Cultural Organization) in the areas of the Universal Declaration on Bioethics and Human Rights and the Universal Declaration of the United Nations of Human Rights, as well as the International Covenant on Civil and Political Rights, and the International Covenant on Economic, Social and Cultural Rights for the

active and conscious use of nanotechnology in the medical field as well as many other areas of science.

Any technology that is capable enough to bring human well-being can detonate destruction in the same way. These concerns have been in the mind of society all the time, for example, regarding the creation of the first synthetic bacteria *"Mycoplasma Laboratorium"*[388], *Transhumanism* tendencies as artificial organs or post-human-robotic-prosthesis-implants [398] [448], nanotechnology for the food industry [449] and for the military modern warfare (kinetic energy motion-exoskeleton) [450] and space industry [451].

The current technocrats maintain the idea that we are no longer *Homo Sapiens*, they say that we are now *Homo Evolutis*, the man who can connect his brain to the computers [402], modifies his environment, genes, weather, and many other variables.

Maybe what started as a challenge, finding desperate the cure for a terrible group of diseases called Cancer, is the product of such manipulation that we did as a species in the environment, food and lifestyle. Maybe and just maybe, the new challenge we face against Cancer, heart diseases, immunological, neuro-degenerative-metabolic diseases, can be overcome by modifying the environment or evolving to post-humans able to replace members and organs of the body by synthetic organs and robotic parts.

Another objective that will require cybernetics, robotics and nanomedicine will be the fact of building stations outside the planet earth, specifically on the moon and Mars. After all, we only have one home, one planet so far, the new race to space will require *Nanomedicine* for overcoming anti-gravity disease conditions. Humankind will also need improved semiconductors made through *Nanotechnology*, nanomaterials for spacecraft or space-bridges (previous modeling and simulation through quantum computing massive storage), but in the end, not even nanotechnology itself will be able to solve all these problems, it will require a 5^{th} industrial revolution. Perhaps this fifth revolution first step is just a change of mentality as a human beings, modifying the socioeconomic policies that make our planet sick, we could get this by using friendly energies and the search for the holy grail: *Artificial photosynthesis* [452] and the *methane to methanol conversion* [453] at low pressures and temperatures. This *5^{th} industrial revolution* could dramatically heal the Cancer that our

planet is currently suffering, and it would have an enormous impact preventing diseases and improving the living conditions on Earth's planet.

6.9.1 Nanotechnology for space and military industry.

In the year 2020 geopolitical board, space is a key sector for world powers and post-modern scientific countries, it is said that we have already entered a new technological battle where artificial intelligence, cybernetics, space engineering and nanotechnology will speed up the interests of national security homeland and military industry in space, but at the same time these trends will allow enormous humankind progresses for space-nanomedicine as well as the development of novel nanomaterials for both space exploration and business-leisure. The idea of putting human beings on a spacecraft for a recreational journey is not novel, it has been contemplated for decades in science-fiction books, but the reality is that outer space is extremely dangerous, guarantee the health of tourists, explorers, war-aircraft pilots and astronauts is not an easy task [454]. The physiology of the human body changes at space context. *Space Medicine* is responsible for studying the changes that occur in a normal way in the human body as well as the disease and organic cellular stress at high altitudes as well as in zero/micro-gravity environments [455]. Moreover, to arrive into the space a multidisciplinary group of post-technological disciplines are needed, such disciplines as *Nanotechnology* [456], *Materials Sciences in Microbiology* [457], *Robotics* [458], *Astro-Biology* [459], *Astro-Physics, Artificial Intelligence* [460], *Space-Medicine* [461], *Military Engineering etc*. working together must guarantee the security of the human beings and the improvement of yield of the materials in the space, capable of resisting ionizing radiations (galactic cosmic radiation, solar UV radiation) [457], extreme temperatures and operate materials having novel features like being reusable or at least replaceable at low cost.

6.9.1.1 Nanotechnology for Space Medicine.

As researchers had predicted, nanomedicine found a fundamental role in the trends that govern aerospace research [462] by means exploration, business and tourism. It is well known human body tends to degenerate within microgravity conditions-context, the biochemical parameters in blood, feces and urine change in space. Equally well known are

the changes in astronaut psychology due to isolation, changes in the digestive, cardiovascular, immunological endocrine and skeletal-muscle systems [463].

The need to incorporate new drug delivery systems has led to the creation of micro and nano-channels that can dispense with the use of valves and infusion pumps. The traditional therapy of drug delivery through syringes, pills and tablets could be a problem in space, since the adverse effects in the microgravity environment can be a shorter drug life and therefore a diminished effectiveness, as well as the lack of absorption of drugs in the intestine and decreased quality of life due to discomfort in the administration of injections.

The nanochannels can administer medications in controlled pulses by means of a remote control and by means of cutaneous patches, the improvement of the effectiveness of administration together with the greater delivery of active molecules in the bloodstream can improve the efficacy of the drugs. Currently, the Houston Methodist Hospital in collaboration with the Center of the Advancement of Science in Space (CASIS) have begun experiments in the ISS to determine the effectiveness of the delivery of drugs and hormones at microgravity environments as well as other scientific groups are working on bacteria and viruses [459], the field of astrobiology and space microbiology is of great interest to study the behavior, genetics, physiology of microorganisms and living beings in space zero gravity conditions [464].

Superparamagnetic iron oxide nanoparticles (SPIONs) with polymeric coating or surfactant can also reach their therapeutic target by means of a magnetic field or inhalable [465]. Finally, MEMS can work in the same way as microchannels from 2 to 200 nm that lead to drugs in a controlled way within the human organism by means of patches or implants with nano-needles and nano-sensors that respond to metabolic changes and they release the drug on schedule [466], allowing the crew to free themselves of the worry of administering medications. The concept can be worked on the same orbiting spacecraft or managed from Earth *"Telemedicine"* [467] by an RF remote control.

DR. MAURICIO A. MEDINA-PÉREZ

APPENDIX

TEM IMAGES

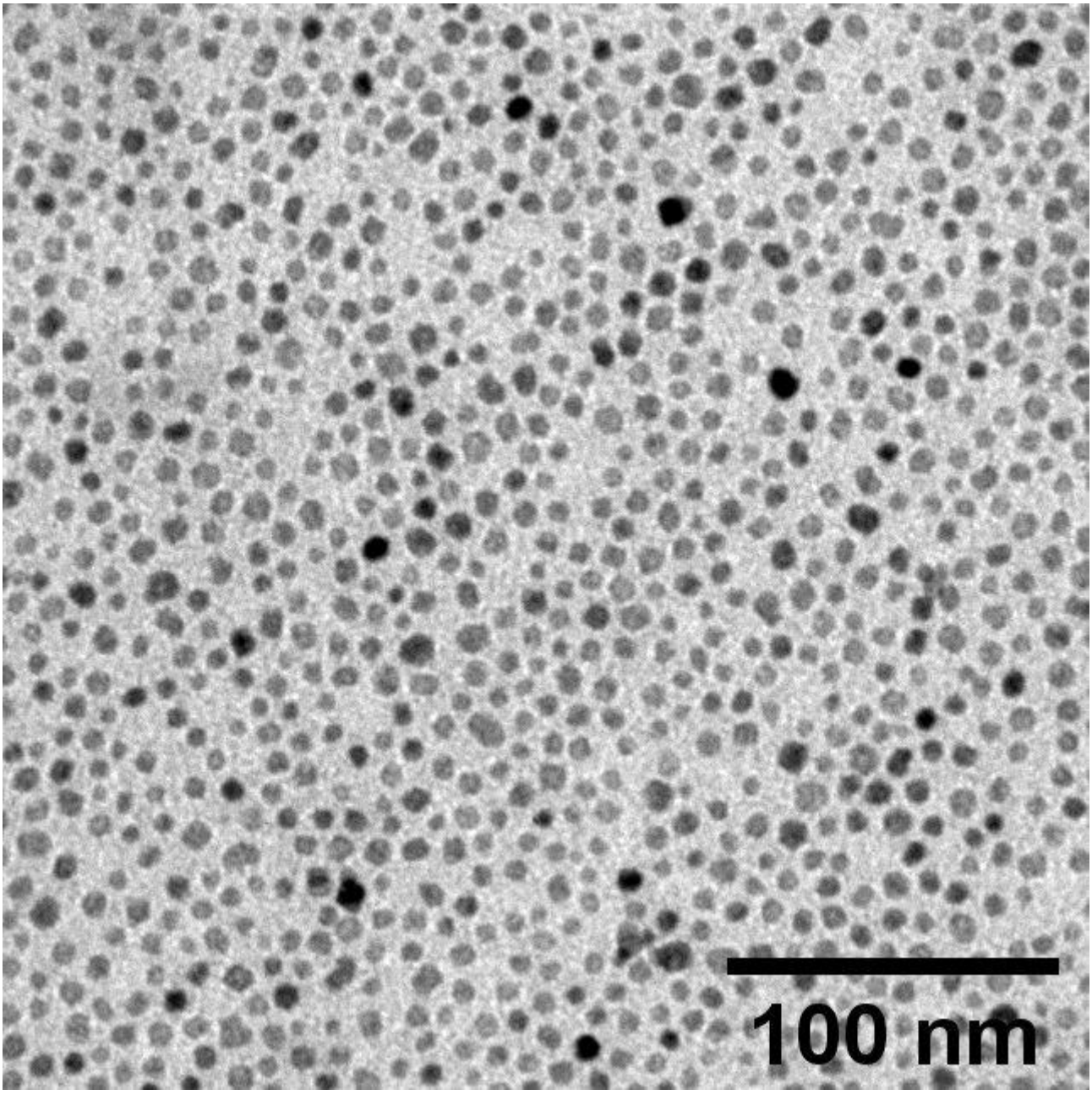

$CoFe_2O_4$ TX-100 0.1 M nanoparticles (NPs)

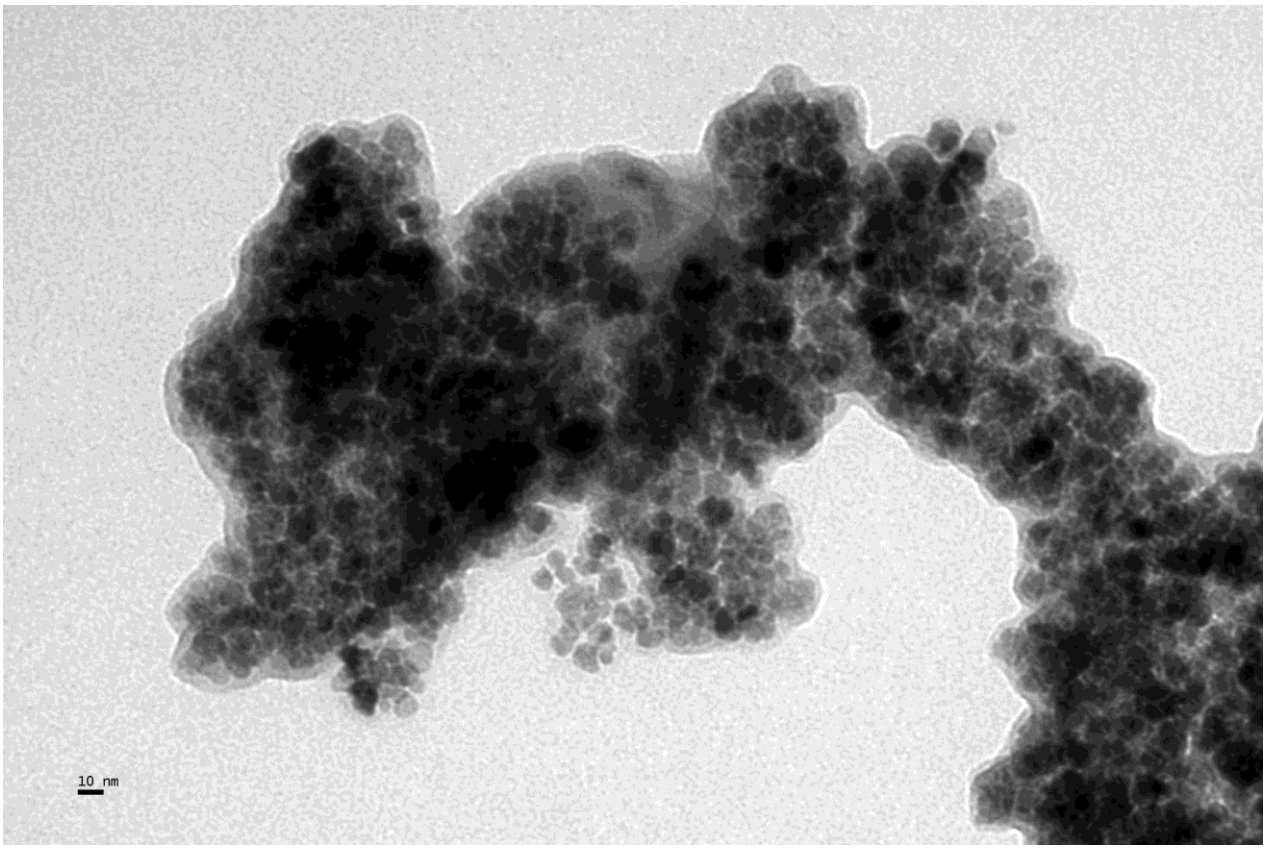

$ZnFe_2O_4$ PEG 0.03M NPs

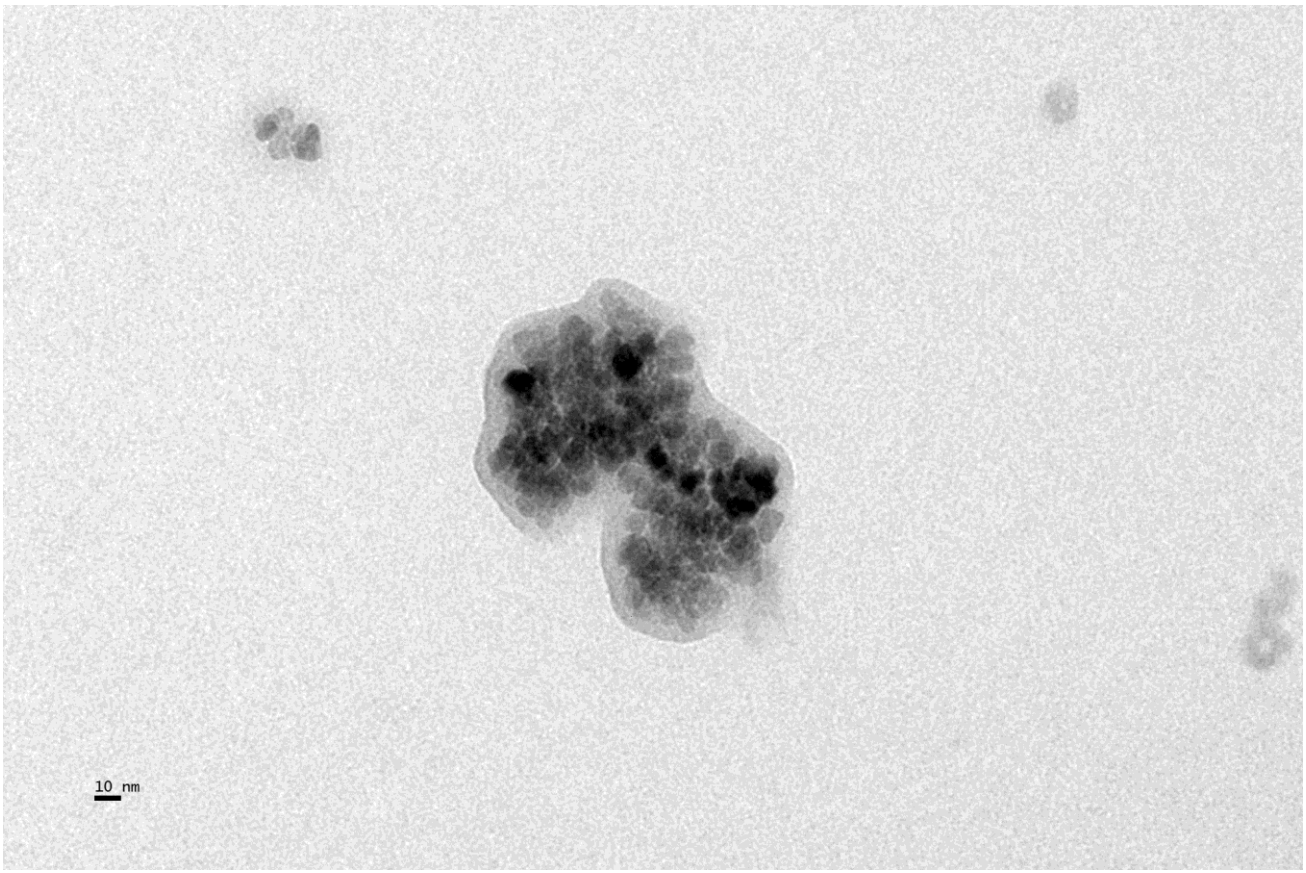

$ZnFe_2O_4$ PEG 0.03M NPs

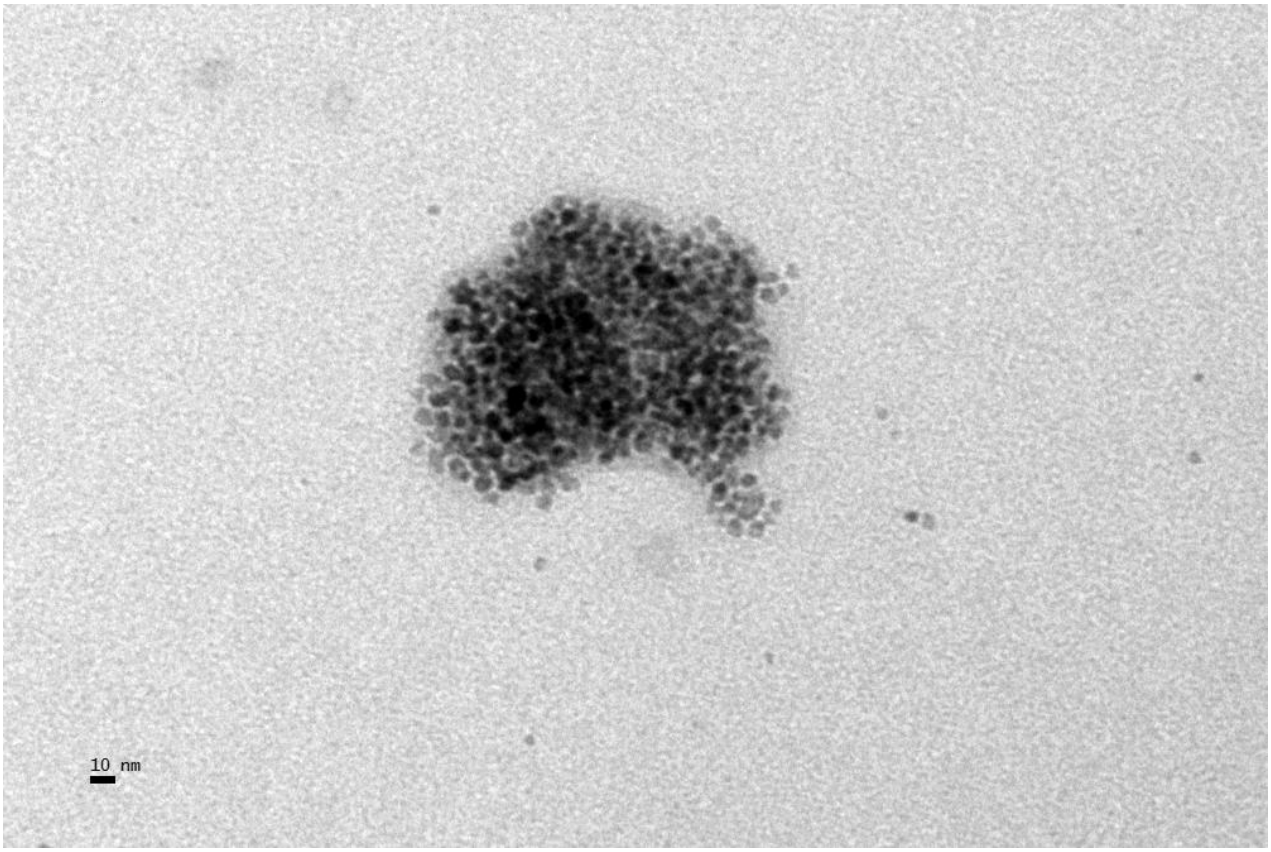

$CoFe_2O_4$ PEG NPS

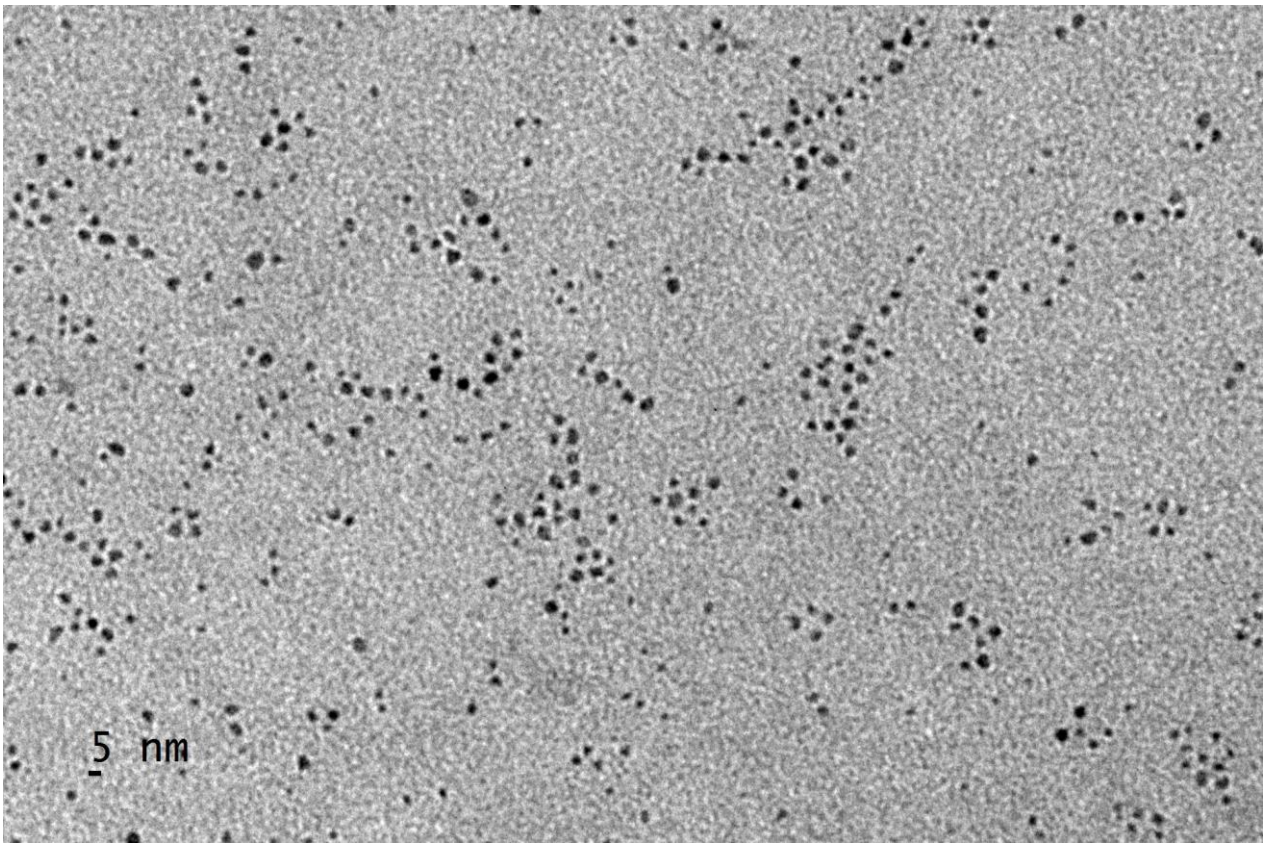

$MnFe_2O_4$ PEG NPs

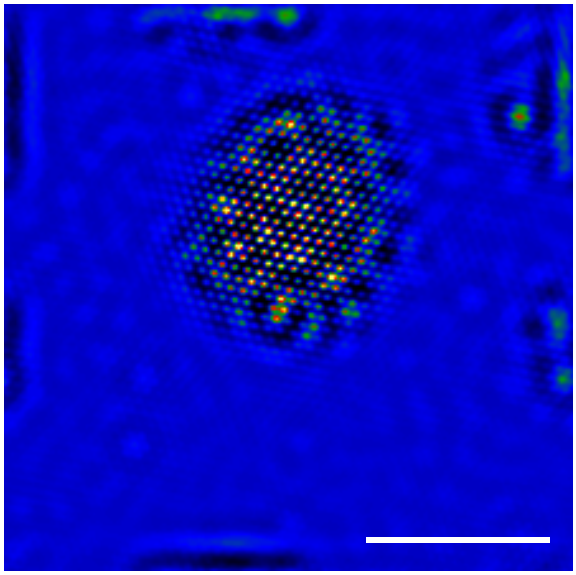

$MnFe_2O_4$ PEG 0.02 Molar NPs 5nm scale bar

PUBLICATIONS

Int J Environ Res Public Health 2020 Mar 20;17(6):2078.

doi: 10.3390/ijerph17062078.

Triple-Negative Breast Cancer: A Review of Conventional and Advanced Therapeutic Strategies

Mauricio A Medina [1], Goldie Oza [2], Ashutosh Sharma [3], L G Arriaga [2], José Manuel Hernández Hernández [4], Vincent M Rotello [5], Jose Tapia Ramirez [6]

Affiliations expand PMID: 32245065

PMCID: PMC7143295
DOI: 10.3390/ijerph17062078
https://pubmed.ncbi.nlm.nih.gov/32245065/

Molecules 2020 Sep 27;25(19):4428.
doi: 10.3390/molecules25194428.

Synthesis, Characterization and Magnetic Hyperthermia of Monodispersed Cobalt Ferrite Nanoparticles for Cancer Therapeutics

Mauricio A Medina [1], Goldie Oza [2], A Ángeles-Pascual [3], Marlene González M [4], R Antaño-López [2], A Vera [5], L Leija [5], Edilso Reguera [4], L G Arriaga [2], José Manuel Hernández Hernández [6], José Tapia Ramírez [7]

Affiliations expand PMID: 32992439

PMCID: PMC7583941
DOI: 10.3390/molecules25194428

https://pubmed.ncbi.nlm.nih.gov/32992439/

REFERENCES

1. Defelipe J. The evolution of the brain, the human nature of cortical circuits, and intellectual creativity. Frontiers in neuroanatomy. 2011;5:29.
2. Masic I, Miokovic M, Muhamedagic B. Evidence based medicine - new approaches and challenges. Acta informatica medica : AIM : journal of the Society for Medical Informatics of Bosnia & Herzegovina : casopis Drustva za medicinsku informatiku BiH. 2008;16(4):219-25.
3. Rogowski W, Payne K, Schnell-Inderst P, Manca A, Rochau U, Jahn B, et al. Concepts of 'personalization' in personalized medicine: implications for economic evaluation. PharmacoEconomics. 2015;33(1):49-59.
4. Pham TD, Ichikawa K. Spatial chaos and complexity in the intracellular space of cancer and normal cells. Theoretical biology & medical modelling. 2013;10:62.
5. Chatterjee DK, Diagaradjane P, Krishnan S. Nanoparticle-mediated hyperthermia in cancer therapy. Therapeutic delivery. 2011;2(8):1001-14.
6. Ruden DM, Bolnick A, Awonuga A, Abdulhasan M, Perez G, Puscheck EE, et al. Effects of Gravity, Microgravity or Microgravity Simulation on Early Mammalian Development. Stem cells and development. 2018;27(18):1230-6.
7. Saini R, Saini S, Sharma S. Nanotechnology: the future medicine. Journal of cutaneous and aesthetic surgery. 2010;3(1):32-3.
8. Ventola CL. The nanomedicine revolution: part 1: emerging concepts. P & T : a peer-reviewed journal for formulary management. 2012;37(9):512-25.
9. Godin B, Sakamoto JH, Serda RE, Grattoni A, Bouamrani A, Ferrari M. Emerging applications of nanomedicine for the diagnosis and treatment of cardiovascular diseases. Trends in pharmacological sciences. 2010;31(5):199-205.
10. Nagaich U. Theranostic nanomedicine: Potential therapeutic epitome. Journal of advanced pharmaceutical technology & research. 2015;6(1):1.
11. Nagaich U. Nanotechnology: The vision of 2025. Journal of advanced pharmaceutical technology & research. 2014;5(3):105-6.
12. Barchiesi D. Lycurgus Cup: inverse problem using photographs for characterization of matter. Journal of the Optical Society of America A, Optics, image science, and vision. 2015;32(8):1544-55.
13. Jeong HH, Mark AG, Alarcon-Correa M, Kim I, Oswald P, Lee TC, et al. Dispersion and shape engineered plasmonic nanosensors. Nature communications. 2016;7:11331.
14. Solaro RJ. Mechanisms of the Frank-Starling law of the heart: the beat goes on. Biophysical journal. 2007;93(12):4095-6.
15. Onoue S, Yamada S, Chan HK. Nanodrugs: pharmacokinetics and safety. International journal of nanomedicine. 2014;9:1025-37.
16. Maysinger D, Moquin A, Choi J, Kodiha M, Stochaj U. Gold nanourchins and celastrol reorganize the nucleo- and cytoskeleton of glioblastoma cells. Nanoscale. 2018;10(4):1716-26.
17. Plascencia-Villa G, Bahena D, Rodriguez AR, Ponce A, Jose-Yacaman M. Advanced microscopy of star-shaped gold nanoparticles and their adsorption-uptake by macrophages. Metallomics : integrated biometal science. 2013;5(3):242-50.
18. Weng J, Ren J. Luminescent quantum dots: a very attractive and promising tool in biomedicine. Current medicinal chemistry. 2006;13(8):897-909.
19. Vigderman L, Manna P, Zubarev ER. Quantitative replacement of cetyl trimethylammonium bromide by cationic thiol ligands on the surface of gold nanorods and their extremely large uptake by cancer cells. Angew Chem Int Ed Engl. 2012;51(3):636-41.
20. Ayala-Orozco C, Urban C, Bishnoi S, Urban A, Charron H, Mitchell T, et al. Sub-100nm gold nanomatryoshkas improve photo-thermal therapy efficacy in large and highly aggressive triple

negative breast tumors. Journal of controlled release : official journal of the Controlled Release Society. 2014;191:90-7.
21. Jung YW, Lee H, Kim JY, Koo EJ, Oh KS, Yuk SH. Pluronic-based core/shell nanoparticles for drug delivery and diagnosis. Current medicinal chemistry. 2013;20(28):3488-99.
22. Kwizera EA, Chaffin E, Wang Y, Huang X. Synthesis and Properties of Magnetic-Optical Core-Shell Nanoparticles. RSC Adv. 2017;7(28):17137-53.
23. Gokcay B, Arda B. Nanotechnology, Nanomedicine; Ethical Aspects. Revista romana de bioetica. 2015;13(3).
24. Yih TC, Moudgil VK. Nanotechnology comes of age to trigger the third industrial revolution. Nanomedicine : nanotechnology, biology, and medicine. 2007;3(4):245.
25. Morigi V, Tocchio A, Bellavite Pellegrini C, Sakamoto JH, Arnone M, Tasciotti E. Nanotechnology in medicine: from inception to market domination. Journal of drug delivery. 2012;2012:389485.
26. Barber J, Tran PD. From natural to artificial photosynthesis. Journal of the Royal Society, Interface. 2013;10(81):20120984.
27. Prasad R, Bhattacharyya A, Nguyen QD. Nanotechnology in Sustainable Agriculture: Recent Developments, Challenges, and Perspectives. Frontiers in microbiology. 2017;8:1014.
28. Katz LM, Dewan K, Bronaugh RL. Nanotechnology in cosmetics. Food and chemical toxicology : an international journal published for the British Industrial Biological Research Association. 2015;85:127-37.
29. Gyles C. Nanotechnology. The Canadian veterinary journal La revue veterinaire canadienne. 2012;53(8):819-22.
30. Ramos AP, Cruz MAE, Tovani CB, Ciancaglini P. Biomedical applications of nanotechnology. Biophysical reviews. 2017;9(2):79-89.
31. Moyano DF, Rotello VM. Nano meets biology: structure and function at the nanoparticle interface. Langmuir : the ACS journal of surfaces and colloids. 2011;27(17):10376-85.
32. Duncan B, Kim C, Rotello VM. Gold nanoparticle platforms as drug and biomacromolecule delivery systems. Journal of controlled release : official journal of the Controlled Release Society. 2010;148(1):122-7.
33. Hu M, Chen J, Li ZY, Au L, Hartland GV, Li X, et al. Gold nanostructures: engineering their plasmonic properties for biomedical applications. Chemical Society reviews. 2006;35(11):1084-94.
34. Derkachova A, Kolwas K, Demchenko I. Dielectric Function for Gold in Plasmonics Applications: Size Dependence of Plasmon Resonance Frequencies and Damping Rates for Nanospheres. Plasmonics. 2016;11:941-51.
35. Jain PK, Huang X, El-Sayed IH, El-Sayed MA. Noble metals on the nanoscale: optical and photothermal properties and some applications in imaging, sensing, biology, and medicine. Accounts of chemical research. 2008;41(12):1578-86.
36. Aslan K, Lakowicz JR, Geddes CD. Plasmon light scattering in biology and medicine: new sensing approaches, visions and perspectives. Current opinion in chemical biology. 2005;9(5):538-44.
37. Hellman F, Hoffmann A, Tserkovnyak Y, Beach GSD, Fullerton EE, Leighton C, et al. Interface-Induced Phenomena in Magnetism. Reviews of modern physics. 2017;89(2).
38. Akbarzadeh A, Samiei M, Davaran S. Magnetic nanoparticles: preparation, physical properties, and applications in biomedicine. Nanoscale research letters. 2012;7(1):144.
39. Ha Y, Ko S, Kim I, Huang Y, Mohanty K, Huh C, et al. Recent Advances Incorporating Superparamagnetic Nanoparticles into Immunoassays. ACS applied nano materials. 2018;1(2):512-21.
40. Jackson R. John Tyndall and the Early History of Diamagnetism. Annals of science. 2015;72(4):435-89.

41. Clore GM, Iwahara J. Theory, practice, and applications of paramagnetic relaxation enhancement for the characterization of transient low-population states of biological macromolecules and their complexes. Chemical reviews. 2009;109(9):4108-39.
42. Nie T, Tang J, Kou X, Gen Y, Lee S, Zhu X, et al. Enhancing electric-field control of ferromagnetism through nanoscale engineering of high-Tc MnxGe1-x nanomesh. Nature communications. 2016;7:12866.
43. Pavlosiuk O, Kaczorowski D, Fabreges X, Gukasov A, Wisniewski P. Antiferromagnetism and superconductivity in the half-Heusler semimetal HoPdBi. Scientific reports. 2016;6:18797.
44. Wahajuddin, Arora S. Superparamagnetic iron oxide nanoparticles: magnetic nanoplatforms as drug carriers. International journal of nanomedicine. 2012;7:3445-71.
45. Stephen ZR, Kievit FM, Zhang M. Magnetite Nanoparticles for Medical MR Imaging. Materials today. 2011;14(7-8):330-8.
46. Grover VP, Tognarelli JM, Crossey MM, Cox IJ, Taylor-Robinson SD, McPhail MJ. Magnetic Resonance Imaging: Principles and Techniques: Lessons for Clinicians. Journal of clinical and experimental hepatology. 2015;5(3):246-55.
47. Hajnal JV, Baudouin CJ, Oatridge A, Young IR, Bydder GM. Design and implementation of magnetization transfer pulse sequences for clinical use. Journal of computer assisted tomography. 1992;16(1):7-18.
48. Lassenberger A, Scheberl A, Stadlbauer A, Stiglbauer A, Helbich T, Reimhult E. Individually Stabilized, Superparamagnetic Nanoparticles with Controlled Shell and Size Leading to Exceptional Stealth Properties and High Relaxivities. ACS applied materials & interfaces. 2017;9(4):3343-53.
49. Estelrich J, Sanchez-Martin MJ, Busquets MA. Nanoparticles in magnetic resonance imaging: from simple to dual contrast agents. International journal of nanomedicine. 2015;10:1727-41.
50. Krishnan KM. Biomedical Nanomagnetics: A Spin Through Possibilities in Imaging, Diagnostics, and Therapy. IEEE transactions on magnetics. 2010;46(7):2523-58.
51. Lam T, Pouliot P, Avti PK, Lesage F, Kakkar AK. Superparamagnetic iron oxide based nanoprobes for imaging and theranostics. Advances in colloid and interface science. 2013;199-200:95-113.
52. Shokrollahi H. Structure, synthetic methods, magnetic properties and biomedical applications of ferrofluids. Materials science & engineering C, Materials for biological applications. 2013;33(5):2476-87.
53. Kellum JA. Determinants of blood pH in health and disease. Crit Care. 2000;4(1):6-14.
54. Moolthiya W, Yuenyao P. The risk of malignancy index (RMI) in diagnosis of ovarian malignancy. Asian Pacific journal of cancer prevention : APJCP. 2009;10(5):865-8.
55. Bridot JL, Faure AC, Laurent S, Riviere C, Billotey C, Hiba B, et al. Hybrid gadolinium oxide nanoparticles: multimodal contrast agents for in vivo imaging. Journal of the American Chemical Society. 2007;129(16):5076-84.
56. Mao X, Xu J, Cui H. Functional nanoparticles for magnetic resonance imaging. Wiley interdisciplinary reviews Nanomedicine and nanobiotechnology. 2016;8(6):814-41.
57. Villafana T. Fundamental physics of magnetic resonance imaging. Radiologic clinics of North America. 1988;26(4):701-15.
58. Sousa F, Sanavio B, Saccani A, Tang Y, Zucca I, Carney TM, et al. Superparamagnetic Nanoparticles as High Efficiency Magnetic Resonance Imaging T2 Contrast Agent. Bioconjugate chemistry. 2017;28(1):161-70.
59. Howell JD. Early Clinical Use of the X-Ray. Transactions of the American Clinical and Climatological Association. 2016;127:341-9.
60. Gibson DJ, Burden ST, Strauss BJ, Todd C, Lal S. The role of computed tomography in evaluating body composition and the influence of reduced muscle mass on clinical outcome in

abdominal malignancy: a systematic review. European journal of clinical nutrition. 2015;69(10):1079-86.
61. Shang DP, Liu CX, Yin Y. A comparison of the different 3D CT scanning modes on the GTV delineation for the solitary pulmonary lesion. Radiation oncology. 2014;9:211.
62. Power SP, Moloney F, Twomey M, James K, O'Connor OJ, Maher MM. Computed tomography and patient risk: Facts, perceptions and uncertainties. World journal of radiology. 2016;8(12):902-15.
63. Chaurand P, Liu W, Borschneck D, Levard C, Auffan M, Paul E, et al. Multi-scale X-ray computed tomography to detect and localize metal-based nanomaterials in lung tissues of in vivo exposed mice. Scientific reports. 2018;8(1):4408.
64. Basu S, Kwee TC, Surti S, Akin EA, Yoo D, Alavi A. Fundamentals of PET and PET/CT imaging. Annals of the New York Academy of Sciences. 2011;1228:1-18.
65. Griffeth LK. Use of PET/CT scanning in cancer patients: technical and practical considerations. Proceedings. 2005;18(4):321-30.
66. Welch MJ, Hawker CJ, Wooley KL. The advantages of nanoparticles for PET. Journal of nuclear medicine : official publication, Society of Nuclear Medicine. 2009;50(11):1743-6.
67. Kaur P, Aliru ML, Chadha AS, Asea A, Krishnan S. Hyperthermia using nanoparticles--Promises and pitfalls. International journal of hyperthermia : the official journal of European Society for Hyperthermic Oncology, North American Hyperthermia Group. 2016;32(1):76-88.
68. Wang C, Hsu CH, Li Z, Hwang LP, Lin YC, Chou PT, et al. Effective heating of magnetic nanoparticle aggregates for in vivo nano-theranostic hyperthermia. International journal of nanomedicine. 2017;12:6273-87.
69. Fischer ER, Hansen BT, Nair V, Hoyt FH, Dorward DW. Scanning electron microscopy. Current protocols in microbiology. 2012;Chapter 2:Unit 2B
70. Jones CG. Scanning electron microscopy: preparation and imaging for SEM. Methods Mol Biol. 2012;915:1-20.
71. Hagen CA, Hawrylewicz EJ, Anderson BT, Tolkacz VK, Cephus ML. Use of the scanning electron microscope for viewing bacteria in soil. Applied microbiology. 1968;16(6):932-4.
72. Hwu JJ, Joy DC. A study of electron beam-induced conductivity in resists. Scanning. 1999;21(4):264-72.
73. Winey M, Meehl JB, O'Toole ET, Giddings TH, Jr. Conventional transmission electron microscopy. Molecular biology of the cell. 2014;25(3):319-23.
74. Yu C, Wang H. Large lateral photovoltaic effect in metal-(oxide-) semiconductor structures. Sensors. 2010;10(11):10155-80.
75. Fahy A, Barr M, Martens J, Dastoor PC. A highly contrasting scanning helium microscope. The Review of scientific instruments. 2015;86(2):023704.
76. Kempen PJ, Thakor AS, Zavaleta C, Gambhir SS, Sinclair R. A scanning transmission electron microscopy approach to analyzing large volumes of tissue to detect nanoparticles. Microscopy and microanalysis : the official journal of Microscopy Society of America, Microbeam Analysis Society, Microscopical Society of Canada. 2013;19(5):1290-7.
77. Tang SY, Zhang W, Soffe R, Nahavandi S, Shukla R, Khoshmanesh K. High resolution scanning electron microscopy of cells using dielectrophoresis. PloS one. 2014;9(8):e104109.
78. Scimeca M, Bischetti S, Lamsira HK, Bonfiglio R, Bonanno E. Energy Dispersive X-ray (EDX) microanalysis: A powerful tool in biomedical research and diagnosis. European journal of histochemistry : EJH. 2018;62(1):2841.
79. Mantele W, Deniz E. UV-VIS absorption spectroscopy: Lambert-Beer reloaded. Spectrochimica acta Part A, Molecular and biomolecular spectroscopy. 2017;173:965-8.
80. Brown JQ, Vishwanath K, Palmer GM, Ramanujam N. Advances in quantitative UV-visible spectroscopy for clinical and pre-clinical application in cancer. Current opinion in biotechnology. 2009;20(1):119-31.

81. Bunaciu AA, Udristioiu EG, Aboul-Enein HY. X-ray diffraction: instrumentation and applications. Critical reviews in analytical chemistry. 2015;45(4):289-99.
82. Jauncey GE. The Scattering of X-Rays and Bragg's Law. Proceedings of the National Academy of Sciences of the United States of America. 1924;10(2):57-60.
83. Hansford GM. Phase-targeted X-ray diffraction. Journal of applied crystallography. 2016;49(Pt 5):1561-71.
84. Ramos IR, Malkin A, Lyng FM. Current Advances in the Application of Raman Spectroscopy for Molecular Diagnosis of Cervical Cancer. BioMed research international. 2015;2015:561242.
85. Keating ME, Byrne HJ. Raman spectroscopy in nanomedicine: current status and future perspective. Nanomedicine (Lond). 2013;8(8):1335-51.
86. Wang Y, Irudayaraj J. Surface-enhanced Raman spectroscopy at single-molecule scale and its implications in biology. Philosophical transactions of the Royal Society of London Series B, Biological sciences. 2013;368(1611):20120026.
87. Zhang C, Zhang D, Cheng JX. Coherent Raman Scattering Microscopy in Biology and Medicine. Annual review of biomedical engineering. 2015;17:415-45.
88. Zarnowiec P, Lechowicz L, Czerwonka G, Kaca W. Fourier Transform Infrared Spectroscopy (FTIR) as a Tool for the Identification and Differentiation of Pathogenic Bacteria. Current medicinal chemistry. 2015;22(14):1710-8.
89. Amenabar I, Poly S, Nuansing W, Hubrich EH, Govyadinov AA, Huth F, et al. Structural analysis and mapping of individual protein complexes by infrared nanospectroscopy. Nature communications. 2013;4:2890.
90. Sutens B, Swusten T, Zhong K, Jochum JK, Van Bael MJ, Van der Eycken EV, et al. Tunability of Size and Magnetic Moment of Iron Oxide Nanoparticles Synthesized by Forced Hydrolysis. Materials. 2016;9(7).
91. Ryu C, Blackburn PW, Blinova AA, Boshier MG. Experimental realization of Josephson junctions for an atom SQUID. Physical review letters. 2013;111(20):205301.
92. Flynn ER, Bryant HC. A biomagnetic system for in vivo cancer imaging. Physics in medicine and biology. 2005;50(6):1273-93.
93. Wang Y, Guo C, Zhang GQ, Wang G, Wu C. Ultrafast quantum computation in ultrastrongly coupled circuit QED systems. Scientific reports. 2017;7:44251.
94. Tsai SR, Hamblin MR. Biological effects and medical applications of infrared radiation. Journal of photochemistry and photobiology B, Biology. 2017;170:197-207.
95. Iravani S, Korbekandi H, Mirmohammadi SV, Zolfaghari B. Synthesis of silver nanoparticles: chemical, physical and biological methods. Research in pharmaceutical sciences. 2014;9(6):385-406.
96. Dastjerdi R, Scherrieble A, Bahrizadeh S, Avareh Sadrabadi F, Hedayat L. A Key Major Guideline for Engineering Bioactive Multicomponent Nanofunctionalization for Biomedicine and Other Applications: Fundamental Models Confirmed by Both Direct and Indirect Evidence. BioMed research international. 2017;2017:2867653.
97. Albanese A, Tang PS, Chan WC. The effect of nanoparticle size, shape, and surface chemistry on biological systems. Annual review of biomedical engineering. 2012;14:1-16.
98. Richards DA, Maruani A, Chudasama V. Antibody fragments as nanoparticle targeting ligands: a step in the right direction. Chemical science. 2017;8(1):63-77.
99. Bhattacharjee S. DLS and zeta potential - What they are and what they are not? Journal of controlled release : official journal of the Controlled Release Society. 2016;235:337-51.
100. Moon KS, Park YB, Bae JM, Oh S. Near-infrared laser-mediated drug release and antibacterial activity of gold nanorod-sputtered titania nanotubes. Journal of tissue engineering. 2018;9:2041731418790315.

101. Sudhakar A. History of Cancer, Ancient and Modern Treatment Methods. Journal of cancer science & therapy. 2009;1(2):1-4.
102. Lampe JW. Dairy products and cancer. Journal of the American College of Nutrition. 2011;30(5 Suppl 1):464S-70S.
103. Bertram JS. The molecular biology of cancer. Molecular aspects of medicine. 2000;21(6):167-223.
104. White MC, Peipins LA, Watson M, Trivers KF, Holman DM, Rodriguez JL. Cancer prevention for the next generation. The Journal of adolescent health : official publication of the Society for Adolescent Medicine. 2013;52(5 Suppl):S1-7.
105. Hecker E. Definitions and terminology in cancer (tumour) etiology. An analysis aiming at proposals for a current internationally standardized terminology. Bulletin of the World Health Organization. 1976;54(1):1-10.
106. Naito Y, Yoshioka Y, Yamamoto Y, Ochiya T. How cancer cells dictate their microenvironment: present roles of extracellular vesicles. Cellular and molecular life sciences : CMLS. 2017;74(4):697-713.
107. Thun MJ, DeLancey JO, Center MM, Jemal A, Ward EM. The global burden of cancer: priorities for prevention. Carcinogenesis. 2010;31(1):100-10.
108. Pandya HJ, Park K, Desai JP. Design and fabrication of a flexible MEMS-based electromechanical sensor array for breast cancer diagnosis. Journal of micromechanics and microengineering : structures, devices, and systems. 2015;25(7).
109. Duesberg P, Mandrioli D, McCormack A, Nicholson JM. Is carcinogenesis a form of speciation? Cell cycle. 2011;10(13):2100-14.
110. Rakoff-Nahoum S. Why cancer and inflammation? The Yale journal of biology and medicine. 2006;79(3-4):123-30.
111. Baena Ruiz R, Salinas Hernandez P. Diet and cancer: risk factors and epidemiological evidence. Maturitas. 2014;77(3):202-8.
112. Lee EY, Muller WJ. Oncogenes and tumor suppressor genes. Cold Spring Harbor perspectives in biology. 2010;2(10):a003236.
113. Huff J. Chemicals and cancer in humans: first evidence in experimental animals. Environmental health perspectives. 1993;100:201-10.
114. Gilbert ES. Ionising radiation and cancer risks: what have we learned from epidemiology? International journal of radiation biology. 2009;85(6):467-82.
115. Ghoncheh M, Pournamdar Z, Salehiniya H. Incidence and Mortality and Epidemiology of Breast Cancer in the World. Asian Pacific journal of cancer prevention : APJCP. 2016;17(S3):43-6.
116. Al-Hajj M, Wicha MS, Benito-Hernandez A, Morrison SJ, Clarke MF. Prospective identification of tumorigenic breast cancer cells. Proceedings of the National Academy of Sciences of the United States of America. 2003;100(7):3983-8.
117. Aebi S, Davidson T, Gruber G, Cardoso F, Group EGW. Primary breast cancer: ESMO Clinical Practice Guidelines for diagnosis, treatment and follow-up. Annals of oncology : official journal of the European Society for Medical Oncology / ESMO. 2011;22 Suppl 6:vi12-24.
118. Cserni G, Chmielik E, Cserni B, Tot T. The new TNM-based staging of breast cancer. Virchows Archiv : an international journal of pathology. 2018;472(5):697-703.
119. Beumer IJ, Persoon M, Witteveen A, Dreezen C, Chin SF, Sammut SJ, et al. Prognostic Value of MammaPrint((R)) in Invasive Lobular Breast Cancer. Biomarker insights. 2016;11:139-46.
120. McVeigh TP, Kerin MJ. Clinical use of the Oncotype DX genomic test to guide treatment decisions for patients with invasive breast cancer. Breast cancer. 2017;9:393-400.
121. Gucalp A, Traina TA. Triple-negative breast cancer: adjuvant therapeutic options. Chemotherapy research and practice. 2011;2011:696208.

122. Nielsen TO, Hsu FD, Jensen K, Cheang M, Karaca G, Hu Z, et al. Immunohistochemical and clinical characterization of the basal-like subtype of invasive breast carcinoma. Clinical cancer research : an official journal of the American Association for Cancer Research. 2004;10(16):5367-74.
123. Sotiriou C, Neo SY, McShane LM, Korn EL, Long PM, Jazaeri A, et al. Breast cancer classification and prognosis based on gene expression profiles from a population-based study. Proceedings of the National Academy of Sciences of the United States of America. 2003;100(18):10393-8.
124. Dai X, Li T, Bai Z, Yang Y, Liu X, Zhan J, et al. Breast cancer intrinsic subtype classification, clinical use and future trends. American journal of cancer research. 2015;5(10):2929-43.
125. Speiser JJ, Ersahin C, Osipo C. The functional role of Notch signaling in triple-negative breast cancer. Vitamins and hormones. 2013;93:277-306.
126. Yao H, He G, Yan S, Chen C, Song L, Rosol TJ, et al. Triple-negative breast cancer: is there a treatment on the horizon? Oncotarget. 2017;8(1):1913-24.
127. Speirs V, Parkes AT, Kerin MJ, Walton DS, Carleton PJ, Fox JN, et al. Coexpression of estrogen receptor alpha and beta: poor prognostic factors in human breast cancer? Cancer research. 1999;59(3):525-8.
128. Jezequel P, Loussouarn D, Guerin-Charbonnel C, Campion L, Vanier A, Gouraud W, et al. Gene-expression molecular subtyping of triple-negative breast cancer tumours: importance of immune response. Breast cancer research : BCR. 2015;17:43.
129. Ahn SG, Kim SJ, Kim C, Jeong J. Molecular Classification of Triple-Negative Breast Cancer. Journal of breast cancer. 2016;19(3):223-30.
130. Lehmann BD, Bauer JA, Chen X, Sanders ME, Chakravarthy AB, Shyr Y, et al. Identification of human triple-negative breast cancer subtypes and preclinical models for selection of targeted therapies. The Journal of clinical investigation. 2011;121(7):2750-67.
131. Masuda H, Baggerly KA, Wang Y, Zhang Y, Gonzalez-Angulo AM, Meric-Bernstam F, et al. Differential response to neoadjuvant chemotherapy among 7 triple-negative breast cancer molecular subtypes. Clinical cancer research : an official journal of the American Association for Cancer Research. 2013;19(19):5533-40.
132. Gu Y, Masiero M, Banham AH. Notch signaling: its roles and therapeutic potential in hematological malignancies. Oncotarget. 2016;7(20):29804-23.
133. Palomero T, Barnes KC, Real PJ, Glade Bender JL, Sulis ML, Murty VV, et al. CUTLL1, a novel human T-cell lymphoma cell line with t(7;9) rearrangement, aberrant NOTCH1 activation and high sensitivity to gamma-secretase inhibitors. Leukemia. 2006;20(7):1279-87.
134. Brennan K, Clarke RB. Combining Notch inhibition with current therapies for breast cancer treatment. Therapeutic advances in medical oncology. 2013;5(1):17-24.
135. Soares R, Balogh G, Guo S, Gartner F, Russo J, Schmitt F. Evidence for the notch signaling pathway on the role of estrogen in angiogenesis. Mol Endocrinol. 2004;18(9):2333-43.
136. Weijzen S, Rizzo P, Braid M, Vaishnav R, Jonkheer SM, Zlobin A, et al. Activation of Notch-1 signaling maintains the neoplastic phenotype in human Ras-transformed cells. Nature medicine. 2002;8(9):979-86.
137. Weng AP, Ferrando AA, Lee W, Morris JPt, Silverman LB, Sanchez-Irizarry C, et al. Activating mutations of NOTCH1 in human T cell acute lymphoblastic leukemia. Science. 2004;306(5694):269-71.
138. Gao J, Long B, Wang Z. Role of Notch signaling pathway in pancreatic cancer. American journal of cancer research. 2017;7(2):173-86.
139. O'Neill CF, Urs S, Cinelli C, Lincoln A, Nadeau RJ, Leon R, et al. Notch2 signaling induces apoptosis and inhibits human MDA-MB-231 xenograft growth. The American journal of pathology. 2007;171(3):1023-36.

140. Espinoza I, Miele L. Notch inhibitors for cancer treatment. Pharmacology & therapeutics. 2013;139(2):95-110.
141. Sharma A, Paranjape AN, Rangarajan A, Dighe RR. A monoclonal antibody against human Notch1 ligand-binding domain depletes subpopulation of putative breast cancer stem-like cells. Molecular cancer therapeutics. 2012;11(1):77-86.
142. Benedito R, Roca C, Sorensen I, Adams S, Gossler A, Fruttiger M, et al. The notch ligands Dll4 and Jagged1 have opposing effects on angiogenesis. Cell. 2009;137(6):1124-35.
143. Espinoza I, Pochampally R, Xing F, Watabe K, Miele L. Notch signaling: targeting cancer stem cells and epithelial-to-mesenchymal transition. OncoTargets and therapy. 2013;6:1249-59.
144. Chan SM, Weng AP, Tibshirani R, Aster JC, Utz PJ. Notch signals positively regulate activity of the mTOR pathway in T-cell acute lymphoblastic leukemia. Blood. 2007;110(1):278-86.
145. Yuan X, Wu H, Xu H, Xiong H, Chu Q, Yu S, et al. Notch signaling: an emerging therapeutic target for cancer treatment. Cancer letters. 2015;369(1):20-7.
146. Heussler HS, Suri M. Sonic hedgehog. Molecular pathology : MP. 2003;56(3):129-31.
147. Kubo M, Nakamura M, Tasaki A, Yamanaka N, Nakashima H, Nomura M, et al. Hedgehog signaling pathway is a new therapeutic target for patients with breast cancer. Cancer research. 2004;64(17):6071-4.
148. Nagase T, Nagase M, Machida M, Fujita T. Hedgehog signalling in vascular development. Angiogenesis. 2008;11(1):71-7.
149. St-Jacques B, Hammerschmidt M, McMahon AP. Indian hedgehog signaling regulates proliferation and differentiation of chondrocytes and is essential for bone formation. Genes & development. 1999;13(16):2072-86.
150. Canto P, Soderlund D, Reyes E, Mendez JP. Mutations in the desert hedgehog (DHH) gene in patients with 46,XY complete pure gonadal dysgenesis. The Journal of clinical endocrinology and metabolism. 2004;89(9):4480-3.
151. Aberger F, Kern D, Greil R, Hartmann TN. Canonical and noncanonical Hedgehog/GLI signaling in hematological malignancies. Vitamins and hormones. 2012;88:25-54.
152. Li Y, Maitah MY, Ahmad A, Kong D, Bao B, Sarkar FH. Targeting the Hedgehog signaling pathway for cancer therapy. Expert opinion on therapeutic targets. 2012;16(1):49-66.
153. Yang N, Zhou TC, Lei XX, Wang C, Yan M, Wang ZF, et al. Inhibition of Sonic Hedgehog Signaling Pathway by Thiazole Antibiotic Thiostrepton Attenuates the CD44+/CD24-Stem-Like Population and Sphere-Forming Capacity in Triple-Negative Breast Cancer. Cellular physiology and biochemistry : international journal of experimental cellular physiology, biochemistry, and pharmacology. 2016;38(3):1157-70.
154. Hui M, Cazet A, Nair R, Watkins DN, O'Toole SA, Swarbrick A. The Hedgehog signalling pathway in breast development, carcinogenesis and cancer therapy. Breast cancer research : BCR. 2013;15(2):203.
155. Habib JG, O'Shaughnessy JA. The hedgehog pathway in triple-negative breast cancer. Cancer medicine. 2016;5(10):2989-3006.
156. Tao Y, Mao J, Zhang Q, Li L. Overexpression of Hedgehog signaling molecules and its involvement in triple-negative breast cancer. Oncology letters. 2011;2(5):995-1001.
157. Chang AL, Arron ST, Migden MR, Solomon JA, Yoo S, Day BM, et al. Safety and efficacy of vismodegib in patients with basal cell carcinoma nevus syndrome: pooled analysis of two trials. Orphanet journal of rare diseases. 2016;11(1):120.
158. Francesca Ghirga MM, Paola Infante. Current trends in Hedgehog signaling pathway inhibition by small molecules. Bioorganic & Medicinal Chemistry Letters. 2018;Volume 28,(Issue 19):3131-40.
159. Pohl SG, Brook N, Agostino M, Arfuso F, Kumar AP, Dharmarajan A. Wnt signaling in triple-negative breast cancer. Oncogenesis. 2017;6(4):e310.

160. Gurney A, Axelrod F, Bond CJ, Cain J, Chartier C, Donigan L, et al. Wnt pathway inhibition via the targeting of Frizzled receptors results in decreased growth and tumorigenicity of human tumors. Proceedings of the National Academy of Sciences of the United States of America. 2012;109(29):11717-22.
161. Zhu Y, Tian Y, Du J, Hu Z, Yang L, Liu J, et al. Dvl2-dependent activation of Daam1 and RhoA regulates Wnt5a-induced breast cancer cell migration. PloS one. 2012;7(5):e37823.
162. Corda G, Sala G, Lattanzio R, Iezzi M, Sallese M, Fragassi G, et al. Functional and prognostic significance of the genomic amplification of frizzled 6 (FZD6) in breast cancer. The Journal of pathology. 2017;241(3):350-61.
163. Krishnamurthy N, Kurzrock R. Targeting the Wnt/beta-catenin pathway in cancer: Update on effectors and inhibitors. Cancer treatment reviews. 2018;62:50-60.
164. Dean M, Fojo T, Bates S. Tumour stem cells and drug resistance. Nature reviews Cancer. 2005;5(4):275-84.
165. Geyer FC, Lacroix-Triki M, Savage K, Arnedos M, Lambros MB, MacKay A, et al. beta-Catenin pathway activation in breast cancer is associated with triple-negative phenotype but not with CTNNB1 mutation. Modern pathology : an official journal of the United States and Canadian Academy of Pathology, Inc. 2011;24(2):209-31.
166. Dey N, Barwick BG, Moreno CS, Ordanic-Kodani M, Chen Z, Oprea-Ilies G, et al. Wnt signaling in triple negative breast cancer is associated with metastasis. BMC cancer. 2013;13:537.
167. Howard B, Ashworth A. Signalling pathways implicated in early mammary gland morphogenesis and breast cancer. PLoS genetics. 2006;2(8):e112.
168. El Ayachi I, Fatima I, Wend P, Alva-Ornelas JA, Runke S, Kuenzinger WL, et al. The WNT10B Network Is Associated with Survival and Metastases in Chemoresistant Triple-Negative Breast Cancer. Cancer research. 2019;79(5):982-93.
169. Park SR, Chen A. Poly(Adenosine diphosphate-ribose) polymerase inhibitors in cancer treatment. Hematology/oncology clinics of North America. 2012;26(3):649-70, ix.
170. De Vos M, Schreiber V, Dantzer F. The diverse roles and clinical relevance of PARPs in DNA damage repair: current state of the art. Biochemical pharmacology. 2012;84(2):137-46.
171. Pleschke JM, Kleczkowska HE, Strohm M, Althaus FR. Poly(ADP-ribose) binds to specific domains in DNA damage checkpoint proteins. The Journal of biological chemistry. 2000;275(52):40974-80.
172. Helleday T. The underlying mechanism for the PARP and BRCA synthetic lethality: clearing up the misunderstandings. Molecular oncology. 2011;5(4):387-93.
173. Murai J, Huang SY, Das BB, Renaud A, Zhang Y, Doroshow JH, et al. Trapping of PARP1 and PARP2 by Clinical PARP Inhibitors. Cancer research. 2012;72(21):5588-99.
174. Gagne JP, Rouleau M, Poirier GG. Structural biology. PARP-1 activation--bringing the pieces together. Science. 2012;336(6082):678-9.
175. Fong PC, Boss DS, Yap TA, Tutt A, Wu P, Mergui-Roelvink M, et al. Inhibition of poly(ADP-ribose) polymerase in tumors from BRCA mutation carriers. The New England journal of medicine. 2009;361(2):123-34.
176. Strom CE, Johansson F, Uhlen M, Szigyarto CA, Erixon K, Helleday T. Poly (ADP-ribose) polymerase (PARP) is not involved in base excision repair but PARP inhibition traps a single-strand intermediate. Nucleic acids research. 2011;39(8):3166-75.
177. Amir Sonnenblick EdA, Hatem A. Azim Jr & Martine Piccart An update on PARP inhibitors—moving to the adjuvant setting. Nature Reviews Clinical Oncology (2015);volume12:pages27–41.
178. Fruman DA, Rommel C. PI3K and cancer: lessons, challenges and opportunities. Nature reviews Drug discovery. 2014;13(2):140-56.
179. Zaytseva YY, Valentino JD, Gulhati P, Evers BM. mTOR inhibitors in cancer therapy. Cancer letters. 2012;319(1):1-7.

180. Sobande F, Dusek L, Matejkova A, Rozkos T, Laco J, Ryska A. EGFR in triple negative breast carcinoma: significance of protein expression and high gene copy number. Ceskoslovenska patologie. 2015;51(2):80-6.
181. Eccles SA. The epidermal growth factor receptor/Erb-B/HER family in normal and malignant breast biology. The International journal of developmental biology. 2011;55(7-9):685-96.
182. Ueno NT, Zhang D. Targeting EGFR in Triple Negative Breast Cancer. Journal of Cancer. 2011;2:324-8.
183. Layman RM, Ruppert AS, Lynn M, Mrozek E, Ramaswamy B, Lustberg MB, et al. Severe and prolonged lymphopenia observed in patients treated with bendamustine and erlotinib for metastatic triple negative breast cancer. Cancer chemotherapy and pharmacology. 2013;71(5):1183-90.
184. Finn RS, Press MF, Dering J, Arbushites M, Koehler M, Oliva C, et al. Estrogen receptor, progesterone receptor, human epidermal growth factor receptor 2 (HER2), and epidermal growth factor receptor expression and benefit from lapatinib in a randomized trial of paclitaxel with lapatinib or placebo as first-line treatment in HER2-negative or unknown metastatic breast cancer. Journal of clinical oncology : official journal of the American Society of Clinical Oncology. 2009;27(24):3908-15.
185. Gunzer K, Joly F, Ferrero JM, Gligorov J, de Mont-Serrat H, Uttenreuther-Fischer M, et al. A phase II study of afatinib, an irreversible ErbB family blocker, added to letrozole in patients with estrogen receptor-positive hormone-refractory metastatic breast cancer progressing on letrozole. SpringerPlus. 2016;5:45.
186. Nabholtz JM, Abrial C, Mouret-Reynier MA, Dauplat MM, Weber B, Gligorov J, et al. Multicentric neoadjuvant phase II study of panitumumab combined with an anthracycline/taxane-based chemotherapy in operable triple-negative breast cancer: identification of biologically defined signatures predicting treatment impact. Annals of oncology : official journal of the European Society for Medical Oncology / ESMO. 2014;25(8):1570-7.
187. Kallab AM, Nalamolu Y, Dainer PM, Jillella AP. A phase II study of weekly paclitaxel and carboplatin in previously untreated patients with advanced non-small-cell lung cancer. Medical oncology. 2005;22(2):145-51.
188. Baselga J, Gomez P, Greil R, Braga S, Climent MA, Wardley AM, et al. Randomized phase II study of the anti-epidermal growth factor receptor monoclonal antibody cetuximab with cisplatin versus cisplatin alone in patients with metastatic triple-negative breast cancer. Journal of clinical oncology : official journal of the American Society of Clinical Oncology. 2013;31(20):2586-92.
189. Carey LA, Rugo HS, Marcom PK, Mayer EL, Esteva FJ, Ma CX, et al. TBCRC 001: randomized phase II study of cetuximab in combination with carboplatin in stage IV triple-negative breast cancer. Journal of clinical oncology : official journal of the American Society of Clinical Oncology. 2012;30(21):2615-23.
190. Velasco G, Sanchez C, Guzman M. Anticancer mechanisms of cannabinoids. Current oncology. 2016;23(2):S23-32.
191. Chakravarti B, Ravi J, Ganju RK. Cannabinoids as therapeutic agents in cancer: current status and future implications. Oncotarget. 2014;5(15):5852-72.
192. Ali R, Wendt MK. The paradoxical functions of EGFR during breast cancer progression. Signal transduction and targeted therapy. 2017;2.
193. Ghadami M, Makita Y, Yoshida K, Nishimura G, Fukushima Y, Wakui K, et al. Genetic mapping of the Camurati-Engelmann disease locus to chromosome 19q13.1-q13.3. American journal of human genetics. 2000;66(1):143-7.
194. Assoian RK, Komoriya A, Meyers CA, Miller DM, Sporn MB. Transforming growth factor-beta in human platelets. Identification of a major storage site, purification, and characterization. The Journal of biological chemistry. 1983;258(11):7155-60.

195. Jamdade VS, Sethi N, Mundhe NA, Kumar P, Lahkar M, Sinha N. Therapeutic targets of triple-negative breast cancer: a review. British journal of pharmacology. 2015;172(17):4228-37.
196. Bhola NE, Balko JM, Dugger TC, Kuba MG, Sanchez V, Sanders M, et al. TGF-beta inhibition enhances chemotherapy action against triple-negative breast cancer. The Journal of clinical investigation. 2013;123(3):1348-58.
197. Wang X, Osada T, Wang Y, Yu L, Sakakura K, Katayama A, et al. CSPG4 protein as a new target for the antibody-based immunotherapy of triple-negative breast cancer. Journal of the National Cancer Institute. 2010;102(19):1496-512.
198. Cooney CA, Jousheghany F, Yao-Borengasser A, Phanavanh B, Gomes T, Kieber-Emmons AM, et al. Chondroitin sulfates play a major role in breast cancer metastasis: a role for CSPG4 and CHST11 gene expression in forming surface P-selectin ligands in aggressive breast cancer cells. Breast cancer research : BCR. 2011;13(3):R58.
199. Kwiatkowska-Borowczyk EP, Gabka-Buszek A, Jankowski J, Mackiewicz A. Immunotargeting of cancer stem cells. Contemporary oncology. 2015;19(1A):A52-9.
200. Atkinson RL, Yang WT, Rosen DG, Landis MD, Wong H, Lewis MT, et al. Cancer stem cell markers are enriched in normal tissue adjacent to triple negative breast cancer and inversely correlated with DNA repair deficiency. Breast cancer research : BCR. 2013;15(5):R77.
201. Hu Y, Fu L. Targeting cancer stem cells: a new therapy to cure cancer patients. American journal of cancer research. 2012;2(3):340-56.
202. Bousquet G, El Bouchtaoui M, Sophie T, Leboeuf C, de Bazelaire C, Ratajczak P, et al. Targeting autophagic cancer stem-cells to reverse chemoresistance in human triple negative breast cancer. Oncotarget. 2017;8(21):35205-21.
203. Yeri A, Gao D. Biosensing using nanoelectromechanical systems. Methods Mol Biol. 2011;726:119-39.
204. Ko J, Carpenter E, Issadore D. Detection and isolation of circulating exosomes and microvesicles for cancer monitoring and diagnostics using micro-/nano-based devices. The Analyst. 2016;141(2):450-60.
205. O'Meara T, Safonov A, Casadevall D, Qing T, Silber A, Killelea B, et al. Immune microenvironment of triple-negative breast cancer in African-American and Caucasian women. Breast cancer research and treatment. 2019.
206. Ventola CL. Progress in Nanomedicine: Approved and Investigational Nanodrugs. P & T : a peer-reviewed journal for formulary management. 2017;42(12):742-55.
207. James JS. DOXIL approved for KS. AIDS treatment news. 1995(no 236):6.
208. Weissig V, Pettinger TK, Murdock N. Nanopharmaceuticals (part 1): products on the market. International journal of nanomedicine. 2014;9:4357-73.
209. Cinkaya A, Akin M, Sengul A. Evaluation of treatment outcomes of triple-negative breast cancer. Journal of cancer research and therapeutics. 2016;12(1):150-4.
210. Rouzier R, Perou CM, Symmans WF, Ibrahim N, Cristofanilli M, Anderson K, et al. Breast cancer molecular subtypes respond differently to preoperative chemotherapy. Clinical cancer research : an official journal of the American Association for Cancer Research. 2005;11(16):5678-85.
211. Kassam F, Enright K, Dent R, Dranitsaris G, Myers J, Flynn C, et al. Survival outcomes for patients with metastatic triple-negative breast cancer: implications for clinical practice and trial design. Clinical breast cancer. 2009;9(1):29-33.
212. Geisler S, Lonning PE, Aas T, Johnsen H, Fluge O, Haugen DF, et al. Influence of TP53 gene alterations and c-erbB-2 expression on the response to treatment with doxorubicin in locally advanced breast cancer. Cancer research. 2001;61(6):2505-12.
213. Carey LA, Dees EC, Sawyer L, Gatti L, Moore DT, Collichio F, et al. The triple negative paradox: primary tumor chemosensitivity of breast cancer subtypes. Clinical cancer research : an official journal of the American Association for Cancer Research. 2007;13(8):2329-34.

214. Byrski T, Huzarski T, Dent R, Marczyk E, Jasiowka M, Gronwald J, et al. Pathologic complete response to neoadjuvant cisplatin in BRCA1-positive breast cancer patients. Breast cancer research and treatment. 2014;147(2):401-5.
215. Vetter M, Fokas S, Biskup E, Schmid T, Schwab F, Schoetzau A, et al. Efficacy of adjuvant chemotherapy with carboplatin for early triple negative breast cancer: a single center experience. Oncotarget. 2017;8(43):75617-26.
216. Sikov WM, Berry DA, Perou CM, Singh B, Cirrincione CT, Tolaney SM, et al. Impact of the addition of carboplatin and/or bevacizumab to neoadjuvant once-per-week paclitaxel followed by dose-dense doxorubicin and cyclophosphamide on pathologic complete response rates in stage II to III triple-negative breast cancer: CALGB 40603 (Alliance). Journal of clinical oncology : official journal of the American Society of Clinical Oncology. 2015;33(1):13-21.
217. Dogan BE, Turnbull LW. Imaging of triple-negative breast cancer. Annals of oncology : official journal of the European Society for Medical Oncology / ESMO. 2012;23 Suppl 6:vi23-9.
218. Verma S, Provencher L, Dent R. Emerging trends in the treatment of triple-negative breast cancer in Canada: a survey. Current oncology. 2011;18(4):180-90.
219. Wahba HA, El-Hadaad HA. Current approaches in treatment of triple-negative breast cancer. Cancer biology & medicine. 2015;12(2):106-16.
220. Rastogi P, Anderson SJ, Bear HD, Geyer CE, Kahlenberg MS, Robidoux A, et al. Preoperative chemotherapy: updates of National Surgical Adjuvant Breast and Bowel Project Protocols B-18 and B-27. Journal of clinical oncology : official journal of the American Society of Clinical Oncology. 2008;26(5):778-85.
221. Ezzat AA, Ibrahim EM, Ajarim DS, Rahal MM, Raja MA, Tulbah AM, et al. Phase II study of neoadjuvant paclitaxel and cisplatin for operable and locally advanced breast cancer: analysis of 126 patients. British journal of cancer. 2004;90(5):968-74.
222. Frasci G, Comella P, Rinaldo M, Iodice G, Di Bonito M, D'Aiuto M, et al. Preoperative weekly cisplatin-epirubicin-paclitaxel with G-CSF support in triple-negative large operable breast cancer. Annals of oncology : official journal of the European Society for Medical Oncology / ESMO. 2009;20(7):1185-92.
223. Goel AK, Nandy M, Sharma G. Cisplatin as neoadjuvant chemotherapy in triple negative breast cancer: Exciting early results. Indian journal of medical and paediatric oncology : official journal of Indian Society of Medical & Paediatric Oncology. 2010;31(3):76-8.
224. Gerber B, Loibl S, Eidtmann H, Rezai M, Fasching PA, Tesch H, et al. Neoadjuvant bevacizumab and anthracycline-taxane-based chemotherapy in 678 triple-negative primary breast cancers; results from the geparquinto study (GBG 44). Annals of oncology : official journal of the European Society for Medical Oncology / ESMO. 2013;24(12):2978-84.
225. Mathe A, Scott RJ, Avery-Kiejda KA. MiRNAs and Other Epigenetic Changes as Biomarkers in Triple Negative Breast Cancer. International journal of molecular sciences. 2015;16(12):28347-76.
226. Rottenberg S, Nygren AO, Pajic M, van Leeuwen FW, van der Heijden I, van de Wetering K, et al. Selective induction of chemotherapy resistance of mammary tumors in a conditional mouse model for hereditary breast cancer. Proceedings of the National Academy of Sciences of the United States of America. 2007;104(29):12117-22.
227. Henderson IC, Berry DA, Demetri GD, Cirrincione CT, Goldstein LJ, Martino S, et al. Improved outcomes from adding sequential Paclitaxel but not from escalating Doxorubicin dose in an adjuvant chemotherapy regimen for patients with node-positive primary breast cancer. Journal of clinical oncology : official journal of the American Society of Clinical Oncology. 2003;21(6):976-83.
228. Rampurwala M, Wisinski KB, O'Regan R. Role of the androgen receptor in triple-negative breast cancer. Clinical advances in hematology & oncology : H&O. 2016;14(3):186-93.

229. Dent R, Trudeau M, Pritchard KI, Hanna WM, Kahn HK, Sawka CA, et al. Triple-negative breast cancer: clinical features and patterns of recurrence. Clinical cancer research : an official journal of the American Association for Cancer Research. 2007;13(15 Pt 1):4429-34.
230. Isakoff SJ. Triple-negative breast cancer: role of specific chemotherapy agents. Cancer journal. 2010;16(1):53-61.
231. Gennari A, Sormani MP, Pronzato P, Puntoni M, Colozza M, Pfeffer U, et al. HER2 status and efficacy of adjuvant anthracyclines in early breast cancer: a pooled analysis of randomized trials. Journal of the National Cancer Institute. 2008;100(1):14-20.
232. Gluz O, Liedtke C, Gottschalk N, Pusztai L, Nitz U, Harbeck N. Triple-negative breast cancer--current status and future directions. Annals of oncology : official journal of the European Society for Medical Oncology / ESMO. 2009;20(12):1913-27.
233. Kilburn LS, Group TNTTM. 'Triple negative' breast cancer: a new area for phase III breast cancer clinical trials. Clinical oncology. 2008;20(1):35-9.
234. Harris LN, Broadwater G, Lin NU, Miron A, Schnitt SJ, Cowan D, et al. Molecular subtypes of breast cancer in relation to paclitaxel response and outcomes in women with metastatic disease: results from CALGB 9342. Breast cancer research : BCR. 2006;8(6):R66.
235. Martin M, Ruiz A, Ruiz Borrego M, Barnadas A, Gonzalez S, Calvo L, et al. Fluorouracil, doxorubicin, and cyclophosphamide (FAC) versus FAC followed by weekly paclitaxel as adjuvant therapy for high-risk, node-negative breast cancer: results from the GEICAM/2003-02 study. Journal of clinical oncology : official journal of the American Society of Clinical Oncology. 2013;31(20):2593-9.
236. Freedman GM, Anderson PR, Li T, Nicolaou N. Locoregional recurrence of triple-negative breast cancer after breast-conserving surgery and radiation. Cancer. 2009;115(5):946-51.
237. Dawood S. Triple-negative breast cancer: epidemiology and management options. Drugs. 2010;70(17):2247-58.
238. Abdulkarim BS, Cuartero J, Hanson J, Deschenes J, Lesniak D, Sabri S. Increased risk of locoregional recurrence for women with T1-2N0 triple-negative breast cancer treated with modified radical mastectomy without adjuvant radiation therapy compared with breast-conserving therapy. Journal of clinical oncology : official journal of the American Society of Clinical Oncology. 2011;29(21):2852-8.
239. Panoff JE, Hurley J, Takita C, Reis IM, Zhao W, Sujoy V, et al. Risk of locoregional recurrence by receptor status in breast cancer patients receiving modern systemic therapy and post-mastectomy radiation. Breast cancer research and treatment. 2011;128(3):899-906.
240. Dragun AE, Pan J, Rai SN, Kruse B, Jain D. Locoregional recurrence in patients with triple-negative breast cancer: preliminary results of a single institution study. American journal of clinical oncology. 2011;34(3):231-7.
241. Toh TB, Lee DK, Hou W, Abdullah LN, Nguyen J, Ho D, et al. Nanodiamond-mitoxantrone complexes enhance drug retention in chemoresistant breast cancer cells. Molecular pharmaceutics. 2014;11(8):2683-91.
242. Ramirez LY, Huestis SE, Yap TY, Zyzanski S, Drotar D, Kodish E. Potential chemotherapy side effects: what do oncologists tell parents? Pediatric blood & cancer. 2009;52(4):497-502.
243. Thun MJ, Henley SJ, Patrono C. Nonsteroidal anti-inflammatory drugs as anticancer agents: mechanistic, pharmacologic, and clinical issues. Journal of the National Cancer Institute. 2002;94(4):252-66.
244. Barenholz Y. Doxil(R)--the first FDA-approved nano-drug: lessons learned. Journal of controlled release : official journal of the Controlled Release Society. 2012;160(2):117-34.
245. Gordon AN, Fleagle JT, Guthrie D, Parkin DE, Gore ME, Lacave AJ. Recurrent epithelial ovarian carcinoma: a randomized phase III study of pegylated liposomal doxorubicin versus topotecan. Journal of clinical oncology : official journal of the American Society of Clinical Oncology. 2001;19(14):3312-22.

246. Gordon AN, Tonda M, Sun S, Rackoff W, Doxil Study I. Long-term survival advantage for women treated with pegylated liposomal doxorubicin compared with topotecan in a phase 3 randomized study of recurrent and refractory epithelial ovarian cancer. Gynecologic oncology. 2004;95(1):1-8.
247. Kotov NA. Chemistry. Inorganic nanoparticles as protein mimics. Science. 2010;330(6001):188-9.
248. Torchilin VP. Micellar nanocarriers: pharmaceutical perspectives. Pharmaceutical research. 2007;24(1):1-16.
249. Baker SN, Baker GA. Luminescent carbon nanodots: emergent nanolights. Angew Chem Int Ed Engl. 2010;49(38):6726-44.
250. Baughman RH, Zakhidov AA, de Heer WA. Carbon nanotubes--the route toward applications. Science. 2002;297(5582):787-92.
251. Huang N, Wang H, Zhao J, Lui H, Korbelik M, Zeng H. Single-wall carbon nanotubes assisted photothermal cancer therapy: animal study with a murine model of squamous cell carcinoma. Lasers in surgery and medicine. 2010;42(9):638-48.
252. Ayala-Orozco C, Urban C, Knight MW, Urban AS, Neumann O, Bishnoi SW, et al. Au nanomatryoshkas as efficient near-infrared photothermal transducers for cancer treatment: benchmarking against nanoshells. ACS nano. 2014;8(6):6372-81.
253. Colombo M, Carregal-Romero S, Casula MF, Gutierrez L, Morales MP, Bohm IB, et al. Biological applications of magnetic nanoparticles. Chemical Society reviews. 2012;41(11):4306-34.
254. Mulvaney P, Parak WJ, Caruso F, Weiss PS. Standardizing Nanomaterials. ACS nano. 2016;10(11):9763-4.
255. Beveridge JS, Buck MR, Bondi JF, Misra R, Schiffer P, Schaak RE, et al. Purification and magnetic interrogation of hybrid Au-Fe3O4 and FePt-Fe3O4 nanoparticles. Angew Chem Int Ed Engl. 2011;50(42):9875-9.
256. Melamed JR, Riley RS, Valcourt DM, Day ES. Using Gold Nanoparticles To Disrupt the Tumor Microenvironment: An Emerging Therapeutic Strategy. ACS nano. 2016;10(12):10631-5.
257. Abdullah LN, Chow EK. Mechanisms of chemoresistance in cancer stem cells. Clinical and translational medicine. 2013;2(1):3.
258. Chow EK, Zhang XQ, Chen M, Lam R, Robinson E, Huang H, et al. Nanodiamond therapeutic delivery agents mediate enhanced chemoresistant tumor treatment. Science translational medicine. 2011;3(73):73ra21.
259. Milane L, Duan ZF, Amiji M. Pharmacokinetics and biodistribution of lonidamine/paclitaxel loaded, EGFR-targeted nanoparticles in an orthotopic animal model of multi-drug resistant breast cancer. Nanomedicine : nanotechnology, biology, and medicine. 2011;7(4):435-44.
260. Miller-Kleinhenz JM, Bozeman EN, Yang L. Targeted nanoparticles for image-guided treatment of triple-negative breast cancer: clinical significance and technological advances. Wiley interdisciplinary reviews Nanomedicine and nanobiotechnology. 2015;7(6):797-816.
261. Zhu H, Dai M, Chen X, Chen X, Qin S, Dai S. Integrated analysis of the potential roles of miRNAmRNA networks in triple negative breast cancer. Molecular medicine reports. 2017;16(2):1139-46.
262. Lu L, Mao X, Shi P, He B, Xu K, Zhang S, et al. MicroRNAs in the prognosis of triple-negative breast cancer: A systematic review and meta-analysis. Medicine. 2017;96(22):e7085.
263. Bertrand N, Wu J, Xu X, Kamaly N, Farokhzad OC. Cancer nanotechnology: the impact of passive and active targeting in the era of modern cancer biology. Advanced drug delivery reviews. 2014;66:2-25.
264. Jabr-Milane LS, van Vlerken LE, Yadav S, Amiji MM. Multi-functional nanocarriers to overcome tumor drug resistance. Cancer treatment reviews. 2008;34(7):592-602.

265. Dana H, Chalbatani GM, Mahmoodzadeh H, Karimloo R, Rezaiean O, Moradzadeh A, et al. Molecular Mechanisms and Biological Functions of siRNA. International journal of biomedical science : IJBS. 2017;13(2):48-57.
266. Guo P, You JO, Yang J, Jia D, Moses MA, Auguste DT. Inhibiting metastatic breast cancer cell migration via the synergy of targeted, pH-triggered siRNA delivery and chemokine axis blockade. Molecular pharmaceutics. 2014;11(3):755-65.
267. Zhang W, Meng J, Ji Y, Li X, Kong H, Wu X, et al. Inhibiting metastasis of breast cancer cells in vitro using gold nanorod-siRNA delivery system. Nanoscale. 2011;3(9):3923-32.
268. Scheinberg DA, Villa CH, Escorcia FE, McDevitt MR. Conscripts of the infinite armada: systemic cancer therapy using nanomaterials. Nature reviews Clinical oncology. 2010;7(5):266-76.
269. Zhang L, Chan JM, Gu FX, Rhee JW, Wang AZ, Radovic-Moreno AF, et al. Self-assembled lipid--polymer hybrid nanoparticles: a robust drug delivery platform. ACS nano. 2008;2(8):1696-702.
270. Scherr M, Battmer K, Schultheis B, Ganser A, Eder M. Stable RNA interference (RNAi) as an option for anti-bcr-abl therapy. Gene therapy. 2005;12(1):12-21.
271. Kulbachinskiy AV. Methods for selection of aptamers to protein targets. Biochemistry Biokhimiia. 2007;72(13):1505-18.
272. Lakhin AV, Tarantul VZ, Gening LV. Aptamers: problems, solutions and prospects. Acta naturae. 2013;5(4):34-43.
273. Turner JJ, Hoos JS, Vonhoff S, Klussmann S. Methods for L-ribooligonucleotide sequence determination using LCMS. Nucleic acids research. 2011;39(21):e147.
274. Ferreira CS, Matthews CS, Missailidis S. DNA aptamers that bind to MUC1 tumour marker: design and characterization of MUC1-binding single-stranded DNA aptamers. Tumour biology : the journal of the International Society for Oncodevelopmental Biology and Medicine. 2006;27(6):289-301.
275. Marimuthu C, Tang TH, Tominaga J, Tan SC, Gopinath SC. Single-stranded DNA (ssDNA) production in DNA aptamer generation. The Analyst. 2012;137(6):1307-15.
276. Luo S, Wang S, Luo N, Chen F, Hu C, Zhang K. The application of aptamer 5TR1 in triple negative breast cancer target therapy. Journal of cellular biochemistry. 2018;119(1):896-908.
277. Alshaer W, Hillaireau H, Vergnaud J, Mura S, Delomenie C, Sauvage F, et al. Aptamer-guided siRNA-loaded nanomedicines for systemic gene silencing in CD-44 expressing murine triple-negative breast cancer model. Journal of controlled release : official journal of the Controlled Release Society. 2018;271:98-106.
278. Pelaz B, Alexiou C, Alvarez-Puebla RA, Alves F, Andrews AM, Ashraf S, et al. Diverse Applications of Nanomedicine. ACS nano. 2017;11(3):2313-81.
279. Bahadar H, Maqbool F, Niaz K, Abdollahi M. Toxicity of Nanoparticles and an Overview of Current Experimental Models. Iranian biomedical journal. 2016;20(1):1-11.
280. Swanner J, Mims J, Carroll DL, Akman SA, Furdui CM, Torti SV, et al. Differential cytotoxic and radiosensitizing effects of silver nanoparticles on triple-negative breast cancer and non-triple-negative breast cells. International journal of nanomedicine. 2015;10:3937-53.
281. Johnstone TC, Suntharalingam K, Lippard SJ. The Next Generation of Platinum Drugs: Targeted Pt(II) Agents, Nanoparticle Delivery, and Pt(IV) Prodrugs. Chemical reviews. 2016;116(5):3436-86.
282. Ahir M, Bhattacharya S, Karmakar S, Mukhopadhyay A, Mukherjee S, Ghosh S, et al. Tailored-CuO-nanowire decorated with folic acid mediated coupling of the mitochondrial-ROS generation and miR425-PTEN axis in furnishing potent anti-cancer activity in human triple negative breast carcinoma cells. Biomaterials. 2016;76:115-32.
283. Shukla R, Bansal V, Chaudhary M, Basu A, Bhonde RR, Sastry M. Biocompatibility of gold nanoparticles and their endocytotic fate inside the cellular compartment: a microscopic overview. Langmuir : the ACS journal of surfaces and colloids. 2005;21(23):10644-54.

284. Michalet X, Pinaud FF, Bentolila LA, Tsay JM, Doose S, Li JJ, et al. Quantum dots for live cells, in vivo imaging, and diagnostics. Science. 2005;307(5709):538-44.
285. Wang LW, Peng CW, Chen C, Li Y. Quantum dots-based tissue and in vivo imaging in breast cancer researches: current status and future perspectives. Breast cancer research and treatment. 2015;151(1):7-17.
286. Sun JZ, Chen C, Jiang G, Tian WQ, Li Y, Sun SR. Quantum dot-based immunofluorescent imaging of Ki67 and identification of prognostic value in HER2-positive (non-luminal) breast cancer. International journal of nanomedicine. 2014;9:1339-46.
287. Zheng HM, Chen C, Wu XH, Chen J, Sun S, Sun JZ, et al. Quantum dot-based in situ simultaneous molecular imaging and quantitative analysis of EGFR and collagen IV and identification of their prognostic value in triple-negative breast cancer. Tumour biology : the journal of the International Society for Oncodevelopmental Biology and Medicine. 2016;37(2):2509-18.
288. Chen C, Yuan JP, Wei W, Tu Y, Yao F, Yang XQ, et al. Subtype classification for prediction of prognosis of breast cancer from a biomarker panel: correlations and indications. International journal of nanomedicine. 2014;9:1039-48.
289. Fudala R, Raut S, Maliwal BP, Zerda TW, Gryczynski I, Simanek E, et al. FRET enhanced fluorescent nanodiamonds. Current pharmaceutical biotechnology. 2014;14(13):1127-33.
290. Yang L, Cao Z, Sajja HK, Mao H, Wang L, Geng H, et al. Development of Receptor Targeted Magnetic Iron Oxide Nanoparticles for Efficient Drug Delivery and Tumor Imaging. Journal of biomedical nanotechnology. 2008;4(4):439-49.
291. Medarova Z, Rashkovetsky L, Pantazopoulos P, Moore A. Multiparametric monitoring of tumor response to chemotherapy by noninvasive imaging. Cancer research. 2009;69(3):1182-9.
292. Guo P, Huang J, Wang L, Jia D, Yang J, Dillon DA, et al. ICAM-1 as a molecular target for triple negative breast cancer. Proceedings of the National Academy of Sciences of the United States of America. 2014;111(41):14710-5.
293. Gobin AM, Lee MH, Halas NJ, James WD, Drezek RA, West JL. Near-infrared resonant nanoshells for combined optical imaging and photothermal cancer therapy. Nano letters. 2007;7(7):1929-34.
294. Kennedy LC, Bickford LR, Lewinski NA, Coughlin AJ, Hu Y, Day ES, et al. A new era for cancer treatment: gold-nanoparticle-mediated thermal therapies. Small. 2011;7(2):169-83.
295. Maluta S, Kolff MW. Role of Hyperthermia in Breast Cancer Locoregional Recurrence: A Review. Breast care. 2015;10(6):408-12.
296. Gobbo OL, Sjaastad K, Radomski MW, Volkov Y, Prina-Mello A. Magnetic Nanoparticles in Cancer Theranostics. Theranostics. 2015;5(11):1249-63.
297. Le Renard PE, Jordan O, Faes A, Petri-Fink A, Hofmann H, Rufenacht D, et al. The in vivo performance of magnetic particle-loaded injectable, in situ gelling, carriers for the delivery of local hyperthermia. Biomaterials. 2010;31(4):691-705.
298. Ruiz A, Hernandez Y, Cabal C, Gonzalez E, Veintemillas-Verdaguer S, Martinez E, et al. Biodistribution and pharmacokinetics of uniform magnetite nanoparticles chemically modified with polyethylene glycol. Nanoscale. 2013;5(23):11400-8.
299. Hayashi K, Nakamura M, Sakamoto W, Yogo T, Miki H, Ozaki S, et al. Superparamagnetic nanoparticle clusters for cancer theranostics combining magnetic resonance imaging and hyperthermia treatment. Theranostics. 2013;3(6):366-76.
300. Ratto F, Matteini P, Centi S, Rossi F, Pini R. Gold nanorods as new nanochromophores for photothermal therapies. Journal of biophotonics. 2011;4(1-2):64-73.
301. Kim J, Chung DJ, Jung SE, Cho SH, Hahn ST, Lee JM. Therapeutic effect of high-intensity focused ultrasound combined with transarterial chemoembolisation for hepatocellular carcinoma <5 cm: comparison with transarterial chemoembolisation monotherapy--preliminary observations. The British journal of radiology. 2012;85(1018):e940-6.

302. Fu Y, Yang W, Wu W, Yan K, Xing BC, Chen MH. Radiofrequency ablation in the management of unresectable intrahepatic cholangiocarcinoma. Journal of vascular and interventional radiology : JVIR. 2012;23(5):642-9.
303. Huang HS, Hainfeld JF. Intravenous magnetic nanoparticle cancer hyperthermia. International journal of nanomedicine. 2013;8:2521-32.
304. Arias LS, Pessan JP, Vieira APM, Lima TMT, Delbem ACB, Monteiro DR. Iron Oxide Nanoparticles for Biomedical Applications: A Perspective on Synthesis, Drugs, Antimicrobial Activity, and Toxicity. Antibiotics. 2018;7(2).
305. Honarvar Z, Hadian Z, Mashayekh M. Nanocomposites in food packaging applications and their risk assessment for health. Electronic physician. 2016;8(6):2531-8.
306. Arora A, Padua GW. Review: nanocomposites in food packaging. Journal of food science. 2010;75(1):R43-9.
307. Matharu RK, Ciric L, Edirisinghe M. Nanocomposites: suitable alternatives as antimicrobial agents. Nanotechnology. 2018;29(28):282001.
308. Roco MC. Nanotechnology: convergence with modern biology and medicine. Current opinion in biotechnology. 2003;14(3):337-46.
309. Jeevanandam J, Barhoum A, Chan YS, Dufresne A, Danquah MK. Review on nanoparticles and nanostructured materials: history, sources, toxicity and regulations. Beilstein journal of nanotechnology. 2018;9:1050-74.
310. Agostinis P, Berg K, Cengel KA, Foster TH, Girotti AW, Gollnick SO, et al. Photodynamic therapy of cancer: an update. CA: a cancer journal for clinicians. 2011;61(4):250-81.
311. Wang X, Hu J, Wang P, Zhang S, Liu Y, Xiong W, et al. Analysis of the in vivo and in vitro effects of photodynamic therapy on breast cancer by using a sensitizer, sinoporphyrin sodium. Theranostics. 2015;5(7):772-86.
312. Kue CS, Kamkaew A, Lee HB, Chung LY, Kiew LV, Burgess K. Targeted PDT agent eradicates TrkC expressing tumors via photodynamic therapy (PDT). Molecular pharmaceutics. 2015;12(1):212-22.
313. Shemesh CS, Moshkelani D, Zhang H. Thermosensitive liposome formulated indocyanine green for near-infrared triggered photodynamic therapy: in vivo evaluation for triple-negative breast cancer. Pharmaceutical research. 2015;32(5):1604-14.
314. Hanahan D, Weinberg RA. Hallmarks of cancer: the next generation. Cell. 2011;144(5):646-74.
315. Liu Z, Li M, Jiang Z, Wang X. A Comprehensive Immunologic Portrait of Triple-Negative Breast Cancer. Translational oncology. 2018;11(2):311-29.
316. Newman AM, Liu CL, Green MR, Gentles AJ, Feng W, Xu Y, et al. Robust enumeration of cell subsets from tissue expression profiles. Nature methods. 2015;12(5):453-7.
317. Yoshihara K, Shahmoradgoli M, Martinez E, Vegesna R, Kim H, Torres-Garcia W, et al. Inferring tumour purity and stromal and immune cell admixture from expression data. Nature communications. 2013;4:2612.
318. Li CW, Lim SO, Hsu JL, Hung MC. Rational combination of immunotherapy for triple negative breast cancer treatment. Chinese clinical oncology. 2017;6(5):54.
319. Ruffell B, Au A, Rugo HS, Esserman LJ, Hwang ES, Coussens LM. Leukocyte composition of human breast cancer. Proceedings of the National Academy of Sciences of the United States of America. 2012;109(8):2796-801.
320. Linsley PS, Greene JL, Brady W, Bajorath J, Ledbetter JA, Peach R. Human B7-1 (CD80) and B7-2 (CD86) bind with similar avidities but distinct kinetics to CD28 and CTLA-4 receptors. Immunity. 1994;1(9):793-801.
321. Maker AV, Attia P, Rosenberg SA. Analysis of the cellular mechanism of antitumor responses and autoimmunity in patients treated with CTLA-4 blockade. Journal of immunology. 2005;175(11):7746-54.

322. Cao Y, Axup JY, Ma JS, Wang RE, Choi S, Tardif V, et al. Multiformat T-cell-engaging bispecific antibodies targeting human breast cancers. Angew Chem Int Ed Engl. 2015;54(24):7022-7.
323. Pardoll DM. The blockade of immune checkpoints in cancer immunotherapy. Nature reviews Cancer. 2012;12(4):252-64.
324. Wimberly H, Brown JR, Schalper K, Haack H, Silver MR, Nixon C, et al. PD-L1 Expression Correlates with Tumor-Infiltrating Lymphocytes and Response to Neoadjuvant Chemotherapy in Breast Cancer. Cancer immunology research. 2015;3(4):326-32.
325. Gibson J. Anti-PD-L1 for metastatic triple-negative breast cancer. The Lancet Oncology. 2015;16(6):e264.
326. Jones LD, Golan D, Hanna SA, Ramachandran M. Artificial intelligence, machine learning and the evolution of healthcare: A bright future or cause for concern? Bone & joint research. 2018;7(3):223-5.
327. Craft JA, 3rd. Artificial Intelligence and the Softer Side of Medicine. Missouri medicine. 2018;115(5):406-9.
328. Cheng JZ, Ni D, Chou YH, Qin J, Tiu CM, Chang YC, et al. Computer-Aided Diagnosis with Deep Learning Architecture: Applications to Breast Lesions in US Images and Pulmonary Nodules in CT Scans. Scientific reports. 2016;6:24454.
329. Houssami N, Lee CI, Buist DSM, Tao D. Artificial intelligence for breast cancer screening: Opportunity or hype? Breast. 2017;36:31-3.
330. Jiang F, Jiang Y, Zhi H, Dong Y, Li H, Ma S, et al. Artificial intelligence in healthcare: past, present and future. Stroke and vascular neurology. 2017;2(4):230-43.
331. Fernández-Martínez JLC, Ana & DeAndrés-Galiana, Enrique J. & Menéndez, Primitiva & Galván, José & Garcıa-Pravia, Carmen. Automatic Classification of Cell Patterns for Triple Negative Breast Cancer Identification. (2014).
332. Tomczak K, Czerwinska P, Wiznerowicz M. The Cancer Genome Atlas (TCGA): an immeasurable source of knowledge. Contemporary oncology. 2015;19(1A):A68-77.
333. Bareche Y, Venet D, Ignatiadis M, Aftimos P, Piccart M, Rothe F, et al. Unravelling triple-negative breast cancer molecular heterogeneity using an integrative multiomic analysis. Annals of oncology : official journal of the European Society for Medical Oncology / ESMO. 2018;29(4):895-902.
334. Elgqvist J. Nanoparticles as Theranostic Vehicles in Experimental and Clinical Applications-Focus on Prostate and Breast Cancer. International journal of molecular sciences. 2017;18(5).
335. Vyas D, Lopez-Hisijos N, Gandhi S, El-Dakdouki M, Basson MD, Walsh MF, et al. Doxorubicin-Hyaluronan Conjugated Super-Paramagnetic Iron Oxide Nanoparticles (DOX-HA-SPION) Enhanced Cytoplasmic Uptake of Doxorubicin and Modulated Apoptosis, IL-6 Release and NF-kappaB Activity in Human MDA-MB-231 Breast Cancer Cells. Journal of nanoscience and nanotechnology. 2015;15(9):6413-22.
336. Meng Q, Meng J, Ran W, Wang J, Zhai Y, Zhang P, et al. Light-Activated Core-Shell Nanoparticles for Spatiotemporally Specific Treatment of Metastatic Triple-Negative Breast Cancer. ACS nano. 2018;12(3):2789-802.
337. Zhang L, Liu C, Gao Y, Li Z, Xing J, Ren W, et al. ZD2-Engineered Gold Nanostar@Metal-Organic Framework Nanoprobes for T1 -Weighted Magnetic Resonance Imaging and Photothermal Therapy Specifically Toward Triple-Negative Breast Cancer. Advanced healthcare materials. 2018;7(24):e1801144.
338. Liang R, Liu L, He H, Chen Z, Han Z, Luo Z, et al. Oxygen-boosted immunogenic photodynamic therapy with gold nanocages@manganese dioxide to inhibit tumor growth and metastases. Biomaterials. 2018;177:149-60.

339. Feng B, Xu Z, Zhou F, Yu H, Sun Q, Wang D, et al. Near infrared light-actuated gold nanorods with cisplatin-polypeptide wrapping for targeted therapy of triple negative breast cancer. Nanoscale. 2015;7(36):14854-64.
340. Liao WS, Ho Y, Lin YW, Naveen Raj E, Liu KK, Chen C, et al. Targeting EGFR of triple-negative breast cancer enhances the therapeutic efficacy of paclitaxel- and cetuximab-conjugated nanodiamond nanocomposite. Acta biomaterialia. 2019;86:395-405.
341. Sanpo N, Berndt CC, Wen C, Wang J. Transition metal-substituted cobalt ferrite nanoparticles for biomedical applications. Acta biomaterialia. 2013;9(3):5830-7.
342. Unni M, Uhl AM, Savliwala S, Savitzky BH, Dhavalikar R, Garraud N, et al. Thermal Decomposition Synthesis of Iron Oxide Nanoparticles with Diminished Magnetic Dead Layer by Controlled Addition of Oxygen. ACS nano. 2017;11(2):2284-303.
343. Allen TM, Cullis PR. Liposomal drug delivery systems: from concept to clinical applications. Advanced drug delivery reviews. 2013;65(1):36-48.
344. Ramimoghadam D, Hussein MZ, Taufiq-Yap YH. The effect of sodium dodecyl sulfate (SDS) and cetyltrimethylammonium bromide (CTAB) on the Properties of ZnO synthesized by hydrothermal method. International journal of molecular sciences. 2012;13(10):13275-93.
345. Simonsen LO, Harbak H, Bennekou P. Cobalt metabolism and toxicology--a brief update. The Science of the total environment. 2012;432:210-5.
346. Horev-Azaria L, Baldi G, Beno D, Bonacchi D, Golla-Schindler U, Kirkpatrick JC, et al. Predictive toxicology of cobalt ferrite nanoparticles: comparative in-vitro study of different cellular models using methods of knowledge discovery from data. Particle and fibre toxicology. 2013;10:32.
347. Jardim KV, Palomec-Garfias AF, Andrade BYG, Chaker JA, Bao SN, Marquez-Beltran C, et al. Novel magneto-responsive nanoplatforms based on MnFe2O4 nanoparticles layer-by-layer functionalized with chitosan and sodium alginate for magnetic controlled release of curcumin. Materials science & engineering C, Materials for biological applications. 2018;92:184-95.
348. Saquib Q, Al-Khedhairy AA, Ahmad J, Siddiqui MA, Dwivedi S, Khan ST, et al. Zinc ferrite nanoparticles activate IL-1b, NFKB1, CCL21 and NOS2 signaling to induce mitochondrial dependent intrinsic apoptotic pathway in WISH cells. Toxicology and applied pharmacology. 2013;273(2):289-97.
349. Li XH, Xu CL, Han XH, Qiao L, Wang T, Li FS. Synthesis and Magnetic Properties of Nearly Monodisperse CoFe2O4Nanoparticles Through a Simple Hydrothermal Condition. Nanoscale research letters. 2010;5(6):1039-44.
350. Teles RHG, Moralles HF, Cominetti MR. Global trends in nanomedicine research on triple negative breast cancer: a bibliometric analysis. International journal of nanomedicine. 2018;13:2321-36.
351. Zhang K, Na T, Wang L, Gao Q, Yin W, Wang J, et al. Human diploid MRC-5 cells exhibit several critical properties of human umbilical cord-derived mesenchymal stem cells. Vaccine. 2014;32(50):6820-7.
352. Naghdi P, Tiraihi T, Ganji F, Darabi S, Taheri T, Kazemi H. Survival, proliferation and differentiation enhancement of neural stem cells cultured in three-dimensional polyethylene glycol-RGD hydrogel with tenascin. Journal of tissue engineering and regenerative medicine. 2016;10(3):199-208.
353. Alkilany AM, Murphy CJ. Toxicity and cellular uptake of gold nanoparticles: what we have learned so far? Journal of nanoparticle research : an interdisciplinary forum for nanoscale science and technology. 2010;12(7):2313-33.
354. Sharma G, Naushad M, Thakur B, Kumar A, Negi P, Saini R, et al. Sodium Dodecyl Sulphate-Supported Nanocomposite as Drug Carrier System for Controlled Delivery of Ondansetron. International journal of environmental research and public health. 2018;15(3).

355. Ravichandran M, Oza G, Velumani S, Ramirez JT, Garcia-Sierra F, Andrade NB, et al. Plasmonic/Magnetic Multifunctional nanoplatform for Cancer Theranostics. Scientific reports. 2016;6:34874.
356. Wang H, Wang L, Song Y, Wang S, Huang X, Xuan Q, et al. CD44(+)/CD24(-) phenotype predicts a poor prognosis in triple-negative breast cancer. Oncology letters. 2017;14(5):5890-8.
357. O'Conor CJ, Chen T, Gonzalez I, Cao D, Peng Y. Cancer stem cells in triple-negative breast cancer: a potential target and prognostic marker. Biomarkers in medicine. 2018;12(7):813-20.
358. Barton VN, Gordon MA, Richer JK, Elias A. Anti-androgen therapy in triple-negative breast cancer. Therapeutic advances in medical oncology. 2016;8(4):305-8.
359. Adan A, Alizada G, Kiraz Y, Baran Y, Nalbant A. Flow cytometry: basic principles and applications. Critical reviews in biotechnology. 2017;37(2):163-76.
360. Givan AL. Flow cytometry: an introduction. Methods Mol Biol. 2011;699:1-29.
361. Mina A, Yoder R, Sharma P. Targeting the androgen receptor in triple-negative breast cancer: current perspectives. OncoTargets and therapy. 2017;10:4675-85.
362. Cochrane DR, Bernales S, Jacobsen BM, Cittelly DM, Howe EN, D'Amato NC, et al. Role of the androgen receptor in breast cancer and preclinical analysis of enzalutamide. Breast cancer research : BCR. 2014;16(1):R7.
363. Ostolska I, Wisniewska M. Application of the zeta potential measurements to explanation of colloidal Cr2O3 stability mechanism in the presence of the ionic polyamino acids. Colloid and polymer science. 2014;292(10):2453-64.
364. Fernandes HP, Cesar CL, Barjas-Castro Mde L. Electrical properties of the red blood cell membrane and immunohematological investigation. Revista brasileira de hematologia e hemoterapia. 2011;33(4):297-301.
365. Tokumasu F, Ostera GR, Amaratunga C, Fairhurst RM. Modifications in erythrocyte membrane zeta potential by Plasmodium falciparum infection. Experimental parasitology. 2012;131(2):245-51.
366. Loof D, Hiller M, Oschkinat H, Koschek K. Quantitative and Qualitative Analysis of Surface Modified Cellulose Utilizing TGA-MS. Materials. 2016;9(6).
367. Petrova OE, Sauer K. High-Performance Liquid Chromatography (HPLC)-Based Detection and Quantitation of Cellular c-di-GMP. Methods Mol Biol. 2017;1657:33-43.
368. Markson JS, Elowitz MB. Synthetic biology of multicellular systems: new platforms and applications for animal cells and organisms. ACS synthetic biology. 2014;3(12):875-6.
369. Stolzenburg S, Rots MG, Beltran AS, Rivenbark AG, Yuan X, Qian H, et al. Targeted silencing of the oncogenic transcription factor SOX2 in breast cancer. Nucleic acids research. 2012;40(14):6725-40.
370. Tapia T, Smalley SV, Kohen P, Munoz A, Solis LM, Corvalan A, et al. Promoter hypermethylation of BRCA1 correlates with absence of expression in hereditary breast cancer tumors. Epigenetics. 2008;3(3):157-63.
371. Winblad N, Lanner F. Biotechnology: At the heart of gene edits in human embryos. Nature. 2017;548(7668):398-400.
372. Parbin S, Kar S, Shilpi A, Sengupta D, Deb M, Rath SK, et al. Histone deacetylases: a saga of perturbed acetylation homeostasis in cancer. The journal of histochemistry and cytochemistry : official journal of the Histochemistry Society. 2014;62(1):11-33.
373. Butler MG. Genomic imprinting disorders in humans: a mini-review. Journal of assisted reproduction and genetics. 2009;26(9-10):477-86.
374. Maier JAH, Mohrle R, Jeltsch A. Design of synthetic epigenetic circuits featuring memory effects and reversible switching based on DNA methylation. Nature communications. 2017;8:15336.
375. Arora BP. Anti-aging medicine. Indian journal of plastic surgery : official publication of the Association of Plastic Surgeons of India. 2008;41(Suppl):S130-3.

376. Duesberg P, McCormack A. Immortality of cancers: a consequence of inherent karyotypic variations and selections for autonomy. Cell cycle. 2013;12(5):783-802.
377. Hayflick L. The Limited in Vitro Lifetime of Human Diploid Cell Strains. Experimental cell research. 1965;37:614-36.
378. Schrader GM, Allender MC, Odoi A. Diagnosis, treatment, and outcome of eastern box turtles (Terrapene carolina carolina) presented to a wildlife clinic in Tennessee, USA, 1995-2007. Journal of wildlife diseases. 2010;46(4):1079-85.
379. Sergiev PV, Artemov AA, Prokhortchouk EB, Dontsova OA, Berezkin GV. Genomes of Strongylocentrotus franciscanus and Lytechinus variegatus: are there any genomic explanations for the two order of magnitude difference in the lifespan of sea urchins? Aging. 2016;8(2):260-71.
380. Munro D, Blier PU. The extreme longevity of Arctica islandica is associated with increased peroxidation resistance in mitochondrial membranes. Aging cell. 2012;11(5):845-55.
381. Russo R, Giordano D, Paredi G, Marchesani F, Milazzo L, Altomonte G, et al. The Greenland shark Somniosus microcephalus-Hemoglobins and ligand-binding properties. PloS one. 2017;12(10):e0186181.
382. Lanner RM, Connor KF. Does bristlecone pine senesce? Experimental gerontology. 2001;36(4-6):675-85.
383. Tomczyk S, Fischer K, Austad S, Galliot B. Hydra, a powerful model for aging studies. Invertebrate reproduction & development. 2015;59(sup1):11-6.
384. Allday MJ, Sinclair A, Parker G, Crawford DH, Farrell PJ. Epstein-Barr virus efficiently immortalizes human B cells without neutralizing the function of p53. The EMBO journal. 1995;14(7):1382-91.
385. Carroll M, Zhou X. Panacea in progress: CRISPR and the future of its biological research introduction. Microbiological research. 2017;201:63-74.
386. Sun W, Ji W, Hall JM, Hu Q, Wang C, Beisel CL, et al. Self-assembled DNA nanoclews for the efficient delivery of CRISPR-Cas9 for genome editing. Angew Chem Int Ed Engl. 2015;54(41):12029-33.
387. Lee CH, Yoon HJ. Medical big data: promise and challenges. Kidney research and clinical practice. 2017;36(1):3-11.
388. Glass JI. Synthetic genomics and the construction of a synthetic bacterial cell. Perspectives in biology and medicine. 2012;55(4):473-89.
389. Shao Y, Molnar LF, Jung Y, Kussmann J, Ochsenfeld C, Brown ST, et al. Advances in methods and algorithms in a modern quantum chemistry program package. Physical chemistry chemical physics : PCCP. 2006;8(27):3172-91.
390. van Mourik T. First-principles quantum chemistry in the life sciences. Philosophical transactions Series A, Mathematical, physical, and engineering sciences. 2004;362(1825):2653-70.
391. Singhal N, Kumar M, Kanaujia PK, Virdi JS. MALDI-TOF mass spectrometry: an emerging technology for microbial identification and diagnosis. Frontiers in microbiology. 2015;6:791.
392. Alvarez-Rodriguez U, Sanz M, Lamata L, Solano E. Quantum Artificial Life in an IBM Quantum Computer. Scientific reports. 2018;8(1):14793.
393. Shi Y, Toga AW. Connectome imaging for mapping human brain pathways. Molecular psychiatry. 2017;22(9):1230-40.
394. Deffner S. Demonstration of entanglement assisted invariance on IBM's quantum experience. Heliyon. 2017;3(11):e00444.
395. Langer F, Schmid CP, Schlauderer S, Gmitra M, Fabian J, Nagler P, et al. Lightwave valleytronics in a monolayer of tungsten diselenide. Nature. 2018;557(7703):76-80.
396. Jedlicka P. Revisiting the Quantum Brain Hypothesis: Toward Quantum (Neuro)biology? Frontiers in molecular neuroscience. 2017;10:366.

397. Li Y, McGrail DJ, Xu J, Li J, Liu NN, Sun M, et al. MERIT: Systematic analysis and characterization of Mutational Effect on RNA Interactome Topology. Hepatology. 2018.
398. McNamee MJ, Edwards SD. Transhumanism, medical technology and slippery slopes. Journal of medical ethics. 2006;32(9):513-8.
399. Bostrom N. Human genetic enhancements: a transhumanist perspective. The Journal of value inquiry. 2003;37(4):493-506.
400. Zhang H, Wu R, Li C, Zang X, Zhang X, Jin H, et al. A Force-Sensing System on Legs for Biomimetic Hexapod Robots Interacting with Unstructured Terrain. Sensors. 2017;17(7).
401. Zeilig G, Weingarden H, Zwecker M, Dudkiewicz I, Bloch A, Esquenazi A. Safety and tolerance of the ReWalk exoskeleton suit for ambulation by people with complete spinal cord injury: a pilot study. The journal of spinal cord medicine. 2012;35(2):96-101.
402. Daly JJ, Huggins JE. Brain-computer interface: current and emerging rehabilitation applications. Archives of physical medicine and rehabilitation. 2015;96(3 Suppl):S1-7.
403. Platt JL, Cascalho M. New and old technologies for organ replacement. Current opinion in organ transplantation. 2013;18(2):179-85.
404. Gregg RD, Sensinger JW. Towards Biomimetic Virtual Constraint Control of a Powered Prosthetic Leg. IEEE transactions on control systems technology : a publication of the IEEE Control Systems Society. 2014;22(1):246-54.
405. Shastry BS. SNPs: impact on gene function and phenotype. Methods Mol Biol. 2009;578:3-22.
406. Cook JA, Shah KB, Quader MA, Cooke RH, Kasirajan V, Rao KK, et al. The total artificial heart. Journal of thoracic disease. 2015;7(12):2172-80.
407. Wrenn SM, Griswold ED, Uhl FE, Uriarte JJ, Park HE, Coffey AL, et al. Avian lungs: A novel scaffold for lung bioengineering. PloS one. 2018;13(6):e0198956.
408. Cerasa A, Pignolo L, Gramigna V, Serra S, Olivadese G, Rocca F, et al. Exoskeleton-Robot Assisted Therapy in Stroke Patients: A Lesion Mapping Study. Frontiers in neuroinformatics. 2018;12:44.
409. Haas BJ, Whited JL. Advances in Decoding Axolotl Limb Regeneration. Trends in genetics : TIG. 2017;33(8):553-65.
410. Ong CS, Yesantharao P, Huang CY, Mattson G, Boktor J, Fukunishi T, et al. 3D bioprinting using stem cells. Pediatric research. 2018;83(1-2):223-31.
411. Pedersen RA, Mascetti V, Mendjan S. Synthetic organs for regenerative medicine. Cell stem cell. 2012;10(6):646-7.
412. Li Y, Zhang D. Artificial Cardiac Muscle with or without the Use of Scaffolds. BioMed research international. 2017;2017:8473465.
413. Gura V, Rivara MB, Bieber S, Munshi R, Smith NC, Linke L, et al. A wearable artificial kidney for patients with end-stage renal disease. JCI insight. 2016;1(8).
414. Klonoff DC. The artificial pancreas: how sweet engineering will solve bitter problems. Journal of diabetes science and technology. 2007;1(1):72-81.
415. Ho AC, Humayun MS, Dorn JD, da Cruz L, Dagnelie G, Handa J, et al. Long-Term Results from an Epiretinal Prosthesis to Restore Sight to the Blind. Ophthalmology. 2015;122(8):1547-54.
416. Miller LE, Zimmermann AK, Herbert WG. Clinical effectiveness and safety of powered exoskeleton-assisted walking in patients with spinal cord injury: systematic review with meta-analysis. Medical devices. 2016;9:455-66.
417. Anthony Atala, MD: Building Organs for the Future. Transplantation. 2016;100(8):1595-6.
418. Pincock S. Anthony Atala: at the cutting edge of regenerative surgery. Lancet. 2011;378(9800):1371.
419. Osaki T, Sivathanu V, Kamm RD. Vascularized microfluidic organ-chips for drug screening, disease models and tissue engineering. Current opinion in biotechnology. 2018;52:116-23.

420. Pasqualini FS, Emmert MY, Parker KK, Hoerstrup SP. Organ Chips: Quality Assurance Systems in Regenerative Medicine. Clinical pharmacology and therapeutics. 2017;101(1):31-4.
421. Esch EW, Bahinski A, Huh D. Organs-on-chips at the frontiers of drug discovery. Nature reviews Drug discovery. 2015;14(4):248-60.
422. Sackmann EK, Fulton AL, Beebe DJ. The present and future role of microfluidics in biomedical research. Nature. 2014;507(7491):181-9.
423. Xiao Y, Zhang B, Liu H, Miklas JW, Gagliardi M, Pahnke A, et al. Microfabricated perfusable cardiac biowire: a platform that mimics native cardiac bundle. Lab on a chip. 2014;14(5):869-82.
424. An F, Qu Y, Liu X, Zhong R, Luo Y. Organ-on-a-Chip: New Platform for Biological Analysis. Analytical chemistry insights. 2015;10:39-45.
425. Whitesides GM. The origins and the future of microfluidics. Nature. 2006;442(7101):368-73.
426. Yi HG, Lee H, Cho DW. 3D Printing of Organs-On-Chips. Bioengineering. 2017;4(1).
427. Conde JP, Madaboosi N, Soares RR, Fernandes JT, Novo P, Moulas G, et al. Lab-on-chip systems for integrated bioanalyses. Essays in biochemistry. 2016;60(1):121-31.
428. Foudeh AM, Fatanat Didar T, Veres T, Tabrizian M. Microfluidic designs and techniques using lab-on-a-chip devices for pathogen detection for point-of-care diagnostics. Lab on a chip. 2012;12(18):3249-66.
429. Unger MA, Chou HP, Thorsen T, Scherer A, Quake SR. Monolithic microfabricated valves and pumps by multilayer soft lithography. Science. 2000;288(5463):113-6.
430. Wu J, Dong M, Santos S, Rigatto C, Liu Y, Lin F. Lab-on-a-Chip Platforms for Detection of Cardiovascular Disease and Cancer Biomarkers. Sensors. 2017;17(12).
431. Neethirajan S, Kobayashi I, Nakajima M, Wu D, Nandagopal S, Lin F. Microfluidics for food, agriculture and biosystems industries. Lab on a chip. 2011;11(9):1574-86.
432. Zhao Y, Chen D, Yue H, French JB, Rufo J, Benkovic SJ, et al. Lab-on-a-chip technologies for single-molecule studies. Lab on a chip. 2013;13(12):2183-98.
433. Gerber D, Maerkl SJ, Quake SR. An in vitro microfluidic approach to generating protein-interaction networks. Nature methods. 2009;6(1):71-4.
434. Madaboosi N, Soares RR, Chu V, Conde JP. A microfluidic immunoassay platform for the detection of free prostate specific antigen: a systematic and quantitative approach. The Analyst. 2015;140(13):4423-33.
435. Sandetskaya N, Moos D, Potter H, Seifert S, Jenerowicz M, Becker H, et al. An integrated versatile lab-on-a-chip platform for the isolation and nucleic acid-based detection of pathogens. Future science OA. 2017;3(2):FSO177.
436. Bagga D, Reichert JL, Koschutnig K, Aigner CS, Holzer P, Koskinen K, et al. Probiotics drive gut microbiome triggering emotional brain signatures. Gut microbes. 2018:1-11.
437. Ercolini D, Fogliano V. Food Design To Feed the Human Gut Microbiota. Journal of agricultural and food chemistry. 2018;66(15):3754-8.
438. Thursby E, Juge N. Introduction to the human gut microbiota. The Biochemical journal. 2017;474(11):1823-36.
439. Gupta S, Allen-Vercoe E, Petrof EO. Fecal microbiota transplantation: in perspective. Therapeutic advances in gastroenterology. 2016;9(2):229-39.
440. De Stefani E, Boffetta P, Ronco AL, Deneo-Pellegrini H, Correa P, Acosta G, et al. Processed meat consumption and risk of cancer: a multisite case-control study in Uruguay. British journal of cancer. 2012;107(9):1584-8.
441. Fernandez J, Garcia L, Monte J, Villar CJ, Lombo F. Functional Anthocyanin-Rich Sausages Diminish Colorectal Cancer in an Animal Model and Reduce Pro-Inflammatory Bacteria in the Intestinal Microbiota. Genes. 2018;9(3).

442. Sozer N, Kokini JL. Nanotechnology and its applications in the food sector. Trends in biotechnology. 2009;27(2):82-9.
443. Sekhon BS. Food nanotechnology - an overview. Nanotechnology, science and applications. 2010;3:1-15.
444. Vernikov VM, Arianova EA, Gmoshinskii IV, Khotimchenko SA, Tutel'ian VA. [Nanotechnology in food production: advances and problems]. Voprosy pitaniia. 2009;78(2):4-17.
445. Ai J, Biazar E, Jafarpour M, Montazeri M, Majdi A, Aminifard S, et al. Nanotoxicology and nanoparticle safety in biomedical designs. International journal of nanomedicine. 2011;6:1117-27.
446. Ray PC, Yu H, Fu PP. Toxicity and environmental risks of nanomaterials: challenges and future needs. Journal of environmental science and health Part C, Environmental carcinogenesis & ecotoxicology reviews. 2009;27(1):1-35.
447. Mahmoodi NM, Arami M. Degradation and toxicity reduction of textile wastewater using immobilized titania nanophotocatalysis. Journal of photochemistry and photobiology B, Biology. 2009;94(1):20-4.
448. Porter A. Bioethics and Transhumanism. The Journal of medicine and philosophy. 2017;42(3):237-60.
449. Singh T, Shukla S, Kumar P, Wahla V, Bajpai VK. Application of Nanotechnology in Food Science: Perception and Overview. Frontiers in microbiology. 2017;8:1501.
450. Fadel TR, Farrell DF, Friedersdorf LE, Griep MH, Hoover MD, Meador MA, et al. Toward the Responsible Development and Commercialization of Sensor Nanotechnologies. ACS sensors. 2016;1(3):207-16.
451. Jia L. Global Governmental Investment in Nanotechnologies. Current nanoscience. 2005;1(3):263-6.
452. Dau H, Fujita E, Sun L. Artificial Photosynthesis: Beyond Mimicking Nature. ChemSusChem. 2017;10(22):4228-35.
453. Tomkins P, Ranocchiari M, van Bokhoven JA. Direct Conversion of Methane to Methanol under Mild Conditions over Cu-Zeolites and beyond. Accounts of chemical research. 2017;50(2):418-25.
454. Ballard SB. The U.S. commercial air tour industry: a review of aviation safety concerns. Aviation, space, and environmental medicine. 2014;85(2):160-6.
455. Grigoriev AI, Agadjanyan AA, Baranov VM, Polyakov VV. On the contribution of space medicine in the public health care. Acta astronautica. 1997;41(4-10):531-6.
456. Hood E. Nanotechnology: looking as we leap. Environmental health perspectives. 2004;112(13):A740-9.
457. Horneck G, Klaus DM, Mancinelli RL. Space microbiology. Microbiology and molecular biology reviews : MMBR. 2010;74(1):121-56.
458. Shaw IG. Robot Wars: US Empire and geopolitics in the robotic age. Security dialogue. 2017;48(5):451-70.
459. Taylor PW. Impact of space flight on bacterial virulence and antibiotic susceptibility. Infection and drug resistance. 2015;8:249-62.
460. Frenger P. Nasa astronauts, prosthetics and the manned space program. Biomedical sciences instrumentation. 2014;50:186-90.
461. Hodkinson PD, Anderton RA, Posselt BN, Fong KJ. An overview of space medicine. British journal of anaesthesia. 2017;119(suppl_1):i143-i53.
462. Ghidini T. Regenerative medicine and 3D bioprinting for human space exploration and planet colonisation. Journal of thoracic disease. 2018;10(Suppl 20):S2363-S75.
463. Demontis GC, Germani MM, Caiani EG, Barravecchia I, Passino C, Angeloni D. Human Pathophysiological Adaptations to the Space Environment. Frontiers in physiology. 2017;8:547.
464. Klaus DM, Benoit MR, Nelson ES, Hammond TG. Extracellular mass transport considerations for space flight research concerning suspended and adherent in vitro cell cultures.

Journal of gravitational physiology : a journal of the International Society for Gravitational Physiology. 2004;11(1):17-27.
465. Miranda MS, Rodrigues MT, Domingues RMA, Costa RR, Paz E, Rodriguez-Abreu C, et al. Development of Inhalable Superparamagnetic Iron Oxide Nanoparticles (SPIONs) in Microparticulate System for Antituberculosis Drug Delivery. Advanced healthcare materials. 2018;7(15):e1800124.
466. Kathuria H, Kochhar JS, Kang L. Micro and nanoneedles for drug delivery and biosensing. Therapeutic delivery. 2018;9(7):489-92.
467. Rayman RB. Telemedicine: military applications. Aviation, space, and environmental medicine. 1992;63(2):135-7.